

---

# Carbanionic Polymerisation of 2-Vinylpyridine

## Influence of Comonomers and Polymer Architectures

---

Dissertation

zur Erlangung des Grades

„Doktor der Naturwissenschaften“

im Promotionsfach Chemie

am Fachbereich Chemie, Pharmazie,  
Geographie und Geowissenschaften der  
Johannes Gutenberg-Universität Mainz

vorgelegt von

Marcel Fickenscher

geboren in Naila

Mainz, 2021

JOHANNES GUTENBERG  
UNIVERSITÄT MAINZ





Die als Dissertation vorgelegte Arbeit wurde in der Zeit von August 2017 bis November 2021 am Department Chemie der Johannes Gutenberg-Universität Mainz im Arbeitskreis von Herrn Prof. Dr. [REDACTED] angefertigt.

Dekanin: Prof. Dr. [REDACTED]

1. Berichterstatter: Prof. Dr. [REDACTED]

2. Berichterstatter: Prof. Dr. [REDACTED]

Tag der mündlichen Prüfung: 15.12.2021

Hiermit versichere ich gemäß § 10 Abs. 3d der Promotionsordnung vom 24.07.2007:

Ich habe die jetzt als Dissertation vorgelegte Arbeit selbst angefertigt und alle benutzten Hilfsmittel (Literatur, Apparaturen, Material) in der Arbeit angegeben.

Ich habe oder hatte die jetzt als Dissertation vorgelegte Arbeit nicht als Prüfungsarbeit für eine andere staatliche oder andere wissenschaftliche Prüfung eingereicht.

Ich hatte weder die jetzt als Dissertation vorgelegte Arbeit noch Teile davon bei einer anderen Fakultät bzw. einem anderen Fachbereich als Dissertation eingereicht.

---

Marcel Fickenscher





*“Fill your heart with what’s important and be done with all the rest.”*

*– Jordan Dreyer –*



# Danksagung

Um diese Arbeit zum Erfolg zu führen, wurde ich von vielen Seiten unterstützt, bei denen ich mich an dieser Stelle von ganzem Herzen bedanken möchte.

Allen voran gilt der größte Dank meinem Doktorvater **Prof. Dr. [REDACTED]** für die Möglichkeit, diese Arbeit in Ihrer Arbeitsgruppe anzufertigen. Die vielen Freiheiten und das damit entgegengebrachte Vertrauen ist nicht selbstverständlich und hat maßgeblich zur Entwicklung eigener Ideen beigetragen. Ihre Unterstützung bei der Umsetzung aller Projekte hat letztlich zum Gelingen dieser Arbeit geführt.

Bei **Prof. Dr. [REDACTED]** möchte ich mich für die hilfreichen Diskussionen während des Gruppenseminars bedanken, welche viele Denkanstöße für meine Projekte gegeben haben.

**[REDACTED]**, **[REDACTED]** und **[REDACTED]** danke ich für ihren Einsatz während ihrer Bachelorarbeiten. Euch zu betreuen hat mir viel Spaß gemacht und ihr habt einen wertvollen Beitrag zu dieser Arbeit geleistet. **[REDACTED]** danke ich für die vielen Diskussionen und Erkenntnisse während seiner Masterarbeit, die auch diese Arbeit vorangebracht haben.

**[REDACTED]** und **[REDACTED]** gilt großer Dank für die Unterstützung im täglichen Laboralltag und die Messung zahlreicher Proben, sowie für viele schöne Momente abseits der täglichen Aufgaben. Ohne euch und euer Bemühen für den Arbeitskreis würde vieles nicht so rund laufen. Gleichermaßen gilt mein Dank auch **[REDACTED]** für die Unterstützung bei allen organisatorischen Fragen. **[REDACTED]** möchte ich für die vielen Glasgeräte danken, die er mit größtem Geschick nach meinen Vorstellungen angefertigt, und so einige Synthesen erst möglich gemacht hat.

**[REDACTED]** danke ich für die große Hilfe bei der Messung der Zug-Dehnungsexperimente.

Für die super Zusammenarbeit, viele schöne Erlebnisse und den guten Zusammenhalt möchte ich dem gesamten Arbeitskreis und allen, die mittlerweile ihre Zeit im Arbeitskreis hinter sich haben, meinen Dank aussprechen. Konferenzen, Hüttenseminare, Grillabende und alle anderen großen und kleinen Events haben die Zeit im Arbeitskreis unvergesslich gemacht. Besonders möchte ich [REDACTED], [REDACTED], [REDACTED], [REDACTED] und [REDACTED] erwähnen, die sowohl bei fachlichen Diskussionen aber auch bei Unternehmungen abseits des Labors immer vollen Einsatz gezeigt haben.

[REDACTED], [REDACTED], [REDACTED] und [REDACTED] danke ich für die vielen hilfreichen und schönen Tage und Abende, sowohl im Arbeitskreis als auch darüber hinaus bei Koch- und Spieleabenden, sowie allen anderen teils intensiven Erlebnissen, die einen guten Ausgleich geschaffen haben und zeigen, dass Kollegen manchmal doch Freunde sind. Ganz besonderer Dank gilt an dieser Stelle [REDACTED], für die vielen Konzerte, auf denen wir gemeinsam waren und all die anderen, unvergesslichen Momente und schönen Unternehmungen der letzten Jahre!  
xoxo

Gleichermaßen bedanke ich mich bei allen meinen Freunden außerhalb des Arbeitskreises, die mich während des Studiums und teilweise auch schon davor begleitet haben, ganz besonders und allen voran bei [REDACTED] und [REDACTED] sowie [REDACTED], [REDACTED], [REDACTED], [REDACTED] und [REDACTED], [REDACTED], [REDACTED] und [REDACTED]. Ohne euch wäre das Studium und vieles darüber hinaus nicht annähernd so schön gewesen – vielen Dank für diese tolle Zeit!

Abschließend möchte ich mich bei einen Eltern [REDACTED] und [REDACTED], sowie meinem Opa [REDACTED] bedanken, die mich zu jeder Zeit unterstützt, und mit ihrem Zutun das Studium und die Promotion erst ermöglicht haben. Vielen Dank für Alles.

---

# Table of Contents

Table of Contents .....	- 1 -
1. Motivation and Objectives .....	- 3 -
2. Abstract .....	- 7 -
3. Zusammenfassung .....	- 11 -
4. Graphical Abstract.....	- 15 -
5. Chapter 1 – Introduction.....	- 17 -
6. Chapter 2 – Introducing a 1,1-diphenylethylene analogue for vinylpyridine: anionic copolymerisation of 3-(1-phenylvinyl)pyridine ( <i>m</i> -PyPE).....	- 57 -
7. Chapter 3 – Increasing the versatility of bifunctional carbanionic initiators with the use of <sup>1</sup> H NMR kinetic studies .....	- 99 -
8. Chapter 4 – Synthesis and characterisation of novel 2-vinylpyridine-isoprene ABA triblock copolymers .....	- 113 -
9. Chapter 5 – Synthesis and characterisation of ABA triblock copolymers based on isoprene and 2-vinylpyridine for TPE applications .....	- 159 -
10. Chapter 6 – End-capping of bifunctional initiated polyisoprene with <i>m</i> -PyPE ..	- 213 -
Curriculum Vitae.....	- 237 -



# 1. Motivation and Objectives

Polymers are a class of materials with an extremely wide range of applications, their properties can be adjusted by the specific properties of the chosen monomers and polymer architectures.<sup>1,2</sup> Particularly in the field of rubber materials, the success story started with the vulcanisation of natural rubber in 1939 by Charles Goodyear and continued with the development of high-performance thermoplastic elastomers, which are typically composed of styrene and dienes such as butadiene or isoprene.<sup>3,4</sup> The academic and industrial interest in such materials is evident in the range of different copolymers, which are characterised by the incorporation of different styrene derivatives or different copolymer architectures.<sup>5</sup>

The living anionic polymerisation in particular is the gold standard for highly controlled syntheses of thermoplastic elastomers (TPEs) with a high content of 1,4-regioisomers in the polydiene block, which represents the elastic soft phase of the material.<sup>6,7</sup> The stepwise addition of the comonomer allows comparatively easy access to block copolymers with exact molecular weights and dispersities. While the known styrene derivatives predominantly feature substitutions with oxygen-containing groups on the phenyl moiety, several nitrogen-bearing styrene derivatives are also reported in literature.<sup>8,9</sup> However, vinylpyridine in particular is an exciting comonomer due to the substitution within the aromatic ring. Especially its use in TPEs would be interesting, as its inherent polarity and the possibility to carry out numerous postpolymerisation modifications could significantly expand the range of possible applications.<sup>10</sup>

The main drawback when using vinylpyridine is the reactivity of the monomer. While autopolymerisation and side reactions during the reaction can easily take place, the active chain end shows high stability and thus low reactivity due to the electron-withdrawing pyridine ring.<sup>6,10</sup> As a result, the possibilities for copolymerisation with hydrocarbon monomers are limited. Neither the random copolymerisation nor the linear synthesis of vinylpyridine-isoprene-vinylpyridine ABA triblock copolymers is possible, since the crossover starting from vinylpyridinylithium is absent.

Given the limited statistical copolymerisation, this led to the question:

*"Is it possible to introduce statistically distributed hydrocarbon side groups into polyvinylpyridine via the careful choice of a new comonomer, to tailor the material properties?"*

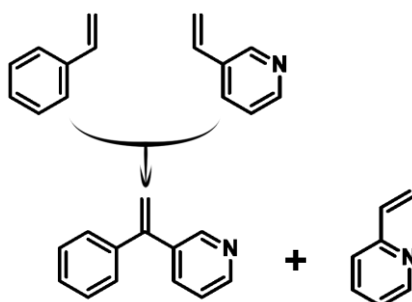


Figure 1: Visualisation of a novel comonomer combining styrene and 2-VP for the statistical copolymerisation with 2-VP.

The use of multivalent initiators in carbanionic polymerisations is well established both in academia and industry.<sup>11-13</sup> Typically, bifunctional initiators are used to reduce the number of reaction steps required in the synthesis of (multi)block copolymers by 1, or, in the case of tri- or oligofunctional initiators, to enable complex polymer architectures.<sup>14</sup> Another possible application for bifunctional initiators is the copolymerisation of reaction-inhibited monomers, thus enabling the overcome of reactivity differences by means of exploiting linear synthesis routes.<sup>15,16</sup> This led to the second question:

*"Is it possible to optimise the use of bifunctional initiators towards a universally applicable route in order to realise novel copolymer architectures based on isoprene and vinylpyridine?"*

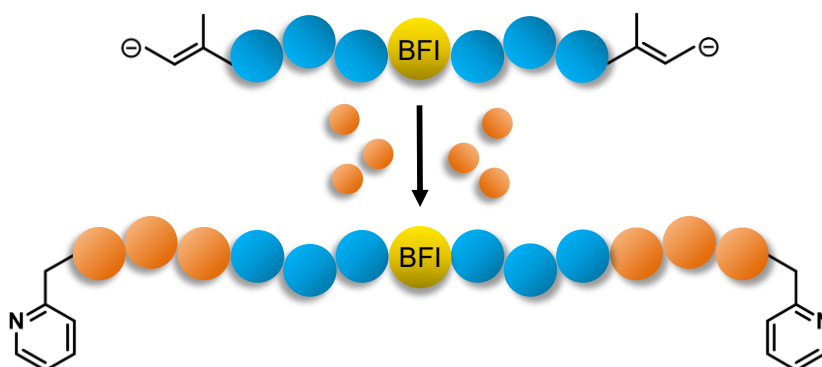


Figure 2: Visualisation of a synthesis route towards 2-VP-isoprene-2-VP ABA triblock copolymers.



## References

- (1) Sarkar, P.; Bhowmick, A. K. Sustainable rubbers and rubber additives. *J. Appl. Polym. Sci.* **2018**, *135* (24), 45701. DOI: 10.1002/app.45701.
- (2) Spontak, R. J.; Patel, N. P. Thermoplastic elastomers: fundamentals and applications. *Current Opinion in Colloid & Interface Science* **2000**, *5* (5-6), 333–340. DOI: 10.1016/S1359-0294(00)00070-4.
- (3) Morton, M.; McGrath, J. E.; Juliano, P. C. Structure-property relationships for styrene-diene thermoplastic elastomers. *J. polym. sci., C Polym. symp.* **1969**, *26* (1), 99–115. DOI: 10.1002/polc.5070260107.
- (4) Calzonetti, J. A.; Laursen, C. J. Patents of Charles Goodyear: His International Contributions to the Rubber Industry. *Rubber Chemistry and Technology* **2010**, *83* (3), 303–321. DOI: 10.5254/1.3525687.
- (5) Knoll, K.; Nießner, N. Styrolux + and styroflex + - from transparent high impact polystyrene to new thermoplastic elastomers: Syntheses, applications and blends with other styrene based polymers. *Macromol. Symp.* **1998**, *132* (1), 231–243. DOI: 10.1002/masy.19981320122.
- (6) Hadjichristidis, N.; Hirao, A., Eds. *Anionic Polymerization: Principles, Practice, Strength, Consequences and Applications*, 1st ed. 2015; SpringerLink Bücher; Springer, 2015. DOI: 10.1007/978-4-431-54186-8.
- (7) Szwarc, M. 'Living' Polymers. *Nature* **1956**, *178* (4543), 1168–1169. DOI: 10.1038/1781168a0.
- (8) Ishizone, T.; Hirao, A.; Nakahama, S. Anionic polymerization of monomers containing functional groups. *Macromolecules* **1993** (26), 6964–6975.
- (9) Hirao, A.; Loykulnant, S.; Ishizone, T. Recent advance in living anionic polymerization of functionalized styrene derivatives. *Progress in Polymer Science* **2002**, *27* (8), 1399–1471. DOI: 10.1016/S0079-6700(02)00016-3.
- (10) Kennemur, J. G. Poly(vinylpyridine) Segments in Block Copolymers: Synthesis, Self-Assembly, and Versatility. *Macromolecules* **2019**, *52* (4), 1354–1370. DOI: 10.1021/acs.macromol.8b01661.
- (11) Schulz, G. G. H.; Höcker, H. 1,3-Bis(1-phenylvinyl)benzene and its reactions with electron transfer reagents. *Makromol. Chem.* **1977**, *178* (9), 2589–2594. DOI: 10.1002/macp.1977.021780909.
- (12) Matmour, R.; Gnanou, Y. Combination of an anionic terminator multifunctional initiator and divergent carbanionic polymerization: application to the synthesis of dendrimer-like polymers and of asymmetric and miktoarm stars. *J. Am. Chem. Soc.* **2008**, *130* (4), 1350–1361. DOI: 10.1021/ja076442t. Published Online: Jan. 3, 2008.
- (13) Lee, P.-C.; Wang, C.-C.; Chen, C.-Y. Synthesis of high-vinyl isoprene and styrene triblock copolymers via anionic polymerization with difunctional t-BuLi initiator. *European Polymer Journal* **2020**, *124*, 109476. DOI: 10.1016/j.eurpolymj.2020.109476.
- (14) Matmour, R.; Gnanou, Y. Synthesis of complex polymeric architectures using multilithiated carbanionic initiators—Comparison with other approaches. *Progress in Polymer Science* **2013**, *38* (1), 30–62. DOI: 10.1016/j.progpolymsci.2012.08.003.

(15) Beinert, G.; Lutz, P.; Franta, E.; Rempp, P. A bifunctional anionic initiator soluble in non-polar solvents. *Makromol. Chem.* **1978**, *179* (2), 551–555. DOI: 10.1002/macp.1978.021790233.

(16) Guyot, P.; Favier, J. C.; Uytterhoeven, H.; Fontanille, M.; Sigwalt, P. New perfectly difunctional organolithium initiators for block copolymer synthesis: Synthesis of dilithium initiators in the absence of polar additives. *Polymer* **1981**, *22* (12), 1724–1728. DOI: 10.1016/0032-3861(81)90394-3.

## 2. Abstract

This thesis describes the copolymerisation of 2-vinylpyridine (2-VP) towards novel copolymer structures. The main objective is to expand the range of applications for P(2-VP) copolymers, in terms of hydrophilicity and thermal properties as well as the synthesis of thermoplastic elastomers (TPEs) with 2-VP hard segments.

**Chapter 1** gives a general introduction and describes the theoretical background of this thesis. Starting from the basics of carbanionic polymerisation, different polymer architectures and the properties of thermoplastic elastomers are described. An overview of the monomers used, isoprene and 2-VP, highlights the necessary conditions for the polymerisations to be carried out. Literature-known 2-VP-isoprene diblock copolymers are reviewed and the microphase separation of 2-VP-hydrocarbon monomer block copolymers is discussed in detail. Finally, the history of bifunctional initiators, which represent the basic building block for the development of the new polymer architectures, is presented. The initiators used in this thesis, double diphenylethylene (DDPE) and 1-bromo-4-(4-bromophenoxy)-2-pentadecylbenzene (DBPPB), are discussed in detail and the respective characteristics are outlined.

**Chapter 2** presents a new monomer and its copolymerisation with 2-VP. 3-(1-phenylvinyl)pyridine (*m*-PyPE) is prepared starting from 3-benzoylpyridine *via* a facile Wittig reaction and embodies the combination of styrene and vinylpyridine, with the purpose of aligning the reactivities of both monomers. While the direct copolymerisation of 2-VP with styrene is not possible, the adjusted reactivity allows the cross-over between the phenyl-bearing comonomer and 2-VP and vice versa, opening up the possibility of randomly introduced hydrocarbon side groups in P(2-VP). The analytical results of the synthesis, based on NMR spectroscopy, confirm the successful copolymerisation. It is demonstrated that the material properties can be efficiently altered and adjusted. As expected, the glass transition temperature  $T_g$  increases in a linear trend with increasing *m*-PyPE content, while the hydrophilicity is

reduced. These results provide a promising basis for the further development of existing applications in which P(2-VP) is used.

**Chapter 3** focuses on the bifunctional initiators for the following copolymerisations of 2-VP with isoprene. DDPE and DBPPB are described in detail with their respective characteristics and a universal route for the use of both initiators for polymerisations is presented. In particular, the kinetics during the activation step is in the foreground and monitored by means of  $^1\text{H}$  NMR spectroscopy to ensure quantitative conversion. Based on this, the optimal working concentration for the use of the initiators is described. The results form the basis for the subsequent triblock syntheses and are generally valid for further conceivable carbanionic polymerisations.

**Chapter 4** describes the synthesis of novel 2-VP-isoprene ABA triblock copolymers. Starting with the synthesis of DDPE, the activation of the initiator is discussed and the quantitative conversion into the active species is confirmed via the endcapping of a polystyrene sample with ethylene oxide. Subsequently, the optimal reaction conditions for block copolymer synthesis are determined experimentally and the synthesis of different series of samples is displayed, confirming that the use of a bifunctional initiator is suitable to circumvent the sequence limitation of a monofunctional initiation. The analysis by means of SEC and NMR spectroscopy confirms the excellent reaction control. A high proportion of 1,4-regioisomers within the isoprene block as well as the correct monomer composition is determined. Furthermore, the known aggregation tendency of the polymers is observed and characterised via SEC and light scattering experiments. Finally, qualitative post-polymerisation modification of the materials by means of protonation as well as preliminary elastomeric properties are shown, the latter indicating the suitability of the polymers as TPEs.

**Chapter 5** covers the synthesis of high molecular weight triblock copolymers from 2-VP and isoprene. The optimisation of the synthesis route is discussed in detail and the resulting polymers are characterised by SEC and NMR spectroscopy. The results obtained show a high fraction of the 1,4-regioisomer within the polyisoprene block, which is an important factor for elastomeric behaviour. Thermal analysis of the glass

transition temperature clearly shows the  $T_g$ s of both blocks, suggesting successful microphase separation. From the synthesised samples, films were prepared using the solvent evaporation technique, which are qualitatively investigated by tensile testing. The results show that the choice of a suitable solvent during film production should be the focus of further research, but the basic suitability of the materials for use as TPEs can already be discerned from the performed measurements.

**Chapter 6** deals with the enfunctionalisation of bifunctionally initiated polyisoprene with *m*-PyPE, an amino functional DPE derivative. The absence of homopolymerisation of *m*-PyPE provides an elegant solution for the introduction of exactly one amino functionality on the living chain. The possibility of postpolymerisation modification of *m*-PyPE allows reversible crosslinking of such telechelics using dihalogenated species or bisphenols. The latter are of particular interest due to the lower toxicity. The theoretical background as well as different synthetic approaches and the respective difficulties are discussed.



### 3. Zusammenfassung

Diese Arbeit thematisiert die Copolymerisation von 2-Vinylpyridin (2-VP) und die Synthese von neuartigen 2-VP Copolymerstrukturen. Das Hauptziel ist die Erweiterung des Anwendungsbereichs von P(2-VP) Copolymeren in Bezug auf Hydrophilie und thermische Eigenschaften, sowie die Synthese von thermoplastischen Elastomeren mit P(2-VP) Hartsegmenten.

**Kapitel 1** gibt eine allgemeine Einführung und beschreibt den theoretischen Hintergrund dieser Arbeit. Ausgehend von den Grundlagen der carbanionischen Polymerisation werden verschiedene Polymerarchitekturen und die Eigenschaften von thermoplastischen Elastomeren beschrieben. Ein Überblick über die verwendeten Monomere Isopren und 2-VP zeigt die notwendigen Bedingungen für die durchzuführenden Polymerisationen. Literaturbekannte 2-VP-Isopren Diblockcopolymeren werden diskutiert und die Mikrophasenseparation von 2-VP Kohlenwasserstoffmonomer Blockcopolymeren wird ausführlich erörtert. Schließlich wird die Geschichte der bifunktionellen Initiatoren, die den Grundbaustein für die Entwicklung der neuen Polymerarchitekturen darstellen, vorgestellt. Die in dieser Arbeit verwendeten Initiatoren, Doppeldiphenylethylen (DDPE) und 1-Brom-4-(4-bromphenoxy)-2-pentadecylbenzol (DBPPB), werden detailliert charakterisiert und die jeweiligen Besonderheiten vorgestellt.

**Kapitel 2** stellt ein neues Monomer und seine Copolymerisation mit 2-VP vor. 3-(1-Phenylvinyl)pyridin (*m*-PyPE) wird ausgehend von 3-Benzoylpyridin über eine Wittig-Reaktion hergestellt und verkörpert die Kombination von Styrol und Vinylpyridin mit dem Ziel, die Reaktivität dieser Monomere anzugleichen. Während die direkte Copolymerisation von 2-VP mit Styrol nicht möglich ist, erlaubt die angepasste Reaktivität des neuen Comonomers *m*-PyPE den Cross-Over zwischen dem phenylsubstituierten Comonomer und 2-VP und umgekehrt, was die Möglichkeit von zufällig eingeführten Kohlenwasserstoff-Seitengruppen in P(2-VP) eröffnet. Die analytischen Ergebnisse der Synthese, basierend auf NMR-Spektroskopie, bestätigen

die erfolgreiche Copolymerisation. Es wird gezeigt, dass die Materialeigenschaften effizient verändert und eingestellt werden können. Wie erwartet, steigt die Glasübergangstemperatur  $T_g$  mit zunehmendem *m*-PyPE-Gehalt linear an, während die Hydrophilie abnimmt. Diese Ergebnisse bilden eine vielversprechende Grundlage für die Weiterentwicklung bestehender Anwendungen, in denen P(2-VP) eingesetzt wird.

**Kapitel 3** konzentriert sich auf die bifunktionellen Initiatoren für die folgenden Copolymerisationen von 2-VP mit Isopren. DDPE und DBPPB werden mit ihren jeweiligen Eigenschaften detailliert beschrieben und eine universelle Route für den Einsatz beider Initiatoren für Polymerisationen vorgestellt. Insbesondere steht die Reaktionskinetik während des Aktivierungsschrittes im Vordergrund und wird mittels  $^1\text{H}$ -NMR-Spektroskopie verfolgt, um den quantitativen Umsatz zu gewährleisten. Darauf aufbauend wird die optimale Initiatorkonzentration beschrieben. Die Ergebnisse bilden die Grundlage für die nachfolgenden Triblocksynthesen und sind universell für weitere denkbare carbanionische Polymerisationen anwendbar.

**Kapitel 4** beschreibt die Synthese von neuartigen 2-VP-Isopren ABA Triblockcopolymeren. Ausgehend von der Synthese von DDPE wird die Aktivierung des Initiators erörtert und die quantitative Umwandlung in die aktive Spezies durch das Endcapping einer Polystyrolprobe mit Ethylenoxid bestätigt. Anschließend werden die optimalen Reaktionsbedingungen für die Synthese von Blockcopolymeren experimentell bestimmt und die Synthese verschiedener Proben gezeigt, was bestätigt, dass der Einsatz eines bifunktionellen Initiators geeignet ist, um die Sequenzbeschränkung der monofunktionellen Reaktionsführung zu umgehen. Die Analyse mittels GPC und NMR-Spektroskopie bestätigt die ausgezeichnete Reaktionskontrolle. Es wird ein hoher Anteil des 1,4-Regioisomers innerhalb des Isoprenblocks sowie die korrekte Monomierzusammensetzung nachgewiesen. Darüber hinaus wird die bekannte Aggregationsneigung der Polymere beobachtet und durch GPC- und Lichtstreuungsexperimente charakterisiert. Schließlich werden die qualitative Modifizierung der Materialien nach der Polymerisation durch Protonierung



sowie erste elastomere Eigenschaften untersucht, wobei letztere auf die Eignung der Polymere für den Einsatz als TPEs hinweisen.

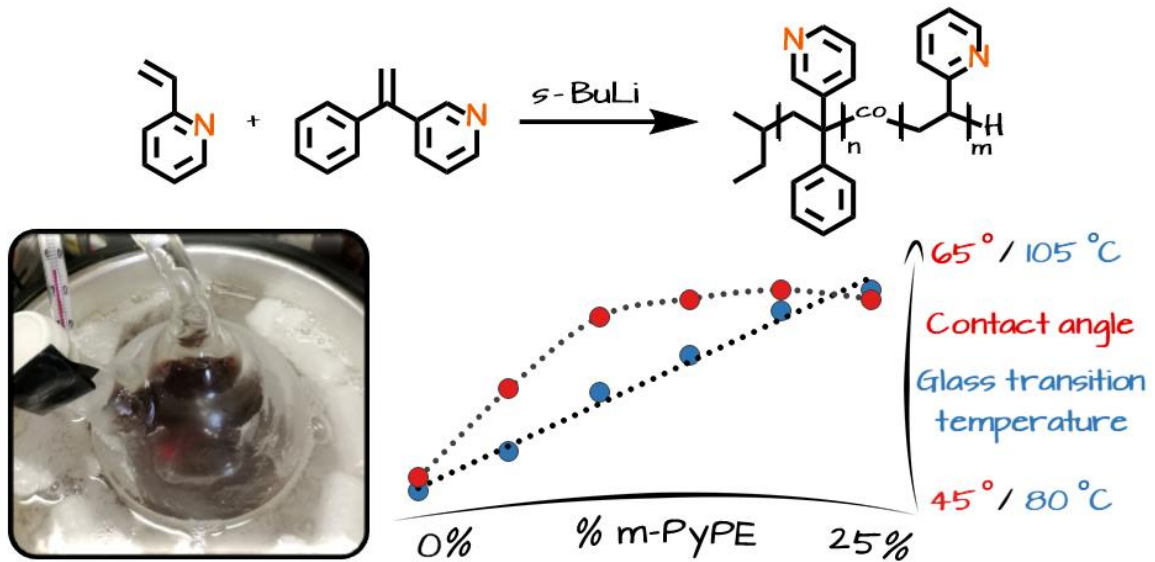
**Kapitel 5** behandelt die Synthese von hochmolekularen Triblockcopolymeren aus 2-VP und Isopren. Die Optimierung der Syntheseroute wird ausführlich erörtert und die resultierenden Polymere werden mittels GPC und NMR-Spektroskopie charakterisiert. Die erzielten Ergebnisse zeigen einen hohen Anteil des gewünschten 1,4-Regioisomers innerhalb des Polyisoprenblocks, der ein wichtiger Faktor für das elastomere Verhalten ist. Die thermische Analyse der Glasübergangstemperatur zeigt deutlich die  $T_g$ s beider Copolymerblöcke, was auf eine erfolgreiche Mikrophasentrennung schließen lässt. Aus den synthetisierten Proben wurden mit Hilfe der Lösungsmittelverdampfungstechnik Filme hergestellt, die durch Zug-Dehungsversuche qualitativ untersucht wurden. Die Ergebnisse zeigen, dass die Wahl eines geeigneten Lösungsmittels bei der Folienherstellung im Fokus weiterer Forschung stehen sollte, die grundsätzliche Eignung der Materialien für den Einsatz als TPEs ist aber bereits durch die durchgeführten Messungen zu erkennen.

**Kapitel 6** beschäftigt sich mit der Enkfunktionalisierung von bifunktionell initiiertem Polyisopren mit *m*-PyPE, einem aminofunktionellen DPE-Derivat. Das Ausbleiben der Homopolymerisation von *m*-PyPE bietet eine elegante Lösung für die Einführung von genau einer Aminofunktionalität am lebenden Kettenende. Die Möglichkeit, *m*-PyPE nach der Polymerisation zu modifizieren, erlaubt die reversible Vernetzung solcher Telechele mit Hilfe von dihalogenierten Spezies oder Bisphenolen. Letztere sind aufgrund ihrer geringeren Toxizität von besonderem Interesse. Der theoretische Hintergrund sowie verschiedene synthetische Ansätze und die jeweiligen Schwierigkeiten werden erörtert.

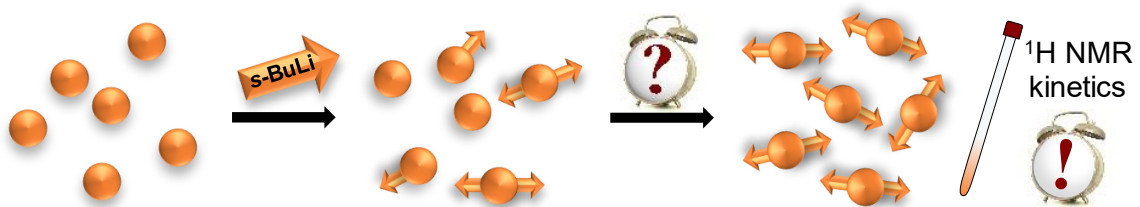


## 4. Graphical Abstract

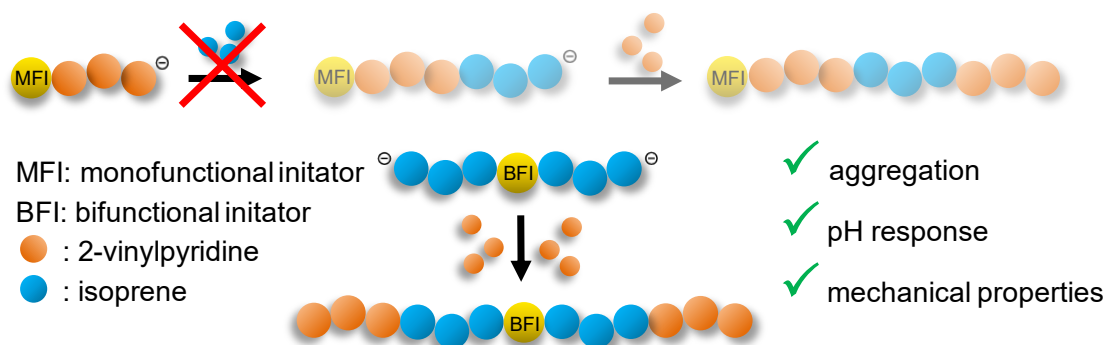
## Chapter 2



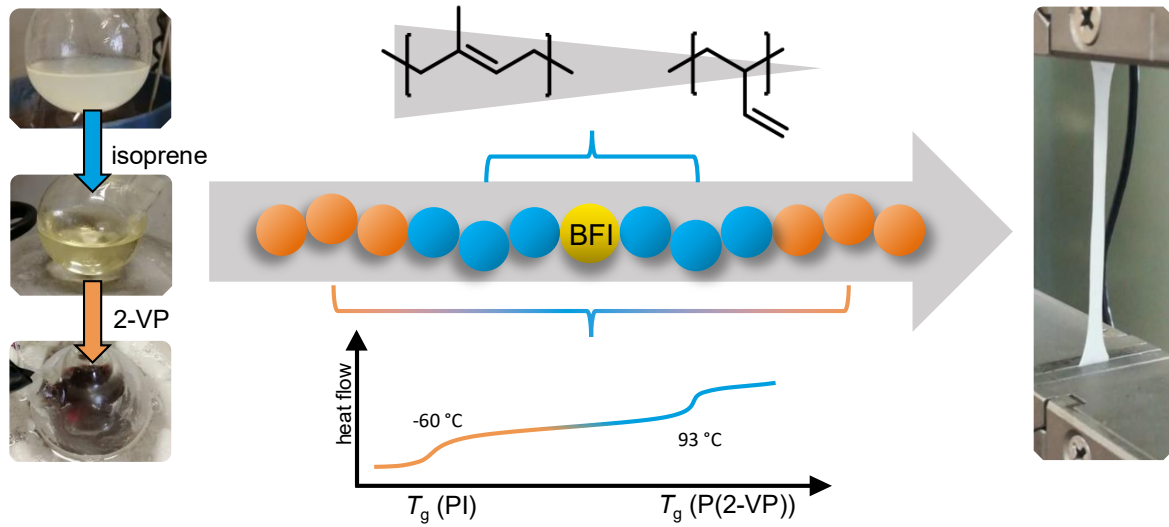
## Chapter 3



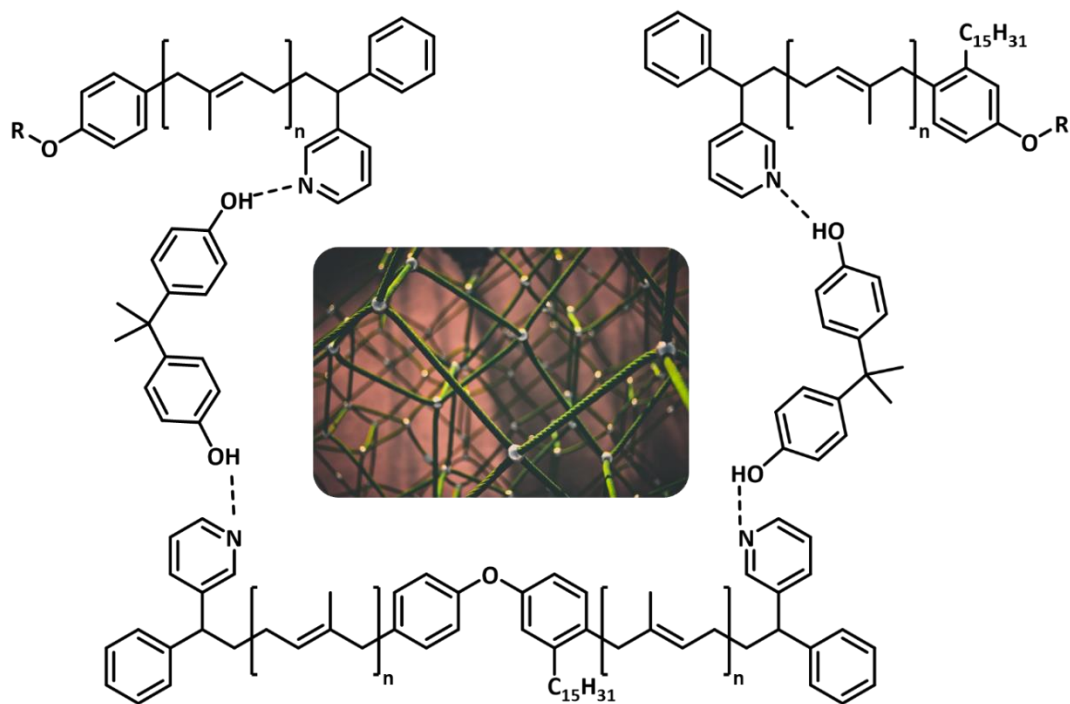
## Chapter 4



## Chapter 5



## Chapter 6



## 5. Chapter 1 – Introduction

After the first report on macromolecules by H. Staudinger in 1920 a tremendous milestones in polymer science was set by Michael Swarcz in 1954 with the development of the *living anionic polymerisation*, which today is an important research field, and by far not limited to academia.<sup>1-5</sup> The global production of plastics rose to 368 million tons in 2019 and is still growing.<sup>6</sup> Especially the possibility to synthesise tailored polymers without any side reactions as well as in the absence of chain transfer or termination reactions enabled the manufacturing of high-precision and high-performance plastics.

### 5.1 Carbanionic Polymerisation

Polymerisation reactions are divided into two main types: Step-growth and chain-growth reactions. While the former require monomers with two functional groups that can form a chemical bond and thus requires high turnover, the latter is characterised by the fact that individual monomers are each capable of adding a new monomer.<sup>7</sup> Chain-growth polymerisation can be further divided into radical, cationic, anionic and coordinative polymerisations.<sup>8</sup> This work is focused on the anionic polymerisation of carbonyl vinyl monomers, which gained considerable attention in 1956 with the polymerisation of styrene with sodium naphthalenide in THF by Michael Szwarc, as shown in Figure 1.<sup>3</sup> The reaction begins with the formation of a naphthalenide radical anion in an electron transfer reaction from sodium followed by the formation of a styrene radical which readily dimerises into the active bifunctional initiator structure. The radical nature of the activation step justifies the use of a polar solvent such as THF, which ultimately slightly limits the scope of this method, as will be discussed later. The bifunctional styrene dimer is now capable of adding additional styrene monomers, leading to the formation of the polymer until all remaining monomer is consumed. The chain ends are then still in an active form which allows the

polymerisation of additional monomer units when they are added to the reaction mixture.

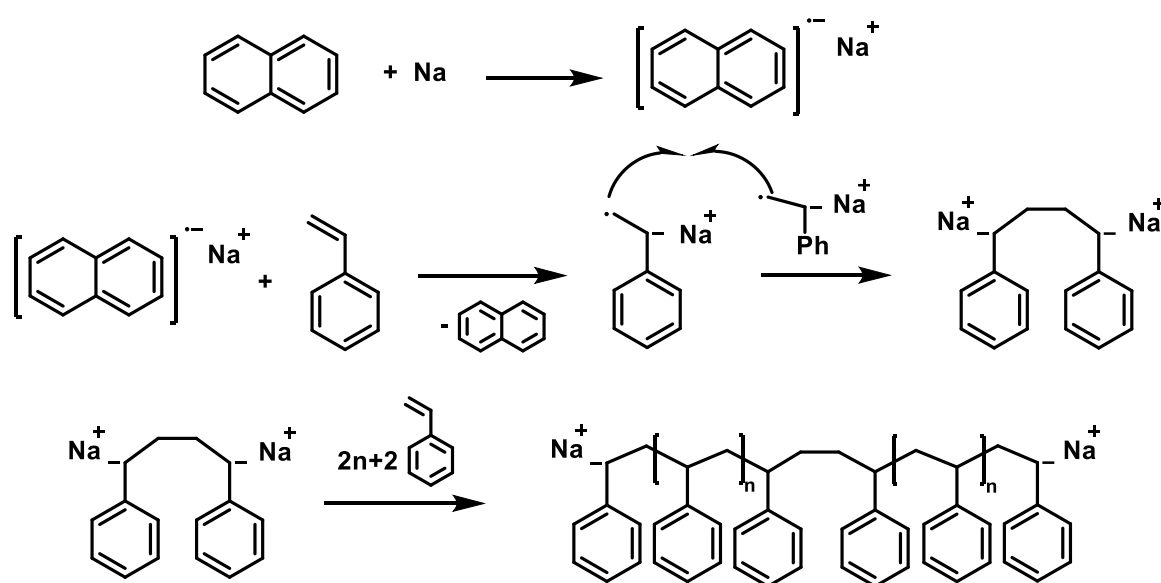


Figure 1: Anionic polymerisation of styrene using sodium naphthalenide as initiator in THF.

Today, alkyl lithium initiators are commonly used to start the polymerisation reaction of many different monomers. An exemplary overview of suitable monomers is given in Figure 2.<sup>9</sup> Especially polystyrene and polydienes as well as substituted polystyrenes e.g. alkyl styrene or *p*-fluorostyrene have been intensively studied.<sup>10-17</sup>

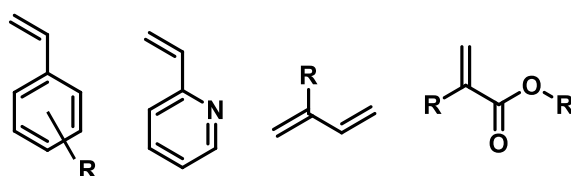


Figure 2: A selection of monomers suitable for anionic vinyl polymerisation. R=H, alkyl, electron withdrawing non-protic group.

To characterise an anionic polymerisation reaction as a *living anionic polymerisation*, several criteria must be met: To ensure homogeneous chain growth, the initiation step must be significantly faster than the propagation rate of the reaction, and there must be no termination or chain transfer reactions throughout the reaction. This then allows the synthesis of well-defined polymers with dispersities  $\mathcal{D}$  of around 1.01-1.10.<sup>18</sup> The dispersity distribution is given in Equation 1 where  $M_w$  is the weight average and  $M_n$  the number average.

$$D = \frac{\bar{M}_w}{\bar{M}_n} \approx 1 + \frac{1}{\overline{DP}_n} \quad \text{Equation 1}$$

Figure 3 shows the three different polymerisation steps: Initiation with *sec*-Butyllithium (*s*-BuLi), propagation and termination with methanol as protic substance.

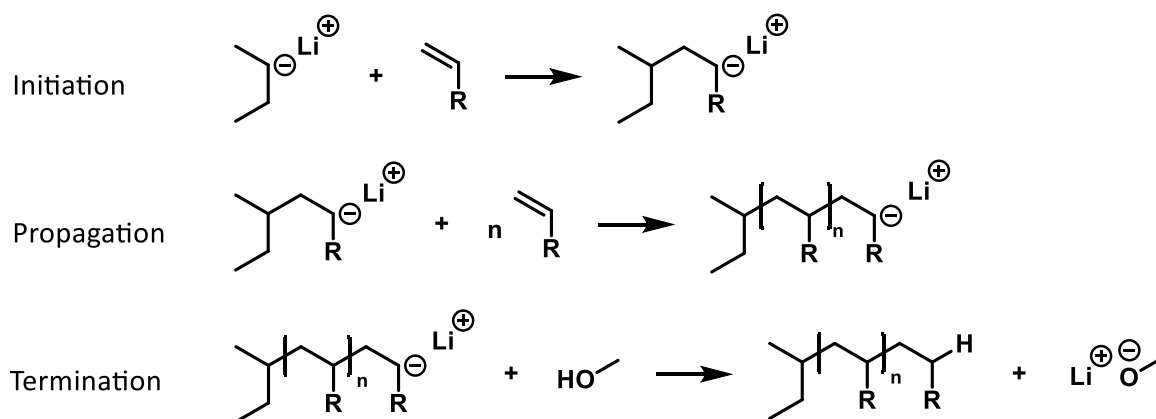


Figure 3: Overview over the reaction steps during a carbanionic polymerisation.

In the absence of side reactions, the carbanion concentration is constant and equals the initiator concentration. Therefore, the monomer consumption of these polymerisations can be described by first order kinetics, shown in Equation 2.

$$-\frac{d[M]}{dt} = k_p[M][M^-] = k_p[M][I^-] \quad \text{Equation 2}$$

To ensure the homogeneous growth of the polymers, the initiation rate of *living anionic polymerisations* is considerably higher than the propagation rate. Therefore, the degree of polymerisation  $\bar{P}_n$  can be adjusted by the monomer-to-initiator ratio, as described by Equation 3.

$$\bar{P}_n = \frac{[M]_0 - [M^-]_t}{[M^-]} = \frac{[M]_0 - [M^-]_t}{[I^-]} \quad \text{Equation 3}$$

Utmost care must be taken with regard to the reaction conditions, as protic impurities as well as oxygen and carbon dioxide lead to the uncontrolled termination or chain coupling as shown in Figure 4.

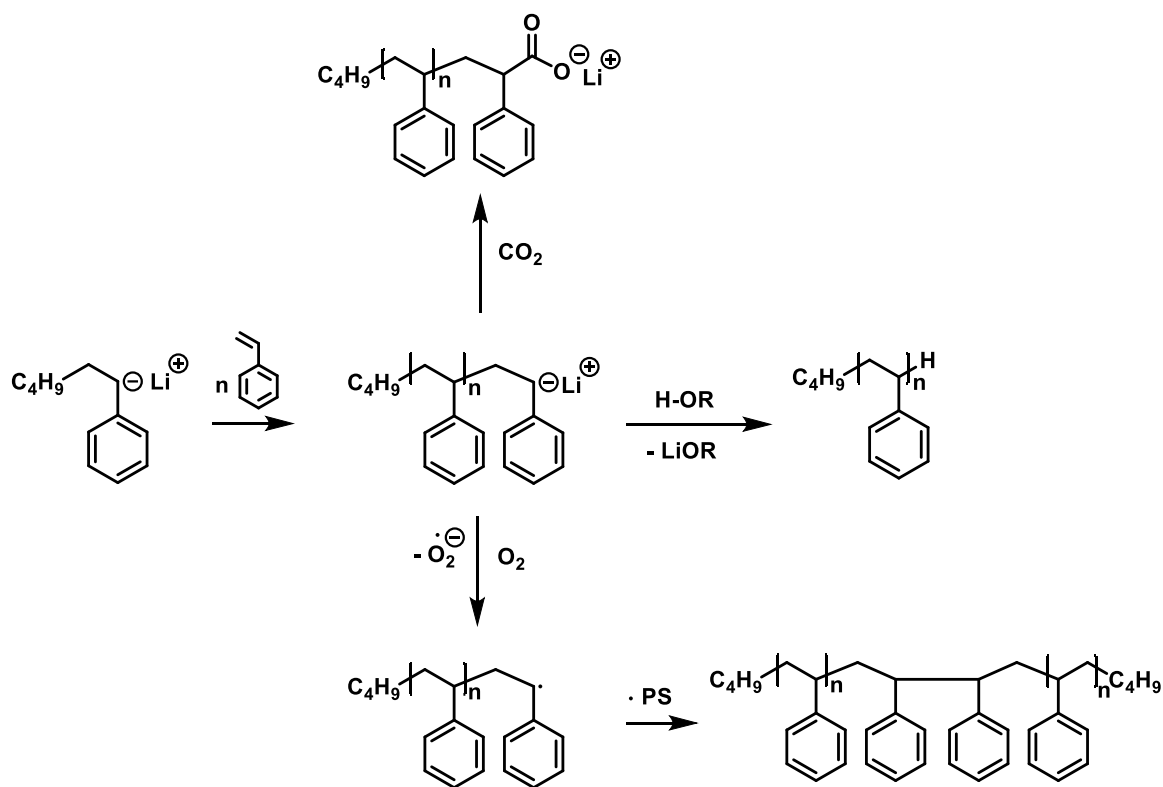


Figure 4: Impurities during the living anionic polymerisation of polystyrene lead to different termination or chain transfer reactions.

Traditionally, the *break seal technique* was used for these kinds of syntheses. Modern reaction conditions use the *Schlenk technique* with teflon caps and rubber seals, high vacuum, several flame drying steps of the sealed apparatus and careful pretreatment of all monomers and solvents, including the removal of stabilisers and traces of water and dissolved gasses with calcium hydrate and repeated *freeze-pump-thaw* cycles.<sup>18</sup>

As described earlier, the chain ends of the growing polymers remain active once the monomer has been fully incorporated, and subsequently begin the polymerisation of additional monomer, if added. This allows the synthesis of more complex polymer architectures and well-defined copolymer structures, a selection from the many variants is shown in Figure 5.<sup>19</sup> Depending on the reactivity of the monomers and the addition strategy, their position along the chain differs. Block copolymers are commonly synthesised via the sequential addition of monomers. This also allows the synthesis of tri- or higher block copolymers and especially ABA triblock copolymers from styrene and butadiene or isoprene are present in the polymer industry.<sup>20,21</sup>



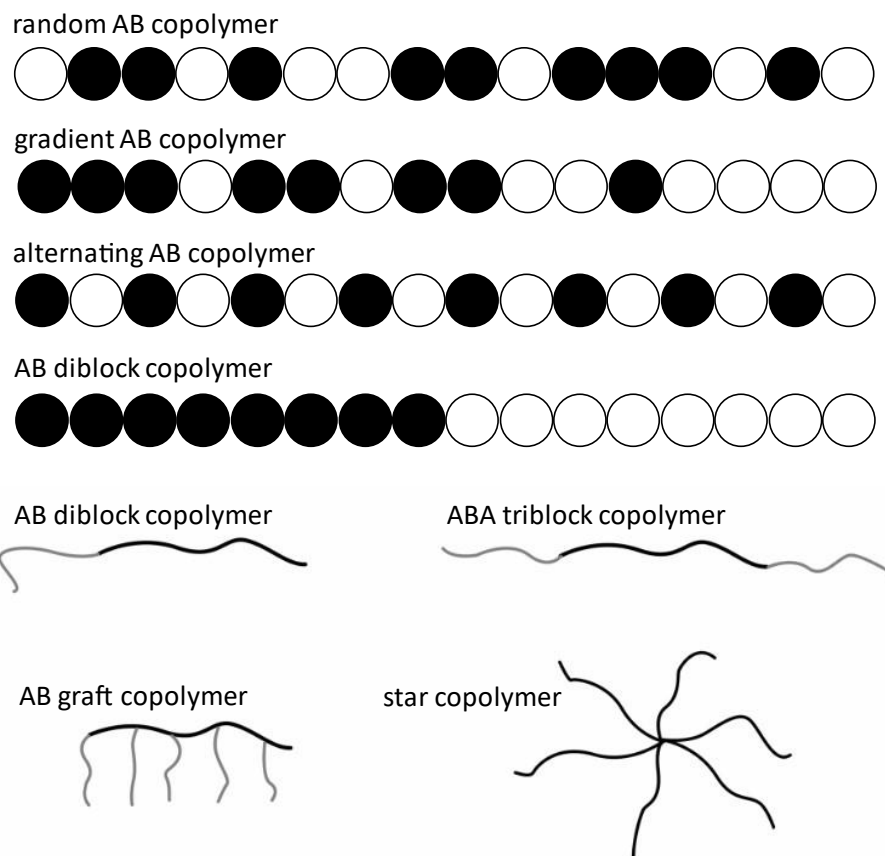


Figure 5: Selection of different (co)polymer architectures.

Copolymers combine properties of their consisting monomers. Random or alternating copolymers show a behaviour that can be described as a mixture of both monomer properties. To a certain degree, this is also true for gradient copolymers yet changes, if the gradient is steeper and the polymer structure becomes block like. Block copolymers generally exhibit the separate characteristics of the homopolymers, particularly concerning the glass transition temperature  $T_g$ , but nevertheless combine their respective properties, e.g. for elasticity and toughness, in one material. Triblock copolymers are of particular interest, as their intermolecular interaction results in enhanced material properties.<sup>22,23</sup> Based on this characterisation three main groups are defined: Elastomers, thermoplastics and duroplastics.

## 5.2 Thermoplastic Elastomers

Elastomers are defined as a class of polymers that display rubber-like elasticity, basically named after their elastic recovery upon mechanical deformation.<sup>24</sup> Elastomers based on natural rubber, obtained by coagulation of the milk sap of the rubber tree *Hevea brasiliensis*, were already used by ancient cultures like the Maya around 200-400 AD.<sup>25</sup> The journey to today's materials continued with the discovery of the vulcanisation process by Charles Goodyear in 1839. The covalent crosslinking of polyisoprene with sulfur to introduce sulfide bridges leads to the hardening of the rubber and thus to highly elastic materials.<sup>24,26</sup> The diverse applications for these materials range from pencil erasers, balls and gloves to automotive tires and much more. The latter in particular represents one of the most widespread groups for polymers of this type after the first air-filled tire was patented by Robert William Thomson in 1847.<sup>27</sup> The molecular structure of these materials was discovered by G. Williams in 1860 via careful pyrolysis of caoutchouc and the isolation of isoprene.<sup>25</sup> In 1910 F. E. Matthews by accident discovered the formation of a rubber-like material from the storage of isoprene over sodium metal for several weeks. He went on to develop other synthetic rubbers by using different dienes and alkali metals such as butadiene and potassium which was patented in Great Britain.<sup>28</sup> With the expiration of the patent in 1926 IG Farben continued with the work on the alkali metal initiated polymerisation and produced the famous synthetic Buna rubber 32, 85 and 115 with different molecular weights for the tire manufacture.<sup>29</sup> In 1929, Walter Bock developed styrene-butadiene copolymers by emulsion polymerisation. These early thermoplastic elastomers (TPEs) show superior material properties in terms of abrasion and improved the existing tire designs.<sup>30</sup> Regardless of the application, the main advantage of these materials is based on not covalent but physical crosslinking and the resulting recyclability. Since their introduction to the market in the 1950s, TPEs have experienced an emerging growth in the polymer industry.<sup>31-33</sup> The established living anionic polymerisation described earlier has now enabled the precise synthesis of similar polymers and is a powerful tool to produce materials with enhanced properties.<sup>34</sup>

TPEs typically consist of a hard phase (e.g. styrene) and a soft phase (e.g. isoprene) that can self-assemble into intermolecular aggregates as a consequence of immiscible polymer blocks which act as crosslinks while being readily moldable for processing.<sup>35</sup>

For AB diblock copolymers, this microphase separation is described by the Flory-Huggins theory, given in Equation 4.<sup>36</sup>

$$\frac{\Delta G_m}{k_B T} = \frac{f_A}{N_A} \ln f_B + f_A f_B \chi_{AB} \quad \text{Equation 4}$$

$\Delta G_m$  represents the Gibbs free energy,  $k_B$  the Boltzmann constant and  $T$  the temperature. The volume fraction of monomers A or B is given by the respective variable  $f$ , while  $N$  describes the degree of polymerisation and  $\chi$  the Flory-Huggins interaction parameter. The entropy of the system is described by the first two terms and always favours the mixing of the phases, however, this effect is only small since polymers commonly have a large degree of polymerisation.<sup>37</sup> The latter term of Equation 4 represents the enthalpy term and the Flory-Huggins interaction parameter affects the segregation significantly.  $\chi_{AB}$  is further described by Equation 5 as the free-energy cost per monomer of contacts between A and B monomers.

$$\chi_{AB} = \frac{Z}{k_B T} \left[ \epsilon_{AB} - \frac{1}{2} (\epsilon_{AA} + \epsilon_{BB}) \right] \quad \text{Equation 5}$$

$Z$  is the number of nearest neighbouring monomers in a copolymer configuration cell and  $\epsilon_{AB}$  the interaction energy per monomer between A and B monomers. Positive values indicate the repulsion between A and B while negative ones indicate a drive towards the mixing.<sup>38</sup> The segregation of the blocks ultimately lead to the formation of domains ranging between 10-100 nm in size.<sup>39</sup> In order to achieve a state that is as favourable as possible in terms of energy, the system strives to minimise the interfaces of the domains.<sup>40</sup> Based on the volume fraction of the monomers, a series of morphologies is possible, as shown in Figure 6.<sup>41</sup> Scheme a) depicts how once the volume fraction of monomer B exceeds a certain value, the block copolymer starts to self-assemble and a spheric (S), a cylindric (C) or a gyroid (G) morphology is formed,

embedded in the phase of the more voluminous comonomer block. If the volume fraction of block B is further increased, a lamellar (L) structure forms until block A starts to form these morphologies in a reversed manner, embedded in the phase of block A. Scheme b) shows the calculated phase diagram, which allows estimation of the block copolymer composition necessary to form a given morphology, while scheme c) displays an experimental diagram for a diblock copolymer of styrene and isoprene including a mixed morphology, the perforated lamellar structure (PL).

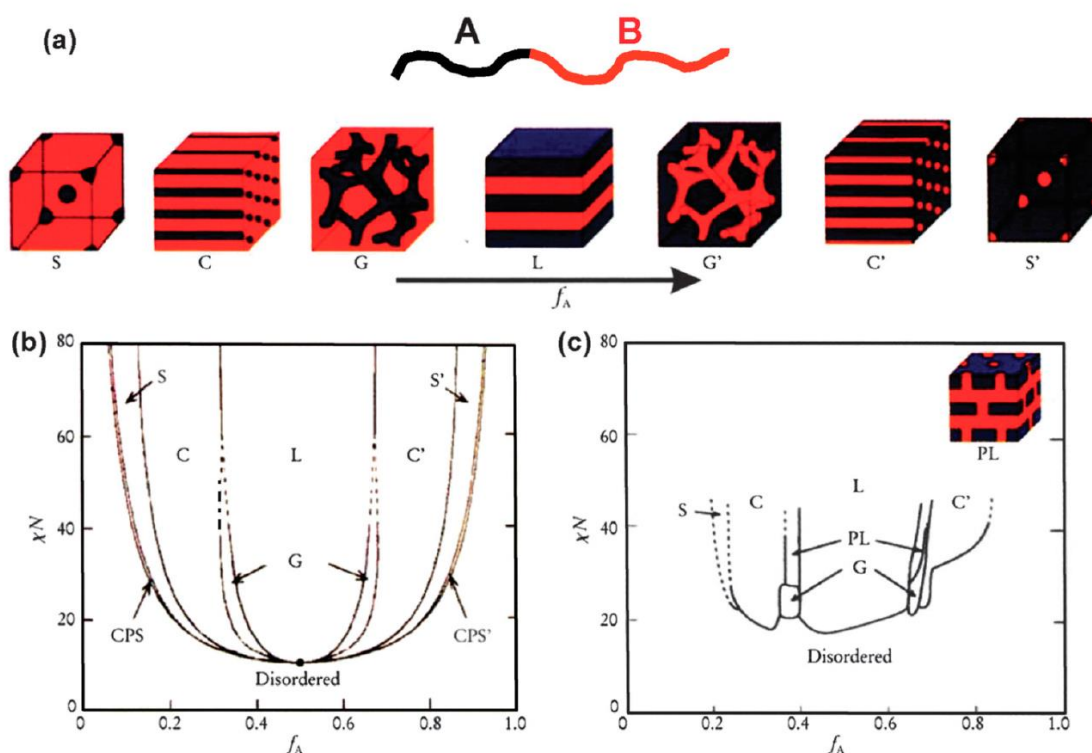
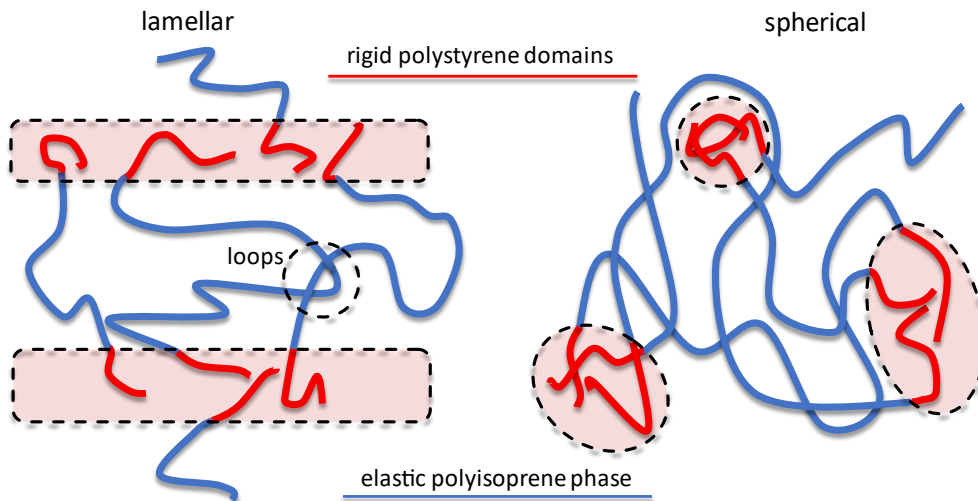


Figure 6: a) Different phase morphologies based on the volume fraction of the monomers. b) Calculated phase diagram for the respective morphologies. c) Experimental phase diagram for a styrene-isoprene block copolymer. (Copyright (2012) Royal Society of Chemistry).<sup>41</sup>

The morphology of ABA triblock copolymers is similar to that of AB diblocks in a good approximation, here the volume fraction is considered by snipping the B block in the middle.<sup>42–44</sup> Figure 7 shows an exemplary, schematic domain arrangement of an ABA triblock copolymer. Compared to diblock copolymers, triblock copolymers exhibit improved mechanical properties because the polymer chains form bridges between the phase separated domains building a physical network that can also be further stabilised by the formation of loops.<sup>40,45,46</sup>



*Figure 7: Schematic domain arrangement of an ABA styrene-isoprene copolymer.*

Increasing the number of blocks enhances this effect as well as a higher molecular weight of the polymers, since the bridging and entangling fraction is increased.<sup>46,47</sup>

Today, the applications of these materials range from general-purpose 3D printing to highly specific medical applications, and many different monomers are used, yet styrene and isoprene are still among the most commonly used.<sup>48</sup>

### 5.3 Isoprene

A variety of dienes is known in literature, yet one of the most common monomers used as low  $T_g$  component, along with butadiene, is isoprene. In 2017 natural rubber (*cis*-1,4-polyisoprene) accounts for 46% of the total global rubber consumption.<sup>49</sup> A selection of different dienes is shown in Figure 8 a).

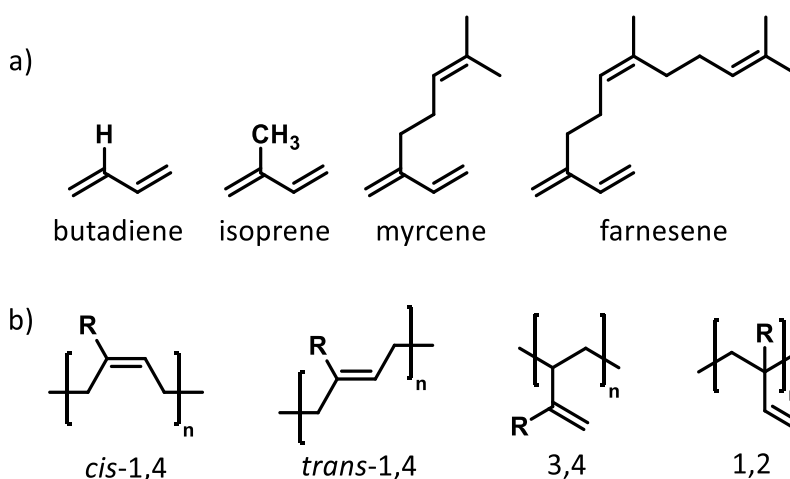


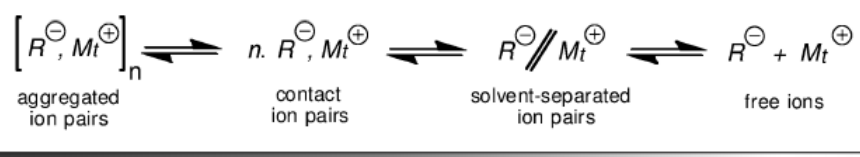
Figure 8: a) Selection of different dienes suitable for the living carbanionic polymerisation.  
b) Different microstructures of polydienes.

Myrcene and farnesene represent a rather novel class of dienes for TPE usage and furthermore represent the trend towards bio-based resources as they are yielded from the renewable resources e.g., turpentine oil or sugar cane.<sup>50–52</sup> The living carbanionic polymerisability of diene monomers is based on the 1,3-conjugated double bond. In the course of the polymerisation reaction, a heterogeneous microstructure is formed and *cis*-1,4-, *trans*-1,4-, 3,4- and 1,2-units are possible, as shown in Figure 8 b).<sup>53</sup> This microstructure is one of the key factors with respect to the properties of polydienes. One main difference between the microstructures is the  $T_g$ , an overview for polyisoprene is given in Table 1.<sup>54–56</sup>

Table 1: Glass transition temperatures of the different isoprene microstructures.

microstructure	$T_g / ^\circ\text{C}$
<i>cis</i> -1,4	-73
<i>trans</i> -1,4	-58
3,4	33
1,2	9

A low  $T_g$  is especially preferred for TPE applications, so the most desired microstructure is the *cis*-1,4 repeating unit.<sup>57</sup> To achieve this, specific parameters must be met during the polymerisation reaction. One of the main factors favouring the *cis*-1,4 microstructure is the solvent. Non-polar solvents like cyclohexane are not able to interact with the living chain ends, leading to a closer ion-pair and therefore allowing the preorganisation of the monomer units.<sup>58</sup> The addition of polar solvents like THF leads to a looser ion-pair and therefore an increased number of 3,4-units. It is noteworthy that the addition of THF also alters the reactivity ratio during the statistical copolymerisation of styrene and isoprene depending on the [THF]/[Li] ratio, thus allowing the copolymer gradient to be adjusted. Figure 9 shows the influence of the solvent on ion-pairs, as described by the Fouss-Winstein spectrum of anion pair interaction.<sup>16,59–62</sup>

Figure 9: Fouss-Winstein spectrum of solvent dependent anion pair interaction.<sup>59</sup>

The widely used alkyl lithium initiators already fulfil the other main requirement: Lithium as counterion. The use of sodium or potassium alters the compositions towards a higher *trans*-1,4 and 3,4 content.<sup>63,64</sup> In contrast to the bigger sodium or potassium counterion, the C-Li coordination complex allows the preorganisation of the monomer unit prior to the addition reaction, as shown in Figure 10.

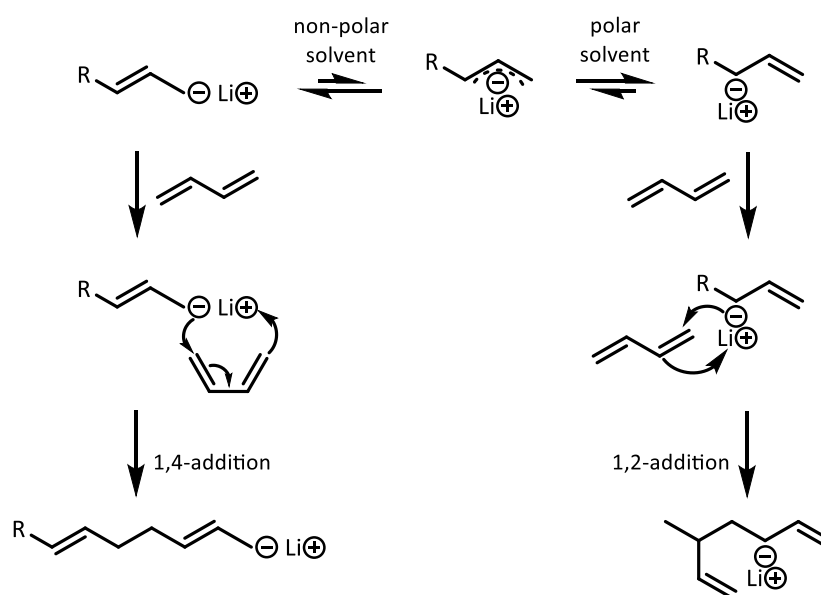


Figure 10: Solvent-dependent preorganisation of butadiene monomers during the living anionic polymerisation.

During the propagation step, a six membered ring structure is formed due to the close C-Li association, resulting in the 1,4-addition of the monomer.<sup>65,66</sup> In summary, the standard reaction conditions chosen for the synthesis of high *cis*-1,4 polyisoprene are non-polar solvents such as cyclohexane and alkyl lithium initiators like *sec*-butyllithium. The microstructure not only influences the  $T_g$  but also alters the aging of the material properties. The dangling double bond of the 1,2- or 3,4-repetitive unit facilitates side reactions that enhance the aging of the polymer. This thermal-oxidative aging leads to a loss of elastomeric properties due to chain scission and cross-linking.<sup>67</sup> Hydrogenation of the polymer is often used for industrial applications to overcome this limited stability, but this also leads to an elevated  $T_g$ .<sup>68</sup>

In 1966, Geoffrey Holden patented his process for the production of P(S-*b*-I-*b*-S) block copolymers for the Shell Oil Company, thus laying the foundation for the modern synthesis of diene-containing and, in particular, isoprene-containing TPEs.<sup>69</sup> The versatility of these materials is evident in the vast number of industrial applications and academic studies that range from simple shoe soles to highly specific stretchable electronic devices, especially when copolymerised with styrene derivatives and styrene itself as the hard phase.<sup>1,18,70</sup> AB, ABA and (tapered) multiblock copolymers were intensively studied with their respective material properties starting from the fairly



poor performance of diblock copolymers to the impressive mechanical properties of polymers with higher block numbers, as shown in Figure 11. A distinct different behaviour is reported between the diblock copolymers and the corresponding multiblock copolymers with the same molecular weight. The lack of domain bridging leads to a considerably earlier break point, while the multiblock copolymers exhibit an elongation of up to 900%.<sup>23,71–76</sup>

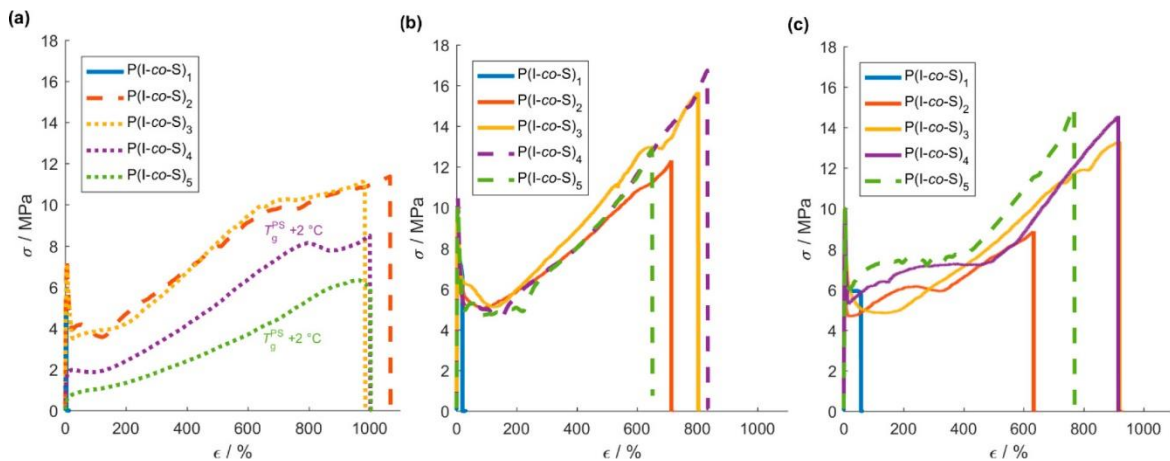


Figure 11: Stress-strain curves of styrene-isoprene block copolymers with varying block numbers and molecular weights (a) 80 kg/mol; b) 240 kg/mol; c) 400 kg/mol), showing the different elasticity between diblock copolymers and those with higher block numbers.<sup>74</sup>

An attempt to push the current limits further, several multigraft copolymers with complex architectures were synthesised and have recently been summarised in a review on superelastomers by Mays et al. in 2017.<sup>77</sup> An overview is given in Figure 12.

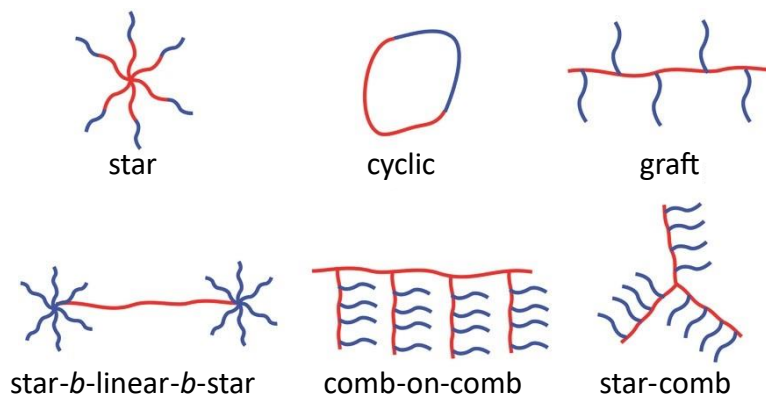


Figure 12: Selection of various complex architectures of block copolymers for the use as superelastomers.<sup>77</sup>

The nonlinear architectures provide a new set of options for further tuning the mechanical properties and introduce additional functionality into the TPEs. In order to synthesise these structures, coupling agents such as chlorosilanes, bifunctional comonomers such as 1,4-bis(phenylethenyl)benzene (PDDPE) or DPE derivatives with functional groups that allow post-polymerisation reactions are used. Compared to commercial Kraton which breaks at 1050% elongation, a tetrafunctional multigraft copolymer with 10 branch points can be elongated up to 2100%.<sup>78</sup> This can be explained by the fact that the PI backbone connects significantly more rigid PS domains compared to linear copolymers. For the same polymer composition, ultimate stress/strain increases linearly with the number of branches as the number of physical cross-links increases. Moreover, a perfectly ordered morphology is not essential for increasing mechanical properties; a high number of branch points compensates for this.

The development in this field demonstrates that it is worthwhile to design new polymers for the application as next-generation high-performance materials. Another approach besides architectural changes to producing isoprene-based TPEs is to completely replace the styrene blocks. Vinylpyridine, in particular, appears to be an attractive comonomer, as it exhibits similar mechanical properties compared to styrene, but due to its polarity shows a chemically different behaviour.

## 5.4 Vinylpyridine

While styrene is one of the most popular monomers used for TPEs, the nitrogen bearing derivative vinylpyridine is less common, yet gives access to polymers with unique properties, as described in the following. Figure 13 shows the three different isomers of vinylpyridine: 2-vinylpyridine (2-VP), 3-vinylpyridine (3-VP) and 4-vinylpyridine (4-VP).

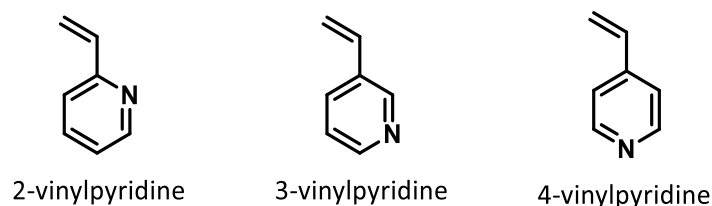


Figure 13: Different isomers of vinylpyridine.

Compared to P(3-VP), P(2-VP) and P(4-VP) as well as the corresponding copolymers are relatively well studied; Szwarcz, among others, published work on the anionic polymerisation of vinylpyridine as early as 1962.<sup>79-86</sup> The latest comprehensive review on polyvinylpyridine (PVP) published by Kennemur in 2019 underlines the versatility of the polymers.<sup>87</sup> 3-VP as monomer is usually left out, which can be addressed to its rather high price. In contrast to styrene, the anionic polymerisation of vinylpyridines usually requires more skill and precisely adjusted reaction conditions due to the increased reactivity and possible side reactions of the monomer.<sup>18</sup> The electron-deficient heterocycle significantly reduces the electron density of the reactive vinyl group, which on the one hand increases the polymerisability, but on the other hand also increases the stability of the living chain end.<sup>88,89</sup> This results in a limitation in the synthesis of block copolymers, which will be discussed in more detail later. The polar character of the pyridine ring limits the solvents during the polymerisation reaction, hydrocarbon solvents such as cyclohexane leads to the precipitation of the polymer during the reaction, therefore, THF commonly is the solvent of choice and reaction temperatures between -78 and -60 °C are necessary.<sup>90</sup> Temperatures higher than that lead to uncontrolled side reactions as the active chain end is able to react with the pyridine ring, as shown in Figure 14, leading to branching and cross-linking.

Due to the two neighbouring carbon atoms, this effect is even more pronounced in the polymerisation of 4-VP.<sup>91</sup>

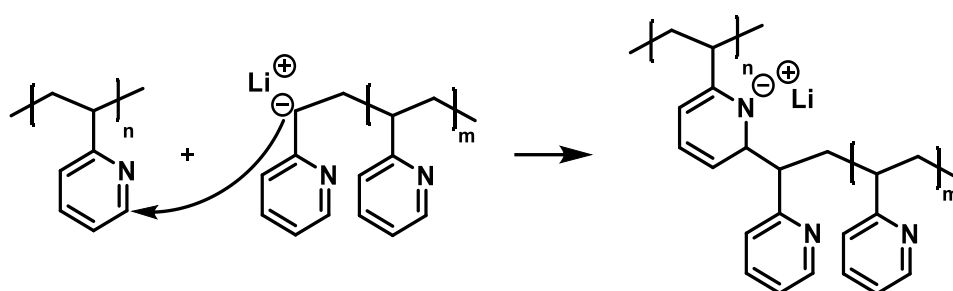


Figure 14: Possible branching and cross-linking side reactions during the polymerisation of 2-VP.

The highly reactive character of vinylpyridine allows its initiation already with comparatively weak bases such as Grignard reagents or enolates.<sup>92</sup> In addition, autopolymerisation of unstabilised vinylpyridines usually starts within one week, even when stored at temperatures around  $-20\text{ }^{\circ}\text{C}$ . This, together with the hygroscopic nature of the monomer, necessitates careful treatment of the monomer prior to the polymerisation. Stabilisers are removed by filtration over basic alumina, water and other protic impurities by stirring over  $\text{CaH}_2$  and if necessary, further drying agents such as trialkylaluminum as well as several distillation and *freeze-pump-thaw* cycles – a process that is comparable to the purification of methacrylates.<sup>93</sup> The propagation reaction proceeds at a comparatively high rate of  $2500 - 3500 \frac{\text{L}}{\text{mol}\cdot\text{s}}$ , depending on the reaction conditions, while the formation of a deep red coloured solution as a result of the  $\pi$ -conjugated anionic chain ends can be observed. Ultimately, PVP can be synthesised with controlled molecular weights and narrow dispersities of 1.1 - 1.2, although it is noteworthy that the estimated molecular weights are about two-thirds lower in SEC measurements compared to PS calibrations, which can be attributed to the reduced hydrodynamic volume of PVP in THF.<sup>9</sup>

The increased stability of the active chain end already mentioned poses particular difficulties in the synthesis of copolymers. In the anionic polymerisation of styrene derivatives, the  $\pi$ -electron density of the vinyl- $\beta$ -carbon directly reflects the reactivities of the monomers and the chemical shift in the  $^{13}\text{C}$  NMR spectrum is a measure thereof.

Table 2 gives an overview over different monomers and their respective shifts in carbon NMR spectroscopy.<sup>94</sup>

Table 2:  $\beta$ -carbon shifts of selected monomers measured via  $^{13}\text{C}$  NMR (a) 400 MHz, b) 15 MHz, c) unknown;  $\text{CDCl}_3$ ) reflect the respective reactivity of different monomers.

monomer	$\beta$ -carbon shift / ppm
styrene	113.93 <sup>a)</sup>
2-VP	118.32 <sup>a)</sup>
4-VP	118.45 <sup>a)</sup>
4-nitrostyrene	118.50 <sup>c)</sup>
methyl methacrylate	125.42 <sup>b)</sup>

The signal of monomers with a lower  $\pi$ -electron density is shifted upfield, which implies that the nucleophilic attack is facilitated, and their reactivity is higher. Conversely, monomers such as 2-VP with a signal shifted downfield, exhibit a lower reactivity for the nucleophilic reaction with the vinyl- $\beta$ -carbon of hydrocarbon monomers. This concept explains the absent cross-over when the reaction starts with 2-VP while the sequential copolymerisation is feasible starting from hydrocarbon monomers, as described in literature.<sup>18</sup>

In view of this, the synthesis pathway for the preparation of copolymers must be well thought out, since hydrocarbon monomers can polymerise vinylpyridine, but this is not possible the other way around. This limitation causes the anionic synthesis of ABA triblock copolymers with vinylpyridine to be challenging, and only possible via detours such as chain coupling or bifunctional initiation.<sup>90,95</sup> With advanced techniques such as difunctional termination or macro terminating agents, the synthesis of star polymers is possible yet also not widely applied.<sup>96,97</sup> For this reason, mainly AB or ABC block copolymers are reported in literature, and although the electron-withdrawing character of the nitrogen atom favours side reactions and limits the possibilities of copolymerisation, it also provides unique properties to the obtained materials. The

nitrogen atom allows a number of post-polymerisation modification possibilities, an overview is given in Figure 15.

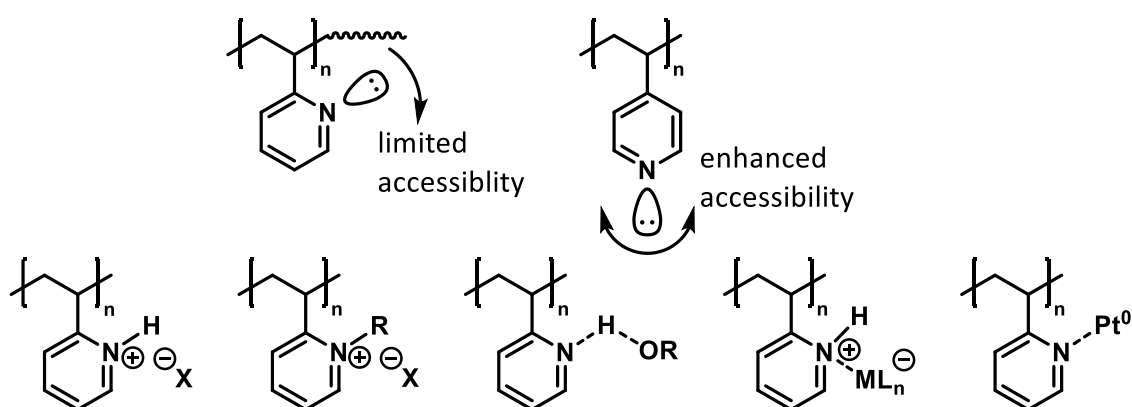


Figure 15: Different accessibility and post-polymerisation modifications of PVP.<sup>87</sup>

The basicity of the pyridinyl side group ( $pK_a = 5.23$ ) facilitates the protonation and thus accounts for its pH-responsive behaviour; PVP becomes water-soluble under acidic conditions.<sup>98</sup> The use of alkyl or aryl halides results in the quaternisation of the nitrogen and thus allows the preparation of polyelectrolyte structures.<sup>99–101</sup> This technique is used for the preparation of block copolymer electrolytes, which are employed in ionic conductors for electrochemical technologies.<sup>102</sup> Alcohols, phenols and other hydrogen bonding compounds also interact with PVP and are readily used for post-polymerisation modification.<sup>103</sup> Depending on the selected reactant, the increase or decrease of the  $\chi$  parameter can be observed, which drastically changes the morphology in copolymers. Targeted introduction also allows the adjustment of the desired microstructure, which is a comparably simple way to obtain complex morphologies such as the gyroid structure.<sup>104–107</sup> Dihalides or bisphenols further exploit this interaction by forming an ionic or hydrogen bond-based network, respectively, as shown in Figure 16.<sup>98,103</sup>

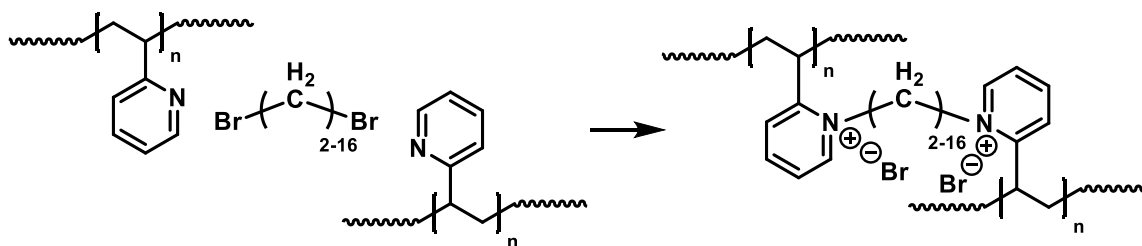


Figure 16: Schematic crosslinking of P(2-VP) with dibromoalkanes comprising from 2 to 16 -CH<sub>2</sub>- units.

It is noteworthy, that there is a distinct difference between the modification of P(2-VP) and P(4-VP), as the nitrogen atom of 4-VP is more exposed. In particular, the efficiency of the modification of P(4-VP) with larger association partners such as metal salts like AuCl<sub>4</sub><sup>-</sup> or Pt<sup>0</sup> nanoparticles is enhanced in comparison to P(2-VP) due to the reduced steric repulsion.<sup>108,109</sup>

For TPE applications, especially block copolymer are of interest. In literature, several reviews topic PVP-containing block copolymers, yet mostly with the aim of loading nanoparticles within the domains. In comparison to PS, P(2-VP) exhibits a similar  $T_g$  of 104 °C for molecular weights above 30 kg/mol but can drop to values around 60 °C for lower molecular weights.<sup>103,110,111</sup> In contrast, the Flory-Huggins parameter significantly differs from that of styrene in PS-*b*-PI copolymers. Currently, no conclusive and reliable values for  $\chi$  can be found in literature, yet the trend  $\chi_{PS-PI} \leq \chi_{P(2-VP)-PS} < \chi_{P(2-VP)-PI}$  is uniformly confirmed and it is expected that  $\chi_{P(2-VP)-PI}$  is at least 1.5 to 3.5 and in some reports even 8 times, higher than  $\chi_{PS-PI}$ . This assumption is supported by the excellent phase separation studied in copolymers and also confirmed in TEM images, as shown in Figure 17 for miktoarm star polymers or manifold reports of linear P(*l*-*b*-S-*b*-2-VP) copolymers found in literature.<sup>112–121</sup>

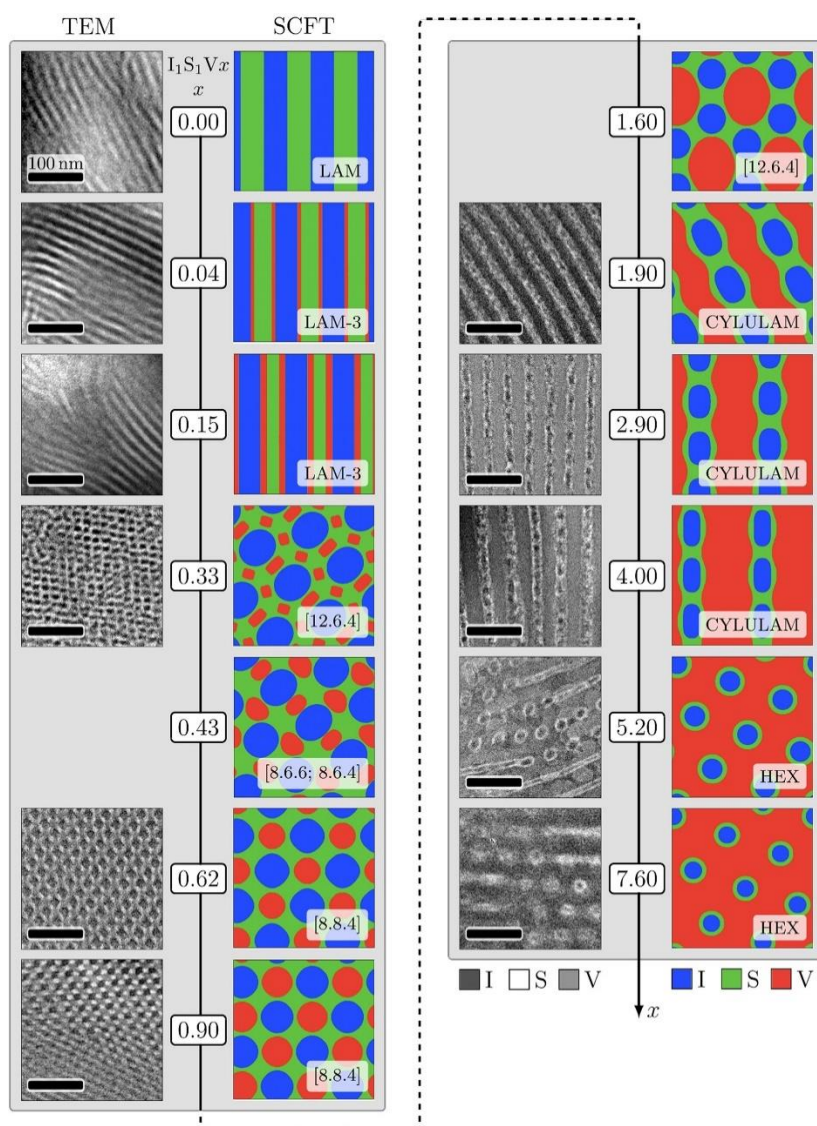


Figure 17: Morphologies of  $P(I-S-2-VP)$  miktoarm star polymers showing excellent phase separation behaviour dependent on the volume fraction of 2-VP.<sup>114</sup>

Several examples for linear  $P(I-b-2-VP)$  block copolymers can be found in literature showing microphase separated polymer films and the successful introduction of palladium nanoparticles into the  $P(2-VP)$  domains.<sup>122–124</sup> Hashimoto et al. studied several polymer films cast from different solvents for a deeper insight into the solvent influence on the microphase-separation of  $P(I-b-2-VP)$ . They report the excellent phase separation behaviour via TEM and SAXS measurements as well as the solvent influence that drastically influences the morphology and spheres, cylinders as well as lamella structures were observed.<sup>125</sup> While this work shows how well films can be made from these polymers and also that the microphase separation of the polymers is as well as expected, no consideration is given to the microstructure of the isoprene block and it



is polymerised in polar solvents. As a result, the fraction of 3,4-isomers predominates and thus no mechanically strainable materials are obtained.

In 1993, Watanabe and Tirrell published the first work on the synthesis of P(I-*b*-2-VP), in which isoprene is polymerised in a first reaction step in the non-polar solvent *n*-heptane. Subsequently, 90% of the *n*-heptane is removed under reduced vacuum and replaced by THF via vacuum distillation to allow the controlled polymerisation of 2-VP at -78 °C. The polymers obtained exhibit narrow dispersities of  $\bar{D} = 1.12 - 1.18$  while the isoprene block consists of 95% 1,4-units.<sup>126</sup> To simplify this relatively complicated procedure, Quirk and Corona-Galvan published a route for the successful synthesis of P(I-*b*-2-VP) in pure hydrocarbon solvents.<sup>127</sup> Using the break-seal technique and lithium chloride as additive to reduce the reactivity of the living 2-VP chain ends by cross-association, isoprene was first polymerised in benzene at 40 – 45 °C. Then, 2-VP was added at 6 – 8 °C and the polymerisation was terminated after only four minutes. The polymers obtained show a very narrow distribution of  $\bar{D} = 1.05 - 1.06$  and 93% 1,4-units. Although the described synthesis is faster in terms of polymerisation time, and does not require a change of solvent, the use of the break-seal technique as well as the extremely short reaction time of 4 minutes is also associated with high synthetic demands.

Overall, the reported characteristics of isoprene-2-VP copolymers demonstrate the potential of 2-VP as a comonomer for the use in TPEs, but so far only AB or ABC block copolymers have been employed and no ABA triblock copolymers with 2-VP as A monomer are reported in the literature as well, which can be ascribed to the demanding nature of their synthesis.<sup>128</sup> To overcome this limitation, bifunctional initiators can be used. However, due to the already described requirements for the living anionic synthesis of isoprene, certain conditions must be met - first and foremost the absence of polar solvents or additives - which will be described in more detail in the following.

## 5.5 Bifunctional Initiators

The general synthesis route for a tri- or multiblock copolymer is described in numerous publications and based on the stepwise addition of the various monomers. If the desired number of blocks is increased, the number of addition steps also increases and thus the risk of introducing impurities which lead to chain termination. Another limitation in the living carbanionic synthesis of block copolymers is the reactivity of the monomers used. As described in chapter 5.4, the crossover from one to another monomer is not possible for some comonomer systems due to strongly different reactivities, making the classical stepwise addition not suitable in all situations. Two prominent examples are shown schematically in Figure 18: The synthesis of block copolymers with hydrocarbon monomers such as styrene or isoprene (blue) and monomers like methacrylate or vinylpyridine (orange).

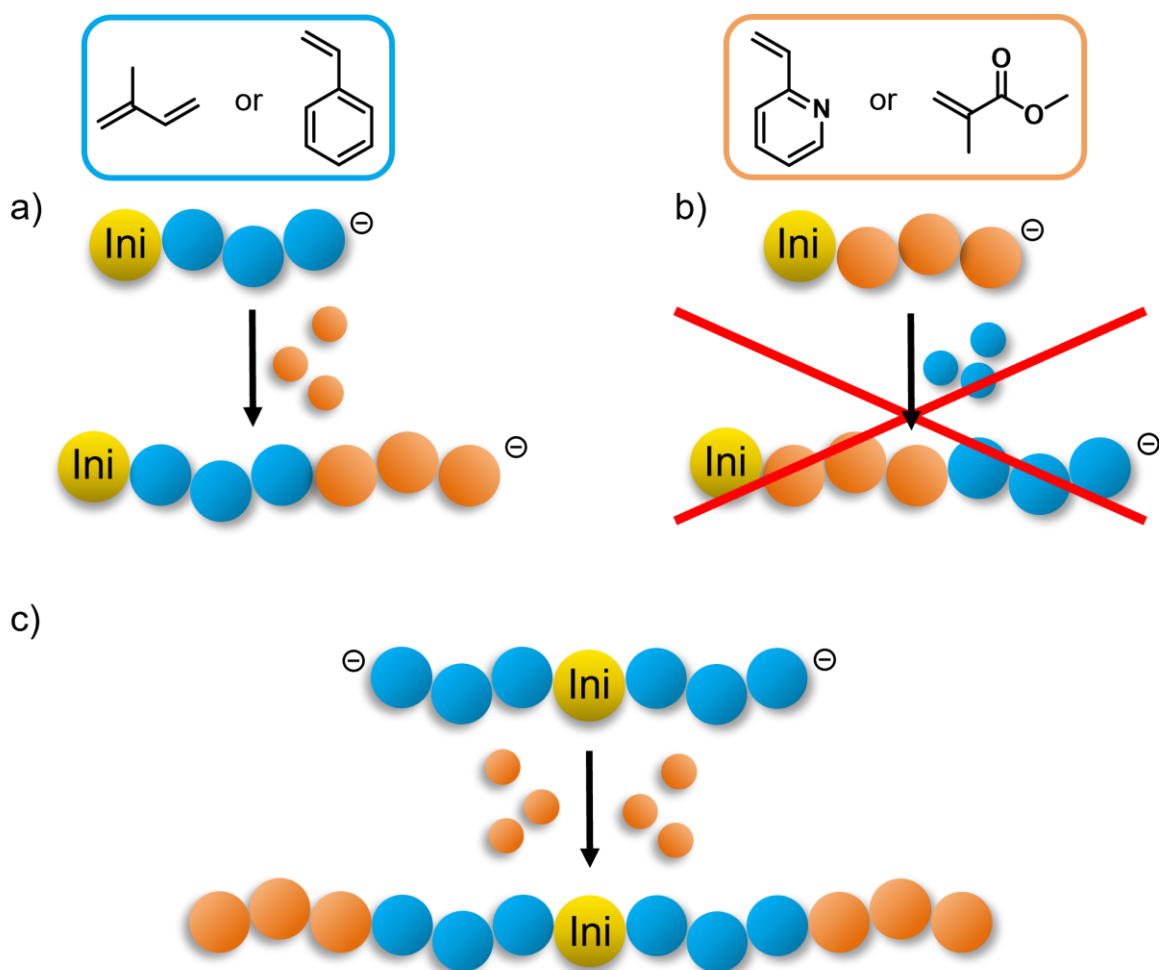


Figure 18: Restricted synthesis of ABA-triblock copolymers (a & b) with non-hydrocarbon outer blocks and circumvention of this limitation with the use of a bifunctional initiator (c).

Starting the synthesis of such ABA triblocks with a monofunctional initiator and the hydrocarbon monomer, the copolymerisation yields only an BA diblock structure while starting with the A monomer will not lead to a block copolymer at all. The use of bifunctional initiators as depicted in Figure 18 c) is an excellent way to circumvent this limitation. Another benefit in favour of the use of bifunctional initiators is the reduction of the required addition steps for the synthesis of multiblock polymers by one, thus reducing the probability of interfering with the polymerisation by impurities.

In the recent decades, many researchers published a variety of different bifunctional initiators, but not all of them are suitable for the anionic polymerisation, especially when it comes to diene polymerisations.<sup>129–131</sup> For example, the well-known potassium-naphthalenide that leads to a radical dimerisation and the formation of two anionic chain ends, is active only in polar solvents.<sup>65</sup> The prevalent requirement to polymerise in non-polar solvents poses the greatest challenge to bi- and multifunctional initiators, as multiple negatively charged molecules tend to aggregate in nonpolar environments, making them ineligible for a homogeneous initiation.<sup>132–136</sup> Various approaches exist to suppress the aggregation and to ensure the solubility and activity in hydrocarbon solvents, which are discussed below using the selected examples from Figure 19.

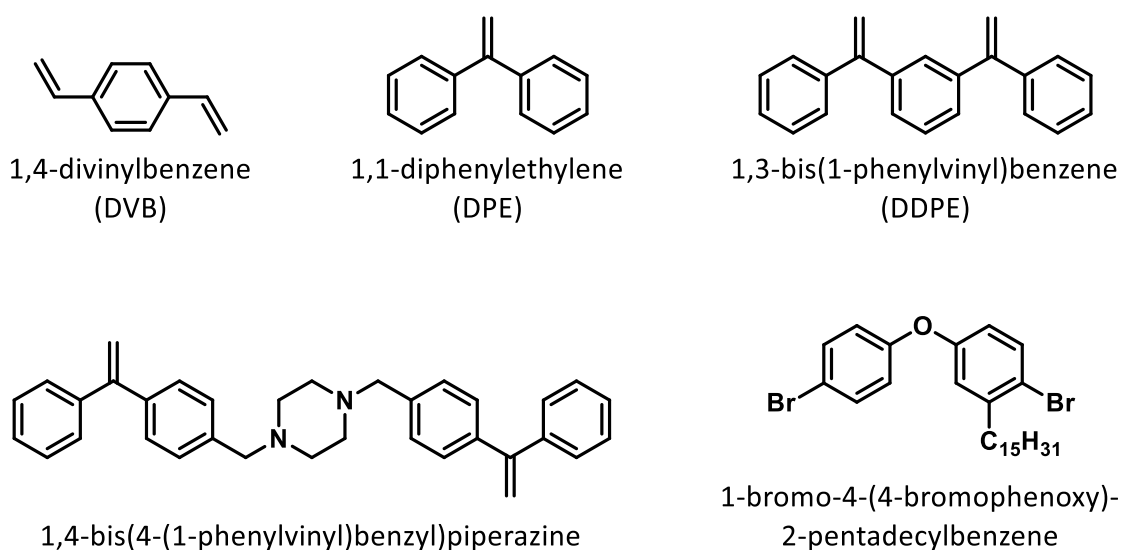


Figure 19: Selection of different bifunctional initiators for the living anionic polymerisation in hydrocarbon solvents.

In general, the activation of bifunctional initiators is always carried out with alkyl lithium compounds, first and foremost *s*-BuLi. During this step, utmost care must be taken to ensure that the stoichiometry is precisely adjusted in order to prevent an excess or shortage of *s*-BuLi. If too much *s*-BuLi is added to the initiator, any remaining *s*-BuLi will start monofunctional chain growth and lead to the formation of di- and triblocks in the product. If not enough *s*-BuLi is used, the initiator is not entirely activated, which also results in monofunctional growth. Depending on the initiator selected, however, chains may also couple or even form a polymer network, since living chain ends react with the free double bond of monofunctionally initiated chains, as depicted in Figure 20.<sup>137</sup>

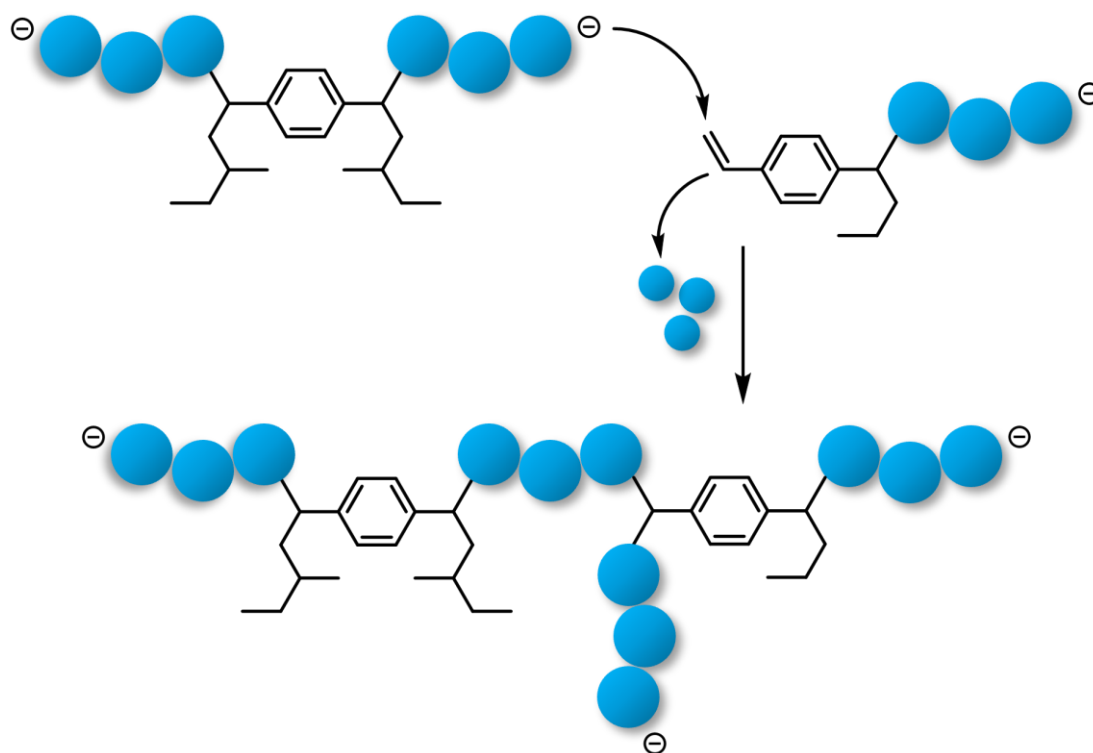


Figure 20: Side reaction of bifunctional initiators exemplified by 1,3-DVB activated with an insufficient amount of *s*-BuLi, resulting in the crosslinking of polymer chains.

One of the earliest examples of bifunctional initiators in non-polar solvents is 1,4-divinylbenzene (DVB), as well as its isomer 1,3-DVB and 1,3- or 1,4-diisopropenylbenzene.<sup>133,138–143</sup> The two vinyl groups readily react with alkyl lithium reagents to form a dianionic species. It is noteworthy, that *t*-BuLi is the activator of choice due to its increased steric demand compared to *s*- or *n*-BuLi, which hampers the

aggregation of the active initiator species, yet it is reported that the association behaviour is still rather strong for this initiator and polar additives are commonly employed.<sup>144</sup> Figure 21 illustrates the dimeric to tetrameric degree of association of dilithiated species based on DFT optimised structures using the example of DVB.<sup>135</sup>

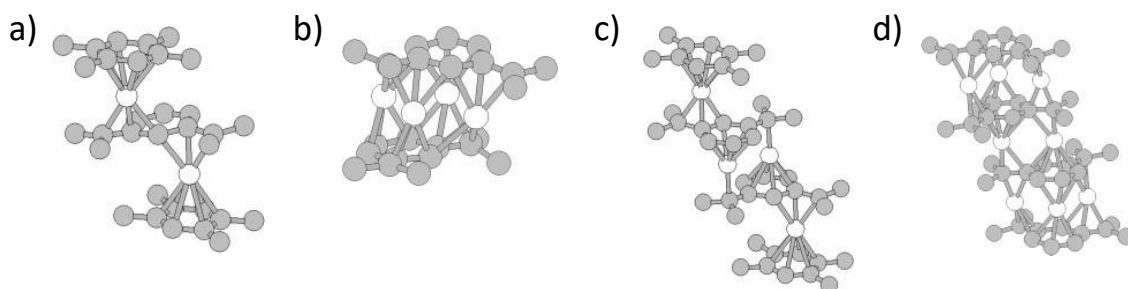


Figure 21: DFT optimised structures of associated DVB-dilithium species. a)  $(\text{Li-DIB-Li})_1(\text{D})_2$ . b)  $(\text{Li-DIB-Li})_2$ . c)  $(\text{Li-DIB-Li})_2(\text{D})_2$ . d)  $(\text{Li-DIB-Li})_4$ .<sup>135</sup>

Due to the small size of DVB, the sterical hindrance that prevents the aggregation of the anionic species is rather low, which also lowers the solubility. Consequently, an attempt was made to increase the size and sterical hindrance which led to DPE and DDPE.

DPE is activated in cyclohexane, with 15 vol% anisole as polar additive and elemental lithium in a dimerisation reaction. Although the active initiator is soluble in this mixture, the process is rather cumbersome as the lithium must be removed by filtration and the concentration must be determined by Gilman double titration before each reaction. The lithium concentration achieved was found to vary between 0.01 and  $0.08 \frac{\text{mmol}}{\text{mL}}$ . Another disadvantage is that the active initiator precipitates upon addition to the actual reaction solution, therefore the *seeding technique* must be used. With this technique, a short isoprenyl or  $\alpha$ -methylstyryl dilithium prepolymer ( $M_n \approx 2000 - 10000 \frac{\text{g}}{\text{mol}}$ ) is formed in a first step, which remains dissolved in the reaction solution and starts the actual polymerisation to ensure a uniform and controlled initiation step for the main polymerisation reaction.<sup>145</sup> It is necessary to mention, that the seeding technique broadens the middle block dispersity, but in most cases this has little effect as long as the molecular weight of the polymer is significantly higher than that of the isoprenyl dilithium precursor.<sup>146</sup>

DDPE (sometimes referred to as *m*-DDPE, MDDPE or PEB) and its *ortho* and *para* derivatives are activated rapidly upon the addition of 2 eq. *s*-BuLi and active in non-polar solvents such as toluene or cyclohexane. The use of DDPE as a bifunctional initiator in nonpolar solvent was first published by Tung et al. in 1978, but DDPE itself as well as a vast number of derivatives have subsequently been studied extensively and efficiently used for the synthesis of various copolymers.<sup>147–159</sup> Several reports on the synthesis of complex polymer architectures, such as star polymers, use DDPE also as coupling agent, as it is also an efficient chain coupling reagent. Therefore, when using DDPE, the exact stoichiometry is even more important than for 1,3-DVB.<sup>160–164</sup> Although in some cases polar additives are added during the activation step, DDPE is reported to produce very well defined polymers even without these.<sup>165</sup> The synthesis of DDPE is possible via two different routes: either by means of a Wittig reaction starting from 1,3-dibenzoylbenzene and methyltriphenylphosphonium bromide, or by means of a Grignard reaction between 1,3-dibenzoylbenzene and methylmagnesium iodide and the subsequent dehydration of the intermediate tertiary alcohol. Both routes require intensive work-up, but the Grignard route avoids the well-known problem of a Wittig reaction, namely the difficult removal of triphenylphosphonium oxide. It is therefore preferable since residues of the polar TPPO can interfere with the living chain end.<sup>155,166,167</sup> The solubility of various derivatives is summarised in a comprehensive review by Bandermann et al. and is based on the steric demand of the bulky phenyl groups, which hinder the aggregation.<sup>168</sup> With respect to the solubility, DDPE is superior to its derivatives with larger alky spacers between the reactive sites and even though the cross-over to the monomer units is reported to be slightly slower, the synthetic effort of the derivatives makes DDPE the initiator of choice for an universal approach of use.

Another possibility to increase the solubility of the active species is the incorporation of intramolecular polar groups, as shown by Long et al. and their reported piperazine-based initiator.<sup>169</sup> The major advantage of such structures is the coordination of the lithium cation by the polar groups within the molecule, which are spatially close to the active site and favour the ion dissociation. This suppresses the

aggregation of the active initiator, but poses no problem during the propagation, since an interaction with the chain end, which becomes more and more distant in the course of the reaction, does not take place. Activation of the initiator was monitored by in situ FTIR analysis and full conversion was achieved after 3 hours. The subsequent addition of isoprene led to the formation of very well defined, monomodal distributed polymer samples with dispersities between 1.06 and 1.09 and molecular weights between 35 and 150  $\frac{\text{kg}}{\text{mol}}$  while 90% 1,4-units were yielded. The synthesis of ABA triblock copolymers with styrene outer blocks also achieved very good results, demonstrating the efficiency of this initiator. Despite the good results, there are no reports found in literature on the use of this initiator, which may be attributed to its rather laborious synthesis.

Gnanou et al. published 1-bromo-4-(4-bromophenoxy)-2-pentadecylbenzene, an initiator similar to the piperazine-based initiator, bearing a polar intramolecular ether group, which has a positive effect on its solubility. In addition, one of the two phenyl rings carries a C<sub>15</sub> alkyl anchor, which prevents the active initiator from precipitating and instead only causes gelation of the initiator solution.<sup>170</sup> In contrast to the initiators discussed so far, the activation in this case has the peculiarity that no addition to double bonds takes place but a lithium-halogen exchange, as shown in Figure 22.

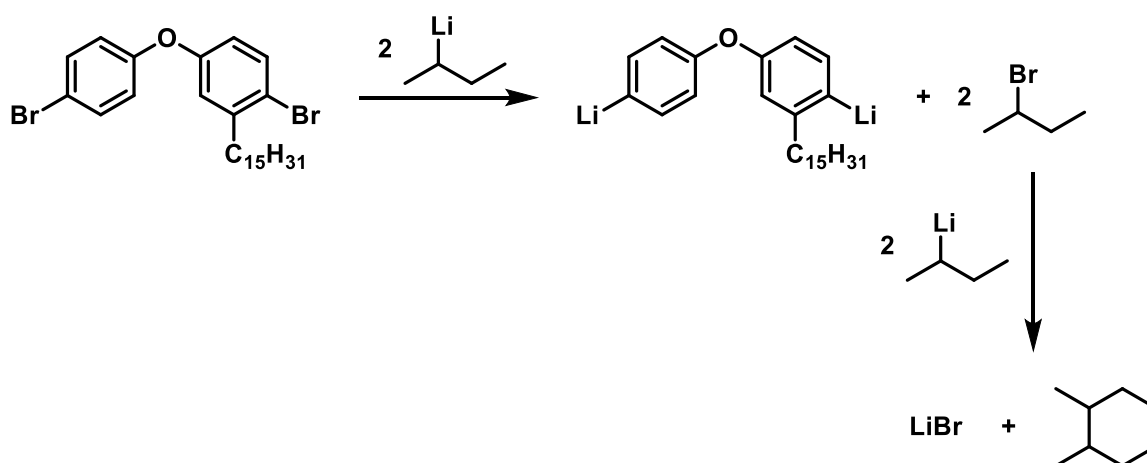


Figure 22: Activation of 1-bromo-4-(4-bromophenoxy)-2-pentadecylbenzene with 2 eq. *s*-BuLi and the subsequent deactivation of the formed 2-bromobutane with another 2 eq. *s*-BuLi to yield 3,4-dimethylhexane and LiBr.

It should be noted that for this initiator a total of 4 eq. *s*-BuLi must be used to convert the 2-bromobutane formed during activation to the inert 3,4-dimethylhexane, which would otherwise react with the living chain ends during polymerisation and thus terminate the polymerisation. The LiBr that is also formed during this reaction does not interfere with the polymerisation, since it precipitates in non-polar solvents. The active initiator species has proven to be efficient for the synthesis of homopolymers and ABA triblock copolymers consisting of styrene and isoprene or butadiene with narrow and monomodal distributions between 1.07 and 1.20 and molecular weights of 2100 - 110900  $\frac{\text{kg}}{\text{mol}}$  while 85 to 91% 1,4-units were obtained. The initiator synthesis starts with 3-pentadecyl phenol, obtained from cashew nut shell liquid as a by-product of agro industry, which reacts with bromobenzene to form 1-pentadecyl-3-phenoxybenzene that is subsequently brominated. The comparatively inexpensive chemicals, as well as the renewable resource 3-pentadecylphenol and the straightforward synthesis route make this initiator particularly interesting.

In summary, all bifunctional initiators differ slightly in their reaction behaviour, so the nature of the intended synthesis must also be considered for a final choice. It must be underlined that for such systems even greater attention must be paid to a correct, preparative working procedure than for the monofunctional living carbanionic polymerisation. Since DDPE and CNI in particular have proven to be comparatively universal with a decent solubility in non-polar solvents, an attempt was made to establish a general working protocol for the broad use of these initiators, which will be discussed in detail in Chapter 3.



## 5.6 References

- (1) Knoll, K.; Nießner, N. Styrolux + and styroflex + - from transparent high impact polystyrene to new thermoplastic elastomers: Syntheses, applications and blends with other styrene based polymers. *Macromol. Symp.* **1998**, *132* (1), 231–243. DOI: 10.1002/masy.19981320122.
- (2) *History 1960s- Kraton Corporation*. <https://kraton.com/company/1960s.php> (accessed 2021-04-15).
- (3) Szwarc, M. 'Living' Polymers. *Nature* **1956**, *178* (4543), 1168–1169. DOI: 10.1038/1781168a0.
- (4) Frey, H.; Johann, T. Celebrating 100 years of "polymer science": Hermann Staudinger's 1920 manifesto. *Polym. Chem.* **2020**, *11* (1), 8–14. DOI: 10.1039/C9PY90161B.
- (5) Staudinger, H. Über Polymerisation. *Ber. dtsh. Chem. Ges. A/B* **1920**, *53* (6), 1073–1085. DOI: 10.1002/cber.19200530627.
- (6) PlasticsEurope. Production of plastics worldwide from 1950 to 2019 (in million metric tons). *Statista* **2021**.
- (7) Koltzenburg, S.; Maskos, M.; Nuyken, O. *Polymere: Synthese, Eigenschaften und Anwendungen*; Springer Berlin Heidelberg, 2014. DOI: 10.1007/978-3-642-34773-3.
- (8) Theato, P.; Klok, H.-A. *Functional polymers by post-polymerization modification: Concepts, guidelines, and applications*; Wiley-VCH, 2013.
- (9) Müller, A. H. E.; Matyjaszewski, K. *Controlled and living polymerizations: Methods and materials*; Wiley-VCH, 2009.
- (10) Tiedemann, P. von; Blankenburg, J.; Maciol, K.; Johann, T.; Müller, A. H. E.; Frey, H. Copolymerization of Isoprene with p-Alkylstyrene Monomers: Disparate Reactivity Ratios and the Shape of the Gradient. *Macromolecules* **2019**, *52* (3), 796–806. DOI: 10.1021/acs.macromol.8b02280.
- (11) Grune, E.; Johann, T.; Appold, M.; Wahlen, C.; Blankenburg, J.; Leibig, D.; Müller, A. H. E.; Gallei, M.; Frey, H. One-Step Block Copolymer Synthesis versus Sequential Monomer Addition: A Fundamental Study Reveals That One Methyl Group Makes a Difference. *Macromolecules* **2018**, *51* (9), 3527–3537. DOI: 10.1021/acs.macromol.8b00404.
- (12) Hirao, A.; Loykulnant, S.; Ishizone, T. Recent advance in living anionic polymerization of functionalized styrene derivatives. *Progress in Polymer Science* **2002**, *27* (8), 1399–1471. DOI: 10.1016/S0079-6700(02)00016-3.
- (13) Kuzma, L. J. Polybutadiene and Polyisoprene Rubbers. In *Rubber Technology*, Third edition; Morton, M., Ed.; Springer US, 1987; pp 235–259. DOI: 10.1007/978-1-4615-7823-9\_8.
- (14) Morton, M., Ed. *Rubber Technology*, Third edition; Springer US, 1987. DOI: 10.1007/978-1-4615-7823-9.
- (15) Morton, M.; Ells, F. R. Absolute rates in anionic copolymerization. *J. Polym. Sci.* **1962**, *61* (171), 25–29. DOI: 10.1002/pol.1962.1206117105.
- (16) Steube, M.; Johann, T.; Hübner, H.; Koch, M.; Dinh, T.; Gallei, M.; Floudas, G.; Frey, H.; Müller, A. H. E. Tetrahydrofuran: More than a "Randomizer" in the Living Anionic Copolymerization of

Styrene and Isoprene: Kinetics, Microstructures, Morphologies, and Mechanical Properties. *Macromolecules* **2020**, *53* (13), 5512–5527. DOI: 10.1021/acs.macromol.0c01022.

(17) Galanos, E.; Grune, E.; Wahlen, C.; Müller, A. H. E.; Appold, M.; Gallei, M.; Frey, H.; Floudas, G. Tapered Multiblock Copolymers Based on Isoprene and 4-Methylstyrene: Influence of the Tapered Interface on the Self-Assembly and Thermomechanical Properties. *Macromolecules* **2019**, *52* (4), 1577–1588. DOI: 10.1021/acs.macromol.8b02669.

(18) Hadjichristidis, N.; Hirao, A. *Anionic Polymerization*; Springer Japan, 2015. DOI: 10.1007/978-4-431-54186-8.

(19) Polymeropoulos, G.; Zapsas, G.; Ntetsikas, K.; Bilalis, P.; Gnanou, Y.; Hadjichristidis, N. 50th Anniversary Perspective : Polymers with Complex Architectures. *Macromolecules* **2017**, *50* (4), 1253–1290. DOI: 10.1021/acs.macromol.6b02569.

(20) Beginn, U. Gradient copolymers. *Colloid Polym Sci* **2008**, *286* (13), 1465–1474. DOI: 10.1007/s00396-008-1922-y.

(21) Bates, C. M.; Bates, F. S. 50th Anniversary Perspective : Block Polymers—Pure Potential. *Macromolecules* **2017**, *50* (1), 3–22. DOI: 10.1021/acs.macromol.6b02355.

(22) Honeker, C. C.; Thomas, E. L. Impact of Morphological Orientation in Determining Mechanical Properties in Triblock Copolymer Systems. *Chem. Mater.* **1996**, *8* (8), 1702–1714. DOI: 10.1021/cm960146q.

(23) Staudinger, U.; Satapathy, B. K.; Thunga, M.; Weidisch, R.; Janke, A.; Knoll, K. Enhancement of mechanical properties of triblock copolymers by random copolymer middle blocks. *European Polymer Journal* **2007**, *43* (6), 2750–2758. DOI: 10.1016/j.eurpolymj.2007.03.022.

(24) Gold, V., Ed. *The IUPAC Compendium of Chemical Terminology*; International Union of Pure and Applied Chemistry (IUPAC), 2019. DOI: 10.1351/goldbook.

(25) Gumboldt, A. Kautschuk nach Maß. *Chemie in unserer Zeit* **1967**, *1* (2), 41–48. DOI: 10.1002/ciuz.19670010203.

(26) Charles Goodyear. Improvement in India-Rubber Fabrics. Patent US3462A.

(27) Robert William Thomson. Improvement in Carriage-Wheels. Patent US5104A.

(28) Matthwes, F. E.; Strange, E. H. Improvements in the Manufacture of Synthetic Caotchouc and the like. Patent GB191024790A.

(29) Requardt, A. Buna - Geburt einer Marke. *Nachr. Chem.* **2016**, *64* (2), 150–153. DOI: 10.1002/nadc.20164046024.

(30) Bock, W.; Wschunkur, E. Verfahren zur Herstellung von kautschukartigen Mischpolymerisaten. Patent DE750980C.

(31) Bhowmick, A. K.; Stephens, H. L., Eds. *Handbook of elastomers*, 2nd ed., rev. and expanded.; Plastics engineering, Vol. 61; Marcel Dekker, 2001.

(32) Banerjee, S. S.; Bhowmick, A. K. High-Temperature Thermoplastic Elastomers Fom Rubber–Plastic Blends: A State-Of-The-Art Review. *Rubber Chemistry and Technology* **2017**, *90* (1), 1–36. DOI: 10.5254/rct.16.83786.

- (33) Legge, N. R. Thermoplastic Elastomers—Three Decades of Progress. *Rubber Chemistry and Technology* **1989**, *62* (3), 529–547. DOI: 10.5254/1.3536257.
- (34) Spontak, R. J.; Patel, N. P. Thermoplastic elastomers: fundamentals and applications. *Current Opinion in Colloid & Interface Science* **2000**, *5* (5-6), 333–340. DOI: 10.1016/S1359-0294(00)00070-4.
- (35) Seymour, R. B.; Kauffman, G. B. Elastomers: III. Thermoplastic elastomers. *J. Chem. Educ.* **1992**, *69* (12), 967. DOI: 10.1021/ed069p967.
- (36) Leibler, L. Theory of Microphase Separation in Block Copolymers. *Macromolecules* **1980**, *13* (6), 1602–1617. DOI: 10.1021/ma60078a047.
- (37) Hiemenz, P. C. *Polymer chemistry*, 2. ed.; CRC Press, 2007.
- (38) Bates, F. S.; Fredrickson, G. H. Block Copolymers—Designer Soft Materials. *Physics Today* **1999**, *52* (2), 32–38. DOI: 10.1063/1.882522.
- (39) Förster, S.; Antonietti, M. Amphiphilic Block Copolymers in Structure-Controlled Nanomaterial Hybrids. *Adv. Mater.* **1998**, *10* (3), 195–217. DOI: 10.1002/(SICI)1521-4095(199802)10:3<195:AID-ADMA195>3.0.CO;2-V.
- (40) Matsen, M. W.; Schick, M. Self-assembly of block copolymers. *Current Opinion in Colloid & Interface Science* **1996**, *1* (3), 329–336. DOI: 10.1016/S1359-0294(96)80128-2.
- (41) Feng, H.; Lu, X.; Wang, W.; Kang, N.-G.; Mays, J. W. Block Copolymers: Synthesis, Self-Assembly, and Applications. *Polymers* **2017**, *9* (10). DOI: 10.3390/polym9100494. Published Online: Oct. 9, 2017.
- (42) Fredrickson, G. H.; Bates, F. S. Dynamics of Block Copolymers: Theory and Experiment. *Annu. Rev. Mater. Sci.* **1996**, *26* (1), 501–550. DOI: 10.1146/annurev.ms.26.080196.002441.
- (43) Storey, R. F.; Chisholm, B. J.; Choate, K. R. Synthesis and Characterization of PS-PIB-PS Triblock Copolymers. *Journal of Macromolecular Science, Part A* **1994**, *31* (8), 969–987. DOI: 10.1080/10601329409349773.
- (44) Matsen, M. W. Effect of Architecture on the Phase Behavior of AB-Type Block Copolymer Melts. *Macromolecules* **2012**, *45* (4), 2161–2165. DOI: 10.1021/ma202782s.
- (45) Zhulina, E. B.; Halperin, A. Lamellar mesogels and mesophases: a self-consistent-field theory. *Macromolecules* **1992**, *25* (21), 5730–5741. DOI: 10.1021/ma00047a026.
- (46) Thunga, M.; Staudinger, U.; Ganß, M.; Weidisch, R.; Knoll, K. Influence of Molecular Weight on Physical and Mechanical Properties of Linear Symmetric S-(S/B)-S Triblock Copolymers. *Macromol. Chem. Phys.* **2008**, NA-NA. DOI: 10.1002/macp.200800440.
- (47) Eastwood, E. A.; Dadmun, M. D. Multiblock Copolymers in the Compatibilization of Polystyrene and Poly(methyl methacrylate) Blends: Role of Polymer Architecture. *Macromolecules* **2002**, *35* (13), 5069–5077. DOI: 10.1021/ma011701z.
- (48) Wang, W.; Lu, W.; Goodwin, A.; Wang, H.; Yin, P.; Kang, N.-G.; Hong, K.; Mays, J. W. Recent advances in thermoplastic elastomers from living polymerizations: Macromolecular architectures and supramolecular chemistry. *Progress in Polymer Science* **2019**, *95*, 1–31. DOI: 10.1016/j.progpolymsci.2019.04.002.

- (49) Sarkar, P.; Bhowmick, A. K. Sustainable rubbers and rubber additives. *J. Appl. Polym. Sci.* **2018**, *135* (24), 45701. DOI: 10.1002/app.45701.
- (50) Tang, C.; Ryu, C. Y., Eds. *Sustainable Polymers from Biomass*; John Wiley & Sons, Incorporated, 2017.
- (51) Behr, A.; Johnen, L. Myrcene as a natural base chemical in sustainable chemistry: a critical review. *ChemSusChem* **2009**, *2* (12), 1072–1095. DOI: 10.1002/cssc.200900186.
- (52) Benjamin, K. R.; Silva, I. R.; Cherubim, J. P.; McPhee, D.; Paddon, C. J. Developing Commercial Production of Semi-Synthetic Artemisinin, and of  $\beta$ -Farnesene, an Isoprenoid Produced by Fermentation of Brazilian Sugar. *Journal of the Brazilian Chemical Society* **2016**. DOI: 10.5935/0103-5053.20160119.
- (53) Worsfold, D. J.; Bywater, S. Anionic Polymerization Of Isoprene. *Can. J. Chem.* **1964**, *42* (12), 2884–2892. DOI: 10.1139/v64-426.
- (54) Mark, J. E. *Physical Properties of Polymers Handbook*, 2. ed.; Springer Science+Business Media, LLC; Springer e-books, 2007. DOI: 10.1007/978-0-387-69002-5.
- (55) Burfield, D. R. Polymer glass transition temperatures. *J. Chem. Educ.* **1987**, *64* (10), 875. DOI: 10.1021/ed064p875.
- (56) Widmaier, J. M.; Meyer, G. C. Glass Transition Temperature of Anionic Polyisoprene. *Rubber Chemistry and Technology* **1981**, *54* (5), 940–943. DOI: 10.5254/1.3535854.
- (57) Stavely, F. W.; Coworkers. Coral Rubber—A Cis -1,4-Polyisoprene. *Rubber Chemistry and Technology* **1956**, *29* (3), 673–686. DOI: 10.5254/1.3542582.
- (58) Margl, P. Mechanisms for anionic butadiene polymerization with alkyl lithium species. *Can. J. Chem.* **2009**, *87* (7), 891–903. DOI: 10.1139/V09-032.
- (59) Matyjaszewski, E.; Muller, E. H. E. *Controlled and Living Polymerizations: From Mechanisms to Applications*; John Wiley & Sons, 2009. DOI: 10.1002/9783527629091.
- (60) Fuoss, R. M. Ionic Association. III. The Equilibrium between Ion Pairs and Free Ions. *J. Am. Chem. Soc.* **1958**, *80* (19), 5059–5061. DOI: 10.1021/ja01552a016.
- (61) Winstein, S.; Clippinger, E.; Fainberg, A. H.; Heck, R.; Robinson, G. C. Salt Effects and Ion Pairs in Solvolysis and Related Reactions. III. 1 Common Ion Rate Depression and Exchange of Anions during Acetolysis 2,3. *J. Am. Chem. Soc.* **1956**, *78* (2), 328–335. DOI: 10.1021/ja01583a022.
- (62) Fumino, K.; Stange, P.; Fossog, V.; Hempelmann, R.; Ludwig, R. Gleichgewicht zwischen Kontakt- und solvensseparierten Ionenpaaren in Mischungen von protischen ionischen Flüssigkeiten und molekularen Lösungsmitteln durch Polarität kontrolliert. *Angew. Chem.* **2013**, *125* (47), 12667–12670. DOI: 10.1002/ange.201303944.
- (63) Stearns, R. S.; Forman, L. E. The stereoregular polymerization of isoprene with lithium and organolithium compounds. *J. Polym. Sci.* **1959**, *41* (138), 381–397. DOI: 10.1002/pol.1959.1204113832.
- (64) Tobolsky, A. V.; Rogers, C. E. Isoprene polymerization by organometallic compounds. II. *J. Polym. Sci.* **1959**, *40* (136), 73–89. DOI: 10.1002/pol.1959.1204013605.

- (65) Hsieh, H. L.; Quirk, R. P. *Anionic Polymerization: Principles and Practical Applications*; Plastics Engineering Ser, v. 34; Chapman and Hall/CRC, 1996.
- (66) Szwarc, M. Living polymers and mechanisms of anionic polymerization. In *Living polymers and mechanisms of anionic polymerization*; Szwarc, M., Ed.; Advances in polymer science (Print), Vol. 49; Springer-Vlg, 1983; pp 1–177. DOI: 10.1007/3-540-12047-5\_1.
- (67) Hamed, G. R.; Zhao, J. Tensile Behavior after Oxidative Aging of Gum and Black-Filled Vulcanizates of SBR and NR. *Rubber Chemistry and Technology* **1999**, *72* (4), 721–730. DOI: 10.5254/1.3538829.
- (68) Gotro, J. T.; Graessley, W. W. Model hydrocarbon polymers: rheological properties of linear polyisoprenes and hydrogenated polyisoprenes. *Macromolecules* **1984**, *17* (12), 2767–2775. DOI: 10.1021/ma00142a058.
- (69) Holden, G.; Milkovich, R. *Process for the preparation of block copolymers*, 1966.
- (70) You, I.; Kong, M.; Jeong, U. Block Copolymer Elastomers for Stretchable Electronics. *Accounts of chemical research* **2019**, *52* (1), 63–72. DOI: 10.1021/acs.accounts.8b00488. Published Online: Dec. 26, 2018.
- (71) Chuangchote, S.; Sirivat, A.; Supaphol, P. Electrospinning of Styrene-Isoprene Copolymeric Thermoplastic Elastomers. *Polym J* **2006**, *38* (9), 961–969. DOI: 10.1295/polymj.PJ2005234.
- (72) Cunningham, R. E.; Treiber, M. R. Preparation and stress–strain properties of ABA-type block polymers of styrene and isoprene or butadiene. *J. Appl. Polym. Sci.* **1968**, *12* (1), 23–34. DOI: 10.1002/app.1968.070120104.
- (73) Zelinski, R.; Childers, C. W. Linear Elastomeric Block Polymers. *Rubber Chemistry and Technology* **1968**, *41* (1), 161–181. DOI: 10.5254/1.3539168.
- (74) Steube, M.; Johann, T.; Galanos, E.; Appold, M.; Rüttiger, C.; Mezger, M.; Gallei, M.; Müller, A. H. E.; Floudas, G.; Frey, H. Isoprene/Styrene Tapered Multiblock Copolymers with up to Ten Blocks: Synthesis, Phase Behavior, Order, and Mechanical Properties. *Macromolecules* **2018**, *51* (24), 10246–10258. DOI: 10.1021/acs.macromol.8b01961.
- (75) Steube, M.; Plank, M.; Gallei, M.; Frey, H.; Floudas, G. Building Bridges by Blending: Morphology and Mechanical Properties of Binary Tapered Diblock/Multiblock Copolymer Blends. *Macromol. Chem. Phys.* **2021**, *222* (4), 2000373. DOI: 10.1002/macp.202000373.
- (76) Morton, M.; McGrath, J. E.; Juliano, P. C. Structure-property relationships for styrene-diene thermoplastic elastomers. *J. polym. sci., C Polym. symp.* **1969**, *26* (1), 99–115. DOI: 10.1002/polc.5070260107.
- (77) Wang, H.; Lu, W.; Wang, W.; Shah, P. N.; Misichronis, K.; Kang, N.-G.; Mays, J. W. Design and Synthesis of Multigraft Copolymer Thermoplastic Elastomers: Superelastomers. *Macromol. Chem. Phys.* **2018**, *219* (1), 1700254. DOI: 10.1002/macp.201700254.
- (78) Weidisch, R.; Gido, S. P.; Uhrig, D.; Iatrou, H.; Mays, J.; Hadjichristidis, N. Tetrafunctional Multigraft Copolymers as Novel Thermoplastic Elastomers. *Macromolecules* **2001**, *34* (18), 6333–6337. DOI: 10.1021/ma001966y.

- (79) Lee, C. L.; Smid, J.; Szwarc, M. Kinetics of anionic polymerization and copolymerization of vinyl pyridines. The penultimate effects. *Trans. Faraday Soc.* **1963**, *59*, 1192. DOI: 10.1039/tf9635901192.
- (80) Hubert, P.; Soum, A.; Fontanille, M. Structure and reactivity of propagating species in anionic polymerization of 2-vinylpyridine initiated by lithium derivatives in toluene. *Macromol. Chem. Phys.* **1995**, *196* (4), 1023–1030. DOI: 10.1002/macp.1995.021960405.
- (81) Matsushita, Y.; Nakao, Y.; Saguchi, R.; Choshi, H.; Nagasawa, M. Studies of Styrene and 2-Vinylpyridine Block Copolymers; Preparation and Characterization. *Polym J* **1986**, *18* (6), 493–499. DOI: 10.1295/polymj.18.493.
- (82) Matsushita, Y.; Shimizu, K.; Nakao, Y.; Choshi, H.; Noda, I.; Nagasawa, M. Preparation and Characterization of Poly(2-vinylpyridine) with Narrow Molecular Weight Distributions. *Polym J* **1986**, *18* (4), 361–366. DOI: 10.1295/polymj.18.361.
- (83) Pratt, L. M.; Khan, I. M.; Hogen-Esch, T. E. Anionic polymerization of 2-vinylpyridine: a computational study of solvent effects on polymerization stereochemistry. *Macromol. Chem. Phys.* **1996**, *197* (11), 3555–3566. DOI: 10.1002/macp.1996.021971106.
- (84) Soum, A.; Fontanille, M.; Sigwalt, P. Anionic polymerization of 2-vinylpyridine initiated by symmetrical organomagnesium compounds in tetrahydrofuran. *J. Polym. Sci. Polym. Chem. Ed.* **1977**, *15* (3), 659–673. DOI: 10.1002/pol.1977.170150313.
- (85) Natalello, A.; Morsbach, J.; Friedel, A.; Alkan, A.; Tonhauser, C.; Müller, A. H. E.; Frey, H. Living Anionic Polymerization in Continuous Flow: Facilitated Synthesis of High-Molecular Weight Poly(2-vinylpyridine) and Polystyrene. *Org. Process Res. Dev.* **2014**, *18* (11), 1408–1412. DOI: 10.1021/op500149t.
- (86) Fragouli, P. G.; Iatrou, H.; Hadjichristidis, N. Synthesis and characterization of linear diblock and triblock copolymers of 2-vinyl pyridine and ethylene oxide. *Polymer* **2002**, *43* (25), 7141–7144. DOI: 10.1016/S0032-3861(02)00455-X.
- (87) Kennemur, J. G. Poly(vinylpyridine) Segments in Block Copolymers: Synthesis, Self-Assembly, and Versatility. *Macromolecules* **2019**, *52* (4), 1354–1370. DOI: 10.1021/acs.macromol.8b01661.
- (88) Schlüter, A.-D.; Hawker, C. J.; Sakamoto, J. *Synthesis of polymers: New structures and methods. Volume 1; Synthesis of polymers, v. 1; Wiley-VCH-Verl., (2012).*
- (89) Hirao, A.; Goseki, R.; Ishizone, T. Advances in Living Anionic Polymerization: From Functional Monomers, Polymerization Systems, to Macromolecular Architectures. *Macromolecules* **2014**, *47* (6), 1883–1905. DOI: 10.1021/ma401175m.
- (90) Watanabe, H.; Shimura, T.; Kotaka, T.; Tirrell, M. Synthesis, characterization, and surface structures of styrene-2-vinylpyridine-butadiene three-block polymers. *Macromolecules* **1993**, *26* (24), 6338–6345. DOI: 10.1021/ma00076a006.
- (91) Luxton, A. R.; Quig, A.; Delvaux, M.-J.; Fetters, L. J. Star-branched polymers: 2. Linking reaction involving 2- and 4-vinyl pyridine and dienyl and styryllithium chain ends. *Polymer* **1978**, *19* (11), 1320–1324. DOI: 10.1016/0032-3861(78)90315-4.
- (92) Soum, A.; Fontanille, M. Living anionic stereospecific polymerization of 2-vinylpyridine. Kinetics of polymerization and nature of active centres. *Makromol. Chem.* **1981**, *182* (6), 1743–1750. DOI: 10.1002/macp.1981.021820615.

- (93) Allen, R. D.; Long, T. E.; McGrath, J. E. Preparation of high purity, anionic polymerization grade alkyl methacrylate monomers. *Polymer Bulletin* **1986**, *15* (2), 127–134. DOI: 10.1007/BF00263389.
- (94) Nakahama, S.; Ishizone, T.; Hirao, A. Anionic living polymerization of styrenes containing electron-withdrawing groups. *Makromolekulare Chemie. Macromolecular Symposia* **1993**, *67* (1), 223–236. DOI: 10.1002/masy.19930670118.
- (95) Masuda, J.; Takano, A.; Nagata, Y.; Noro, A.; Matsushita, Y. Nanophase-separated synchronizing structure with parallel double periodicity from an undecablock terpolymer. *Physical review letters* **2006**, *97* (9), 98301. DOI: 10.1103/PhysRevLett.97.098301. Published Online: Aug. 29, 2006.
- (96) Natalello, A.; Tonhauser, C.; Berger-Nicoletti, E.; Frey, H. A Combined DPE/Epoxyde Termination Strategy for Hydroxyl End-Functional Poly(2-vinylpyridine) and Amphiphilic AB 2 - Miktoarm Stars. *Macromolecules* **2011**, *44* (24), 9887–9890. DOI: 10.1021/ma2023793.
- (97) Kim, H.; Kang, B.-G.; Choi, J.; Sun, Z.; Yu, D. M.; Mays, J.; Russell, T. P. Morphological Behavior of A 2 B Block Copolymers in Thin Films. *Macromolecules* **2018**, *51* (3), 1181–1188. DOI: 10.1021/acs.macromol.7b02601.
- (98) Fréchet, J. M. J.; Meftahi, M. V. de. Poly(vinyl pyridine)s: Simple reactive polymers with multiple applications. *Brit. Poly.J.* **1984**, *16* (4), 193–198. DOI: 10.1002/pi.4980160407.
- (99) Cho, Y.-H.; Yang, J.-E.; Lee, J.-S. Size control of polymeric nanoparticles from polystyrene-b-poly(2-vinylpyridine). *Materials Science and Engineering: C* **2004**, *24* (1-2), 293–295. DOI: 10.1016/j.msec.2003.09.060.
- (100) Fuoss, R. M.; Maclay, W. N. Polyelectrolytes. VI. Viscosities of 4-polyvinylpyridine hydrochloride in methanol at 25°. *J. Polym. Sci.* **1951**, *6* (3), 305–317. DOI: 10.1002/pol.1951.120060306.
- (101) Kee, R. A.; Gauthier, M. Arborescent Polystyrene- graft -poly(2-vinylpyridine) Copolymers: Synthesis and Enhanced Polyelectrolyte Effect in Solution. *Macromolecules* **2002**, *35* (17), 6526–6532. DOI: 10.1021/ma011124e.
- (102) Arges, C. G.; Kambe, Y.; Suh, H. S.; Ocola, L. E.; Nealey, P. F. Perpendicularly Aligned, Anion Conducting Nanochannels in Block Copolymer Electrolyte Films. *Chem. Mater.* **2016**, *28* (5), 1377–1389. DOI: 10.1021/acs.chemmater.5b04452.
- (103) Urakawa, O.; Yasue, A. Glass Transition Behaviors of Poly (Vinyl Pyridine)/Poly (Vinyl Phenol) Revisited. *Polymers* **2019**, *11* (7). DOI: 10.3390/polym11071153. Published Online: Jul. 5, 2019.
- (104) Hofman, A. H.; Terzic, I.; Stuart, M. C. A.; Brinke, G. ten; Loos, K. Hierarchical Self-Assembly of Supramolecular Double-Comb Triblock Terpolymers. *ACS macro letters* **2018**, *7* (10), 1168–1173. DOI: 10.1021/acsmacrolett.8b00570. Published Online: Sep. 13, 2018.
- (105) Lim, H. S.; Lee, J.-H.; Walsh, J. J.; Thomas, E. L. Dynamic swelling of tunable full-color block copolymer photonic gels via counterion exchange. *ACS nano* **2012**, *6* (10), 8933–8939. DOI: 10.1021/nn302949n. Published Online: Oct. 10, 2012.
- (106) Lin, E.-L.; Hsu, W.-L.; Chiang, Y.-W. Trapping Structural Coloration by a Bioinspired Gyroid Microstructure in Solid State. *ACS nano* **2018**, *12* (1), 485–493. DOI: 10.1021/acsnano.7b07017. Published Online: Dec. 20, 2017.

- (107) Ruokolainen; Makinen; Torkkeli; Makela; Serimaa; Brinke; Ikkala. Switching supramolecular polymeric materials with multiple length scales. *Science (New York, N.Y.)* **1998**, *280* (5363), 557–560. DOI: 10.1126/science.280.5363.557.
- (108) Aizawa, M.; Buriak, J. M. Nanoscale patterning of two metals on silicon surfaces using an ABC triblock copolymer template. *J. Am. Chem. Soc.* **2006**, *128* (17), 5877–5886. DOI: 10.1021/ja060366x.
- (109) Mayer, A. B.; Mark, J. E. Colloidal gold nanoparticles protected by water-soluble homopolymers and random copolymers. *European Polymer Journal* **1998**, *34* (1), 103–108. DOI: 10.1016/S0014-3057(97)00074-8.
- (110) Brandrup, J.; Immergut, E. H.; Grulke, E. A., Eds. *Polymer handbook*, 4th ed.; A Wiley-Interscience publication; Wiley, 1999.
- (111) Papadopoulos, P.; Peristeraki, D.; Floudas, G.; Koutalas, G.; Hadjichristidis, N. Origin of Glass Transition of Poly(2-vinylpyridine). A Temperature- and Pressure-Dependent Dielectric Spectroscopy Study. *Macromolecules* **2004**, *37* (21), 8116–8122. DOI: 10.1021/ma048555s.
- (112) Hirschberg, V.; Faust, L.; Rodrigue, D.; Wilhelm, M. Effect of Topology and Molecular Properties on the Rheology and Fatigue Behavior of Solid Polystyrene/Polyisoprene Di- and Triblock Copolymers. *Macromolecules* **2020**, *53* (13), 5572–5587. DOI: 10.1021/acs.macromol.0c00632.
- (113) Dai, K. Determining the temperature-dependent Flory interaction parameter for strongly immiscible polymers from block copolymer segregation measurements. *Polymer* **1994**, *35* (1), 157–161. DOI: 10.1016/0032-3861(94)90065-5.
- (114) Chernyy, S.; Mahalik, J. P.; Kumar, R.; Kirkensgaard, J. J. K.; Arras, M. M. L.; Kim, H.; Schulte, L.; Ndoni, S.; Smith, G. S.; Mortensen, K.; Sumpter, B. G.; Russell, T. P.; Almdal, K. On the morphological behavior of ABC miktoarm stars containing poly(cis 1,4-isoprene), poly(styrene), and poly(2-vinylpyridine). *J. Polym. Sci. Part B: Polym. Phys.* **2018**, *56* (22), 1491–1504. DOI: 10.1002/polb.24733.
- (115) Jiang, K.; Zhang, J.; Liang, Q. Self-Assembly of Asymmetrically Interacting ABC Star Triblock Copolymer Melts. *The journal of physical chemistry. B* **2015**, *119* (45), 14551–14562. DOI: 10.1021/acs.jpcc.5b08187. Published Online: Nov. 2, 2015.
- (116) Zhang, G.; Qiu, F.; Zhang, H.; Yang, Y.; Shi, A.-C. SCFT Study of Tiling Patterns in ABC Star Terpolymers. *Macromolecules* **2010**, *43* (6), 2981–2989. DOI: 10.1021/ma902735t.
- (117) Zioga, A.; Sioula, S.; Hadjichristidis, N. Synthesis and morphology of model 3-miktoarm star terpolymers of styrene, isoprene and 2-vinyl pyridine. *Macromol. Symp.* **2000**, *157* (1), 239–250. DOI: 10.1002/1521-3900(200007)157:1<239:AID-MASY239>3.0.CO;2-I.
- (118) Asai, Y.; Takano, A.; Matsushita, Y. Asymmetric Double Tetragonal Domain Packing from ABC Triblock Terpolymer Blends with Chain Length Difference. *Macromolecules* **2016**, *49* (18), 6940–6946. DOI: 10.1021/acs.macromol.6b01670.
- (119) Mogi, Y.; Kotsuji, H.; Kaneko, Y.; Mori, K.; Matsushita, Y.; Noda, I. Preparation and morphology of triblock copolymers of the ABC type. *Macromolecules* **1992**, *25* (20), 5408–5411. DOI: 10.1021/ma00046a043.



- (120) Asai, Y.; Takano, A.; Matsushita, Y. Creation of Cylindrical Morphologies with Extremely Large Oblong Unit Lattices from ABC Block Terpolymer Blends. *Macromolecules* **2015**, *48* (5), 1538–1542. DOI: 10.1021/ma5025818.
- (121) Asai, Y.; Yamada, K.; Yamada, M.; Takano, A.; Matsushita, Y. Formation of Tetragonally-Packed Rectangular Cylinders from ABC Block Terpolymer Blends. *ACS macro letters* **2014**, *3* (2), 166–169. DOI: 10.1021/mz400647v.
- (122) Tsutsumi, K.; Funaki, Y.; Hirokawa, Y.; Hashimoto, T. Selective Incorporation of Palladium Nanoparticles into Microphase-Separated Domains of Poly(2-vinylpyridine)- block -polyisoprene. *Langmuir* **1999**, *15* (16), 5200–5203. DOI: 10.1021/la990246l.
- (123) Hashimoto, T.; Okumura, A.; Tanabe, D. Visualization of Isolated Poly(2-vinylpyridine)- block -Polyisoprene Chains Adhered to Isolated Palladium Nanoparticles †. *Macromolecules* **2003**, *36* (19), 7324–7330. DOI: 10.1021/ma034471s.
- (124) Akasaka, S.; Mori, H.; Osaka, T.; Mareau, V. H.; Hasegawa, H. Controlled Introduction of Metal Nanoparticles into a Microdomain Structure. *Macromolecules* **2009**, *42* (4), 1194–1202. DOI: 10.1021/ma802674k.
- (125) Funaki, Y.; Kumano, K.; Nakao, T.; Jinnai, H.; Yoshida, H.; Kimishima, K.; Tsutsumi, K.; Hirokawa, Y.; Hashimoto, T. Influence of casting solvents on microphase-separated structures of poly(2-vinylpyridine)- block -polyisoprene. *Polymer* **1999**, *40* (25), 7147–7156. DOI: 10.1016/S0032-3861(99)00112-3.
- (126) Watanabe, H.; Tirrell, M. Measurement of forces in symmetric and asymmetric interactions between diblock copolymer layers adsorbed on mica. *Macromolecules* **1993**, *26* (24), 6455–6466. DOI: 10.1021/ma00076a023.
- (127) Quirk, R. P.; Corona-Galvan, S. Controlled Anionic Synthesis of Polyisoprene–Poly(2-vinylpyridine) Diblock Copolymers in Hydrocarbon Solution. *Macromolecules* **2001**, *34* (5), 1192–1197. DOI: 10.1021/ma001044v.
- (128) Miskaki, C.; Moutsios, I.; Manesi, G.-M.; Artopoiadis, K.; Chang, C.-Y.; Bersenev, E. A.; Moschovas, D.; Ivanov, D. A.; Ho, R.-M.; Avgeropoulos, A. Self-Assembly of Low-Molecular-Weight Asymmetric Linear Triblock Terpolymers: How Low Can We Go? *Molecules* **2020**, *25* (23), 5527. DOI: 10.3390/molecules25235527. Published Online: Nov. 25, 2020.
- (129) Matmour, R.; Gnanou, Y. Synthesis of complex polymeric architectures using multilithiated carbanionic initiators—Comparison with other approaches. *Progress in Polymer Science* **2013**, *38* (1), 30–62. DOI: 10.1016/j.progpolymsci.2012.08.003.
- (130) Bartz, T.; Klapper, M.; Müllen, K. Dihydroanthracene dimers as novel bifunctional initiators for anionic polymerization. *Acta Polym.* **1994**, *45* (3), 248–251. DOI: 10.1002/actp.1994.010450317.
- (131) Quirk, R. P. Anionic Polymerization of Nonpolar Monomers. In *Polymer Science*, 2nd ed.; Moeller, M., Matyjaszewski, K., Eds.; Elsevier Science, 2012; pp 559–590. DOI: 10.1016/B978-0-444-53349-4.00076-5.
- (132) Boutillier, J.-M.; Favier, J.-C.; Hémerly, P.; Sigwalt, P. Various types of aggregates in mono- or bifunctional polyisoprenyllithium in hydrocarbons. *Polymer* **1996**, *37* (23), 5197–5203. DOI: 10.1016/0032-3861(96)00348-5.

- (133) Lee, J. S.; Quirk, R. P.; Foster, M. D. Synthesis and Characterization of Well-Defined, Regularly Branched Polystyrenes Utilizing Multifunctional Initiators. *Macromolecules* **2005**, *38* (13), 5381–5392. DOI: 10.1021/ma050207i.
- (134) Theodosopoulos, G. V.; Hurley, C. M.; Mays, J. W.; Sakellariou, G.; Baskaran, D. Trifunctional organolithium initiator for living anionic polymerization in hydrocarbon solvents in the absence of polar additives. *Polym. Chem.* **2016**, *7* (24), 4090–4099. DOI: 10.1039/C6PY00720A.
- (135) Janssens, K.; Loozen, E.; Yakimansky, A.; van Beylen, M. Kinetic study of the initiation reaction by a dilithium initiator used for the preparation of ABA triblock copolymers in non-polar medium. *Polymer* **2009**, *50* (23), 5368–5373. DOI: 10.1016/j.polymer.2009.09.045.
- (136) Matmour, R.; Lebreton, A.; Tsitsilianis, C.; Kallitsis, I.; Héroguez, V.; Gnanou, Y. Tri- and Tetracarbanionic Initiators by a Lithium/Halide Exchange Reaction: Application to Star-Polymer Synthesis. *Angew. Chem.* **2005**, *117* (2), 288–291. DOI: 10.1002/ange.200461056.
- (137) Sun, W.; He, J.; Wang, X.; Zhang, C.; Zhang, H.; Yang, Y. Synthesis of Dendritic Polystyrenes from an Anionic Inimer. *Macromolecules* **2009**, *42* (19), 7309–7317. DOI: 10.1021/ma9006768.
- (138) Lutz, P.; Franta, E.; Rempp, P. An efficient bifunctional lithium-organic initiator to be used in apolar solvents. *Polymer* **1982**, *23* (13), 1953–1959. DOI: 10.1016/0032-3861(82)90223-3.
- (139) Beinert, G.; Lutz, P.; Franta, E.; Rempp, P. A bifunctional anionic initiator soluble in non-polar solvents. *Makromol. Chem.* **1978**, *179* (2), 551–555. DOI: 10.1002/macp.1978.021790233.
- (140) Sanderson, R. D.; Costa, G.; Summers, G. J.; Summers, C. A. The synthesis of a hydrocarbon-soluble organolithium anionic initiator. A gas-liquid chromatography study of the efficiency of the reaction of *s*-butyllithium with *p*-divinylbenzene. *Polymer* **1999**, *40* (19), 5429–5437. DOI: 10.1016/S0032-3861(98)00762-9.
- (141) Foss, R. P.; Jacobson, H. W.; Cripps, H. N.; Sharkey, W. H. Block and Graft Copolymers of Pivalolactone. II. ABA and ABA-g-A Copolymers with Dienes. *Macromolecules* **1976**, *9* (2), 373–374. DOI: 10.1021/ma60050a043.
- (142) Jou, C.-D.; Hsieh, H. C.-C.; Tsiang, R. C.-C. Efficiency of *n*-butyllithium/*m*-diisopropenylbenzene diadduct as a dicarbanion initiator in the making of  $\alpha,\omega$ -hydroxyl terminated polybutadiene using oxetane as the capping agent. *Polymer* **1997**, *38* (23), 5869–5877. DOI: 10.1016/S0032-3861(97)00137-7.
- (143) Lee, P.-C.; Wang, C.-C.; Chen, C.-Y. Synthesis of high-vinyl isoprene and styrene triblock copolymers via anionic polymerization with difunctional *t*-BuLi initiator. *European Polymer Journal* **2020**, *124*, 109476. DOI: 10.1016/j.eurpolymj.2020.109476.
- (144) Li, H.-J.; Tsiang, R. C.-C. Preparation and characterization of a linear poly(4-vinyl pyridine)-*b*-polybutadiene-*b*-poly(4-vinylpyridine) using a *t*-butyllithium/*m*-diisopropenylbenzene diadduct as a dicarbanion initiator. *Polymer* **2000**, *41* (15), 5601–5610. DOI: 10.1016/S0032-3861(99)00810-1.
- (145) Fetters, L. J.; Morton, M. Synthesis and Properties of Block Polymers. I. Poly- $\alpha$ -methylstyrene-Polyisoprene-Poly- $\alpha$ -methylstyrene. *Macromolecules* **1969**, *2* (5), 453–458. DOI: 10.1021/ma60011a002.
- (146) Fetters, L. J. Procedures for Homogeneous Anionic Polymerization. *Journal of research of the National Bureau of Standards. Section A, Physics and chemistry* **1966**, *70A* (5), 421–433. DOI: 10.6028/jres.070A.035.

- (147) Tung, L. H.; Lo, G. Y.-S.; Beyer, D. E. Dilithium Anionic Initiators Based on Double 1,1-Diphenylethylene Compounds. *Macromolecules* **1978**, *11* (3), 616–617. DOI: 10.1021/ma60063a036.
- (148) Hofmans, J.; van Beylen, M. Synthesis and development of a dilithium initiator and its use for the preparation of ABA-block copolymers in non-polar medium: the use of  $\pi$ -complexing additives. *Polymer* **2005**, *46* (2), 303–318. DOI: 10.1016/j.polymer.2004.11.015.
- (149) Iatrou, H.; Mays, J. W.; Hadjichristidis, N. Regular Comb Polystyrenes and Graft Polyisoprene/Polystyrene Copolymers with Double Branches (“Centipedes”). Quality of (1,3-Phenylene)bis(3-methyl-1-phenylpentylidene)dilithium Initiator in the Presence of Polar Additives. *Macromolecules* **1998**, *31* (19), 6697–6701. DOI: 10.1021/ma980738p.
- (150) Tung, L. H.; Lo, G. Y.-S. Hydrocarbon-Soluble Di- and Multifunctional Organolithium Initiators. *Macromolecules* **1994**, *27* (7), 1680–1684. DOI: 10.1021/ma00085a003.
- (151) Lu, Z.; Xu, H.; Li, Y.; Hu, Y. Synthesis of a difunctional organolithium compound as initiator for the polymerization of styrene-butadiene/isoprene-styrene triblock copolymer. *J. Appl. Polym. Sci.* **2006**, *100* (2), 1395–1402. DOI: 10.1002/app.23666.
- (152) Ma, H. W.; Wang, B.; Zhang, C. Q.; Li, Y.; Hu, Y. M.; Wang, Y. R. Synthesis and characterization of poly[(4-vinylphenyl)dimethylsilane]-b-polybutadiene-b-poly[(4-vinylphenyl)dimethylsilane] (PVPDMS-b-PBd-b-PVPDMS). *Chinese Chemical Letters* **2011**, *22* (11), 1371–1374. DOI: 10.1016/j.ccllet.2011.05.004.
- (153) Yu, J. M.; Dubois, P.; Teyssié, P.; Jérôme, R. Syndiotactic Poly(methyl methacrylate) (sPMMA)–Polybutadiene (PBD)–sPMMA Triblock Copolymers: Synthesis, Morphology, and Mechanical Properties. *Macromolecules* **1996**, *29* (19), 6090–6099. DOI: 10.1021/ma9603950.
- (154) Lepoittevin, B.; Hémerly, P. Synthesis of high-molecular-weight cyclic and multicyclic polystyrenes. *Polym. Adv. Technol.* **2002**, *13* (10-12), 771–776. DOI: 10.1002/pat.257.
- (155) Lo, G. Y.-S.; Otterbacher, E. W.; Pews, R. G.; Tung, L. H. Studies on Dilithium Initiators. 4. Effect of Structure Variations. *Macromolecules* **1994**, *27* (8), 2241–2248. DOI: 10.1021/ma00086a039.
- (156) Vasilakopoulos, T. C.; Hadjichristidis, N. Influence of (1,3-phenylene)bis(3-methyl-1-phenylpentylidene)dilithium initiator concentration on the modality of polybutadiene. *J. Polym. Sci. A Polym. Chem.* **2013**, *51* (4), 824–835. DOI: 10.1002/pola.26435.
- (157) Zhang, X.; Zhang, C.; Wang, Y.; Li, Y. Synthesis and characterization of symmetrical triblock copolymers containing crystallizable high-trans-1,4-polybutadiene. *Polymer Bulletin* **2010**, *65* (3), 201–213. DOI: 10.1007/s00289-009-0192-2.
- (158) Guyot, P.; Favier, J. C.; Uytterhoeven, H.; Fontanille, M.; Sigwalt, P. New perfectly difunctional organolithium initiators for block copolymer synthesis: Synthesis of dilithium initiators in the absence of polar additives. *Polymer* **1981**, *22* (12), 1724–1728. DOI: 10.1016/0032-3861(81)90394-3.
- (159) Bastelberger, T.; Höcker, H. Divinylidene Compounds and Their Role as Key Compounds for the Synthesis of Blockcopolymers. *Angew. Makromol. Chemie* **1984**, *125* (1), 53–67. DOI: 10.1002/apmc.1984.051250105.

- (160) Bae, Y. C.; Coca, S.; Canale, P. L.; Faust, R. Coupling Reaction of Living Polyisobutylene Using Bis(diphenylethenyl) Compounds as Coupling Agents. In *Cationic Polymerization*; Faust, R., Shaffer, T. D., Eds.; ACS Symposium Series; American Chemical Society, 1997; pp 198–210. DOI: 10.1021/bk-1997-0665.ch016.
- (161) Liu, G.; Ma, H.; Lee, H.; Xu, H.; Cheng, S.; Sun, H.; Chang, T.; Quirk, R. P.; Wang, S.-Q. Long-chain branched polymers to prolong homogeneous stretching and to resist melt breakup. *Polymer* **2013**, *54* (24), 6608–6616. DOI: 10.1016/j.polymer.2013.10.007.
- (162) Ma, J. Synthesis of well-defined macrocyclic block copolymers using living coupling agent method. *Macromol. Symp.* **1995**, *91* (1), 41–49. DOI: 10.1002/masy.19950910105.
- (163) Wang, X.; Xia, J.; He, J.; Yu, F.; Li, A.; Xu, J.; Lu, H.; Yang, Y. Synthesis and Characterization of ABC-type Star and Linear Block Copolymers of Styrene, Isoprene, and 1,3-Cyclohexadiene. *Macromolecules* **2006**, *39* (20), 6898–6904. DOI: 10.1021/ma061214p.
- (164) Xie, C.; Ju, Z.; Zhang, C.; Yang, Y.; He, J. Dendritic Block and Dendritic Brush Copolymers through Anionic Macroinimer Approach. *Macromolecules* **2013**, *46* (4), 1437–1446. DOI: 10.1021/ma3025317.
- (165) Quirk, R. P.; Ma, J.-J. Dilithium initiators based on 1,3-bis(1-phenylethenyl)benzene. Tetrahydrofuran and lithiumsec-butoxide effects. *Polym. Int.* **1991**, *24* (4), 197–206. DOI: 10.1002/pi.4990240402.
- (166) Batesky, D. C.; Goldfogel, M. J.; Weix, D. J. Removal of Triphenylphosphine Oxide by Precipitation with Zinc Chloride in Polar Solvents. *The Journal of organic chemistry* **2017**, *82* (19), 9931–9936. DOI: 10.1021/acs.joc.7b00459. Published Online: Sep. 28, 2017.
- (167) Bae, Y. C.; Faust, R. Addition Reaction of Living Polyisobutylene to “Double” Diphenylethylenes. Synthesis of 1,1-Diphenylethylene-Functionalized Polyisobutylene Macromonomers. *Macromolecules* **1998**, *31* (26), 9379–9383. DOI: 10.1021/ma981231h.
- (168) Bandermann, F.; Speikamp, H.-D.; Weigel, L. Bifunctional anionic initiators: A critical study and overview. *Makromol. Chem.* **1985**, *186* (10), 2017–2024. DOI: 10.1002/macp.1985.021861005.
- (169) Schultz, A. R.; Bobade, S.; Scott, P. J.; Long, T. E. Hydrocarbon-Soluble Piperazine-Containing Dilithium Anionic Initiator for High Cis -1,4 Isoprene Polymerization. *Macromol. Chem. Phys.* **2018**, *219* (1), 1700201. DOI: 10.1002/macp.201700201.
- (170) Matmour, R.; More, A. S.; Wadgaonkar, P. P.; Gnanou, Y. High performance poly(styrene-*b*-diene-*b*-styrene) triblock copolymers from a hydrocarbon-soluble and additive-free dicarbanionic initiator. *J. Am. Chem. Soc.* **2006**, *128* (25), 8158–8159. DOI: 10.1021/ja062695v.

## 6. Chapter 2 – Introducing a 1,1-diphenylethylene analogue for vinylpyridine: anionic copolymerisation of 3-(1-phenylvinyl)pyridine (*m*-PyPE)

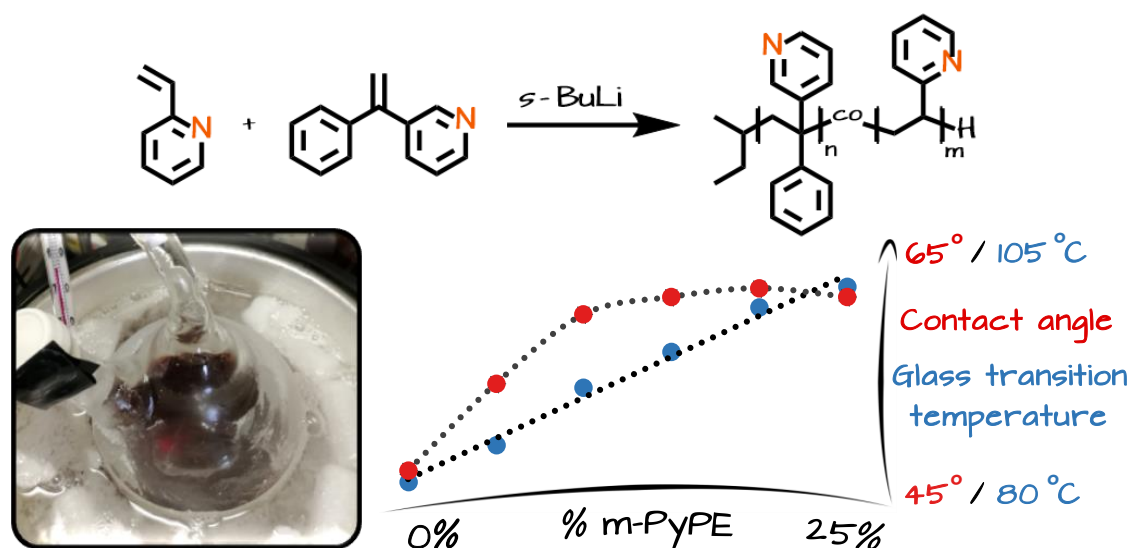
Marcel Fickenscher, [REDACTED] and [REDACTED] \*

M. Sc. Marcel Fickenscher, B. Sc. [REDACTED], Prof. [REDACTED]  
Department of Chemistry, Johannes Gutenberg University Mainz, Duesbergweg 10-14,  
55128 Mainz, Germany  
E-Mail: [REDACTED]

*Polym. Chem.*, **2021**,12, 3576-3581; DOI: 10.1039/D1PY00302J

Keywords: 2-vinylpyridine, DPE derivatives, carbanionic polymerisation

### 6.1 TOC & Short Abstract



3-(1-Phenylvinyl)pyridine is a structural analogue of 1,1-diphenylethylene, with one phenyl group replaced by pyridine. Its suitability for the random copolymerisation with vinylpyridine is demonstrated and the resulting copolymers are characterised.

## 6.2 Abstract

3-(1-phenylvinyl)pyridine (*m*-PyPE), prepared by Wittig reaction from the readily available 3-benzoylpyridine, represents a structural analog of 1,1-diphenylethylene (DPE), one phenyl group being replaced by pyridine. The suitability of *m*-PyPE for the copolymerisation with vinylpyridine is reflected by the  $^{13}\text{C}$  NMR shifts of the  $\beta$ -carbon of 2-vinylpyridine (2-VP; 118.32 ppm) and *m*-PyPE (115.83 ppm, measured in  $\text{CDCl}_3$ ), which possess predictive character for carbanionic copolymerisation. In analogy to DPE and its manifold reported derivatives, carbanionic homopolymerisation of *m*-PyPE was not possible, due to its steric bulk. Copolymers of 2-VP and *m*-PyPE with varied composition have been synthesised with an incorporated amount of *m*-PyPE of up to 25% with respect to 2-VP. Full conversion as well as the targeted incorporation ratio were verified by NMR experiments. An increase of the glass transition temperatures of the resulting copolymers with increasing *m*-PyPE content was observed by differential scanning calorimetry, and the difference in hydrophilicity compared to that of P(2-VP) was determined by contact angle measurements. *m*-PyPE offers potential also for functional termination of other living anionic polymerisations.

### 6.3 Introduction

Ever since the first reports on the anionic polymerisation of 2- and 4-vinylpyridine (2-VP, 4-VP) by Szwarc et al. appeared in 1962, the respective polymers have attracted interest among many researchers, which is reflected in a first review article from 1984.<sup>1,2</sup> The latest comprehensive review, published by Kennemur et al. in 2019, shows that poly(vinylpyridine) (PVP) is further developed in different directions based on the peculiar properties of the electron deficient pyridine ring.<sup>3</sup> The more expensive and challenging synthesis of PVP compared to that of polystyrene is rewarded with unique properties of the resulting materials. The hydrophilic behaviour of PVP in contrast to the non-polar polystyrene, combined with the possibility to perform post polymerisation reactions like quaternisation, complexation of metal ions and oxidation to N-oxides offers a broad range of applications, for instance antibacterial modification of cotton or the mechanical enhancement of tires, to name only two examples of many.<sup>4-10</sup> In contrast to the post polymerisation reactions, the possibilities to modify PVP during the polymerisation itself are limited due to the rather low reactivity of the heteroatom-bearing chain end as well as the required reaction conditions (e.g. polar solvents, low temperatures).

Hirao et al. demonstrated that the reactivity of styrenic vinyl monomers is mirrored by the  $\beta$ -carbon shift in  $^{13}\text{C}$  NMR spectroscopy.<sup>11</sup> An increase of the chemical shift of the signal can be explained with the electron withdrawing nitrogen in the aromatic system. The result is an enhanced delocalisation of the negative charge of the active chain end, which on the one hand leads to a reduced reactivity of the growing polymer chain, but on the other hand also to an increased polymerisability of the monomer during homopolymerisation. Ultimately, this limits the possibilities for the synthesis of copolymers. While block copolymers are easily available, random copolymerisation of VP with styrene or other hydrocarbon monomers is not possible. The active PVP chain end is not capable to cross over to styrene and common styrene-based monomers.<sup>12-20</sup> As a result, tailoring the thermal properties like the glass transition temperature of PVP

is difficult because copolymerisation with 1,1-diphenylethylene (DPE), as reported in literature for styrene monomers, is not possible for P(2-VP).<sup>21-24</sup>

DPE has been used in numerous works, either as a monomer to control the monomer sequence, mainly in combination with styrene, or to moderate chain end reactivity to switch to other monomers with different reactivity.<sup>25,26,27</sup> However, the respective analog for the polymerisation of VP is not known. A variety of functionalised DPE derivatives have been developed for the synthesis of complex star polymer architectures.<sup>28</sup> Recently a DPE analog with a cyclopropyl group has been introduced by Ma et al., demonstrating the current interest in this field.<sup>29</sup>

As an analogue of DPE, in this work we have studied 3-(1-phenylvinyl)pyridine (*m*-PyPE, abbreviation for *m*-pyridinylphenylethylene), a DPE analogous structure that is obtained by replacing one phenyl group of DPE by a pyridine moiety. We demonstrate that *m*-PyPE can be copolymerised with 2-VP to introduce a hydrocarbon side group into PVP, which changes the hydrophilicity as well as the thermal properties of the resulting copolymers.



## 6.4 Results and Discussion

### Synthesis and sample overview

In the following we describe the synthesis of the comonomer *m*-PyPE as well as its anionic copolymerisation. All reactions were performed under standard reaction conditions, described in detail in the experimental part. Various Wittig reactions leading to 1,1-disubstituted alkenes were described by Akita et al. in a general manner.<sup>30</sup> Starting from the readily available 3-benzoylpyridine, a Wittig reaction with methyltriphenylphosphonium bromide and *n*-butyllithium as a base was performed to obtain I in a yield of 68% after careful purification (Figure 1).

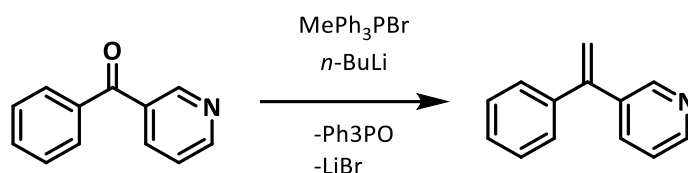


Figure 1: Wittig reaction of 3-benzoylpyridine, affording the monomer *m*-PyPE.

The use of this specific isomer is critical for the success of the synthesis. 2-benzoylpyridine, which more closely corresponds to 2-VP, was not suitable because it was too reactive in the workup process and oligomerised spontaneously during distillation. It is a well-known problem that the removal of the triphenylphosphine oxide (TPPO) as a side product of the Wittig reaction is challenging.<sup>31</sup> Nevertheless, we were able to remove all traces of TPPO via twofold distillation under reduced pressure. The purity of the product was verified by means of TLC, <sup>1</sup>H, <sup>13</sup>C and <sup>31</sup>P NMR spectroscopy; no signals other than those expected could be observed (Figures S1-S3).

### Copolymerisation of *m*-PyPE with 2-vinylpyridine

Table 1 gives an overview of the  $\beta$ -carbon NMR shifts of styrene, DPE and the respective pyridine analogues.

Table 1:  $\beta$ -carbon shifts of selected monomers measured via  $^{13}\text{C}$  NMR (400 MHz,  $\text{CDCl}_3$ , Figure S4) reflect the respective reactivity.

monomer	( $\beta$ -)carbon shift $\Delta\delta$ [ppm]
styrene	113.93
2-VP	118.32
4-VP	118.45
DPE	114.41
<i>m</i> -PyPE	115.83

According to the chemical shift  $\Delta\delta$  it is expected that the reactivity of the living *m*-PyPE chain end is too low to react with styrene. On the other hand, the reaction between a living VP chain end and DPE is unlikely. Consequently, the only way to statistically introduce a phenyl side group in PVP is the copolymerisation with *m*-PyPE, as the rather electron deficient character that is reflected by the given shift is closer to the one of 2-VP.<sup>11</sup>

It is well-known that due to the steric bulk, DPE cannot be homopolymerised, and in copolymerisation with styrene only single DPE units are incorporated between styrene moieties.<sup>23</sup> To ensure the same behaviour for *m*-PyPE, an attempt to homopolymerise it was made. The typical colour change to dark red can be observed as soon as *s*-BuLi is added. The initial reaction of *s*-BuLi with *m*-PyPE leads to the formation of the carbanionic adduct, yet no further addition of *m*-PyPE to an anionically charged product can be observed.  $^1\text{H}$  NMR spectroscopy shows the residual double bond signal of the unreacted *m*-PyPE, and the product to educt ratio matches the *s*-BuLi equivalents that were used during the initiation step (Figure S5). This confirms the

expectation that the steric hindrance of the bulky aromatic groups is sufficient to prevent the addition of more than one *m*-PyPE unit after another.

A variety of copolymers with 2-VP with a targeted molecular weight of  $10 \text{ kg}\cdot\text{mol}^{-1}$  and different amounts of incorporated *m*-PyPE have been synthesised to establish polymerisability of *m*-PyPE. Since homopolymerisation of *m*-PyPE was not possible, and in analogy to the widely investigated copolymerisation of DPE, the theoretical limit of incorporation *m*-PyPE is assumed to be 50% for the statistical copolymerisation of with 2-VP. However, the content of *m*-PyPE in the monomer mixture was varied between 0% and 25% at maximum with respect to 2-VP in this study. Increasing the *m*-PyPE amount beyond 25% is possible, yet full monomer conversion and quantitative yields were not achieved anymore and residual *m*-PyPE signals can be observed in NMR spectra of the copolymers.

Anionic copolymerisation was carried out in a carefully dried all-glass reaction apparatus, sealed with rubber and Teflon caps. The solution of both monomers in THF was initiated with *s*-BuLi and stirred at  $-64 \text{ }^\circ\text{C}$  for 4 h, to ensure full monomer conversion, while side reactions are suppressed due to the low temperature.<sup>3,16</sup> Ultimately, the reaction was quenched with methanol, and the polymer was precipitated as a colourless solid in petroleum ether with quantitative yields (Figure 2).

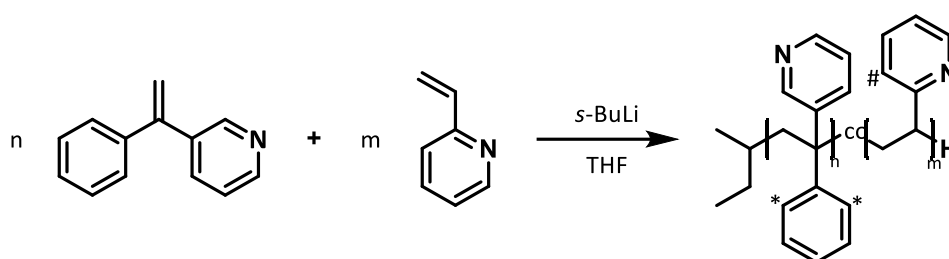


Figure 2: Synthesis of 2-VP - *m*-PyPE copolymers by carbanionic copolymerisation. The carbon atoms used to calculate the incorporation ratio are marked with \* and #.

An overview of all resulting copolymers is given in Table 2. Figure 3 shows well-defined SEC traces for all copolymers with monomodal molecular weight distributions.

Table 2: Characterisation data of copolymer samples with theoretical molecular weight of 10 kg/mol. SEC measurements were performed in DMF with toluene as an internal standard, PS calibration and UV detector. NMR measurements: solvent DMSO- $d_6$ .

ID	$m\text{-PyPE}_{\text{theo}}$ [mol%]	$M_{n, \text{SEC, exp}}$ [ $\text{kg}\cdot\text{mol}^{-1}$ ]	$M_{n, \text{NMR, exp}}$ [ $\text{kg}\cdot\text{mol}^{-1}$ ]	$\bar{D}$	$m\text{-PyPE}_{\text{calc}}$ [mol%]	$m\text{-PyPE}_{\text{theo}}$ [mol%]	$M_{n, \text{SEC, exp}}$ [ $\text{kg}\cdot\text{mol}^{-1}$ ]
1	0	8.4	9.3	1.10	0	0	8.4
2	5	7.3	8.7	1.09	4.3	5	7.3
3	10	8.6	8.7	1.25	10.2	10	8.6
4	15	7.9	6.4	1.23	14.4	15	7.9
6	20	9.0	8.2	1.38	21.2	20	9.0
7	25	7.8	7.7	1.28	24.9	25	7.8

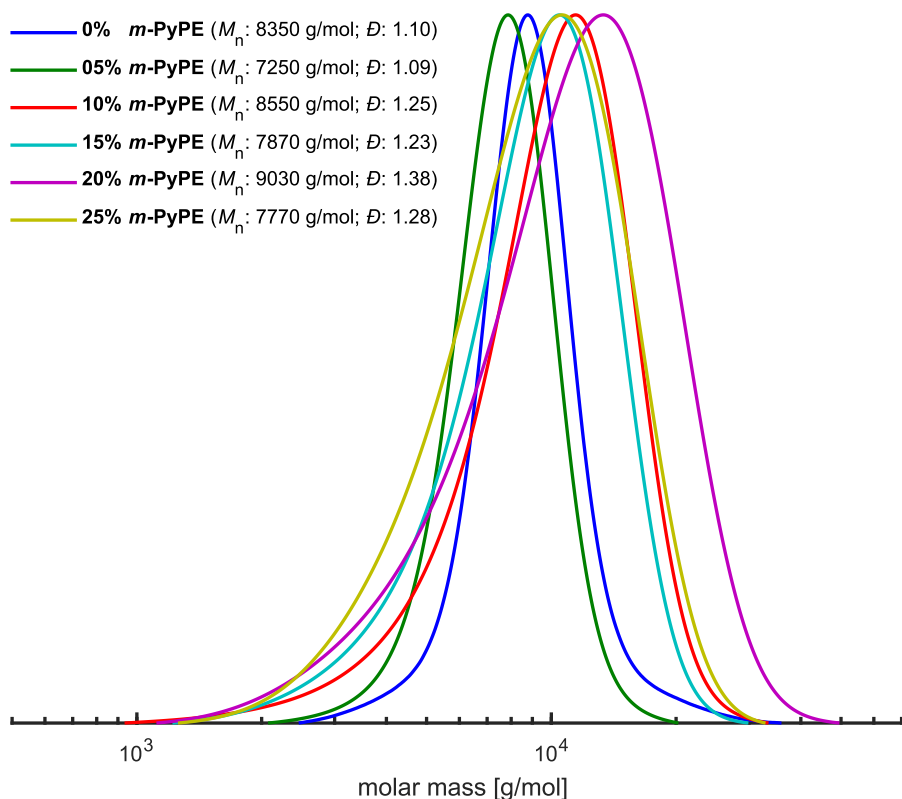


Figure 3: SEC traces of the P(2-VP-co-*m*-PyPE) samples, measured in DMF with toluene as internal standard, polystyrene calibration and an UV detector.

The deviation of the determined molecular weight from the theoretical value of  $10 \text{ kg}\cdot\text{mol}^{-1}$  is ascribed to an underestimation of P(2-VP) when using PS standards, as also reported in literature.<sup>32</sup>

The increasing dispersity of the samples with increasing amount of incorporated *m*-PyPE is tentatively ascribed to the expected hindered crossover from 2-VP to *m*-PyPE. This hypothesis is supported by the observation that full conversion is not possible, when more than 25% *m*-PyPE is used. This suggests that 2-VP exhibits considerably higher reactivity in this monomer pair. Attempts to measure the reaction kinetics using the online NMR spectroscopy approach have been unsuccessful to date as the required cooling does not allow the sample preparation without the polymerisation prior to the measurement. Offline NMR characterisation is also not suitable for this system, the necessary workup prior to the sample measurement would remove residual 2-VP. These difficulties impede the determination of the reactivity ratios as well as the distribution of the monomer gradient along the chains. Yet, SEC characterisation also evidences the absence of shoulders or severe tailing of the elugrams, supporting a controlled synthesis, i.e. the absence of side reactions such as chain transfer reactions or chain coupling, which would result in a bi- or multimodal distribution.

Detailed characterisation of the copolymers via NMR spectroscopy gives insight regarding the incorporation ratio of *m*-PyPE and the overall conversion.  $^1\text{H}$  NMR spectra show no unreacted 2-VP or *m*-PyPE, as the signals of the double bonds completely disappeared (e.g. Figure S9). For the determination of the molecular weight via  $^1\text{H}$  NMR spectroscopy, the common method is to calculate the ratio of the initiator butyl group integral and the polymer backbone integral. However, due to the small butyl signal, the integration is affected by errors in the signal-to-noise ratio (SNR) as well as the defined integral limits. Nevertheless, the values calculated with this approach (Table 1) are all in a similar range, slightly below the targeted molecular weight. In combination with the results of SEC characterisation, this demonstrates controlled copolymerisation and *m*-PyPE is fully incorporated. To further support this,

DOSY NMR spectra (see SI) also show the absence of signals other than residual solvents and the copolymer. Due to the overlapping signals it is not possible to determine the incorporation ratio via  $^1\text{H}$  NMR studies, therefore Inverse-Gated (IG)  $^{13}\text{C}$  NMR measurements are the method of choice. All copolymers were analysed via IG  $^{13}\text{C}$  NMR to determine the exact incorporation ratios. Figure 4 shows an exemplary spectrum (sample 6) as well as an overview of all samples, in which the increasing *m*-PyPE signal can be recognised.

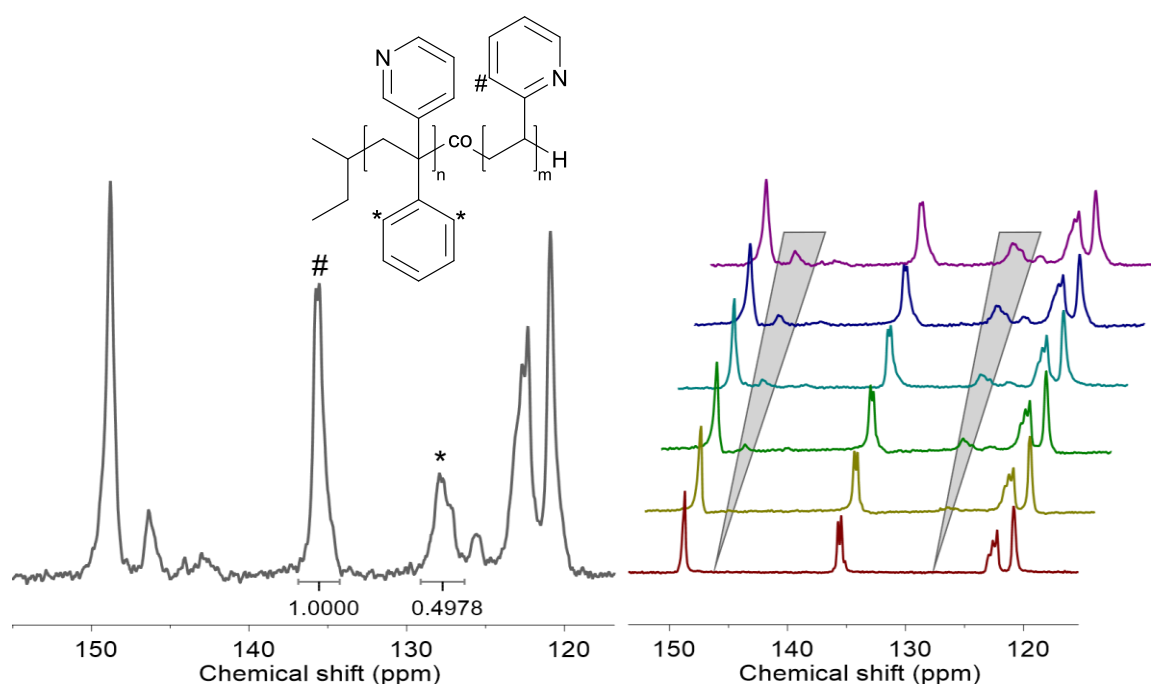


Figure 4: Left: IG  $^{13}\text{C}$  NMR of sample 6. The integral represents the incorporation ratio of *m*-PyPE. Right: IG  $^{13}\text{C}$  NMR spectra of all samples. The *m*-PyPE signal can be clearly distinguished at 127.7 ppm.

For the calculation of the incorporated amount of *m*-PyPE, the integral ratio between the signals marked with # (2-VP, 135.6 ppm, 1H) and \* (*m*-PyPE, 127.7 ppm, 2H) was determined. The percentage of *m*-PyPE with respect to 2-VP is given by the following Equation 1 when I(#) is normalised to 1:

$$\text{mol\% } m\text{-PyPE}_{\text{calc}} = 0.5 \cdot I(*) \quad \text{Equation 1}$$

During the spectra processing, the signal-to-noise ratio can be determined. This allows the estimation of an error, as it gives an indication of the maximum baseline content

in the signal and leads to an assumed error range between 33% (5% incorporation) and 10% (25% incorporation). Nevertheless, all the results fit well with the theoretical values given in Table 1, confirming the incorporation of *m*-PyPE.

#### Physical Properties of the P(2-VP-*co*-*m*-PyPE) copolymers

The incorporation of *m*-PyPE is expected to have a strong influence on the hydrophilicity of the copolymers. To study this effect a series of contact angle measurements was performed. A microscope slide was coated with the polymer by solvent evaporation of a 10w% polymer solution in THF, and the contact angle of a water droplet on the surface was measured. The larger the measured contact angle, the more hydrophobic is the surface, as the surface tension of the droplet minimises the contact area with the glass surface. The results are shown in Figure 5 and Table S1 and demonstrate clearly that the hydrophilicity is reduced with increasing amount of *m*-PyPE due to the hydrophobic phenyl groups.

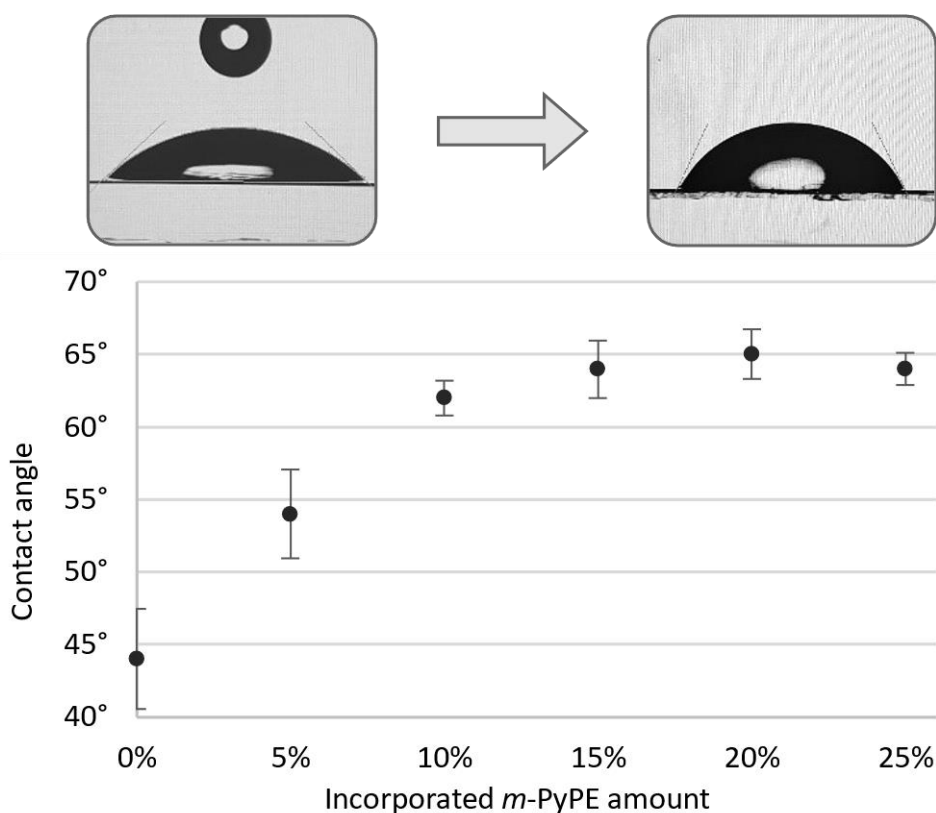


Figure 5: Increasing contact with increased *m*-PyPE incorporation. A clear trend is observable with a plateau, reached at 65 °.

A strong effect is already observed with only 5% of *m*-PyPE, which shifts the contact angle by nearly 10°. The value reaches a plateau at around 65°, which sets the limit for tailoring the hydrophilicity of the copolymers. It is noteworthy that the polymers are still rather hydrophilic in comparison to pure polystyrene, as VP is the dominating monomer unit.

Another effect of the copolymerisation of *m*-PyPE is its influence on the glass transition temperature ( $T_g$ ). In the case of copolymerisation of DPE with styrene, a significant increase of the  $T_g$  from 100 °C up to 180 °C for 50% incorporation is observed.<sup>23</sup> DSC measurements were performed to study the change of the thermal properties of the copolymers. In analogy to DPE, the bulky *m*-PyPE structure leads to a loss of flexibility of the polymer backbone. Consequently, the  $T_g$  increases in a linear manner with increasing *m*-PyPE content (Figure 6).

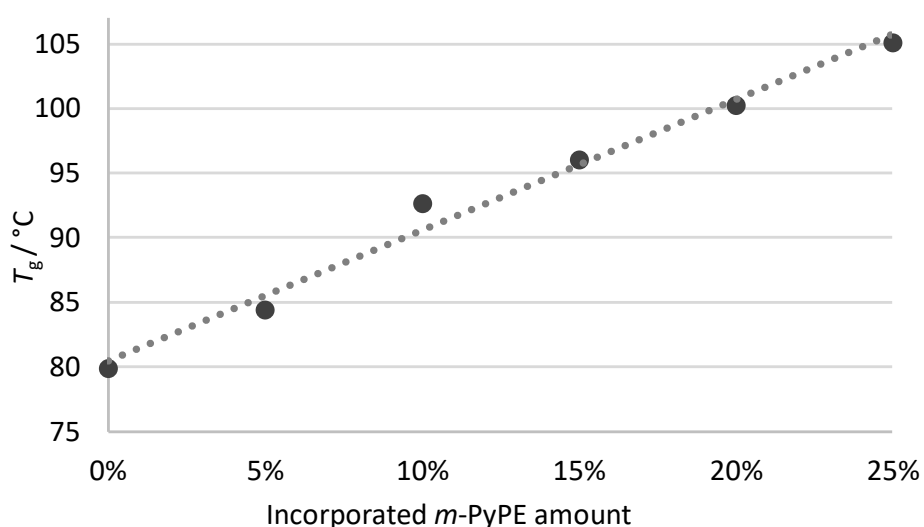


Figure 6: Incorporation of the rigid *m*-PyPE units leads to a linear increase of the glass transition temperature from 80 °C up to 105 °C.

The linear trend also shows that tailoring of the glass transition is possible in a wide range of more than 20 °C. Especially for technical applications this modification is of interest and may improve existing P(2-VP) applications e.g. its use in tires.<sup>33</sup>



## 6.5 Experimental

### Materials and methods

3-Benzoylpyridine was purchased from TCI Chemicals and used without further purification. Methyltriphenylphosphonium bromide was purchased from Acros Organics and used without further purification. 2-Vinylpyridine was purchased from Acros Organics and filtered over basic aluminium oxide to remove the stabiliser and protic impurities and freshly distilled prior to use. All solvents (Fisher Chemical, Carl Roth GmbH + Co. KG) were carefully dried with  $\text{CaH}_2$  (Sigma Aldrich) or Butyllithium (Sigma Aldrich) and freshly distilled prior to use.

### Nuclear magnetic resonance (NMR) spectroscopy

$^1\text{H}$  measurements were performed on a Bruker Avance II 400 at a magnetic field strength of 400 MHz. Inverse-Gated (IG)  $^{13}\text{C}$  measurements were performed using a Bruker Avance III HD 400 at a magnetic field strength of 400 MHz.  $\text{DMSO-d}_6$  was used as solvent for all measurements.

### Size exclusion chromatography (SEC)

All SEC measurements were performed with an Agilent 1100 Series chromatograph, equipped with HEMA columns (300/100/40, 95 cm length, 0.8 cm width, 50 °C) and an Agilent G1314A UV detector. Solvent: DMF, internal standard: toluene, calibration: polystyrene.

### Differential scanning calorimetry (DSC)

The DSC experiments were performed with a Perkin Elmer 8500 differential scanning calorimeter in a temperature range from -50 to 170 °C and a heating rate of 10 - 20 °C/min for the determination of the  $T_g$ .

### Contact angle measurements

The contact angle was measured with a Dataphysics contact angle system OCA with ultrapure water as fluid component.

## Synthesis procedures

### Monomer synthesis

In a carefully dried all-glass apparatus featuring a mechanical stirrer, a dropping funnel and a reflux condenser, 53.6 g (150.1 mmol, 1.1 eq.) methyltriphenyl-phosphonium bromide was dissolved in 350 mL freshly distilled THF. For the formation of the Wittig reagent 62.8 mL (156.9 mmol, 1.2 eq.) 2.5M *n*-BuLi solution in cyclohexane were slowly added via the dropping funnel, the temperature was kept around 0 °C with an ice-water bath. After 30 minutes of stirring, a solution of 24.8 g (135.25 mmol, 1 eq.) 3-benzoylpyridine in 25 mL THF was added via syringe and the cooling bath was removed. The conversion was observed via TLC and upon completion the reaction was quenched with water. Separation of the organic phase and distillation under reduced pressure ( $1 \cdot 10^{-3}$  mbar, b.p. 142 °C) yields *m*-PyPE as a colourless oil in a yield of 68%.

R<sub>f</sub>: 0.52 (cyclohexane/ethylacetate 8:3)

<sup>1</sup>H NMR (DMSO-d<sub>6</sub>, 400 MHz) δ [ppm] = 8.56 (dd, 1H, *J* = 4.8, 1.7 Hz, H-12), 8.54 (dd, 1H, *J* = 2.3, 0.9 Hz, H-14), 7.67 (ddd, 1H, *J* = 7.9, 2.3, 1.6 Hz, H-10), 7.43-7.30 (m, 6H, H-1 to H-4, H-6, H-11), 5.61 (d, 2H, *J* = 13.1 Hz, H-9), 3.35 (H<sub>2</sub>O), 2.50 (DMSO).

<sup>13</sup>C NMR (DMSO-d<sub>6</sub>, 400 MHz) δ [ppm] = 148.9 (C-10), 148.5 (C-12), 146.1 (C-1), 139.8 (C-9), 136.3 (C-3), 135.2 (C-14), 128.5 (C-4, C-8), 128.2 (C-6), 127.6 (C-5, C-7), 123.4 (C-13), 116.3 (C-2), 39.5 (DMSO).

### Polymer synthesis

All polymerisations were carried out on a 2 g scale using a carefully dried all-glass apparatus with rubber seals and Teflon caps as well as standard high vacuum techniques. *m*-PyPE was placed in the reactor and stirred under dynamic vacuum for at least 18 hours to remove traces of water, due to the high boiling point the treatment with CaH<sub>2</sub> was not suitable. 2-VP was purified by filtration over basic aluminium oxide to remove the stabiliser and protic impurities. Subsequently, it was degassed and stirred over calcium hydride for at least 18 hours, freshly distilled prior to use and

added to the reactor via syringe. Degassed THF was stirred over *n*-BuLi using DPE as an indicator and directly distilled in the reaction flask as required. The reactor was cooled to -64 °C with a chloroform/dry ice bath prior to the addition of *s*-BuLi as an initiator via syringe. Successful initiation was observed by the immediate formation of the typical dark red coloured anionic chain end. The solution was stirred for 3 to 4 h and quenched with methanol, which leads to the immediate disappearance of the red colour. The resulting polymers were precipitated in petroleum ether and dried under reduced pressure for several days. The copolymers were obtained as a colourless solid in quantitative yields.

## 6.6 Conclusion

3-(1-phenylvinyl)pyridine (*m*-PyPE) has been obtained by a facile Wittig reaction from the respective ketone. *m*-PyPE represents an analogue of the well-known 1,1-diphenylethylene, albeit with a rather low electron density due to the pyridine ring. Thus, it may be viewed as a DPE analog for the vinylpyridine polymerisation, which is also confirmed by the  $^{13}\text{C}$  NMR shifts of the  $\beta$ -carbon of 2-VP (118.32 ppm) and *m*-PyPE (115.83 ppm). A variety of copolymers of 2-VP and *m*-PyPE with up to 24.9% of *m*-PyPE incorporation was prepared by anionic copolymerisation. The copolymers exhibited narrow to moderate molecular weight distributions. The composition of the polymers was determined via quantitative IG  $^{13}\text{C}$  NMR studies. Incorporation of *m*-PyPE has a significant impact on the properties of 2-VP polymers, which is reflected by the change in hydrophilicity as well as the increasing glass transition temperature that increased up to 105 °C.

This study is an interesting starting point for further structures: In analogy to DPE, the use of *m*-PyPE as a terminating agent for other anionically prepared hydrocarbon polymers should permit the introduction of exactly one functional pyridine end group for further post polymerisation reactions. Also, increasing the incorporated amount of *m*-PyPE by adding 2-VP via syringe pump or in-situ NIR kinetic experiments to study reactivity ratios and therefore the distribution of the monomers along the PVP chain could give more insight in the polymerisation behaviour of vinylpyridines. Especially the latter one – in combination with the change in hydrophilicity and the increased glass transition temperature – could have a strong effect in blending experiments with VP-diene copolymers.<sup>34-36</sup>

## 6.7 References

- (1) Lee, C. L.; Smid, J.; Szwarc, M. Kinetics of anionic polymerization and copolymerization of vinyl pyridines. The penultimate effects. *Trans. Faraday Soc.* **1963**, *59*, 1192. DOI: 10.1039/TF9635901192.
- (2) Fréchet, J. M. J.; Meftahi, M. V. de. Poly(vinyl pyridine)s: Simple reactive polymers with multiple applications. *Brit. Poly. J.* **1984**, *16* (4), 193–198. DOI: 10.1002/pi.4980160407.
- (3) Kennemur, J. G. Poly(vinylpyridine) Segments in Block Copolymers: Synthesis, Self-Assembly, and Versatility. *Macromolecules* **2019**, *52* (4), 1354–1370.
- (4) Mössmer, S.; Spatz, J. P.; Möller, M.; Aberle, T.; Schmidt, J.; Burchard, W. Solution Behavior of Poly(styrene)- block -poly(2-vinylpyridine) Micelles Containing Gold Nanoparticles. *Macromolecules* **2000**, *33* (13), 4791–4798. DOI: 10.1021/ma992006i.
- (5) Alexandridis, P.; Tsianou, M. Block copolymer-directed metal nanoparticle morphogenesis and organization. *European Polymer Journal* **2011**, *47* (4), 569–583. DOI: 10.1016/j.eurpolymj.2010.10.021.
- (6) Rancatore, B. J.; Bai, P.; Xu, T. Organic Semiconductor-Based Supramolecular Nanocomposites. *Macromolecules* **2016**, *49* (11), 4155–4163. DOI: 10.1021/acs.macromol.6b00383.
- (7) Ernst, H.; Rittinghausen, S.; Bartsch, W.; Creutzenberg, O.; Dasenbrock, C.; Görlitz, B.-D.; Hecht, M.; Kairies, U.; Muhle, H.; Müller, M.; Heinrich, U.; Pott, F. Pulmonary inflammation in rats after intratracheal instillation of quartz, amorphous SiO<sub>2</sub>, carbon black, and coal dust and the influence of poly-2-vinylpyridine-N-oxide (PVNO). *Experimental and Toxicologic Pathology* **2002**, *54* (2), 109–126. DOI: 10.1078/0940-2993-00241.
- (8) Cho, Y.-H.; Yang, J.-E.; Lee, J.-S. Size control of polymeric nanoparticles from polystyrene-b-poly(2-vinylpyridine). *Materials Science and Engineering: C* **2004**, *24* (1-2), 293–295. DOI: 10.1016/j.msec.2003.09.060.
- (9) H. Inoue. Polysoaps derived from poly-2-vinylpyridine. *Kolloid-Z.u.Z.Polymer* **1964**, *195* (2), 102–110. DOI: 10.1007/BF01503657.
- (10) Cen, L.; Neoh, K. G.; Kang, E. T. Antibacterial activity of cloth functionalized with N-alkylated poly(4-vinylpyridine). *J. Biomed. Mater. Res.* **2004**, *71A* (1), 70–80. DOI: 10.1002/jbm.a.30125.
- (11) Nakahama, S.; Ishizone, T.; Hirao, A. Anionic living polymerization of styrenes containing electron-withdrawing groups. *Makromolekulare Chemie. Macromolecular Symposia* **1993**, *67* (1), 223–236. DOI: 10.1002/masy.19930670118.
- (12) Gosnell, A. B.; Gervasi, J. A.; Woods, M. D. K.; Stannett, V. Anionic Grafting of Polystyrene and Polyisoprene to Living Poly(2-vinylpyridine). *J. polym. sci., C Polym. symp.* **1969**, *22* (2), 611–620. DOI: 10.1002/polc.5070220206.
- (13) Spatz, J. P.; Mößmer, S.; Möller, M. Mineralization of Gold Nanoparticles in a Block Copolymer Microemulsion. *Chem. Eur. J.* **1996**, *2* (12), 1552–1555. DOI: 10.1002/chem.19960021213.
- (14) Spatz, J. P.; Sheiko, S.; Möller, M. Ion-Stabilized Block Copolymer Micelles: Film Formation and Intermicellar Interaction. *Macromolecules* **1996**, *29* (9), 3220–3226. DOI: 10.1021/ma951712q.

- (15) Zha, W.; Han, C. D.; Lee, D. H.; Han, S. H.; Kim, J. K.; Kang, J. H.; Park, C. Origin of the Difference in Order–Disorder Transition Temperature between Polystyrene- block -poly(2-vinylpyridine) and Polystyrene- block -poly(4-vinylpyridine) Copolymers. *Macromolecules* **2007**, *40* (6), 2109–2119. DOI: 10.1021/ma062516u.
- (16) Luxton, A. R.; Quig, A.; Delvaux, M.-J.; Fetters, L. J. Star-branched polymers:2. Linking reaction involving 2- and 4-vinyl pyridine and dienyland styryllithium chain ends. *Polymer* **1978**, *19* (11), 1320–1324. DOI: 10.1016/0032-3861(78)90315-4.
- (17) Yushu Matsushita; Yasushi Nakao; Ryuichi Saguchi; Haruhisa Choshi; Mitsuru Nagasawa. Studies of Styrene and 2-Vinylpyridine Block Copolymers; Preparation and Characterization. *Polym J* **1986**, *18* (6), 493–499. DOI: 10.1295/polymj.18.493.
- (18) Pitsikalis, M.; Sioula, S.; Pispas, S.; Hadjichristidis, N.; Cook, D. C.; Li, J.; Mays, J. W. Linking reactions of living polymers with bromomethylbenzene derivatives:Synthesis and characterization of star homopolymers and graft copolymers with polyelectrolyte branches. *J. Polym. Sci. A Polym. Chem.* **1999**, *37* (23), 4337–4350. DOI: 10.1002/(SICI)1099-0518(19991201)37:23<4337:AID-POLA10>3.0.CO;2-8.
- (19) Mai, Y.; Eisenberg, A. Selective localization of preformed nanoparticles in morphologically controllable block copolymer aggregates in solution. *Accounts of chemical research* **2012**, *45* (10), 1657–1666. DOI: 10.1021/ar2003144.
- (20) Yang Wang; Xinhe Xu; Peng Xu; Xiaobo Feng; Yanyan Zhang; Feiya Fu; Xiangdong Liu. Controllable self-assembly of polystyrene-block-poly(2-vinylpyridine). *Polymer International* **2018**, *67* (6), 619–626. DOI: 10.1002/pi.5550.
- (21) Zhang, Y.; Han, L.; Ma, H.; Yang, L.; Liu, P.; Shen, H.; Li, C.; Li, Y. The investigation on synthesis of periodic polymers with 1,1-diphenylethylene (DPE) derivatives via living anionic polymerization. *Polymer* **2019**, *169*, 95–105. DOI: 10.1016/j.polymer.2019.02.033.
- (22) Hirao, A.; Loykulnant, S.; Ishizone, T. Recent advance in living anionic polymerization of functionalized styrene derivatives. *Progress in Polymer Science* **2002**, *27* (8), 1399–1471. DOI: 10.1016/S0079-6700(02)00016-3.
- (23) Hutchings, L. R.; Brooks, P. P.; Shaw, P.; Ross-Gardner, P. Fire and Forget!:One-Shot Synthesis and Characterization of Block-Like Statistical Terpolymers via Living Anionic Polymerization. *J. Polym. Sci. A Polym. Chem.* **2018**, *57* (3), 382–394. DOI: 10.1002/pola.29208.
- (24) Knoll, K.; Schneider, M.; Oepen, S. A Forgotten Class of High T<sub>g</sub> Thermoplastic Materials:Anionic Copolymers of Styrene and 1, 1-Diphenylethylene. In *Ionic Polymerizations and Related Processes*; Puskas, J. E., Michel, A., Barghi, S., Eds.; Springer Netherlands, 1999; pp 219–221. DOI: 10.1007/978-94-011-4627-2\_13.
- (25) Yang, L.; Ma, H.; Han, L.; Liu, P.; Shen, H.; Li, C.; Li, Y. Sequence Features of Sequence-Controlled Polymers Synthesized by 1,1-Diphenylethylene Derivatives with Similar Reactivity during Living Anionic Polymerization. *Macromolecules* **2018**, *51* (15), 5891–5903. DOI: 10.1021/acs.macromol.8b01491.
- (26) Hutchings, L. R.; Brooks, P. P.; Parker, D.; Mosely, J. A.; Sevinc, S. Monomer Sequence Control via Living Anionic Copolymerization:Synthesis of Alternating, Statistical, and Telechelic Copolymers

and Sequence Analysis by MALDI ToF Mass Spectrometry. *Macromolecules* **2015**, *48* (3), 610–628. DOI: 10.1021/ma5016038.

(27) Liu, K.; Li, A.; Yang, Z.; Jiang, A.; Xie, F.; Li, S.; Xia, J.; She, Z.; Tang, K.; Zhou, C. Synthesis of strictly alternating copolymers by living carbanionic copolymerization of diphenylethylene with 1,3-pentadiene isomers. *Polym. Chem.* **2019**, *10* (14), 1787–1794. DOI: 10.1039/C9PY00008A.

(28) Higashihara, T.; Inoue, K.; Nagura, M.; Hirao, A. Successive synthesis of well-defined star-branched polymers by an iterative approach based on living anionic polymerization. *Macromol. Res.* **2006**, *14* (3), 287–299. DOI: 10.1007/BF03219084.

(29) Bai, H.; Leng, X.; Han, L.; Yang, L.; Li, C.; Shen, H.; Lei, L.; Zhang, S.; Wang, X.; Ma, H. Thermally Controlled On/Off Switch in a Living Anionic Polymerization of 1-Cyclopropylvinylbenzene with an Anion Migrated Ring-Opening Mechanism. *Macromolecules* **2020**. DOI: 10.1021/acs.macromol.0c01589.

(30) Tomita, R.; Yasu, Y.; Koike, T.; Akita, M. Direct C-H trifluoromethylation of di- and trisubstituted alkenes by photoredox catalysis. *Beilstein journal of organic chemistry* **2014**, *10*, 1099–1106. DOI: 10.3762/bjoc.10.108.

(31) Batesky, D. C.; Goldfogel, M. J.; Weix, D. J. Removal of Triphenylphosphine Oxide by Precipitation with Zinc Chloride in Polar Solvents. *The Journal of organic chemistry* **2017**, *82* (19), 9931–9936. DOI: 10.1021/acs.joc.7b00459.

(32) Hadjichristidis, N.; Hirao, A., Eds. *Anionic Polymerization: Principles, Practice, Strength, Consequences and Applications*, 1st ed. 2015; Springer, 2015. DOI: 10.1007/978-4-431-54186-8.

(33) Bönnemann, H.; Brijoux, W. Organocobalt-Catalyzed Synthesis of Pyridines. In *Advances in heterocyclic chemistry: Vol. 48*; Katritzky, A. R., Ed.; Advances in Heterocyclic Chemistry; Academic Press, 1990; pp 177–222. DOI: 10.1016/S0065-2725(08)60339-6.

(34) Schulz, M. F.; Khandpur, A. K.; Bates, F. S.; Almdal, K.; Mortensen, K.; Hajduk, D. A.; Gruner, S. M. Phase Behavior of Polystyrene–Poly(2-vinylpyridine) Diblock Copolymers. *Macromolecules* **1996**, *29* (8), 2857–2867. DOI: 10.1021/ma951714a.

(35) Zha, W.; Han, C. D.; Moon, H. C.; Han, S. H.; Lee, D. H.; Kim, J. K. Exfoliation of organoclay nanocomposites based on polystyrene-block-polyisoprene-block-poly(2-vinylpyridine) copolymer: Solution blending versus melt blending. *Polymer* **2010**, *51* (4), 936–952. DOI: 10.1016/j.polymer.2009.12.030.

(36) Zhou, Z.-L.; Eisenberg, A. Ionomeric blends. II. Compatibility and dynamic mechanical properties of sulfonated cis-1,4-polyisoprenes and styrene/4-vinylpyridine copolymer blends. *J. Polym. Sci. Polym. Phys. Ed.* **1983**, *21* (4), 595–603. DOI: 10.1002/pol.1983.180210409.

## 6.8 Supporting Information

### *m*-PyPE characterisation

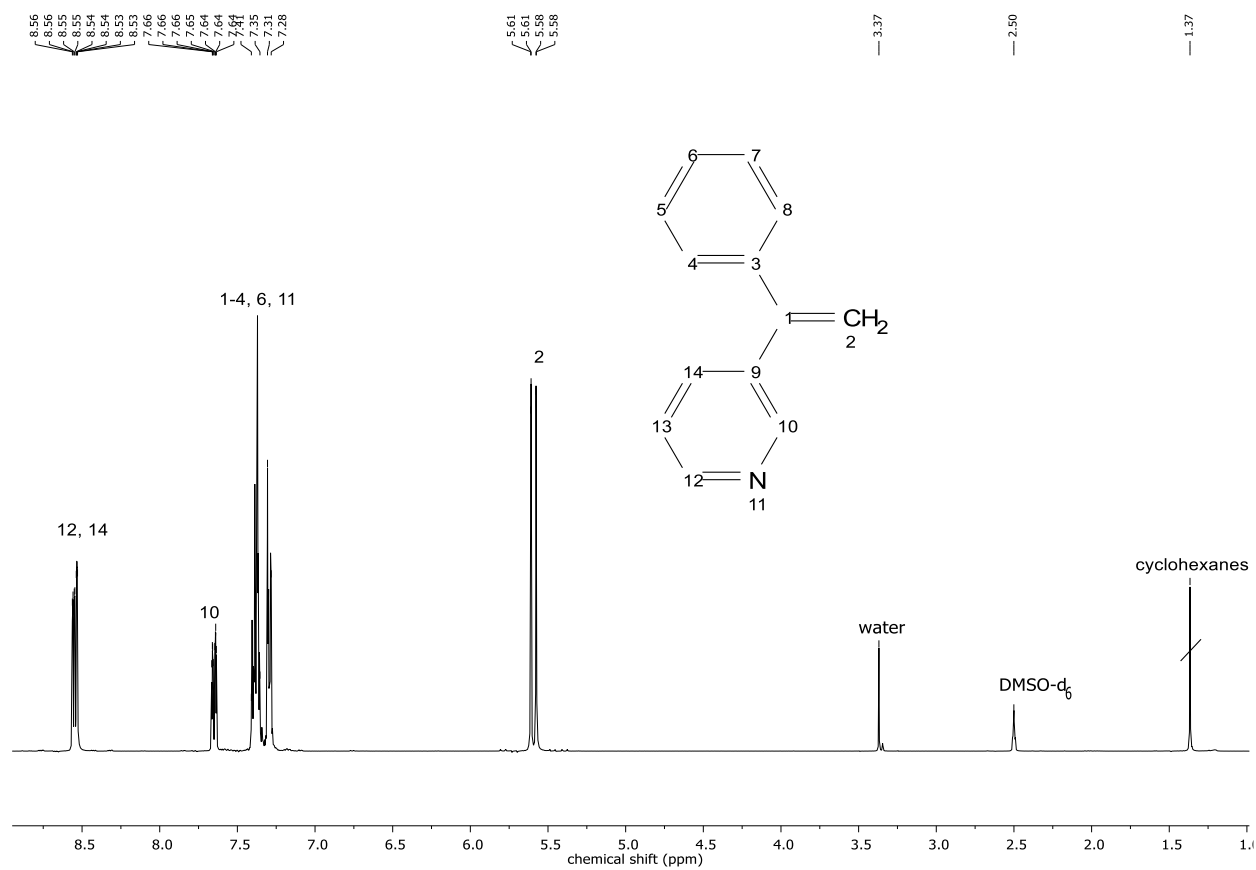


Figure S1:  $^1\text{H}$  NMR spectrum (400 MHz,  $\text{DMSO-d}_6$ ) of *m*-PyPE.



Chapter 2 – Introducing a 1,1-diphenylethylene analogue for vinylpyridine: anionic copolymerisation of 3-(1-phenylvinyl)pyridine (m-PyPE) - Supporting Information

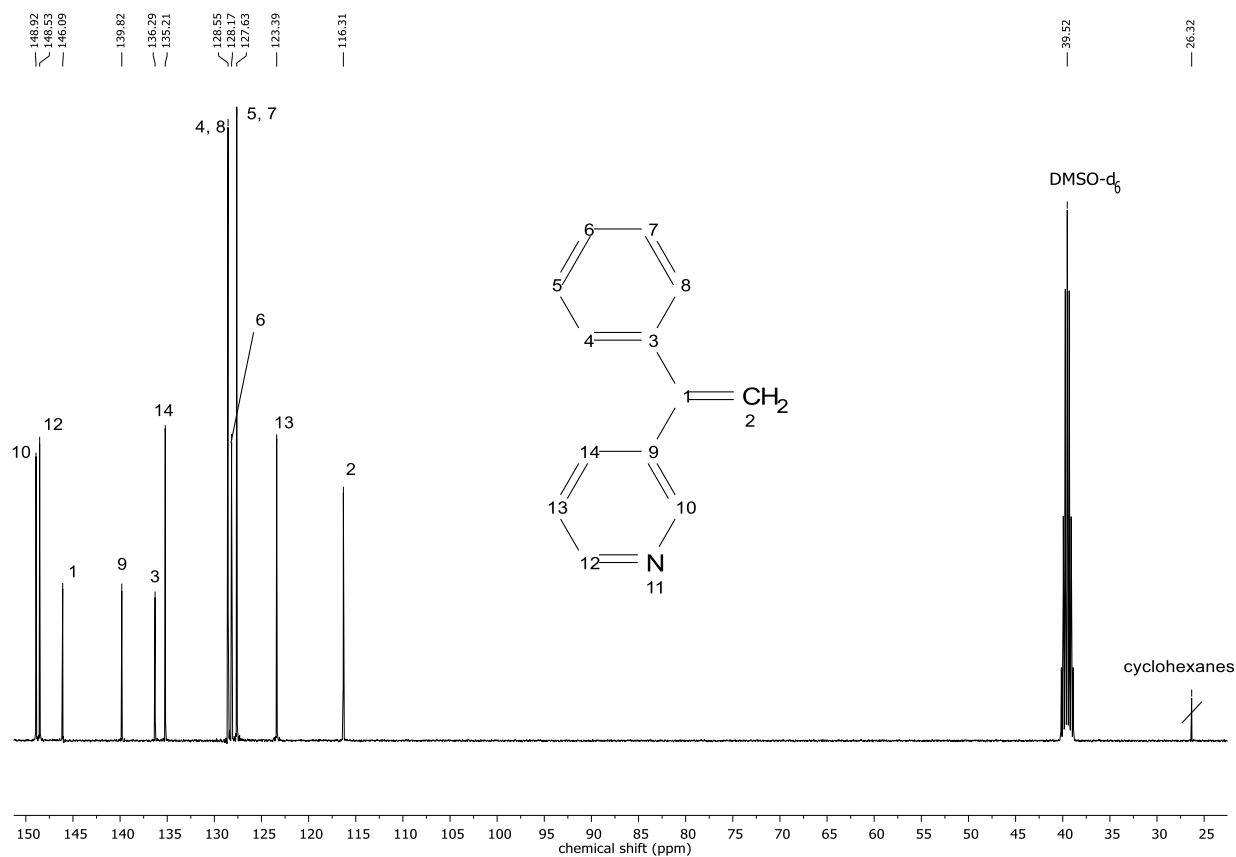


Figure S2: <sup>13</sup>C NMR spectrum (400 MHz, DMSO-d<sub>6</sub>) of m-PyPE.

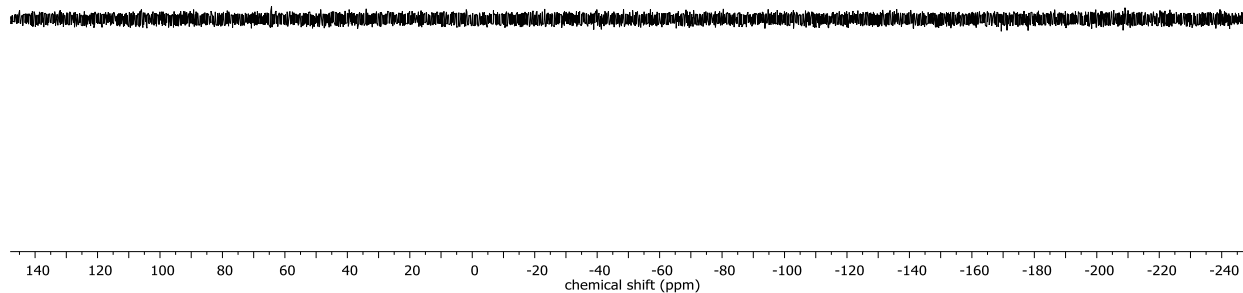


Figure S3: <sup>31</sup>P NMR spectrum (400 MHz, DMSO-d<sub>6</sub>) of m-PyPE, showing the absence of TPPO.

Chapter 2 – Introducing a 1,1-diphenylethylene analogue for vinylpyridine: anionic copolymerisation of 3-(1-phenylvinyl)pyridine (m-PyPE) - Supporting Information

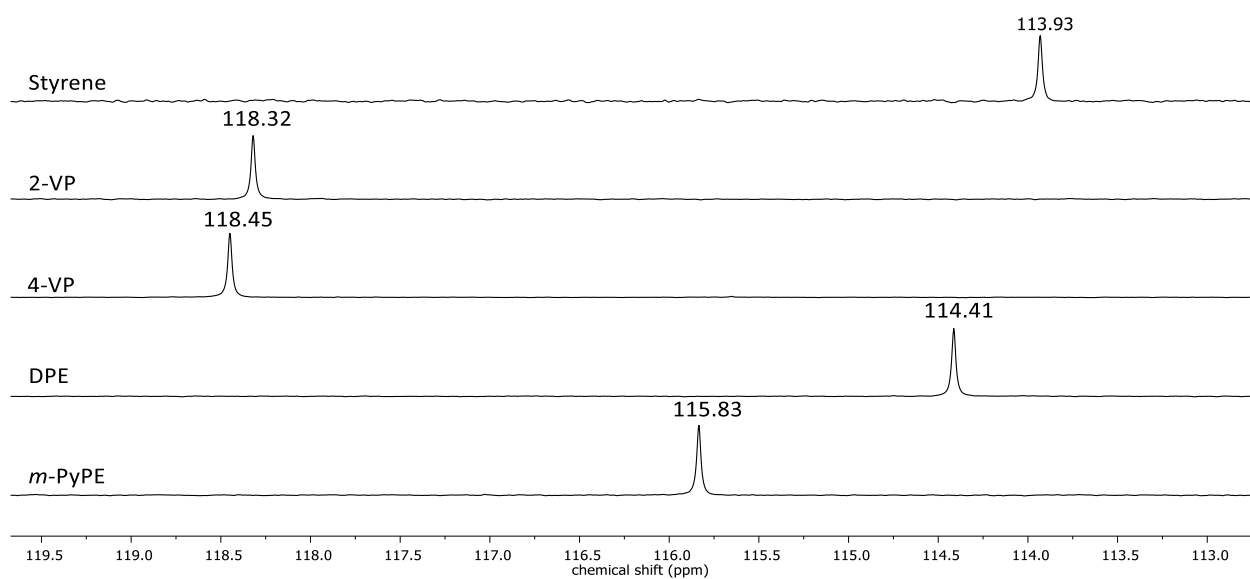


Figure S4:  $^{13}\text{C}$  NMR spectrum (400 MHz,  $\text{CDCl}_3$ ) of different monomers, showing the respective  $\beta$ -carbon shifts.

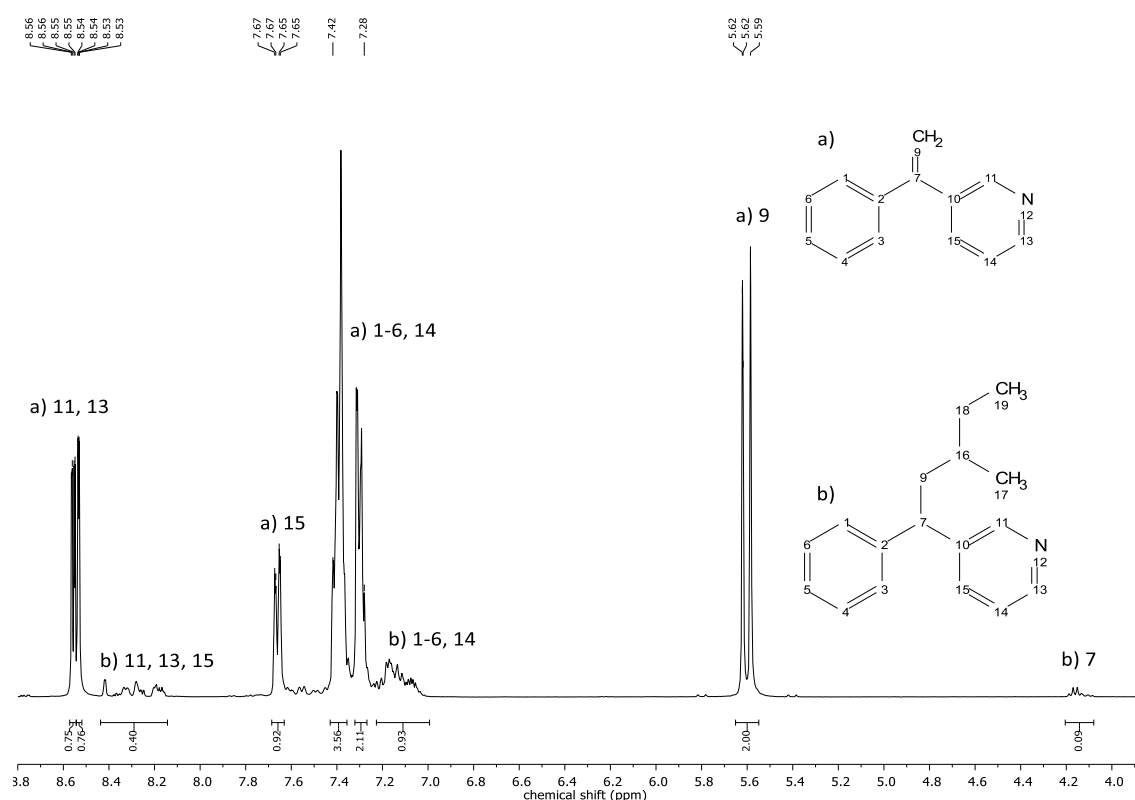


Figure S5:  $^1\text{H}$  NMR spectrum (400 MHz,  $\text{DMSO-d}_6$ ) of *s*-BuLi initiated m-PyPE, showing only the addition of the butyl group and no polymerisation products.

### Copolymer NMR spectroscopy characterisation

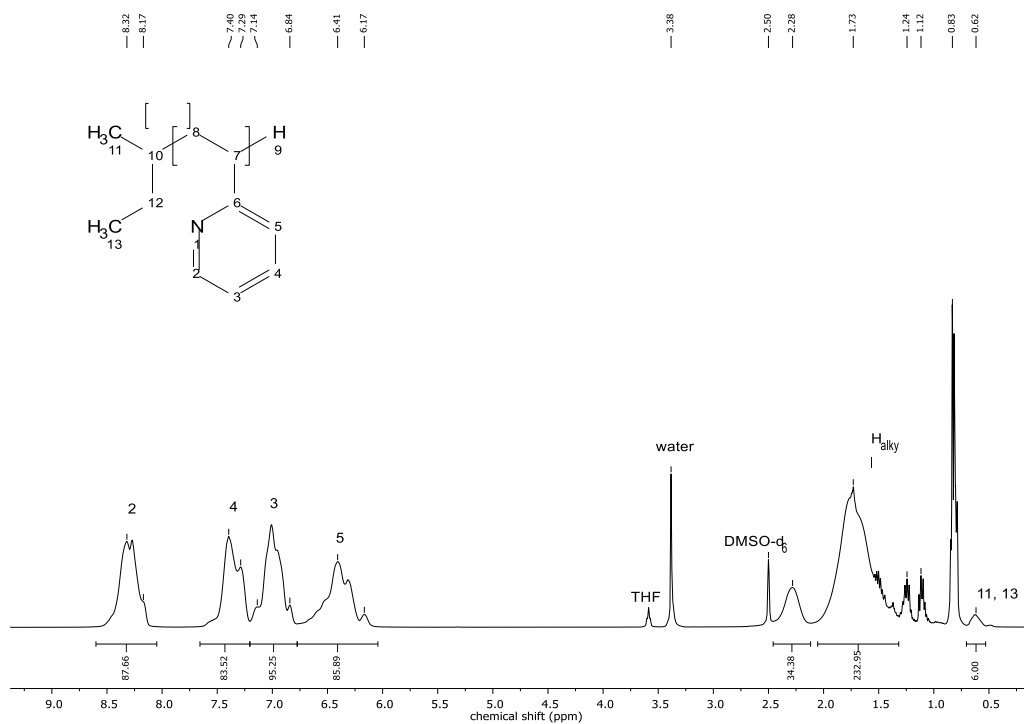


Figure S6: <sup>1</sup>H NMR spectrum (DMSO-d<sub>6</sub>, 400 MHz) of P(2-VP).

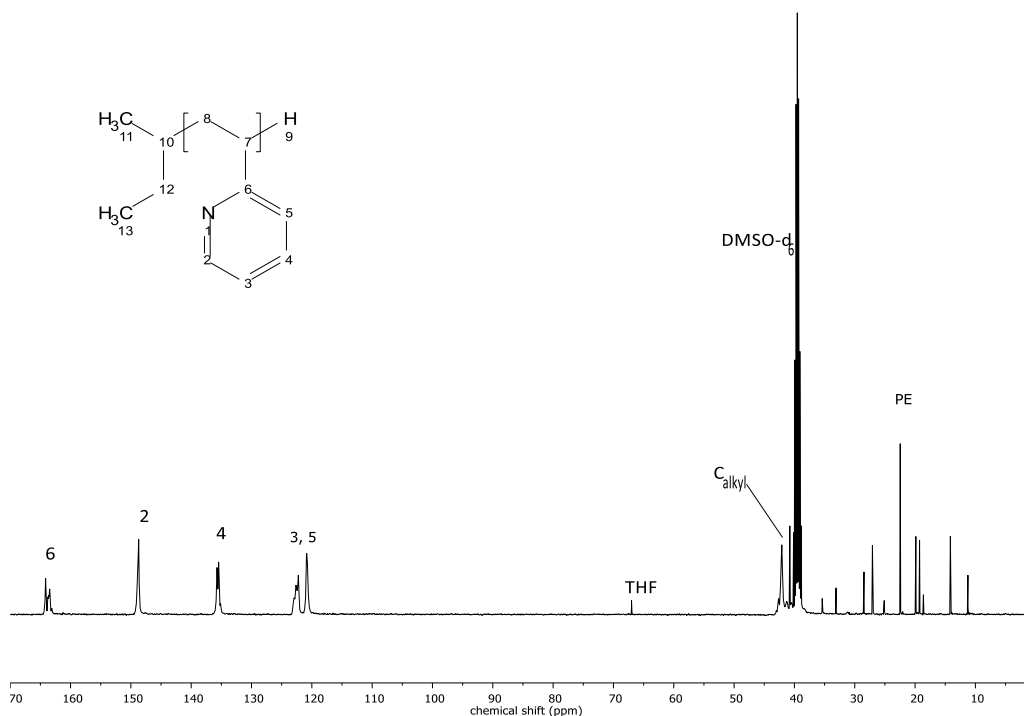


Figure S7: IG <sup>13</sup>C NMR spectrum (DMSO-d<sub>6</sub>, 400 MHz) of P(2-VP).

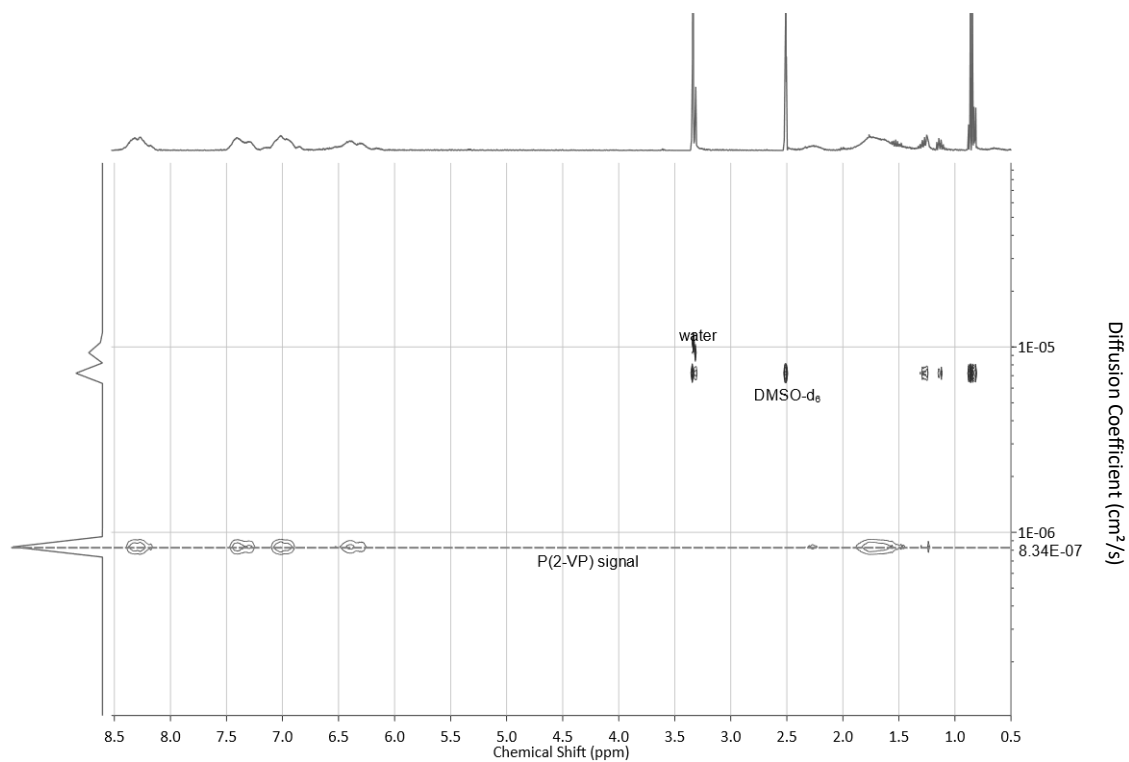


Figure S8: DOSY NMR spectrum (DMSO-*d*<sub>6</sub>, 400 MHz) of P(2-VP).

Chapter 2 – Introducing a 1,1-diphenylethylene analogue for vinylpyridine: anionic copolymerisation of 3-(1-phenylvinyl)pyridine (m-PyPE) - Supporting Information

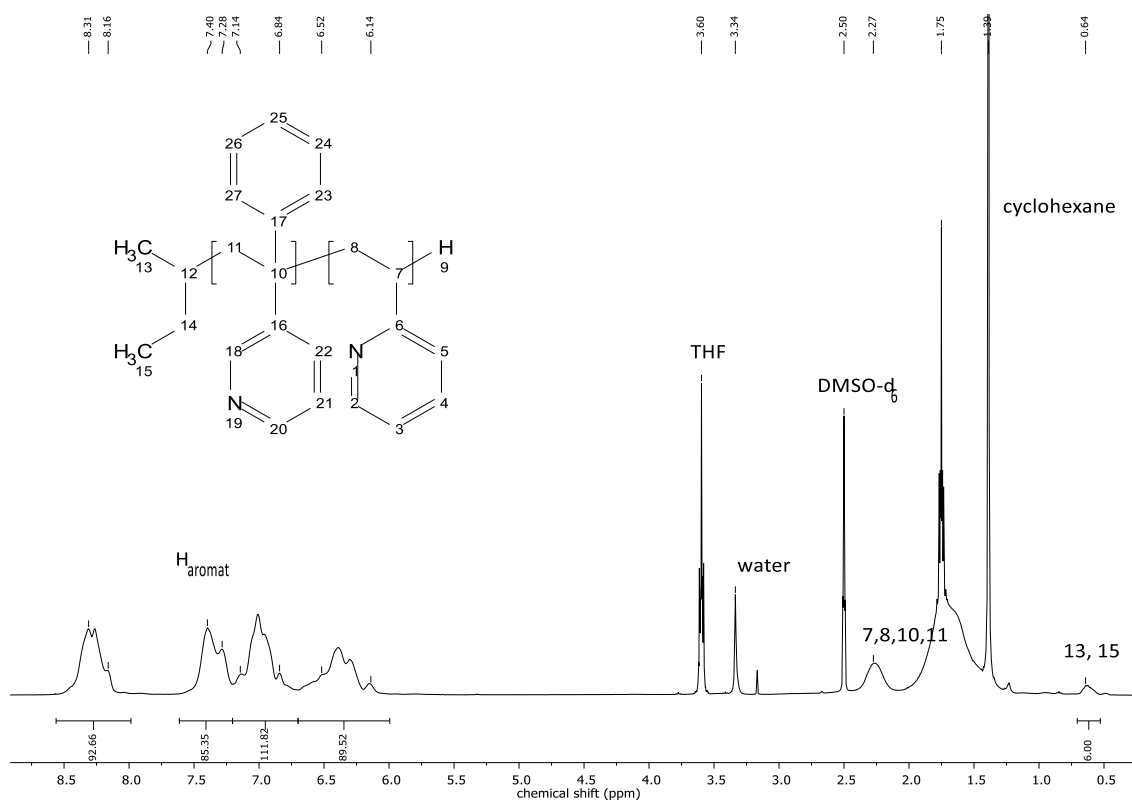


Figure S9: <sup>1</sup>H NMR spectrum (DMSO-d<sub>6</sub>, 400 MHz) of P(2-VP-stat-m-PyPE); 5% m-PyPE.

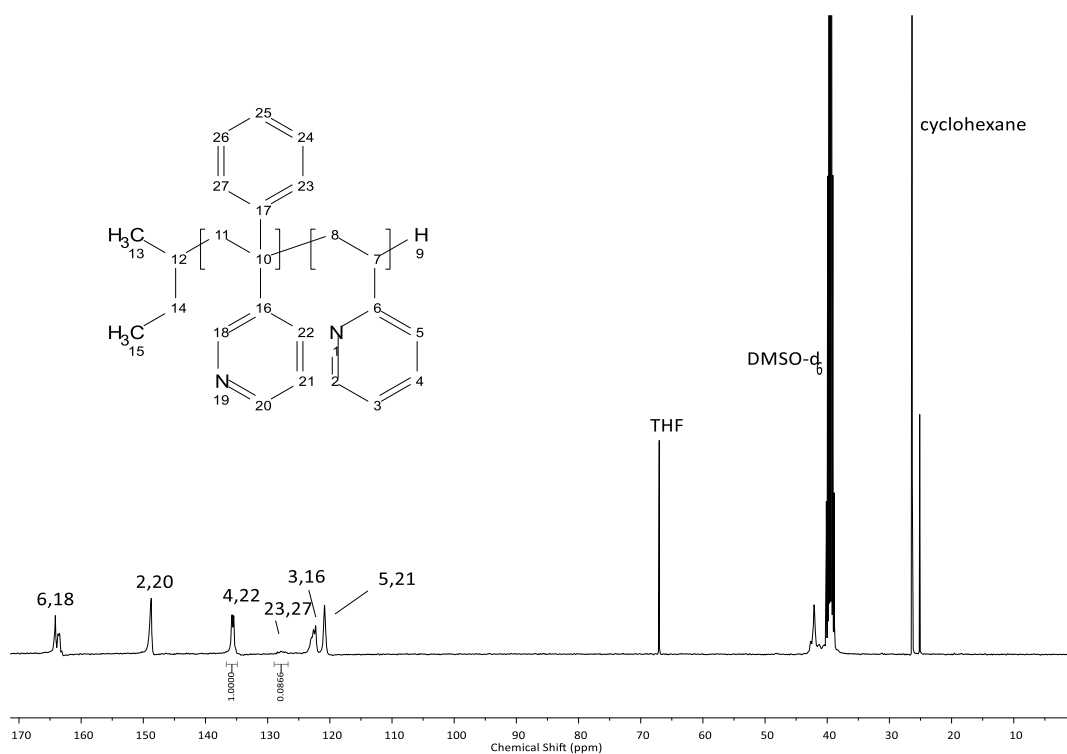


Figure S10: IG <sup>13</sup>C NMR spectrum (DMSO-d<sub>6</sub>, 400 MHz) of P(2-VP-stat-m-PyPE); 5% m-PyPE.

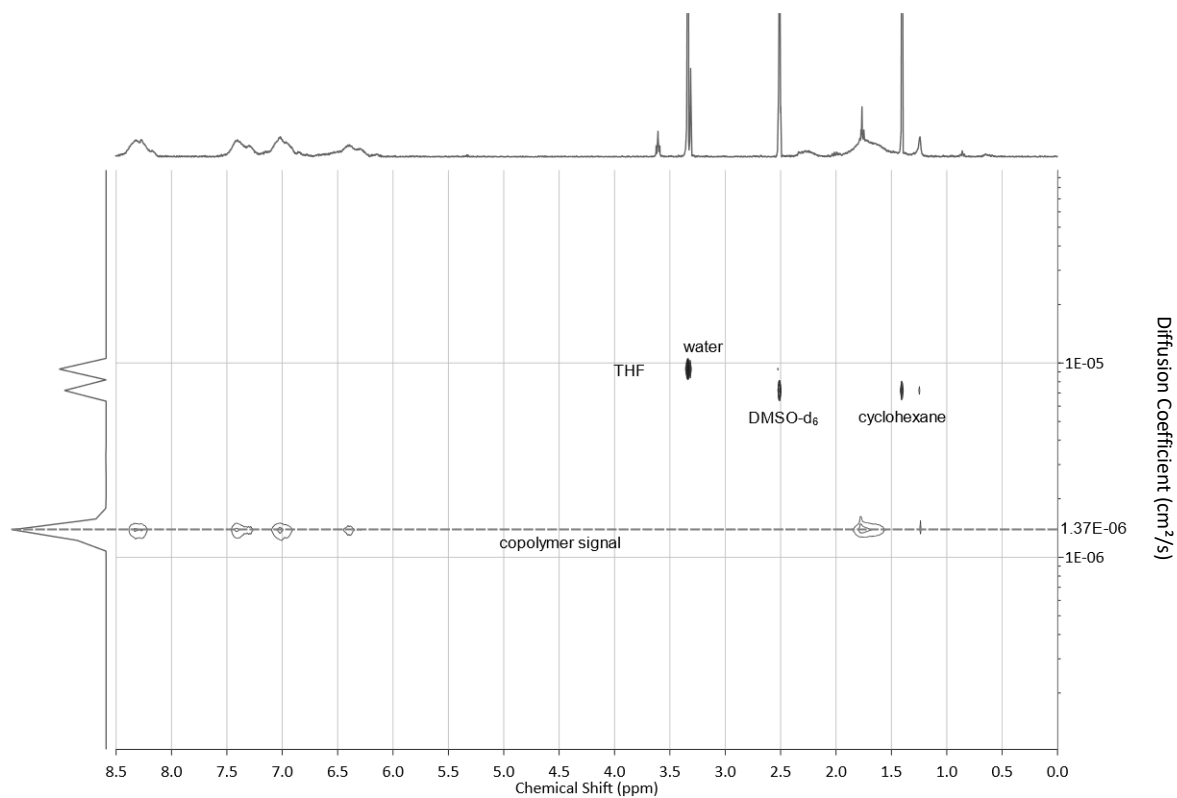


Figure S11: DOSY NMR spectrum (DMSO-d<sub>6</sub>, 400 MHz) of P(2-VP-stat-m-PyPE); 5% m-PyPE.

Chapter 2 – Introducing a 1,1-diphenylethylene analogue for vinylpyridine: anionic copolymerisation of 3-(1-phenylvinyl)pyridine (m-PyPE) - Supporting Information

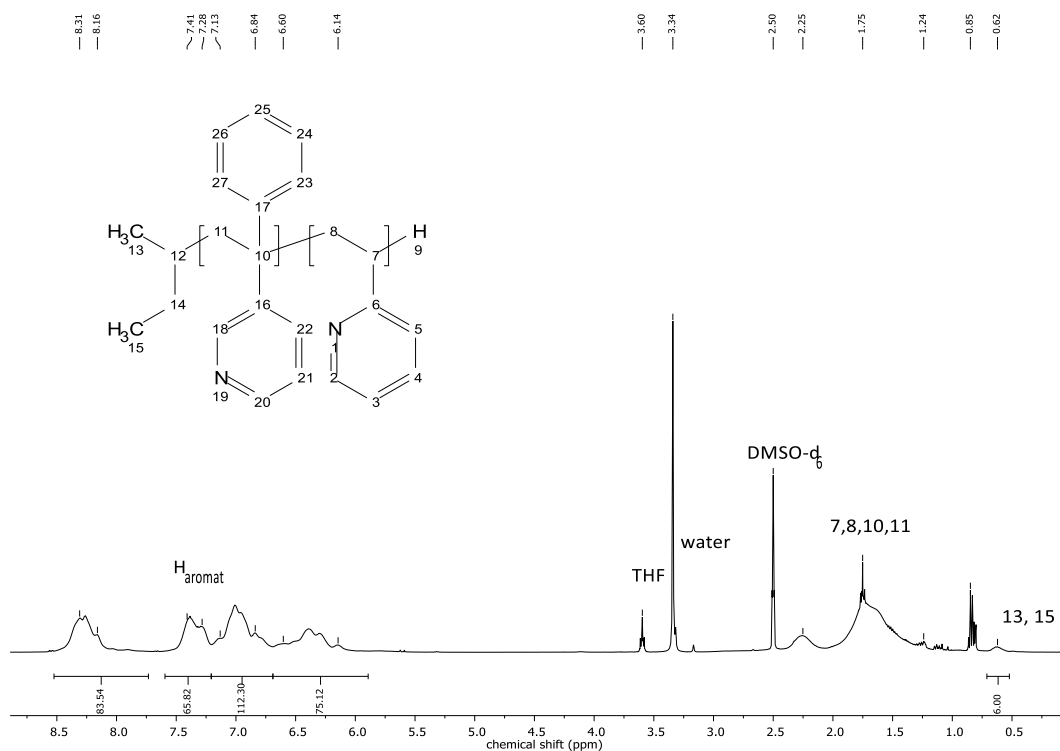


Figure S12: <sup>1</sup>H NMR spectrum (DMSO-d<sub>6</sub>, 400 MHz) of P(2-VP-stat-m-PyPE); 10% m-PyPE.

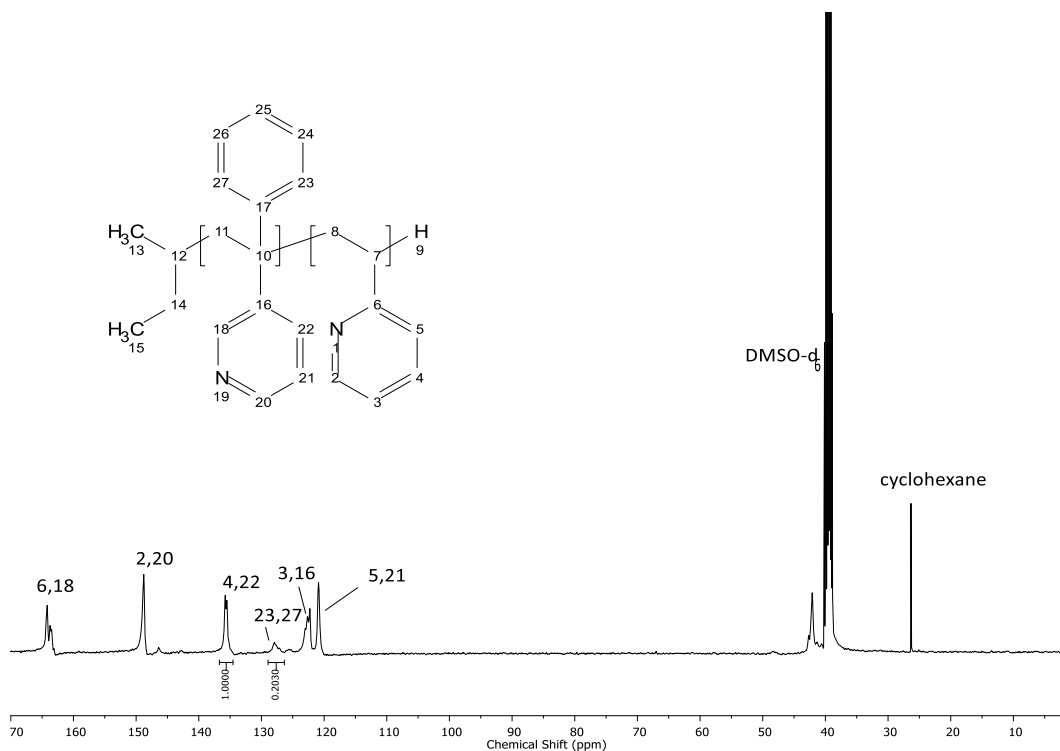


Figure S13: IG <sup>13</sup>C NMR spectrum (DMSO-d<sub>6</sub>, 400 MHz) of P(2-VP-stat-m-PyPE); 10% m-PyPE.

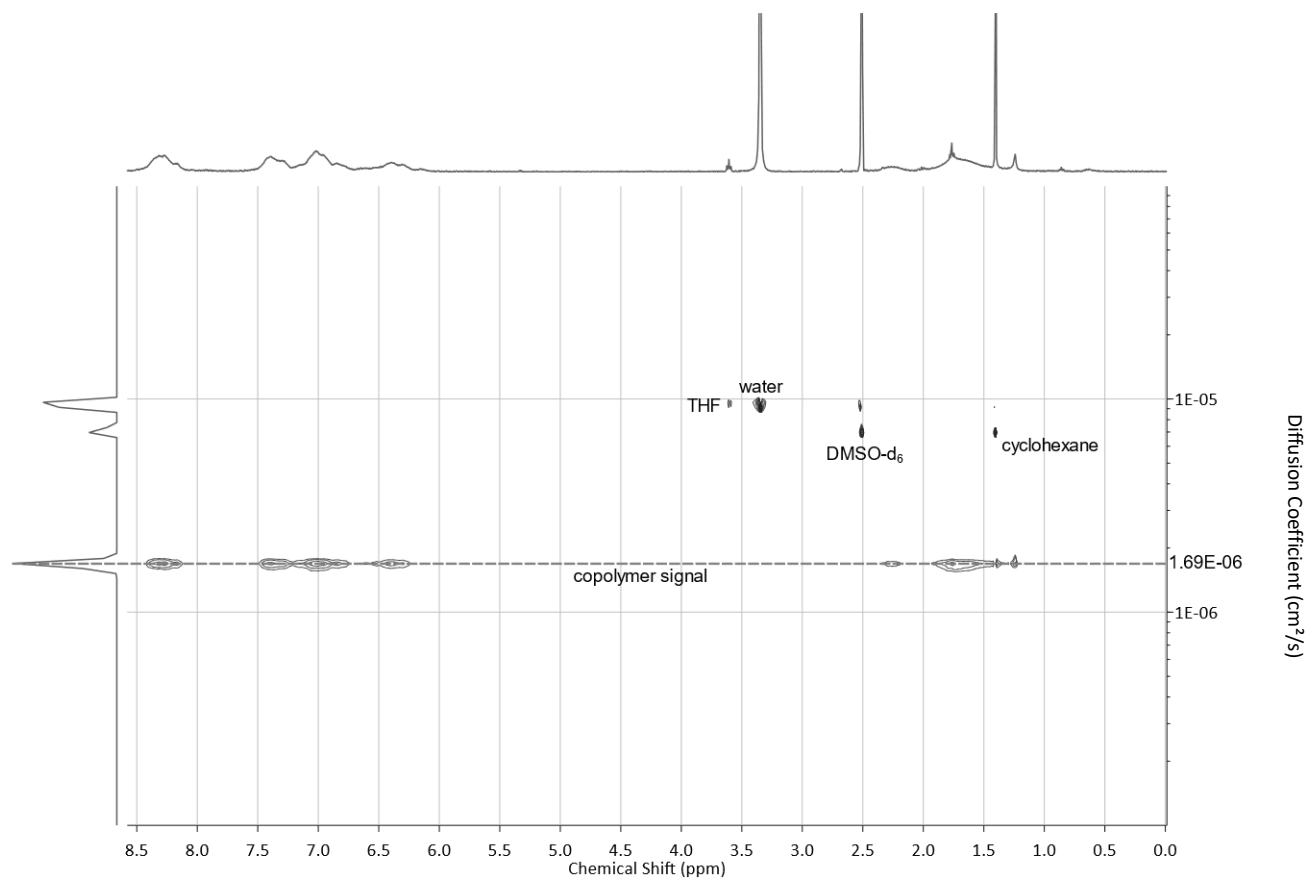


Figure S14: DOSY NMR spectrum (DMSO-d<sub>6</sub>, 400 MHz) of P(2-VP-stat-m-PyPE); 10% m-PyPE.



Chapter 2 – Introducing a 1,1-diphenylethylene analogue for vinylpyridine: anionic copolymerisation of 3-(1-phenylvinyl)pyridine (m-PyPE) - Supporting Information

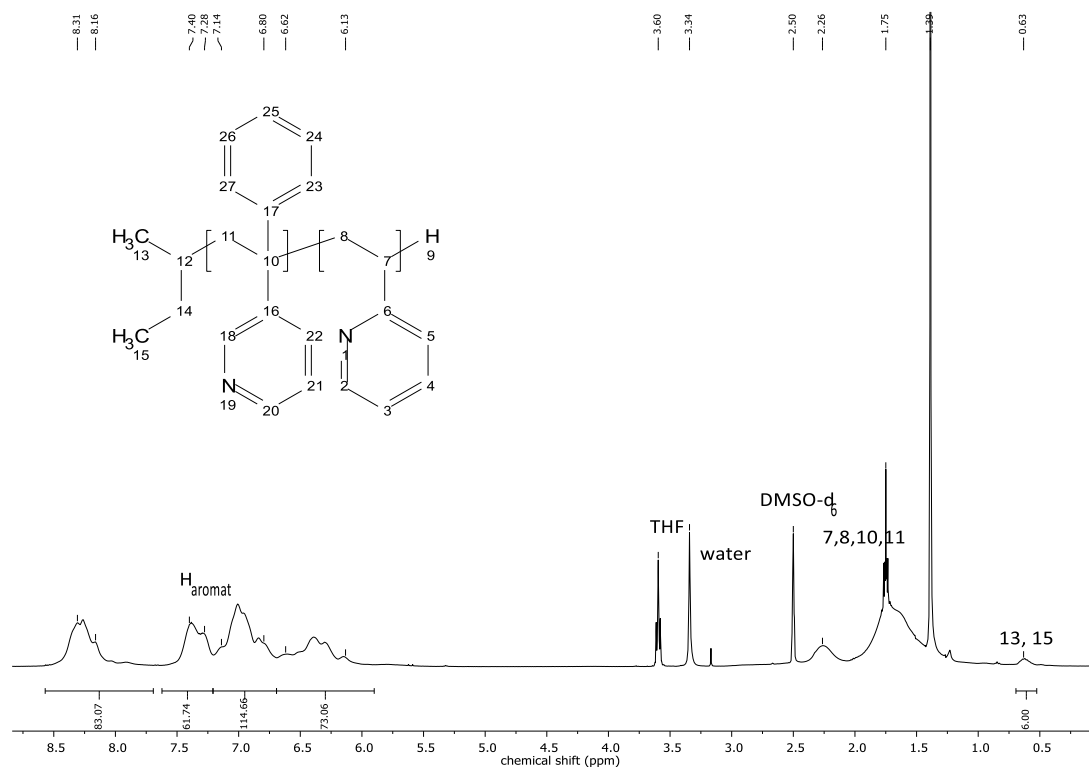


Figure S15: <sup>1</sup>H NMR spectrum (DMSO-d<sub>6</sub>, 400 MHz) of P(2-VP-stat-m-PyPE); 15% m-PyPE.

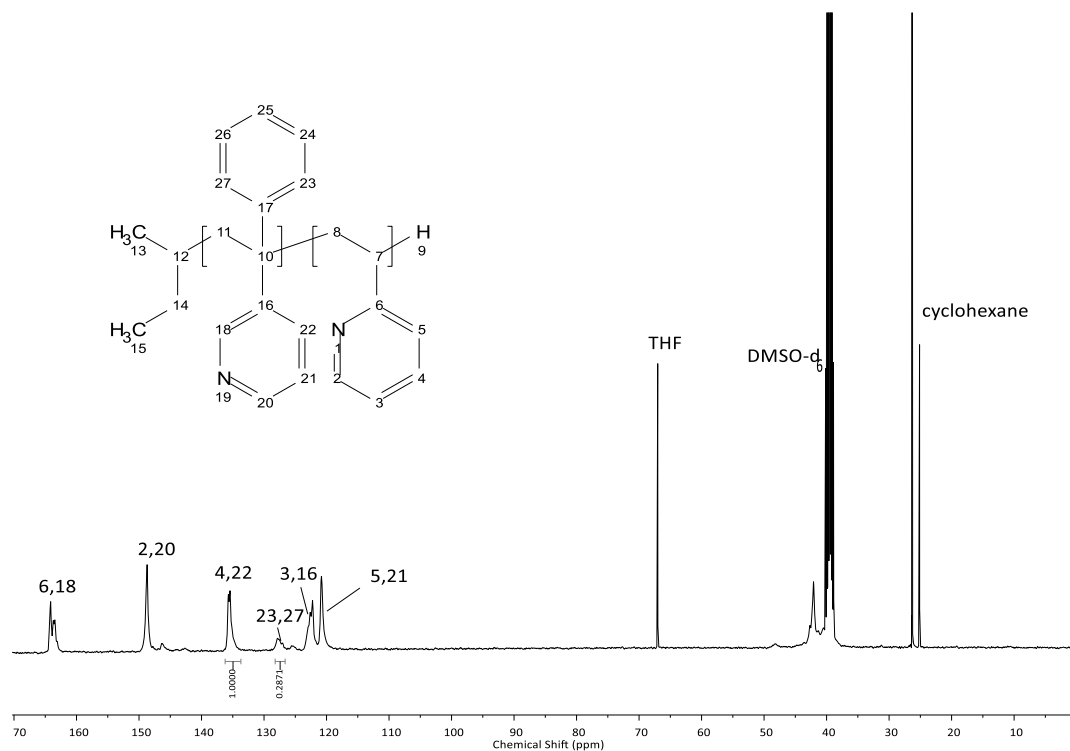


Figure S16: IG <sup>13</sup>C NMR spectrum (DMSO-d<sub>6</sub>, 400 MHz) of P(2-VP-stat-m-PyPE); 15% m-PyPE.

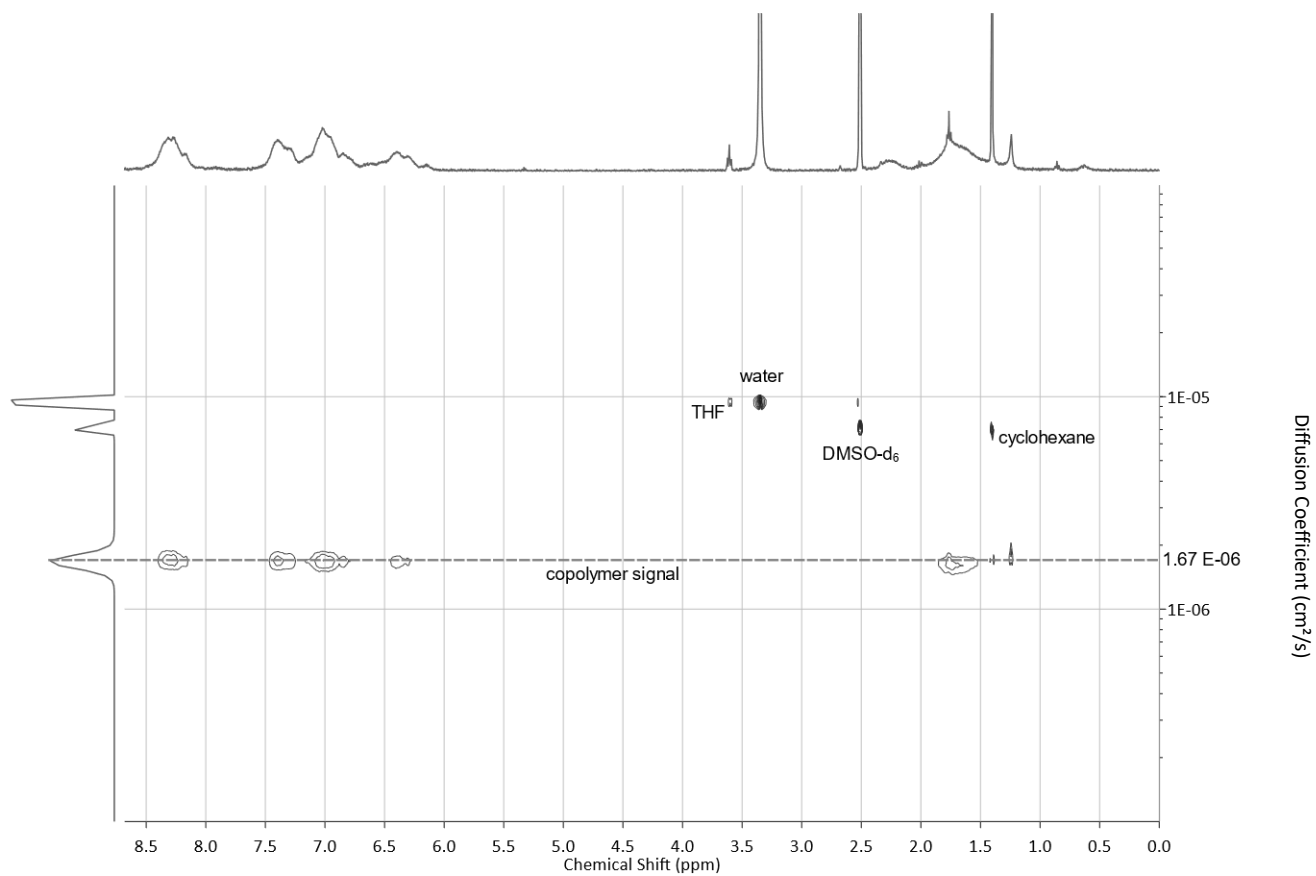


Figure S17: DOSY NMR spectrum (DMSO-d<sub>6</sub>, 400 MHz) of P(2-VP-stat-m-PyPE); 15% m-PyPE.

Chapter 2 – Introducing a 1,1-diphenylethylene analogue for vinylpyridine: anionic copolymerisation of 3-(1-phenylvinyl)pyridine (m-PyPE) - Supporting Information

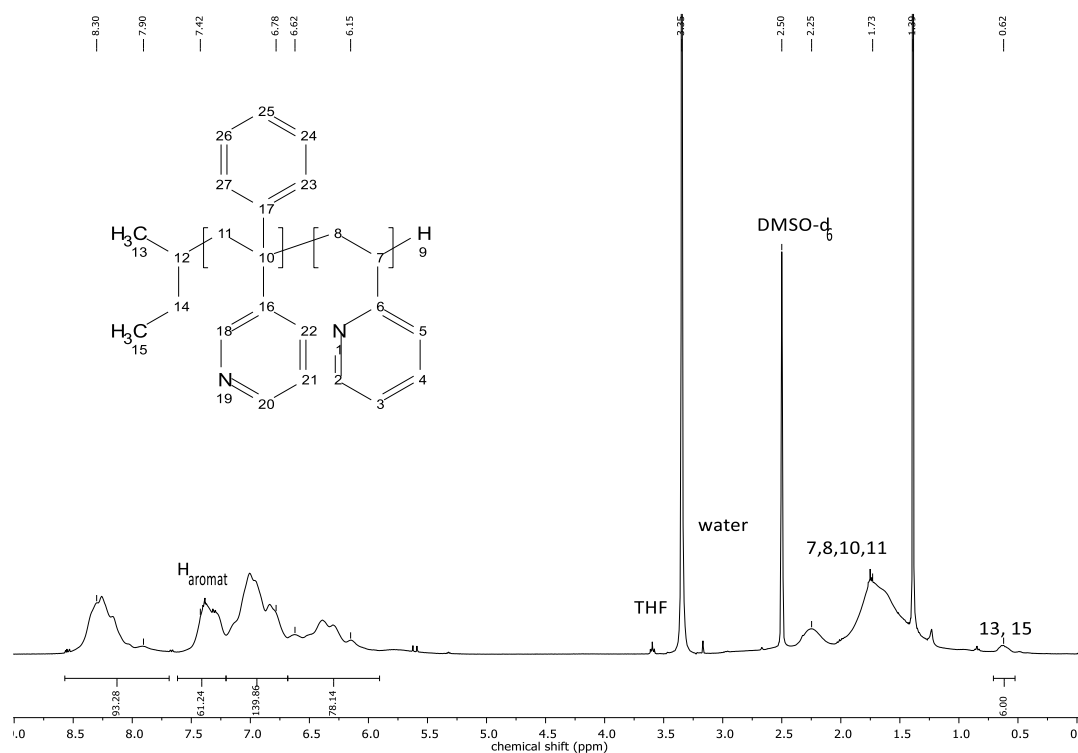


Figure S18: <sup>1</sup>H NMR spectrum (DMSO-d<sub>6</sub>, 400 MHz) of P(2-VP-stat-m-PyPE); 20% m-PyPE.

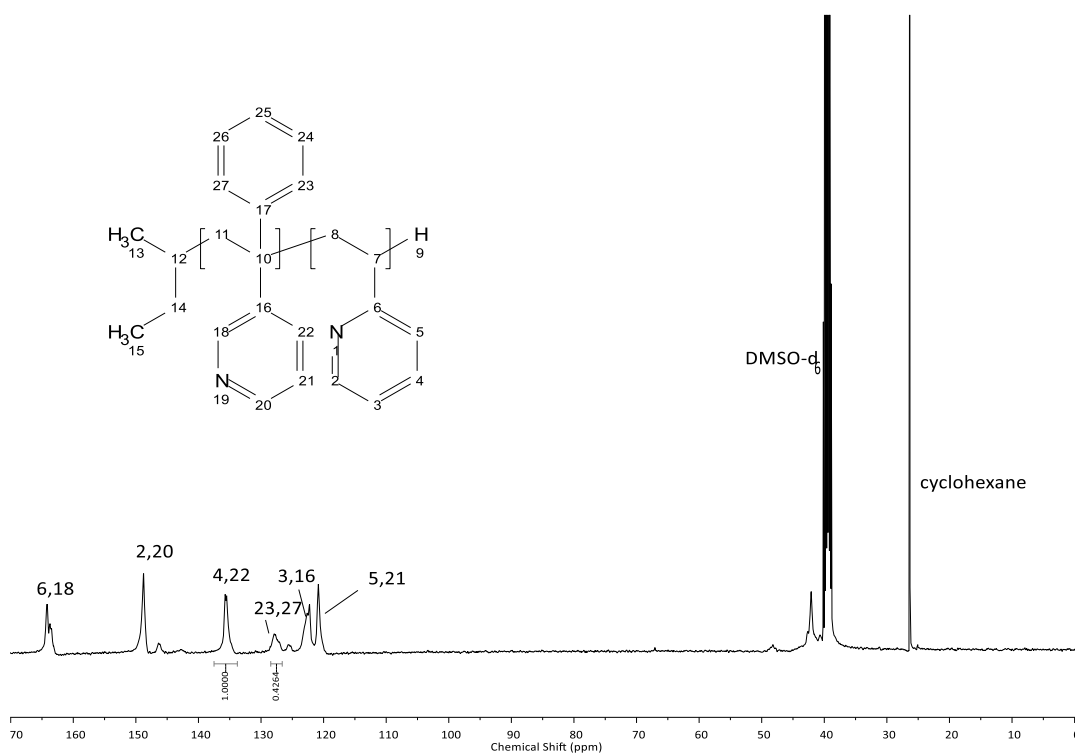


Figure S19: IG <sup>13</sup>C NMR spectrum (DMSO-d<sub>6</sub>, 400 MHz) of P(2-VP-stat-m-PyPE); 20% m-PyPE.

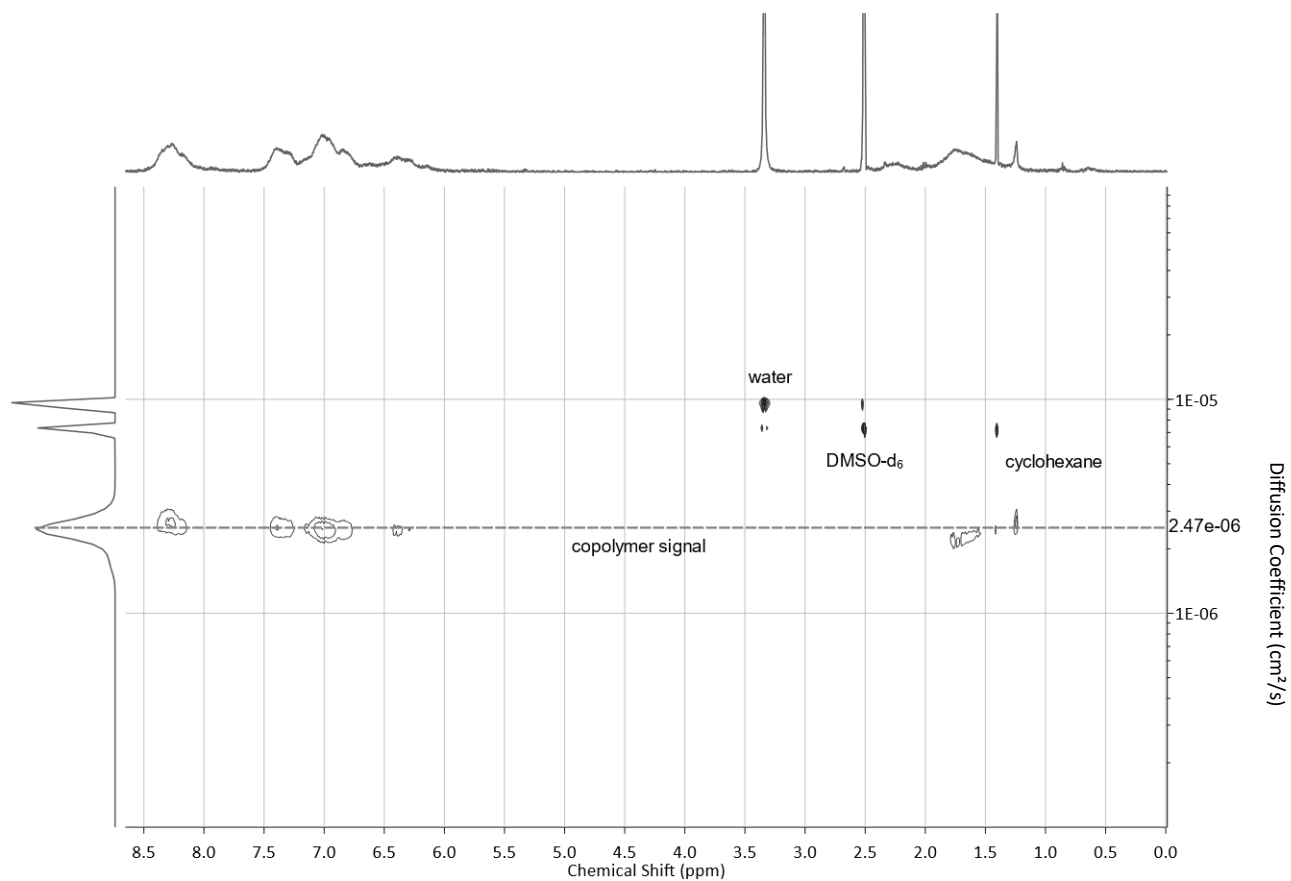


Figure S20: DOSY NMR spectrum (DMSO-d<sub>6</sub>, 400 MHz) of P(2-VP-stat-m-PyPE); 20% m-PyPE.

Chapter 2 – Introducing a 1,1-diphenylethylene analogue for vinylpyridine: anionic copolymerisation of 3-(1-phenylvinyl)pyridine (m-PyPE) - Supporting Information

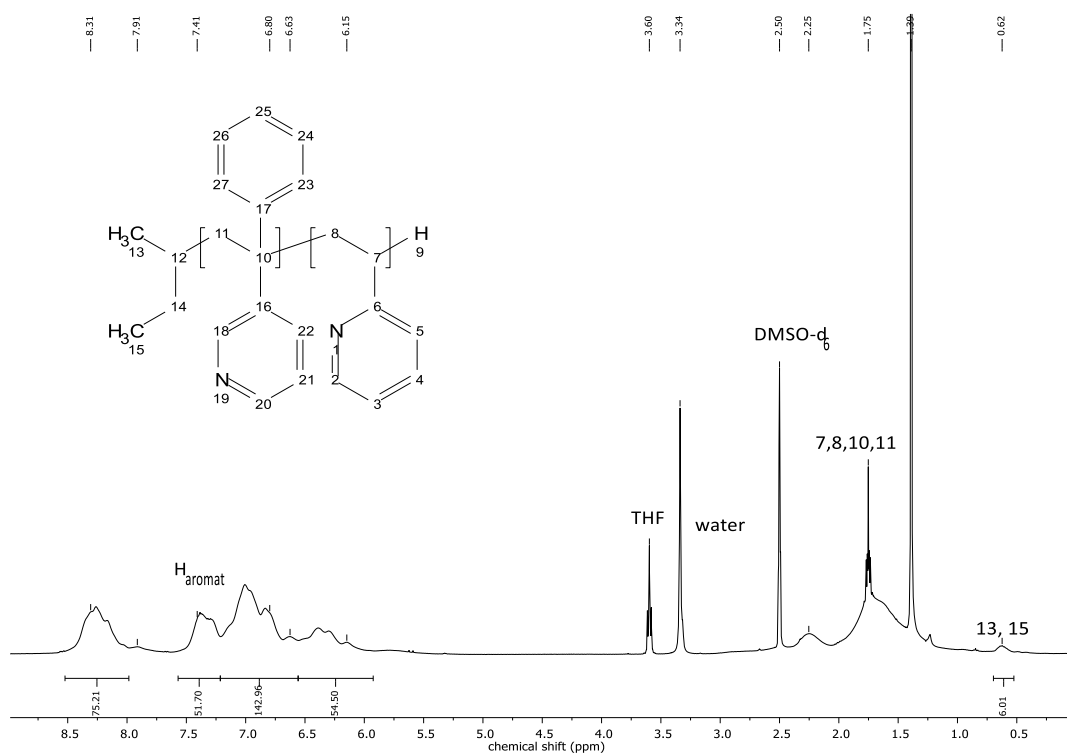


Figure S21: <sup>1</sup>H NMR spectrum (DMSO-d<sub>6</sub>, 400 MHz) of P(2-VP-stat-m-PyPE); 25% m-PyPE.

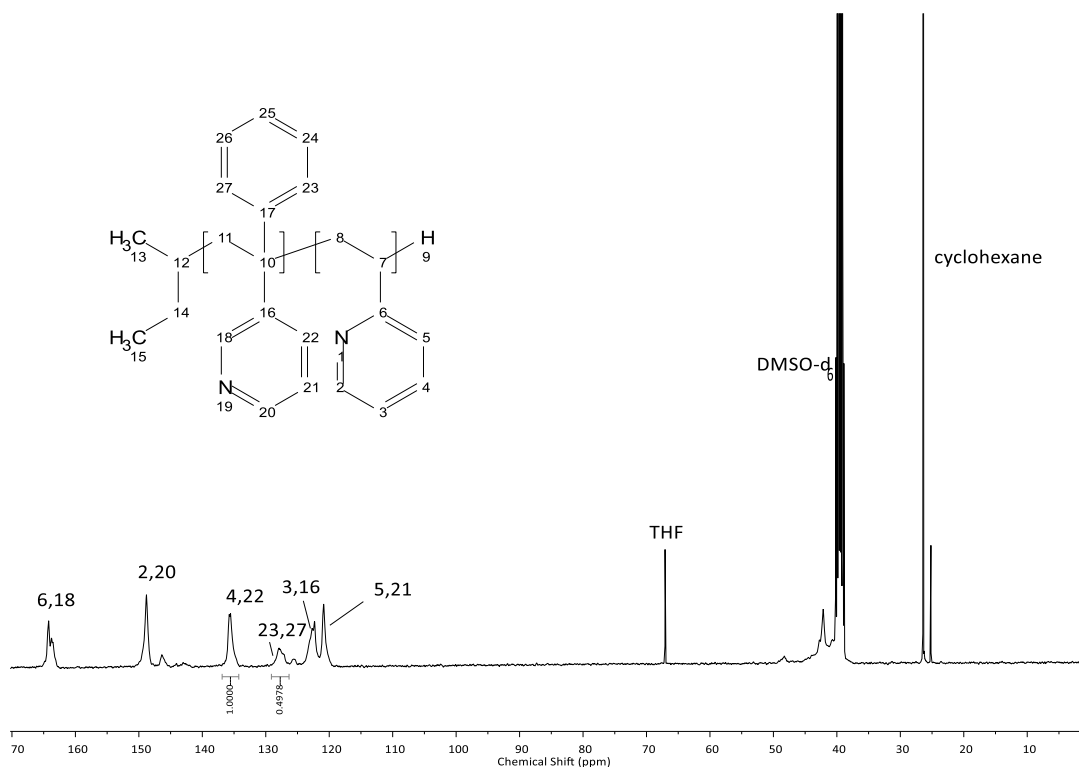


Figure S22: IG <sup>13</sup>C NMR spectrum (DMSO-d<sub>6</sub>, 400 MHz) of P(2-VP-stat-m-PyPE); 25% m-PyPE.

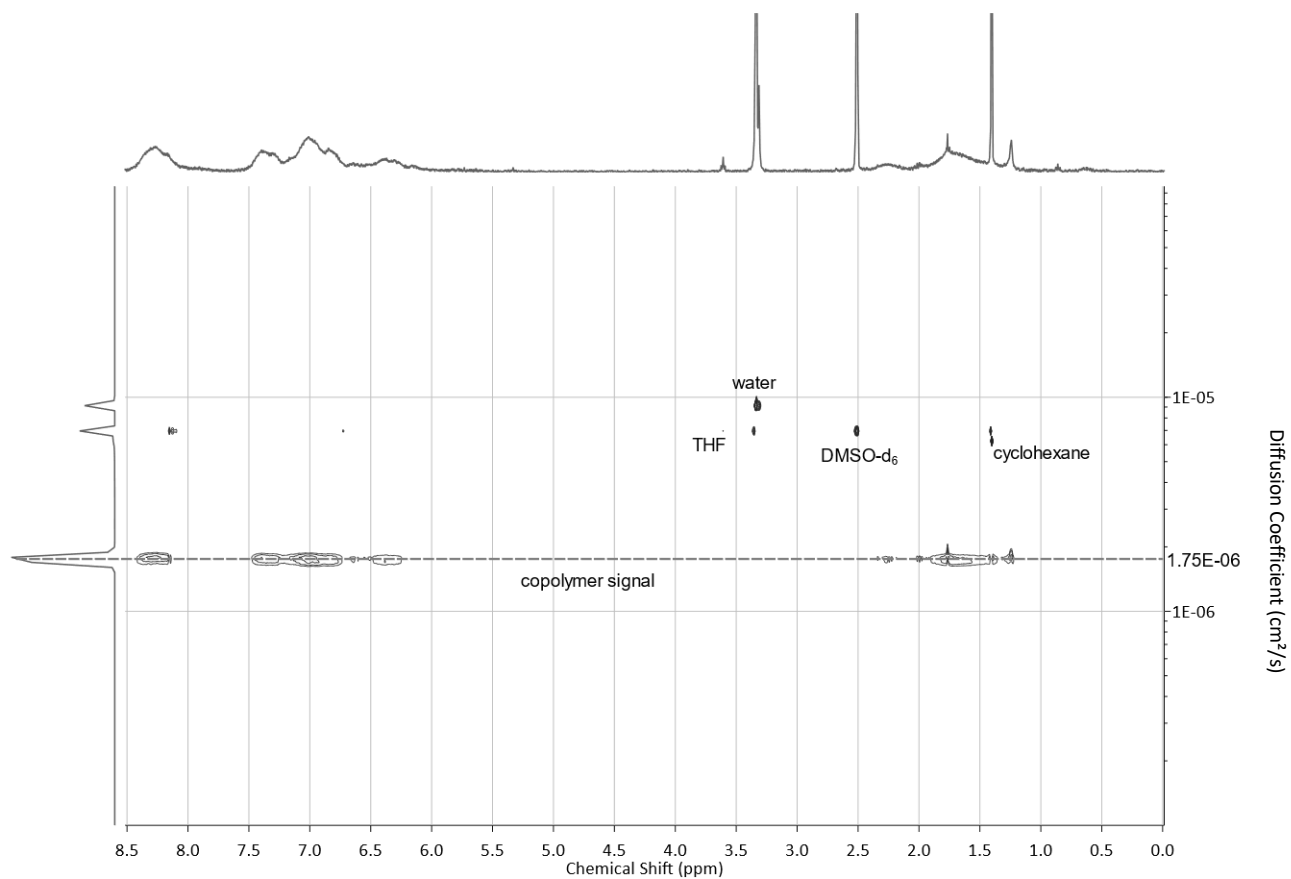


Figure S23: DOSY NMR spectrum (DMSO- $d_6$ , 400 MHz) of P(2-VP-stat-m-PyPE); 25% m-PyPE.

## Differential scanning calorimetry

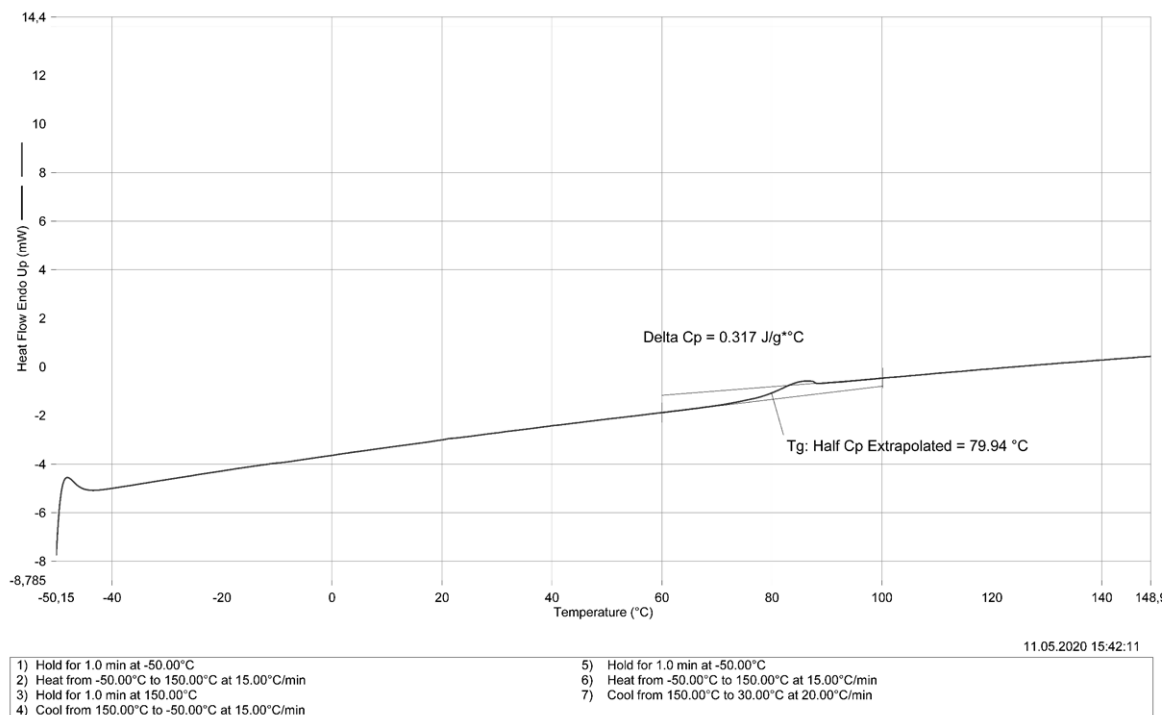


Figure S24: DSC curve of P(2-VP).

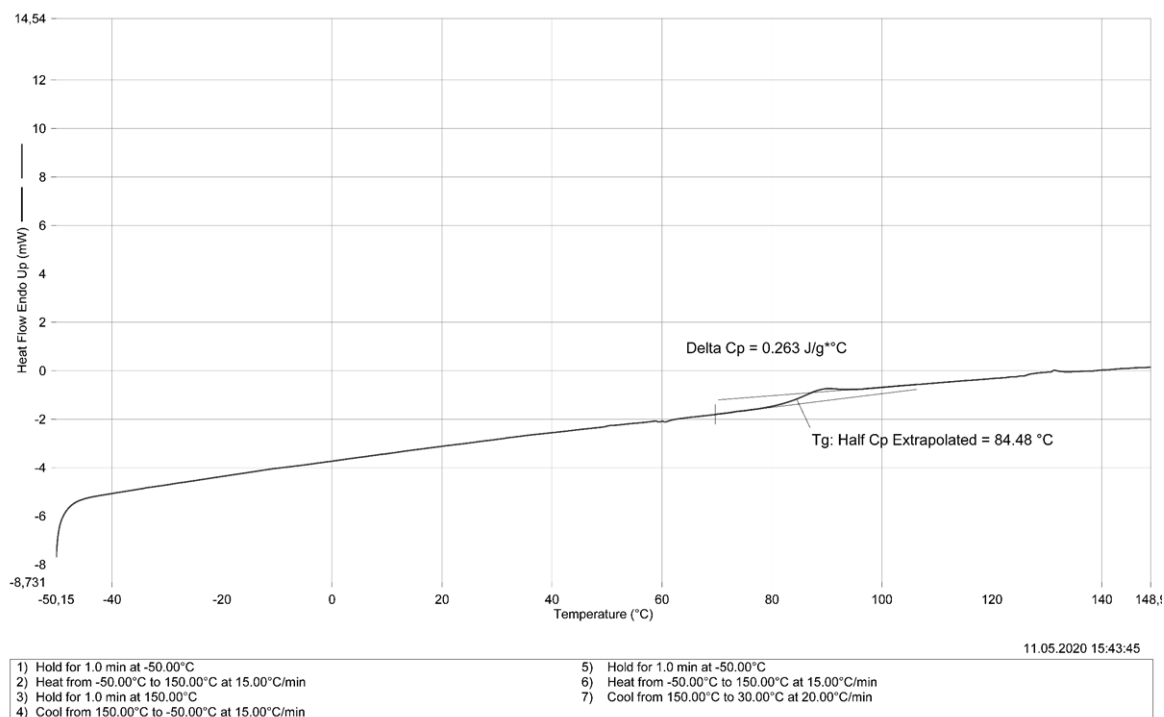


Figure S25: DSC curve of P(2-VP-stat-m-PyPE); 5% m-PyPE.

## Chapter 2 – Introducing a 1,1-diphenylethylene analogue for vinylpyridine: anionic copolymerisation of 3-(1-phenylvinyl)pyridine (m-PyPE) - Supporting Information

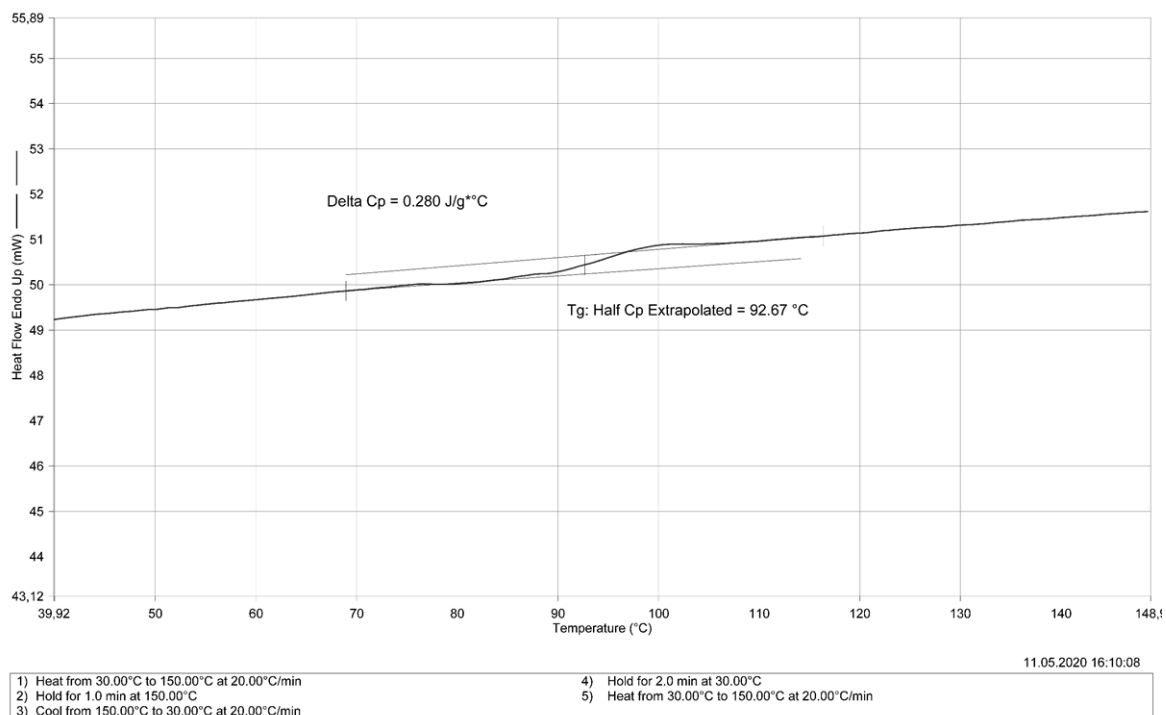


Figure S26: DSC curve of P(2-VP-stat-m-PyPE); 10% m-PyPE.

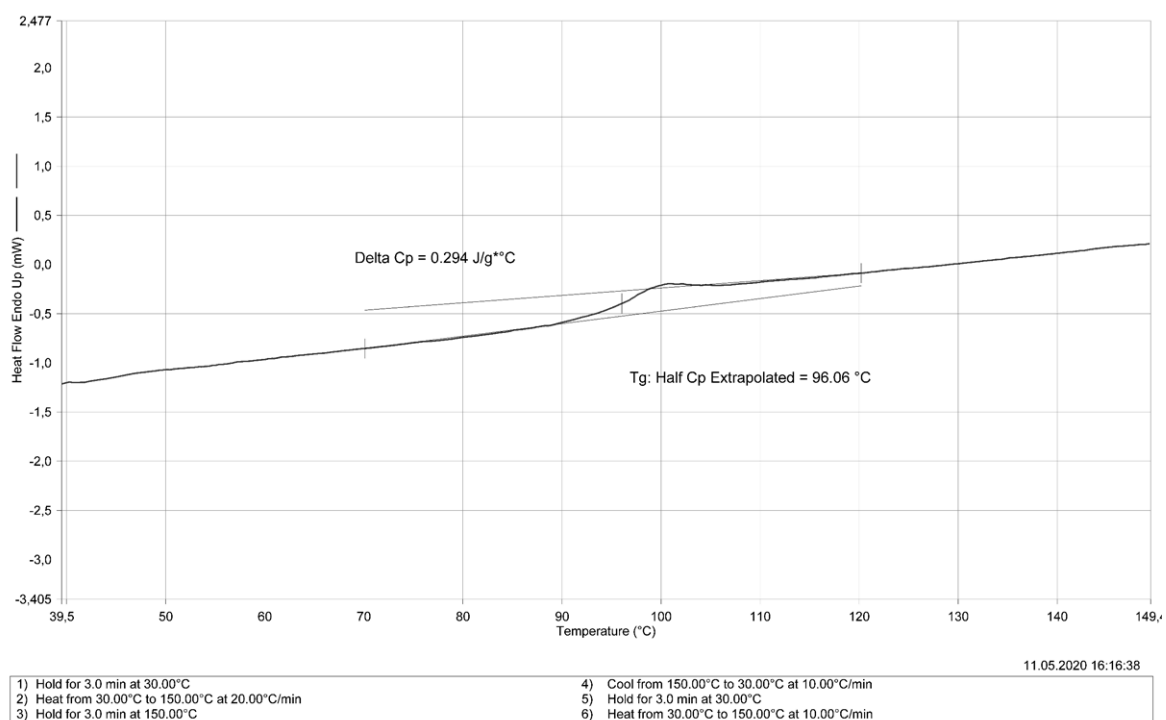


Figure S27: DSC curve of P(2-VP-stat-m-PyPE); 15% m-PyPE.



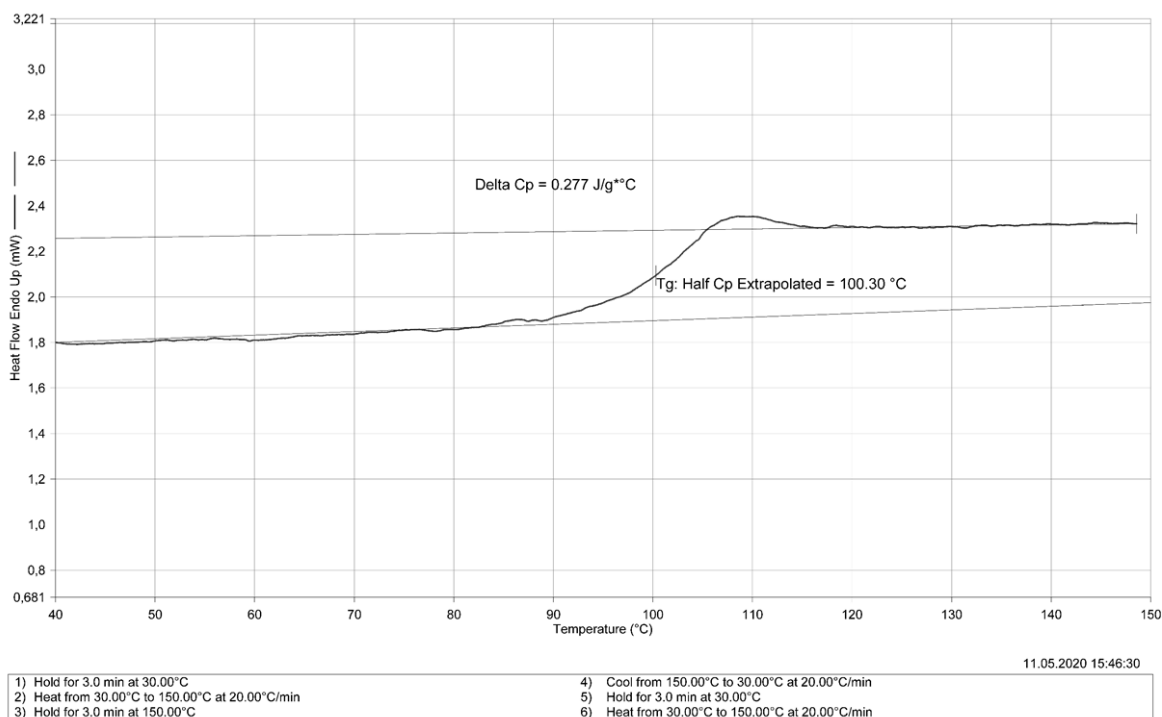


Figure S28: DSC curve of P(2-VP-stat-m-PyPE); 20% m-PyPE.

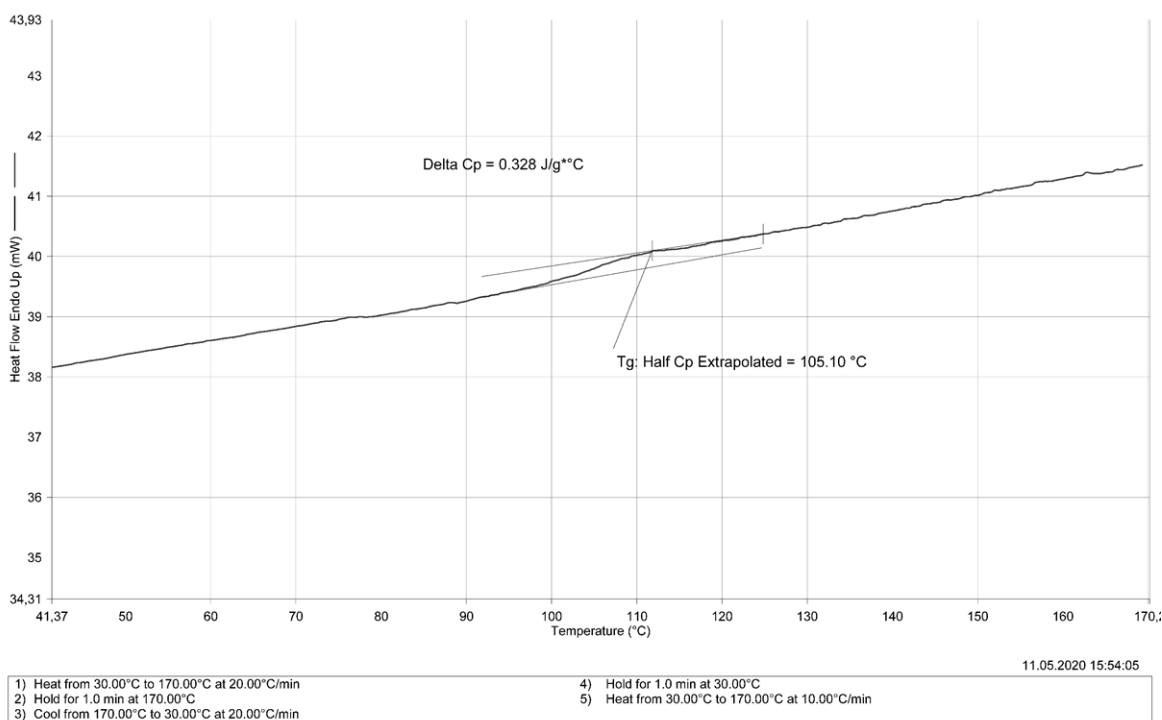


Figure S29: DSC curve of P(2-VP-stat-m-PyPE); 25% m-PyPE.

### Contact angle measurements



Figure S30: Exemplary contact angle of P(2-VP).

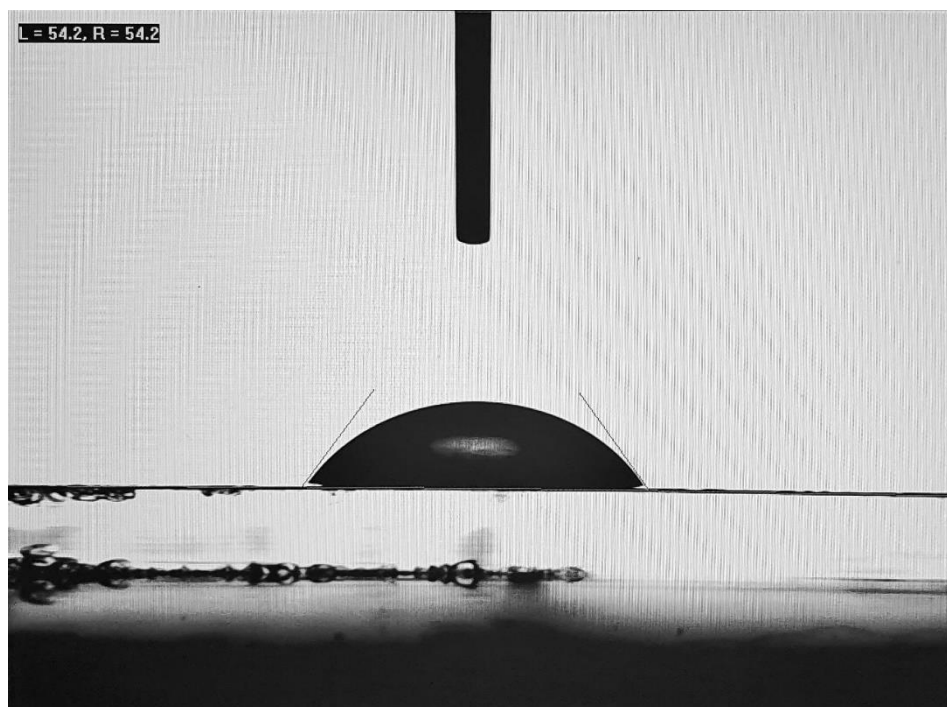


Figure S31: Exemplary contact angle of P(2-VP-stat-m-PyPE); 5% m-PyPE.



Figure S32: Exemplary contact angle of *P*(2-VP-*stat*-*m*-PyPE); 10% *m*-PyPE.

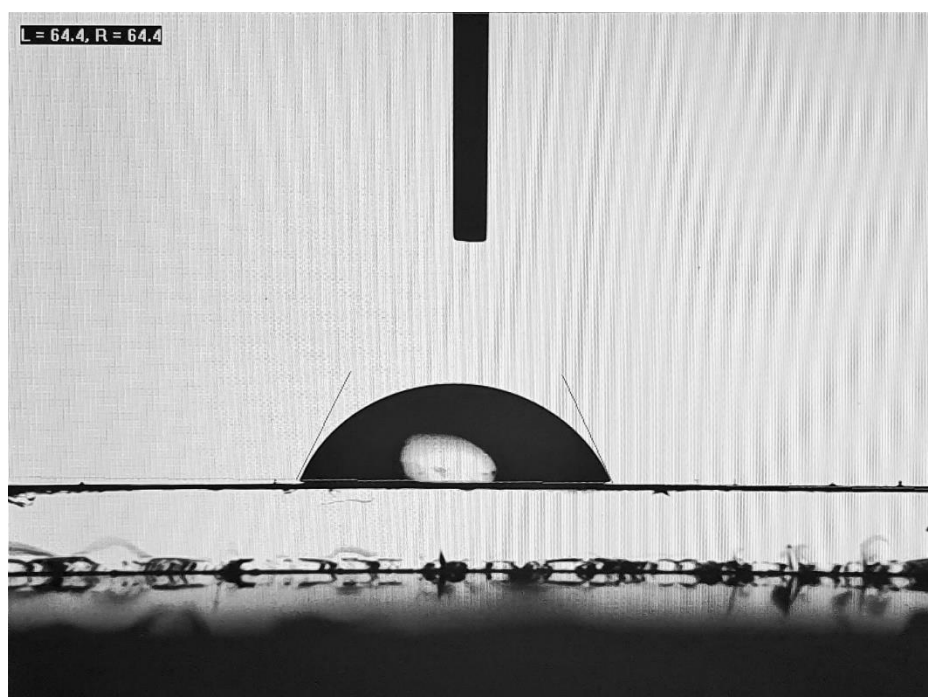


Figure S33: Exemplary contact angle of *P*(2-VP-*stat*-*m*-PyPE); 15% *m*-PyPE.

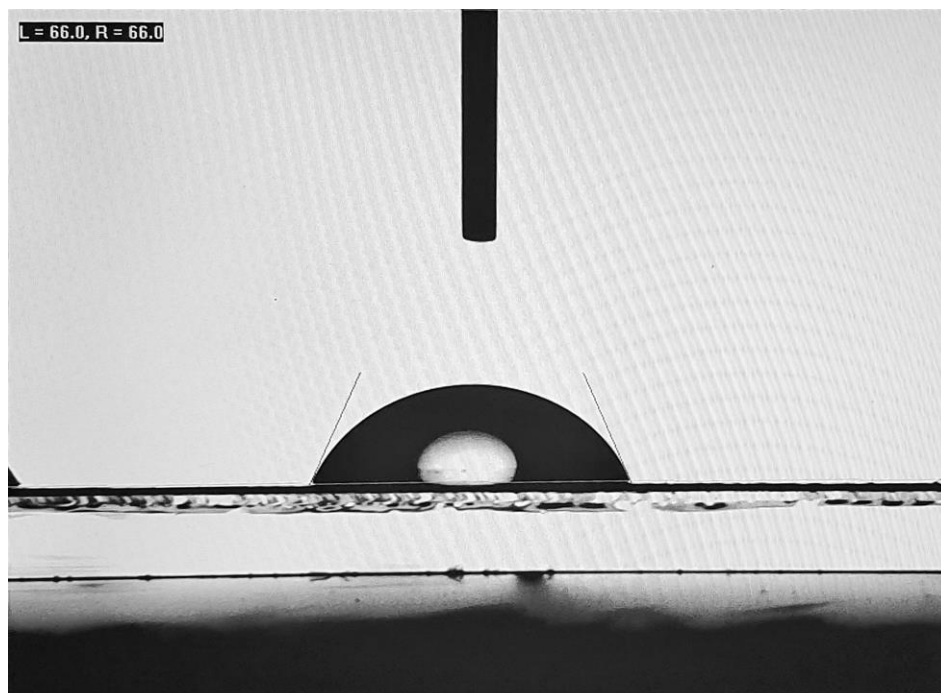


Figure S34: Exemplary contact angle of *P*(2-VP-stat-*m*-PyPE); 20% *m*-PyPE.



Figure S35: Exemplary contact angle of *P*(2-VP-stat-*m*-PyPE); 25% *m*-PyPE.

Table S1: Overview of all measured contact angles and the resulting average.

%m-PyPE	M1 / °	M2 / °	M3 / °	M4 / °	M5 / °	M6 / °	$\overline{\text{CA}}$ / °
0	45.3	45.2	41	41.1	43.6	50.3	44
5	57	54.4	54.2	49.6	-	-	54
10	63.2	61.9	60	61.2	62.1	-	62
15	60.7	66.1	64.5	63.6	64.4	-	64
20	66.9	63.3	65.6	67.4	66	63.5	65
25	63.5	64.3	64.8	63.2	64.4	61.8	64



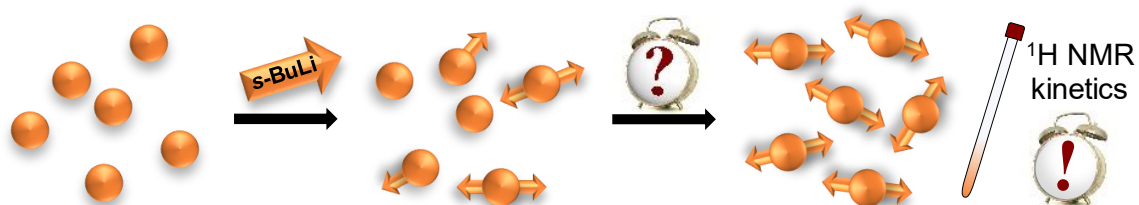
## 7. Chapter 3 – Increasing the versatility of bifunctional carbanionic initiators with the use of $^1\text{H}$ NMR kinetic studies

Marcel Fickenscher, [REDACTED] and [REDACTED] \*

M. Sc. Marcel Fickenscher, B. Sc. [REDACTED], Prof. [REDACTED]  
Department of Chemistry, Johannes Gutenberg University Mainz, Duesbergweg 10-14,  
55128 Mainz, Germany  
E-Mail: [REDACTED]

Keywords: bifunctional initiators, carbanionic polymerisations, activation kinetics studies

### 7.1 TOC & Short Abstract



Herein we present a method for the optimisation of the versatility of bifunctional carbanionic initiators in nonpolar media. To prevent the known aggregation of these structures, the activation process of precisely concentrated stock solutions is followed with  $^1\text{H}$  NMR experiments to find the perfect time for the addition of monomers which also simplifies the use of these initiators.

## 7.2 Abstract

Despite various publications that deal with bifunctional initiators there is still a lack of knowledge regarding some of the activation kinetics. In this study, we report the successful measurement of the activation kinetics of two commonly used bifunctional carbanionic initiators: 1,3-bis(1-phenylvinyl)benzene (DDPE) and 1-bromo-4-(4-bromophenoxy)-2-pentadecylbenzene (DBP). In order to optimize the reaction conditions for the general utilisation and to get a better understanding of the practical aspect of the activation process of these initiators, we follow their reaction with *s*-butyllithium in benzene via online and offline  $^1\text{H}$  NMR kinetic studies. As a result, we are able to present optimised conditions for the improved use of these initiators in terms of the concentration of the activated solution, the complete conversion into the dilithiated species and therefore the perfect time to start the polymerisation reaction.



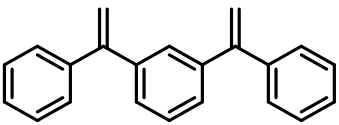
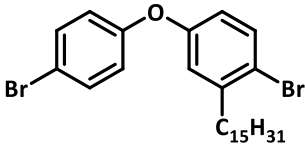
### 7.3 Introduction

Multifunctional initiators are a powerful tool for the synthesis of block copolymers via living anionic polymerisation. With the help of a bifunctional initiator it is possible to reduce the number of steps for the synthesis of ABA triblock copolymers by one, higher functional ones allow access to even more complex polymer architectures.<sup>1-3</sup> One of the earliest examples for these initiators is potassium naphthalenide, yet it is not suitable for all monomers as it requires polar solvents for an efficient initiation.<sup>4</sup> Especially for the synthesis of thermoplastic elastomers (TPEs) with a diene middle block, the use of nonpolar solvents is crucial for a high 1,4-microstructure and therefore the mechanical properties of the resulting material.<sup>5,6</sup> *m*-Divinylbenzene is the simplest initiator that is reported in literature for the bifunctional initiation of hydrocarbon monomers in nonpolar media, yet it is not the best choice.<sup>7</sup> The greatest challenge when using bifunctional carbanionic initiators is the intermolecular association of the dianionic species under the given conditions, which ultimately leads to the formation of inactive precipitates.<sup>8,9</sup> This effect is increased for small molecules with easily accessible anionic sites and leads to a poor performance of *m*-divinylbenzene in terms of the reaction control.<sup>10,11</sup> To overcome this limitation, several other bifunctional initiators have been developed that are active in nonpolar media.<sup>11-13</sup> The most popular one is 1,3-bis(1-phenylvinyl)benzene (DDPE), which represents an approach to suppress the aggregation with the sterically demanding benzene moieties. In 2006 Gnanou et al. published 1-bromo-4-(4-bromophenoxy)-2-pentadecylbenzene (DBPPB), where the precipitation of the aggregated dianions is hindered due to the long alkyl chain.<sup>14</sup> While there are other examples of bifunctional initiators in the literature that meet this requirements, the ones chosen in this study might be the most promising because both synthesis and application are the least complicated.

## 7.4 Results and Discussion

In practice, various factors affect the usability of the activated initiator species: temperature, solvent and concentration are the most influential ones, as these parameters have a strong impact on the activation and association kinetics. In this study, we chose room temperature and benzene as solvent to provide the most versatile conditions. Although both initiators are also soluble in the more common solvent cyclohexane, benzene was chosen on the one hand because of its increased solubility properties for monomers and polymers, and on the other hand because of the increased interaction with  $\text{Li}^+$ , which also promotes the solubility of the dianionic species.<sup>15,16</sup> The concentration of the active initiator solution is based on preexperimental results and values given in literature.<sup>14</sup> In general, a higher concentrated initiator solution tends to form insoluble aggregates or gels in such a strong manner that it averts the homogeneous start of the polymerisation reaction. In contrast, a concentration that is too low leads to extremely long activation times and makes it almost impossible to determine the optimal time to add monomers. The targeted molecular weight as well as the desired sample amount is of interest due to the handling of the normally very small amounts of initiator that are necessary. Hence, an initiator with a higher molar mass is advantageous in the synthesis of high molecular weight polymers. These usually require lower molar amounts of initiator; if its molar mass is higher, the required mass or volume also increases, making it easier to handle. Since the precise stoichiometry between *s*-BuLi and the bifunctional initiator is utmost important for a monomodal weight distribution of the resulting polymer, it is extremely cumbersome in practice to weigh the initiator for each synthesis. The preparation of water- and oxygen-free, non-activated initiator stock solutions of certain concentrations has proven to be very helpful. An overview of the key parameters of both initiators is given in Table 1.

Table 1: Key parameters of both bifunctional initiators.

	 DDPE	 DBPPB
molar mass [ $\text{g}\cdot\text{mol}^{-1}$ ]	282.39	538.41
appearance	colourless, viscous liquid	colourless, fine powder
synthesis steps	2	3
eq. <i>s</i> -butyllithium ( <i>s</i> -BuLi)	2	4
$[\text{c}]_{\text{stock solution}}$ [ $\text{mol}\cdot\text{L}^{-1}$ ]	0.1	0.01
$^1\text{H}$ NMR kinetics	online	offline

Since the precise stoichiometry between *s*-BuLi and the bifunctional initiator is utmost important for a monomodal weight distribution of the resulting polymer, it is extremely cumbersome in practice to weigh the initiator for each synthesis. The preparation of water- and oxygen-free, non-activated initiator stock solutions of certain concentrations has proven to be very helpful. An overview of the key parameters of both initiators is given in Table 1. For DDPE, the range of applicable concentrations varies between 0.05 M and 0.5 M, yet 0.1 M seems to be the best combination of activation speed and solution volume. The concentration range of DBPPB is stricter. The gelation resulting from the association during the activation does not allow concentrations above 0.1 M, otherwise the homogeneous cross over to the monomer units is no longer possible. To achieve the best polymerisation results, it is important to wait long enough before adding the monomer so that all initiator molecules are activated, but not too long to avoid the formation of insoluble aggregates. Therefore,  $^1\text{H}$  NMR kinetic measurements were carried out to follow the conversion in the course

of the reaction. Figure 1 shows the time-dependent change in signals. See Figure S1 - S4 for additional information.

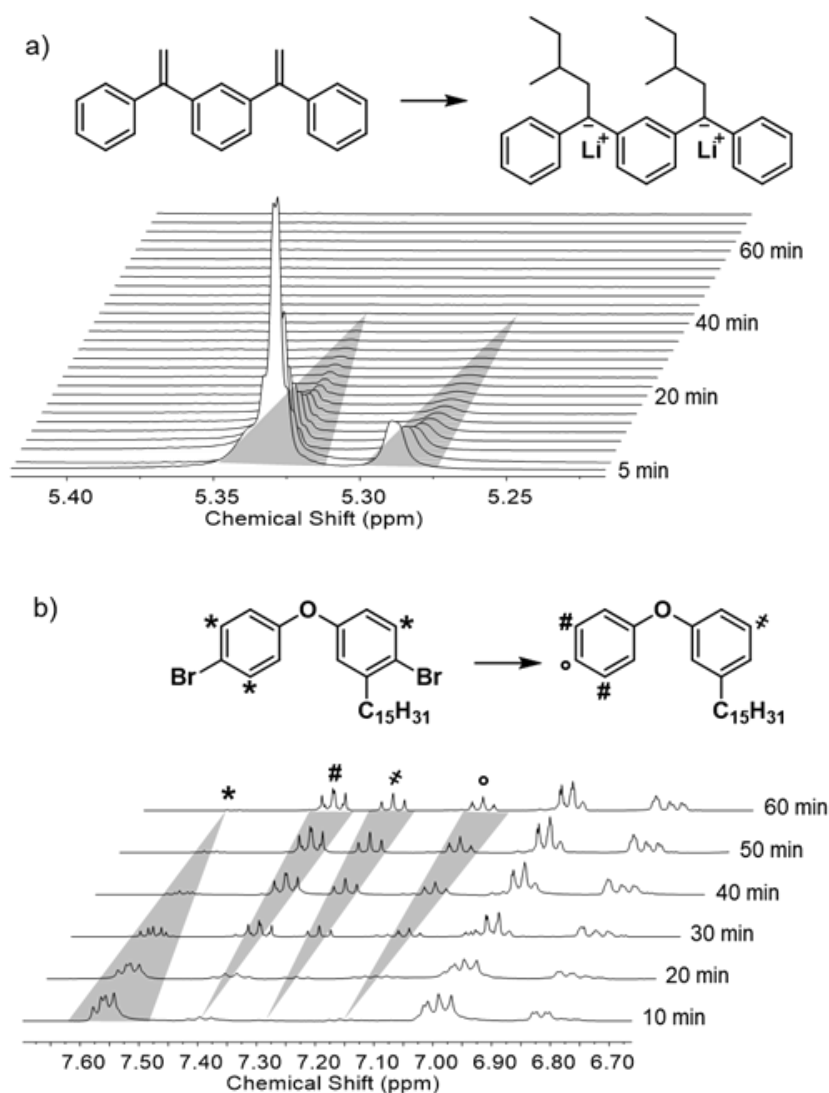


Figure 1: Time-dependent changes in relevant signals during the activation of a) DDPE (0.1 M,  $^1\text{H}$  NMR, solvent: benzene- $d_6$ , 400 MHz) and b) DBPPB (0.01 M,  $^1\text{H}$  NMR, solvent: benzene  $d_6$ , 400 MHz).

The activation of DDPE can easily be observed via online  $^1\text{H}$  NMR kinetics. In the course of the reaction, the decreasing double bond signals between 5.27 and 5.35 ppm shows the progressive addition of  $s\text{-BuLi}$ . After 40 minutes the signal has completely disappeared, no further changes can be observed, and the quantitative activation of the initiator is completed. The activation of DBPPB is observed via offline  $^1\text{H}$  NMR kinetics. Due to the different activation mechanism the online measurement is not

possible as there is no proton signal that disappears. The lithium-halogen exchange directly forms the negative charge, this structural change cannot be observed with  $^1\text{H}$  NMR spectroscopy. To follow the course of the reaction, an equivalent of the *s*-BuLi/DBPPB reaction mixture was treated with methanol to quench the reaction and analyzed afterwards. The change in the signal composition is presented in Figure 1 b). As the reaction progresses, the multiplet between 7.52 and 7.57 ppm which resembles the three protons positioned next to the bromine atoms depletes. However, the expected three new triplets are growing at the same rate at 7.38, 7.27 and 7.12 ppm. After 60 minutes the multiplet signal vanished completely, which shows the quantitative lithium-halogen exchange and thus complete activation. Both solutions are then ready to use and can be further diluted if necessary.

## 7.5 Experimental

### Materials and methods

Both initiators were synthesised according to preciously published procedures.<sup>14,17</sup> *s*-BuLi (1.3 M solution in hexanes) was purchased from Acros Organics and used without further treatment. Benzene- $\text{d}_6$  (99.96% purity) was purchased from Deutero GmbH and used without further treatment. Benzene was purchased from Carl Roth GmbH + Co. KG, degassed, stirred over *s*-BuLi and diphenylethylene as indicator for one night and freshly distilled prior to use. Methanol (HPLC grade) was purchased from Fisher Scientific GmbH and degassed prior to use.

$^1\text{H}$  NMR experiments were carried out on a Bruker Avance II 400 spectrometer, equipped with a 5 mm BBFO sample head with z-gradient and ATM.

### Sample preparation

Both initiators were freeze-dried with benzene and dried in dynamic vacuum for one night. Stock solutions of defined concentrations (DDPE: 0.1 M, DBPPB: 0.01 M) were prepared with benzene- $\text{d}_6$  or dry and degassed benzene under inert argon atmosphere in the glovebox.

DDPE: 1 mL (0.1 mmol, 1 eq.) of the prepared stock solution was transferred into an NMR tube and thoroughly closed with a rubber sealing cap. *s*-BuLi (0.15 mL, 0.2 mmol, 2 eq.) was added via syringe which led to the typically red coloured anionic solution. The first spectrum was measured within one minute, the following ones were taken at two-minute intervals.

DBPPB: 10 mL (0.1 mmol, 1 eq.) of the prepared stock solution were transferred into a glass tube equipped with a magnetic stirring bar. *s*-BuLi (0.31 mL, 0.4 mmol, 4 eq.) was added via syringe to start the activation reaction. Every ten minutes a 1 mL aliquot was taken from the reaction mixture and quenched with 0.1 mL methanol. The solvent was removed under reduced pressure and the solid residue was dissolved in 0.7 mL benzene- $\text{d}_6$  subsequently to perform the  $^1\text{H}$  NMR analysis.

## 7.6 Conclusion

Bifunctional initiators are a powerful tool for the synthesis of complex copolymers, yet their use is demanding with regard to the synthesis skills and equipment - especially the intermolecular association during the activation step is one of the biggest challenges. We were able to increase the versatility by the preparation of stock solutions with optimised concentrations. This not only simplifies handling in general, but also dramatically minimises the stoichiometric error for each synthesis. We successfully followed the activation reaction of the prepared stock solutions via  $^1\text{H}$  NMR experiments and were able to find the perfect time for further dilution and the monomer addition which reduces the probability that inactive aggregates will form. All in all, this optimised reaction procedure increases the accessibility of this kind of initiator to a larger audience.

## 7.7 References

- (1) Müller, A. H. E.; Matyjaszewski, K., Eds. *Controlled and living polymerizations: Methods and materials*; Wiley-VCH, 2009. DOI: 10.1002/9783527629091.
- (2) Lee, J. S.; Quirk, R. P.; Foster, M. D. *Synthesis and Characterization of Well-Defined, Regularly Branched Polystyrenes Utilizing Multifunctional Initiators*. *Macromolecules* 2005, 38 (13), 5381–5392. DOI: 10.1021/ma050207i.
- (3) W. Sun, J. He, X. Wang, C. Zhang, H. Zhang, and Y. Yang. *Synthesis of Dendritic Polystyrenes from an Anionic Inimer*. *Macromolecules* 2009, 42 (19), 7309–7317. DOI: 10.1021/ma9006768.
- (4) Szwarc, M. 'Living' Polymers. *Nature* 1956, 178 (4543), 1168–1169. DOI: 10.1038/1781168a0.
- (5) Knoll, K.; Nießner, N. *Styrolux + and styroflex + - from transparent high impact polystyrene to new thermoplastic elastomers: Syntheses, applications and blends with other styrene based polymers*. *Macromol. Symp.* 1998, 132 (1), 231–243. DOI: 10.1002/masy.19981320122.
- (6) Steube, M.; Johann, T.; Hübner, H.; Koch, M.; Dinh, T.; Gallei, M.; Floudas, G.; Frey, H.; Müller, A. H. E. *Tetrahydrofuran: More than a "Randomizer" in the Living Anionic Copolymerization of Styrene and Isoprene: Kinetics, Microstructures, Morphologies, and Mechanical Properties*. *Macromolecules* 2020, 53 (13), 5512–5527. DOI: 10.1021/acs.macromol.0c01022.
- (7) Beinert, G.; Lutz, P.; Franta, E.; Rempp, P. *A Bifunctional Anionic Initiator Soluble in Non-polar Solvents*. *Makromol. Chem.* 1978, 179 (2), 551–555. DOI: 10.1002/macp.1978.021790233.
- (8) Bywater, S.; Worsfold, D. J. *Alkylolithium anionic polymerization initiators in hydrocarbon solvents*. *Journal of Organometallic Chemistry* 1967, 10 (1), 1–6. DOI: 10.1016/S0022-328X(00)81711-8.
- (9) Hofmans, J.; van Beylen, M. *Synthesis and development of a dilithium initiator and its use for the preparation of ABA-block copolymers in non-polar medium: The use of  $\pi$ -complexing additives*. *Polymer* 2005, 46 (2), 303–318. DOI: 10.1016/j.polymer.2004.11.015.
- (10) Cazumbá, A.; Tauchert, E.; Nicolini, L. F.; Moutinho, M.; Pinto, J. C. *Preparation of Multifunctional Anionic Initiators Through Reactions Between n-Butyl Lithium and Divinylbenzene*. *Macromol. Symp.* 2019, 383 (1), 1800069. DOI: 10.1002/masy.201800069.
- (11) Bandermann, F.; Speikamp, H.-D.; Weigel, L. *Bifunctional anionic initiators: A critical study and overview*. *Makromol. Chem.* 1985, 186 (10), 2017–2024. DOI: 10.1002/macp.1985.021861005.
- (12) Schultz, A. R.; Bobade, S.; Scott, P. J.; Long, T. E. *Hydrocarbon-Soluble Piperazine-Containing Dilithium Anionic Initiator for High Cis -1,4 Isoprene Polymerization*. *Macromol. Chem. Phys.* 2018, 219 (1), 1700201. DOI: 10.1002/macp.201700201.
- (13) Lo, G. Y.-S.; Otterbacher, E. W.; Pews, R. G.; Tung, L. H. *Studies on Dilithium Initiators. 4. Effect of Structure Variations*. *Macromolecules* 1994, 27 (8), 2241–2248. DOI: 10.1021/ma00086a039.
- (14) Matmour, R.; More, A. S.; Wadgaonkar, P. P.; Gnanou, Y. *High performance poly(styrene-b-diene-b-styrene) triblock copolymers from a hydrocarbon-soluble and additive-free dicarbanionic initiator*. *Journal of the American Chemical Society* 2006, 128 (25), 8158–8159. DOI: 10.1021/ja062695v.



(15) Ma, J. C.; Dougherty, D. A. The Cation- $\pi$  Interaction. *Chemical reviews* 1997, 97 (5), 1303–1324. DOI: 10.1021/cr9603744.

(16) Tsuzuki, S.; Yoshida, M.; Uchamaru, T.; Mikami, M. The Origin of the Cation/ $\pi$  Interaction: The Significant Importance of the Induction in Li<sup>+</sup> and Na<sup>+</sup> Complexes. *J. Phys. Chem. A* 2001, 105 (4), 769–773. DOI: 10.1021/jp003287v.

(17) Lattermann, G.; Höcker, H. Darstellung und charakterisierung von einigen neuen bis(1-phenylvinyl)-verbindungen. *Makromol. Chem.* 1974, 175 (10), 2865–2874. DOI: 10.1002/macp.1974.021751007.

## 7.8 Supporting Information

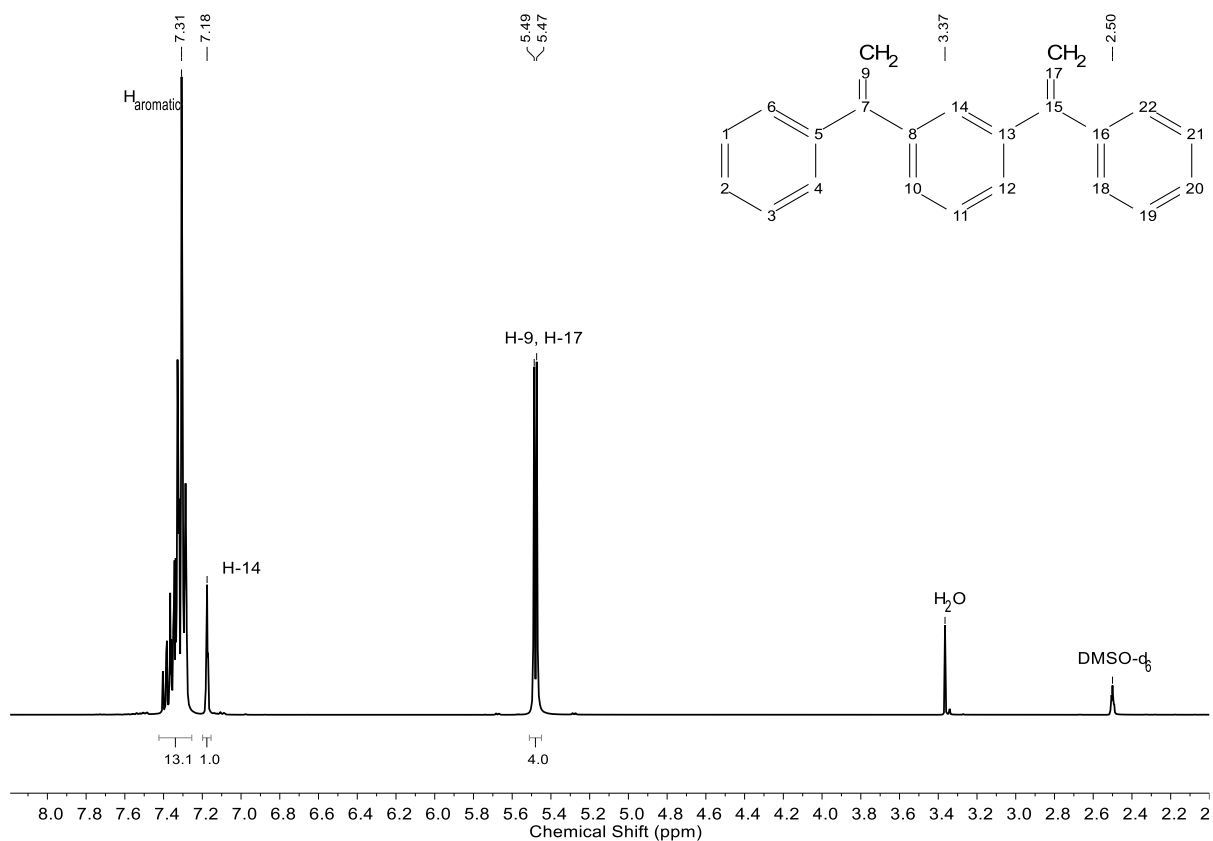


Figure S1:  $^1\text{H}$  NMR spectrum of non-activated DDPE (solvent:  $\text{DMSO-d}_6$ , 400 MHz).

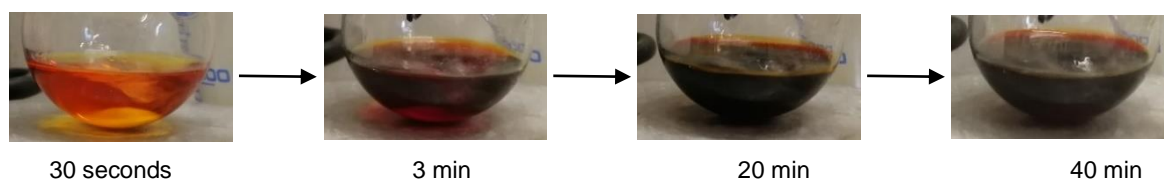


Figure S2: Visible change to the typical dark red coloured anionic solution during the activation of DDPE.

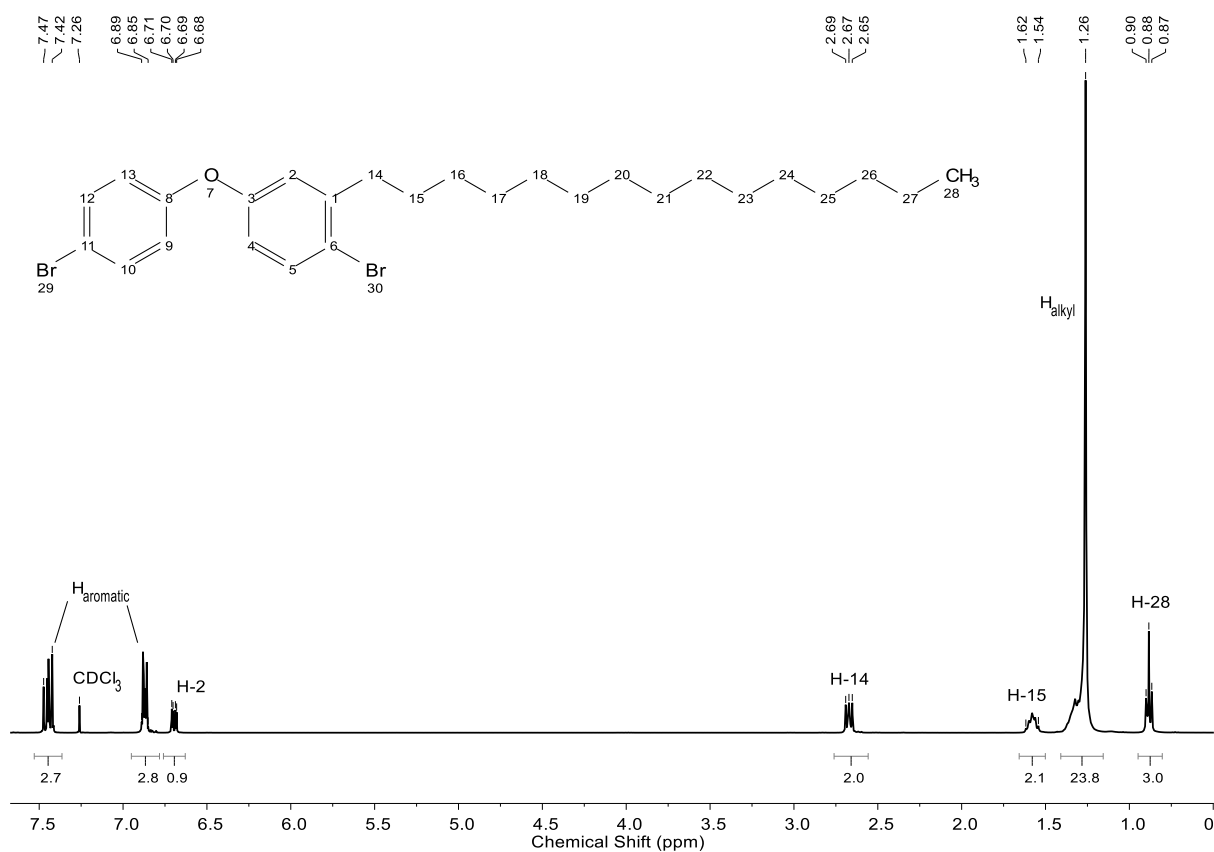


Figure S3:  $^1\text{H}$  NMR spectrum of non-activated DBPPB (solvent:  $\text{CDCl}_3$ , 400 MHz).

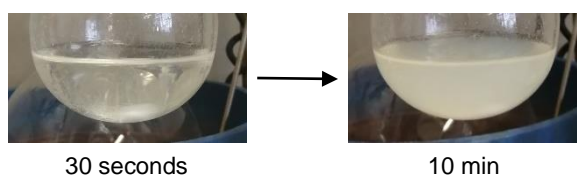


Figure S4: Visible cloudiness during the activation of the DBPPB solution, resulting from the precipitating LiBr.



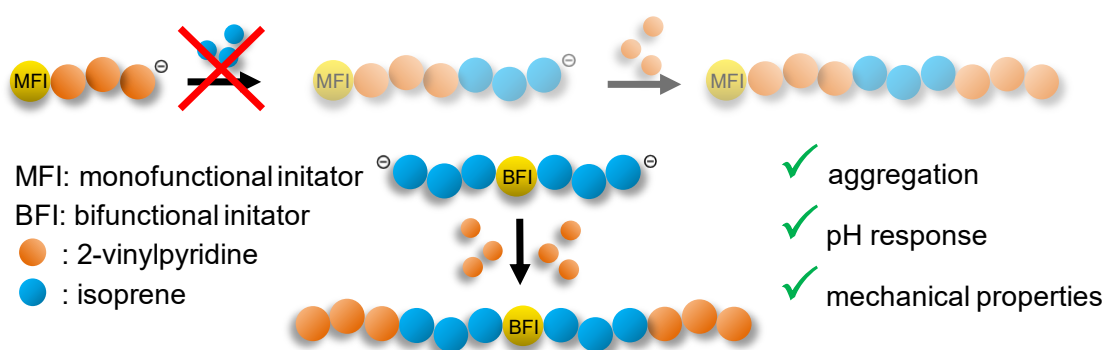
## 8. Chapter 4 – Synthesis and characterisation of novel 2-vinylpyridine-isoprene ABA triblock copolymers

Marcel Fickenscher, [REDACTED] and [REDACTED]\*

M. Sc. Marcel Fickenscher, B. Sc. [REDACTED], Prof. [REDACTED]  
Department of Chemistry, Johannes Gutenberg University Mainz, Duesbergweg 10-14,  
55128 Mainz, Germany  
E-Mail: [REDACTED]

Keywords: 2-vinylpyridine, isoprene, carbanionic polymerisations, triblock copolymers

### 8.1 TOC & Short Abstract



Copolymerisation of 2-vinylpyridine and isoprene, starting from a bifunctional initiator, yields novel ABA triblock structures that cannot be accessed *via* a linear synthesis route. The polymers are analysed by means of SEC and NMR spectroscopy and the observed aggregation tendency is investigated.

## 8.2 Abstract

Since the reactivities between monomers are different, it is not possible to synthesise linear ABA triblock copolymers from every conceivable monomer pair by monofunctional initiation, if the reactivity of A is insufficient to polymerise monomer B. Double 1,1-diphenylethylene (DDPE) is an efficient bifunctional carbanionic initiator and allows the synthesis of ABA triblock copolymer structures starting from monomer B, if the latter is reactive enough to cross-over to monomer A. In this work, novel ABA triblock copolymers have been synthesised with 2-vinylpyridine (2-VP) end blocks and an isoprene midblock with a high number of the 1,4-regioisomer. First, the applicability of the bifunctional initiator in nonpolar media has been optimised, followed by the careful two-step polymer synthesis, including the intermediate addition of a polar solvent to allow for polymerisation of 2-VP at low temperatures, forming the P(2-VP) end blocks. Ultimately, two different sets of polymers have been prepared, differing in monomer composition (15-70-15 and 20-60-20 mol% for the blocks) and molecular weight (10 - 27 kg·mol<sup>-1</sup>). The molar monomer ratio as well as the isoprene microstructure were verified by <sup>1</sup>H NMR and DSC experiments. SEC and light scattering experiments gave qualitative insight into the solution behaviour of the polymers and provided a reliable trend regarding their aggregation characteristics. An increased particle size with increasing molecular weight was observed, while polymers with the same molecular weight but higher 2-VP content showed a reduced particle size due to the enhanced interaction of the P(2-VP) blocks. In addition, pH-dependent solubility and first indications of mechanical resilience are reported, raising the prospect of new type of functional TPE materials.

### 8.3 Introduction

Block copolymers are a well-known class of materials with a wide range of applications, and styrene-diene block copolymers in particular are often in focus.<sup>1</sup> The large number of more than 1600 publications on styrene-butadiene or styrene-isoprene block copolymers between 2000 and 2019 clearly underlines their importance.<sup>2</sup> Due to their excellent mechanical properties compared to AB diblock copolymers, especially ABA triblock copolymers or higher multiblock copolymers are of special interest. Common applications range from everyday thermoplastic elastomers (TPEs) and high-performance polymers for medical uses to novel approaches for highly specific electronics.<sup>3-6</sup> To broaden the range of possible applications, the use of functional styrene derivatives is an interesting starting point, and several examples were published as early as 1963.<sup>7-9</sup>

Another suitable monomer that has received little attention in terms of copolymerisations with isoprene is 2-vinylpyridine (2-VP), which, however, is an interesting alternative to styrene due to its quite similar mechanical properties but significantly different polar character.<sup>10</sup> The manifold possibilities for post-polymerisation modifications as well as different applications of vinylpyridine copolymers were presented in a comprehensive perspective article by Kennemur from 2019, which impressively demonstrates the rather simple access to tailor-made materials with unique properties.<sup>11</sup> In addition the polymerisation of functional styrene derivatives often requires the use of protective groups. This is not necessary for vinylpyridine, albeit low temperatures are required to suppress possible side reactions described in the literature.<sup>12,13</sup>

The living anionic polymerisation is the gold standard for controlled polymerisation reactions, as it allows for the synthesis of well-defined structures with narrow molecular weight distributions.<sup>14,15</sup> In particular, the carbanionic synthesis of polyisoprene is well understood, and the preparation of polymers

with a high content of 1,4-regioisomers, which is essential for low glass transition temperatures and the mechanical properties, is achieved without encountering problems by using non-polar solvents and lithium initiators.<sup>16–19</sup> In contrast to styrene, a polar solvent is essential for the polymerisation of 2-VP, which makes the synthesis of 2-VP/isoprene polymers particularly challenging due to the different reaction conditions. Nevertheless, some examples can be found in literature. Watanabe and Tirrell published the sequential synthesis, starting with the polymerisation of isoprene in *n*-heptane. Subsequently, 90% of the solvent was removed under reduced pressure and replaced by THF, followed by the addition of 2-VP at -78 °C to ensure the controlled polymerisation.<sup>20</sup> Polymers with narrow dispersities of 1.12-1.18 and a high content of 1,4-polyisoprene microstructure of 93% were obtained. Quirk and Corona-Galvan report the synthesis of P(*l-b*-2-VP) initiated in pure hydrocarbon solvents (benzene) in the presence of LiCl with very narrow dispersities of 1.01-1.06 and 93% 1,4-units. The use of LiCl is critical for the success of the synthesis, as it suppresses side reactions during the polymerisation of 2-VP, while working at comparatively elevated temperatures of 6-8 °C.<sup>21</sup> Kurata et al. report the gas permeability of P(*l-b*-2-VP) thin-films and conclude that it resembles that of SBS block copolymers closely in all respects at temperatures between 25-60 °C. The permeation is mainly governed by the mobility of the rubbery PI phase with a high 1,4-microstructure, while the glassy P(2-VP) domains remain inert.<sup>22</sup> Further insight into the material properties were provided by Hashimoto et al. They report the effect of casting solvents for the preparation of thin-films and demonstrate the excellent phase separation behaviour of the polymers and the formation of spherical, cylindrical and lamellar morphologies *via* TEM and SAXS measurements.<sup>23</sup> Furthermore, they studied the selective incorporation of Pd nanoparticles into the P(2-VP) domains of the respective thin-films, demonstrating the potential of these materials as substrate for metal catalysts or optical devices. It should be noted, that the polymers reported by Hashimoto et al. were synthesised in THF, resulting in a high 3,4-content of PI.<sup>24</sup> While no



conclusive reports for the exact Flory-Huggins interaction parameter  $\chi$  can be found in literature yet, the trend  $\chi_{(PS-PI)} \leq \chi_{(P(2-VP)-PS)} < \chi_{(PI-P(2-VP))}$  is uniformly confirmed and it is expected that  $\chi_{(PI-P(2-VP))}$  is at least 1.5 to 3.5 and in some reports even 8 times, higher than  $\chi_{(PS-PI)}$ .<sup>11,25-31</sup> Different reports on the solution behaviour of copolymers with strongly immiscible blocks show their ability to form non-conventional micellar shapes, e.g. toroids.<sup>32,33</sup> Chang et al. investigated the self-assembly of P(*l-b-2-VP*) and report the formation of stable toroidal micelles with highly uniform size and shape with the opportunity to grow gold nanoparticles along the ring surface.<sup>34</sup>

Overall, the manifold properties already reported, show the potential of these copolymers which renders the synthesis of ABA triblock copolymers of the type P(2-VP)-*b*-PI-*b*-P(2-VP) particularly interesting. For a wide range of possible applications, it is desirable to maximise the number of 1,4-units in the PI block, which is why sequential synthesis in different solvents is necessary. While the sequential polymerisation of AB diblock copolymers is achieved with established synthesis protocols, the synthesis of ABA triblock copolymers is a challenging task, since the cross-over from 2-VP to isoprene is not possible.<sup>21</sup> The living vinylpyridine chain end shows reduced nucleophilicity due to the electron-withdrawing character of the nitrogen atom. The reactivity of the living chain ends is mirrored by the  $\beta$ -carbon shift in <sup>13</sup>C NMR, as demonstrated by Hirao et al. for different styrene derivatives containing electron-withdrawing groups. For the monomers used in this study, the reactivity follows the order isoprene > 2-VP; to simplify the comparison, the values for styrene and 4-VP are also given in Table 1.<sup>35</sup>

Table 1: ( $\beta$ -)carbon shifts of selected monomers measured via  $^{13}\text{C}$  NMR (400 MHz,  $\text{CDCl}_3$ , Figure S1) reflect the respective reactivity.

monomer	( $\beta$ -)carbon shift / [ppm]
isoprene	113.54 C-1 / 116.67 C-4
styrene	113.93
2-VP	118.32
4-VP	118.45

The difference of  $\sim 5$  ppm between 2-VP and the C-1 carbon of isoprene which is nucleophilically attacked during the polymerisation indicates that a corresponding cross-over originating from 2-VP is not possible. The earlier described synthesis of diblock copolymers is possible by starting with isoprene in a non-polar solvent followed by the sequential addition of a polar solvent and vinylpyridine in a second step. However, triblock copolymers cannot be produced in the same manner. The use of a bifunctional initiator can overcome this limitation and generates a living dilithiopolyisoprene precursor that readily reacts with 2-VP to form the desired ABA structure.

Due to the dianionic charge of comparatively small molecules, bifunctional initiators tend to aggregate in non-polar solvents, making them unavailable for uniform, effective initiation. Nevertheless, several structures have been developed that prevent aggregation, relying on different strategies. Figure 1 gives an overview of different bifunctional initiators. Gnanou et al. use an intramolecular polar ether group and an alkyl anchor to prevent the dianionic initiator (I) from precipitating. Additionally, the activation mechanism is a lithium-halogen exchange on both benzene moieties, resulting in the necessary addition of two additional eq. *s*-BuLi, which readily converts the intermediary bromobutane to 3,4-dimethylhexane, thus avoiding the quenching of any living chain ends during the polymerisation process.<sup>36</sup> Another approach is structure

(II). Long et al. use an intramolecular piperazine group, which suppresses the ion association *via* coordination of the lithium cations.<sup>37</sup> An earlier example and, among numerous other publications, also the initiator used in this work is structure (III), diphenylethylene (DPPE). The sterically demanding benzyl moieties prevent the assembly of several active DDPE molecules.<sup>38–41</sup> Starting from DDPE, we herein report the synthesis of novel P(2-VP-*b*-I-*b*-2VP) triblock copolymers.

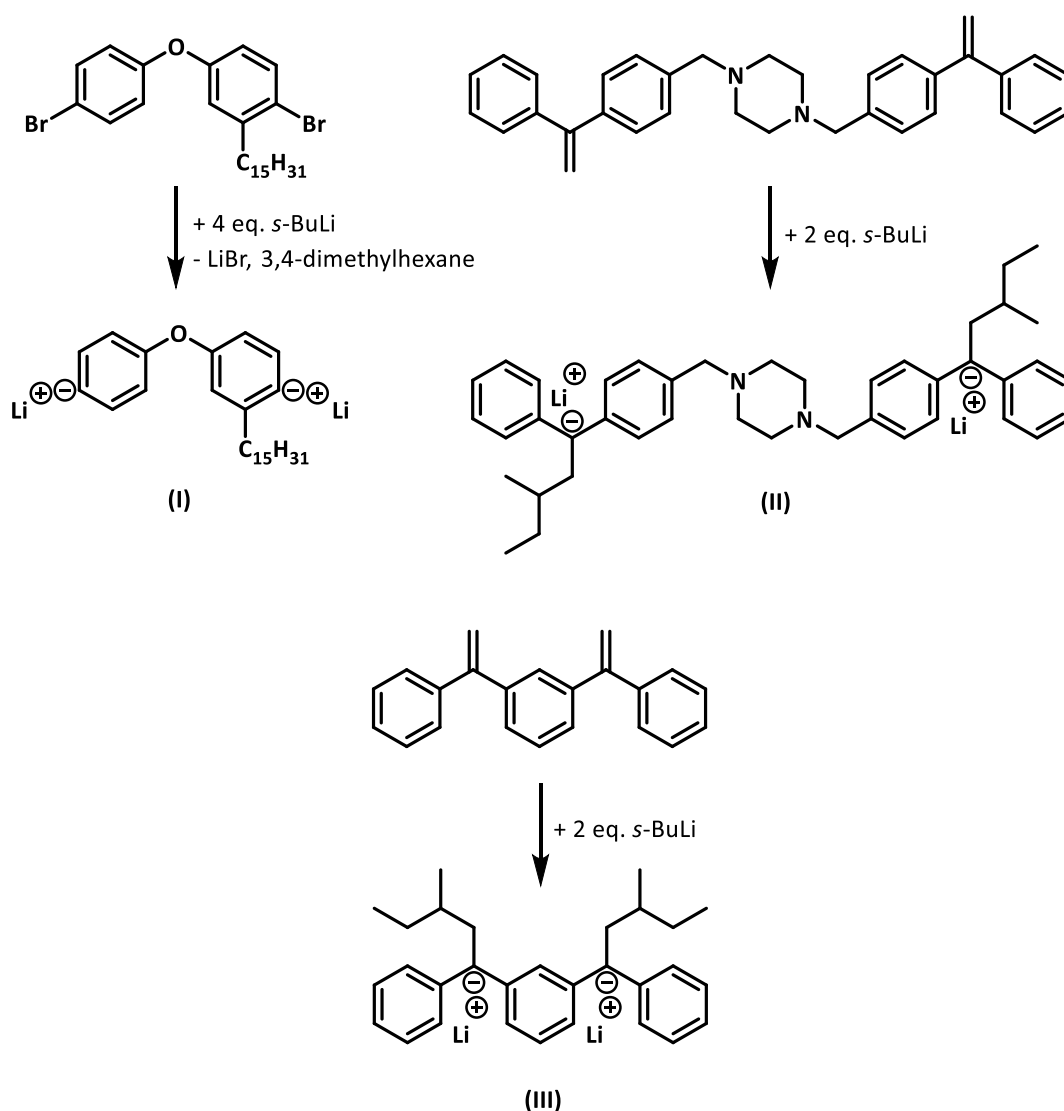


Figure 1: Bifunctional anionic initiators for use in non-polar solvents and the respective activation with *s*-BuLi to form the active initiator species. (I) published by Gnanou et al., an intramolecular polar ether group and the long alkyl anchor suppress precipitation. (II) published by Long et al., the intramolecular piperazine moiety promotes ion dissociation. (III) DDPE, the bulky benzene moieties sterically hinder aggregation of the activated dianionic species.<sup>36–41</sup>

## 8.4 Results and Discussion

### Synthesis and sample overview

In the following, the synthesis of the bifunctional initiator DDPE as well as the sequential carbanionic polymerisation of P(2-VP-*b*-I-*b*-2-VP) are described.

### Initiator synthesis

Although the Wittig reaction of 1,3-dibenzoylbenzene with methyl triphenylphosphonium bromide is the commonly reported method for this synthesis, the troublesome removal of the by-product triphenylphosphine oxide led to the choice of a different strategy.<sup>42</sup> In analogy to the synthesis of DPE, DDPE was prepared using the Grignard reaction.<sup>43</sup> While two different synthesis routes are conceivable, the reaction of 1,3-diacetylbenzene with a phenylmagnesium halogenide leads to insufficient results and poor yields of only 25%. In contrast, the reaction of the readily available 1,3-dibenzoylbenzene with methylmagnesium iodide yields good results, which can be attributed to the lower steric hindrance in the transition state, since the Grignard reagent is less bulky, and the three-ring structure is already pre-formed. In the first step of the reaction, both ketone groups are converted by the Grignard reagent and subsequent hydrolysis to the tertiary alcohol, which eliminates water under weak acidic conditions and elevated temperature to ultimately form both double bonds (Figure 2). After careful purification III was obtained in a yield of 91%.

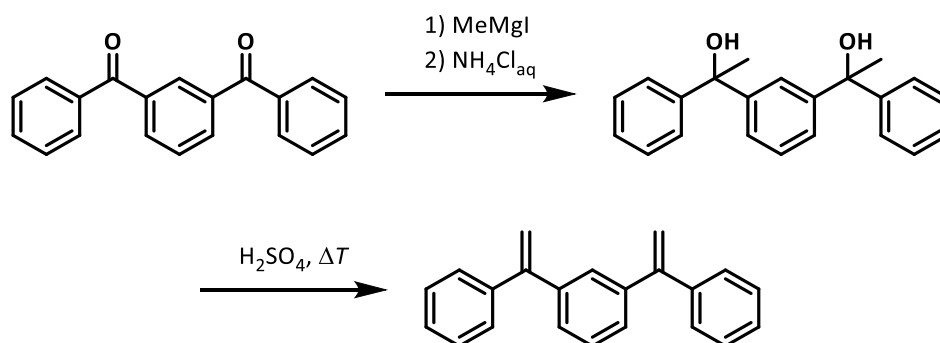


Figure 2: Grignard reaction of 1,3-dibenzoylbenzene and subsequent dehydrogenation, affording the bifunctional initiator DDPE.

To guarantee the required purity and to verify full activation of the initiator, styrene was polymerised and end-capped with ethyleneoxide (EO) in a model reaction, similar to the publication by Bates et. al.<sup>44</sup>  $^1\text{H}$  NMR spectroscopy demonstrates, by means of the correct ratio between initiator signal and EO signal, that exactly one EO unit is added to each living anionic chain end. The SEC trace shows a monomodal distribution with a dispersity of 1.1, proving the efficiency of the synthesised DDPE as bifunctional initiator (see Figures S4, S5). Since the incomplete activation of the initiator (Figure 1) leads to side reactions such as chain coupling during the polymerisation, the addition of *s*-BuLi to the double bonds of DDPE was followed using online  $^1\text{H}$  NMR spectroscopy. The decrease of the corresponding signal is tracked to determine the optimal time for the addition of the monomer. The data show that after 30 minutes, 99% conversion can be observed (see Figure S6).

#### Polymer synthesis

All polymerisation reactions were carried out using standard high-vacuum techniques in carefully dried all-glass reaction vessels, sealed with rubber and Teflon caps. DDPE was initially placed in the reaction flask, lyophilised with pre-dried benzene, and stirred in dynamic vacuum at room temperature for one night. Both monomers were degassed in several freeze-pump-thaw cycles, dried over  $\text{CaH}_2$  for one night, and freshly distilled prior to the reaction. Figure 3 gives an overview of the polymerisation steps. A 0.1 M solution of DDPE in benzene is activated with *s*-BuLi for 60 minutes, followed by the addition of further benzene for sufficient dilution during isoprene polymerisation. Isoprene is added *via* syringe and stirred for 2 h. After full conversion of isoprene, the reaction flask was cooled to  $-64\text{ }^\circ\text{C}$  and THF was condensed into the reaction mixture under reduced pressure. To prevent the reaction mixture from freezing during the polymerisation, it is necessary to add at least the same volume of THF with respect to benzene (Figure S7). 2-VP was injected *via* syringe and allowed to polymerise for 1 h prior to quenching of the reaction mixture with methanol. In the course of the reaction, two important colour changes are observed that can be taken as an indication for successful transformation of the chain ends: Starting from the active solution of DDPE

with a red colour, the addition of isoprene and the subsequent formation of the isoprenyllithium chain end turns the solution to a pale yellow colour, which changes back to red once 2-VP is added (Figure 3). Since the purification of the resulting polymers is challenging due to the amphiphilic character and precipitation is difficult, the solvent was removed under reduced pressure to afford P(2-VP-*b*-I-*b*-2-VP) with quantitative yields.

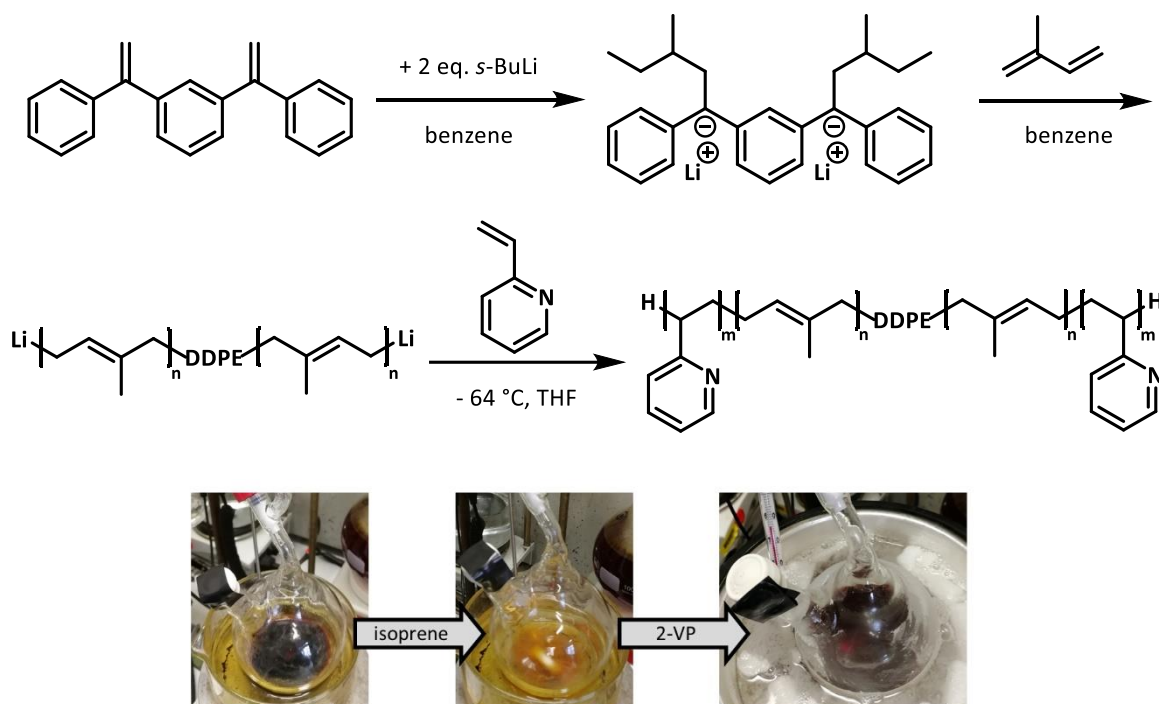


Figure 3: Sequential polymerisation scheme for 2-VP-isoprene ABA triblock copolymers starting from the bifunctional initiator DDPE. The observable colour change indicates the successful cross-over to the respective monomer during the reaction steps.

Two sets of polymers with varied molar monomer ratios were synthesised to establish the triblock copolymer synthesis: 15-70-15 and 20-60-20 with different molecular weights in dependence of the 2-VP outer blocks molecular weights, which were chosen between 2 and 4 kg mol<sup>-1</sup> to investigate the influence of the monomer composition and P(2-VP) block size.

### Characterisation of the block copolymers

An overview of all resulting copolymers is given in Table 2, Figure 4 shows the SEC traces of both copolymer sets.

*Table 2: Characterisation data of copolymer samples with theoretical molecular weights, SEC measurements were performed in DMF with toluene as an internal standard, PS calibration and UV detector. NMR measurements were performed in CDCl<sub>3</sub> and 400 MHz.*

Sample	$M_{n, \text{tar}}$ [kg·mol <sup>-1</sup> ]	$M_{n, \text{SEC, exp}}$ [kg·mol <sup>-1</sup> ]	$M_{n, \text{NMR, exp}}$ [kg·mol <sup>-1</sup> ]	$\bar{D}$	1,4-units [%]
15-70-15 - 2k	13.3	5.8	25.1	1.1	91.3
15-70-15 - 3k	20.0	10.6	23.0	1.2	91.8
15-70-15 - 4k	26.6	16.1	30.5	1.2	91.7
20-60-20 - 2k	10	5.8	13.6	1.1	93.5
20-60-20 - 3k	15	8.5	12.8	1.1	90.9
20-60-20 - 4k	20	10.8	17.8	1.2	91.2

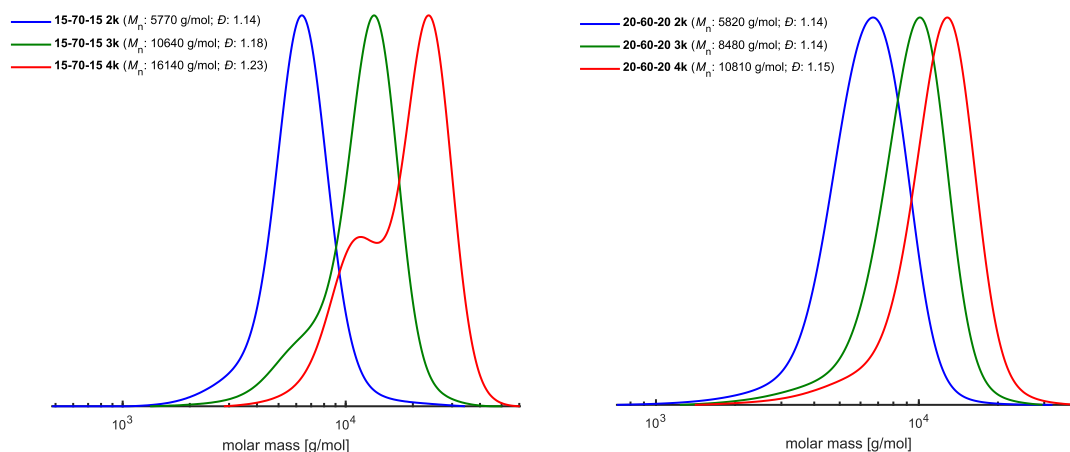


*Figure 4: SEC traces of the P(2-VP-b-I-b-2-VP) samples, measured in DMF with toluene as internal standard, polystyrene calibration and an UV detector.*

The shoulders of the 15-70-15 set can be attributed to chain termination from protic impurities introduced during the addition of 2-VP; thus representing an isoprene homopolymer. The proportion of homopolymer was determined to be 9% and 27%,

respectively by means of a multiarea data evaluation. The rather high value of 27% underlines the immense caution with respect to predrying required during the synthesis, however, it does not pose a problem for the subsequent characterisation of the polymers. Furthermore, this displays the successful synthesis, as this bimodality clearly demonstrates the presence of the triblock copolymers. The excellent, monomodal SEC traces of the 20-60-20 series show that the synthesis strategy used is suitable since, no bimodality can be observed in this case.

A significant discrepancy between the theoretical molecular weight and the respective experimental values can be observed as well. In view of the SEC experiments, this effect is ascribed to an underestimation of the vinylpyridine blocks when using PS standards, as reported in literature.<sup>45</sup> For the reported triblock structures, this effect is particularly pronounced as a result of the aggregation behaviour, which further reduces the hydrodynamic radius. Another factor contributing to the underestimation is the mid-block, as isoprene also has a lower molecular weight compared to the PS standard, which will be discussed in more detail later. Apart from the known underestimation, both sets of polymer samples show the expected shift to higher molecular weights with an increasing targeted molecular weight, indicating their successful synthesis.

In case of NMR determination, the variation of the molecular weight is attributed to the difficult integration of the initiator signal. Since the aromatic signals of DDPE and 2-VP overlap, the terminal *s*-BuLi alkyl protons are used for the integration. In this case, however, due to the low intensity and the proximity to the alkyl backbone signal of the polymer, their integration is particularly difficult and error-prone. To further support the efficient copolymerisation, an exemplary DOSY NMR spectrum of sample 20-60-20 4k was measured (Figure S14). It shows the absence of signals other than for benzene-*d*<sub>6</sub> and the copolymer, demonstrating the formation of the P(2-VP-*b*-I-*b*-2-VP) triblock copolymer structure. In contrast to the molecular weight, the microstructure composition of the isoprene middle block can be determined for all samples,



according to Equation 1. The percentage of 3,4-units is given by the integral ratio of both vinyl signals (1,4-units: 5.1 ppm, 1H; 3,4-units: 4.7 ppm, 2H; see ESI):

$$\%(3,4) = \frac{(0.5 \cdot I(3,4))}{I(1,4) + 0.5 \cdot I(3,4)} \cdot 100 \quad \text{Equation 1}$$

The resulting values demonstrate the possibility to achieve a high content of 1,4-units of over 90% for every sample (Table 2). This is also reflected by the glass transition temperature  $T_g$  of the polyisoprene middle block. It varies between -60 and -65 °C and is in good accordance with values reported in literature for high molecular weight 1,4-isoprene polymers (see ESI).<sup>46</sup> Due to the relatively low molecular weights of the 2-VP blocks, it was only possible to observe a  $T_g$  of 81 °C for the 4k sample of the 15-70-15 series. As described in literature, the lack of a detectable  $T_g$  is ascribed to the low volume of the 2-VP blocks. Since isoprene forms the main component in these polymers, it is difficult to observe both  $T_g$ s. This effect is amplified by the sensitivity limit of the DSC measurement, it is no longer sufficient to map a  $T_g$  since the heat capacity step  $\Delta C_p$  at the  $T_g$  is inversely proportional to the temperature.<sup>47,48</sup> For the 20-60-20 series, the observed  $T_g$ s are still weakly pronounced, but determinable for all polymers. A clear trend can be seen, as expected the  $T_g$  increases together with the molecular weight of the block from 40 to 66 °C. The values are in agreement with literature and clearly indicate the presence of a defined 2-VP block.<sup>49,50</sup>

In addition to the polyisoprene microstructure, NMR spectroscopy also allows the determination of the monomer ratio *via* the signal ratio of 2-VP (8.20 ppm, 1H, normalised to 1) to both isoprene signals, following Equation 2:

$$\begin{aligned} \text{mol\% (isoprene)} &= 100 \cdot \frac{(I(1,4) + 0.5 \cdot I(3,4))}{I(2\text{-VP}) + (I(1,4) + 0.5 \cdot I(3,4))} \\ &= 100 \cdot \frac{(I(1,4) + 0.5 \cdot I(3,4))}{1 + (I(1,4) + 0.5 \cdot I(3,4))} \end{aligned} \quad \text{Equation 2}$$

The calculated values are in excellent agreement with the theoretically planned monomer composition and deviate by no more than 3% (see Table S2). These results,

in addition with the high 1,4-content of the polymers demonstrates that the desired control over the reaction by means of living anionic polymerisation was achieved.

#### Solution behaviour

As described earlier, the respective diblock copolymers of isoprene and 2-VP tend to form aggregates. A first indication of similar aggregation behaviour of the triblock copolymer structures is the reduced hydrodynamic radius of the polymers, which is mirrored by a lower apparent molecular weight in the SEC elugrams. In addition to the already discussed main signal of the polymers, a second distribution mode can be observed at very high molecular weights via SEC, as shown in Figure 5.

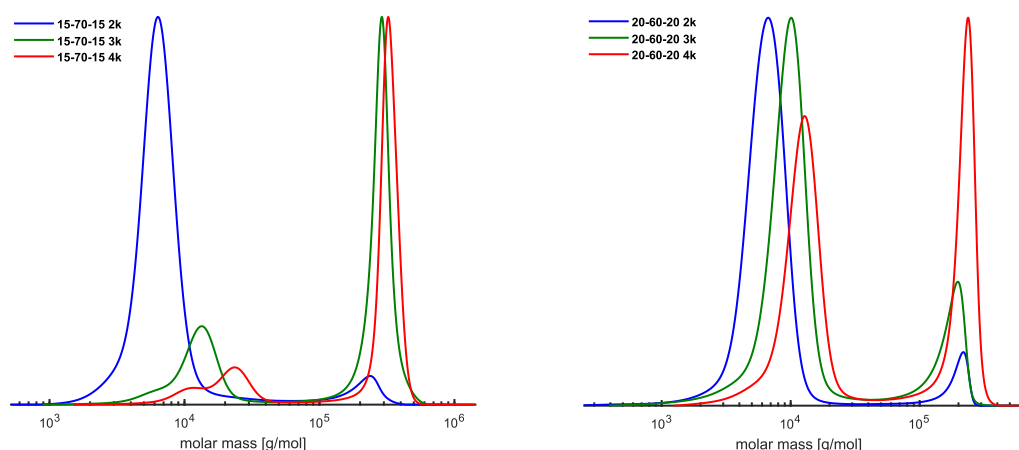


Figure 5: Complete SEC traces of the polymer samples. The molecular weights and dispersities provided refer to the very narrowly distributed, high molecular weight signal, indicating the aggregation of  $P(2\text{-VP-}b\text{-I-}b\text{-2-VP})$ .

This is of particular interest since such signals often indicate an uncontrolled side reaction, which can, however, be ruled out in this case. The most likely case of incomplete activation of the initiator, which would lead to chain coupling and cross-linking, can be excluded; an uncontrolled reaction would be accompanied by a significant broadening of the distribution. In addition, cross-linking side reactions would result in an insoluble product that cannot be detected *via* SEC as it is separated out while passing the pre-column. The presence of the homopolymer signal along with the main signal in the 15-70-15 4k sample also precludes the high  $M_n$  signal from being the actual product signal. This is further

supported by the fact that the molecular weight of these polymers is known to be underestimated in SEC elugrams, rather than drastically overestimated as would be the case here. Therefore, the high molecular weight, together with the very narrow distribution of the signals allows for the conclusion that these are well-defined aggregates of the respective P(2-VP-*b*-I-*b*-2-VP)s. For a qualitative estimation of the aggregation number  $z_A$ , the molecular weight of both signals was used for the calculation, according to Equation 3:

$$z_A = \frac{M_n^{\max}(\text{aggregate})}{M_n^{\max}(\text{single})} \quad \text{Equation 3}$$

Since it can be assumed that the isoprene homopolymer fraction is not involved in aggregation and to minimise the calculation error due to the shoulder of the signals in the 15-70-15 series, the signal maxima were used. Table 3 shows the corresponding results.

*Table 3: Calculated aggregation number  $z_A$  from SEC traces and determined particle size from light scattering measurements in DMF.*

Sample	$M_n^{\max}(\text{single})$ [kg·mol <sup>-1</sup> ]	$M_n^{\max}(\text{aggregate})$ [kg·mol <sup>-1</sup> ]	$z_A$	particle size [nm]
15-70-15 - 2k	6.4	237.9	37.4	68
15-70-15 - 3k	13.4	290.9	21.8	74
15-70-15 - 4k	23.6	323.0	13.7	113
20-60-20 - 2k	6.7	218.9	32.6	32
20-60-20 - 3k	10.1	196.9	19.5	38
20-60-20 - 4k	12.8	238.3	18.6	45

The apparent aggregation number decreases with increasing molecular weight. This effect is attributed to the increased block lengths. We hypothesise that the polar 2-VP blocks are solubilised and form the shell of the aggregate, while isoprene forms the core.<sup>51</sup> As the chain length increases, the steric demand of

the 2-VP shell increases, reducing the number of isoprene blocks that fit in the core, ultimately decreasing the overall number of chains within an aggregate while the hydrodynamic radius is increased.

Comparing the results of both polymer sets, the same conclusion can be drawn: While the polymers of the 15-70-15 set show an overall larger hydrodynamic radius, the aggregates of the 20-60-20 set are apparently smaller, due to the fact that the longer 2-VP blocks have a larger steric demand compared to the isoprene blocks, and at the same time the smaller isoprene blocks can form a core of more units, which is also reflected in the lower reduction of  $z_A$  with increasing  $M_n$ . With regard to the signal intensity between that of the individual chains and that of the aggregates, a further trend can be observed for both polymer series. The proportion of aggregates within the respective sample increases with the length of the 2-VP blocks. This can be attributed to the fact that the longer 2-VP blocks interact more easily due to their good solubility in DMF, thus favouring the tendency to form aggregates.

To further characterise the polymers, all samples were subjected to light scattering measurements using a zetasizer for the determination of the particle size. Figure 6 displays the dependence of the particle size on the targeted molecular weight.

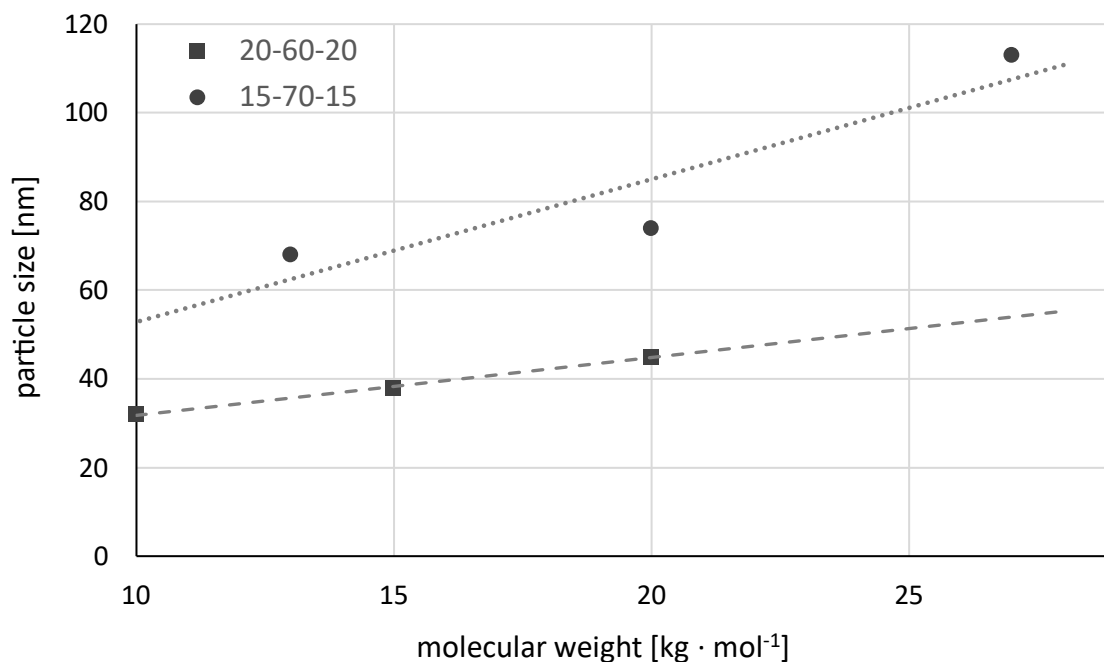
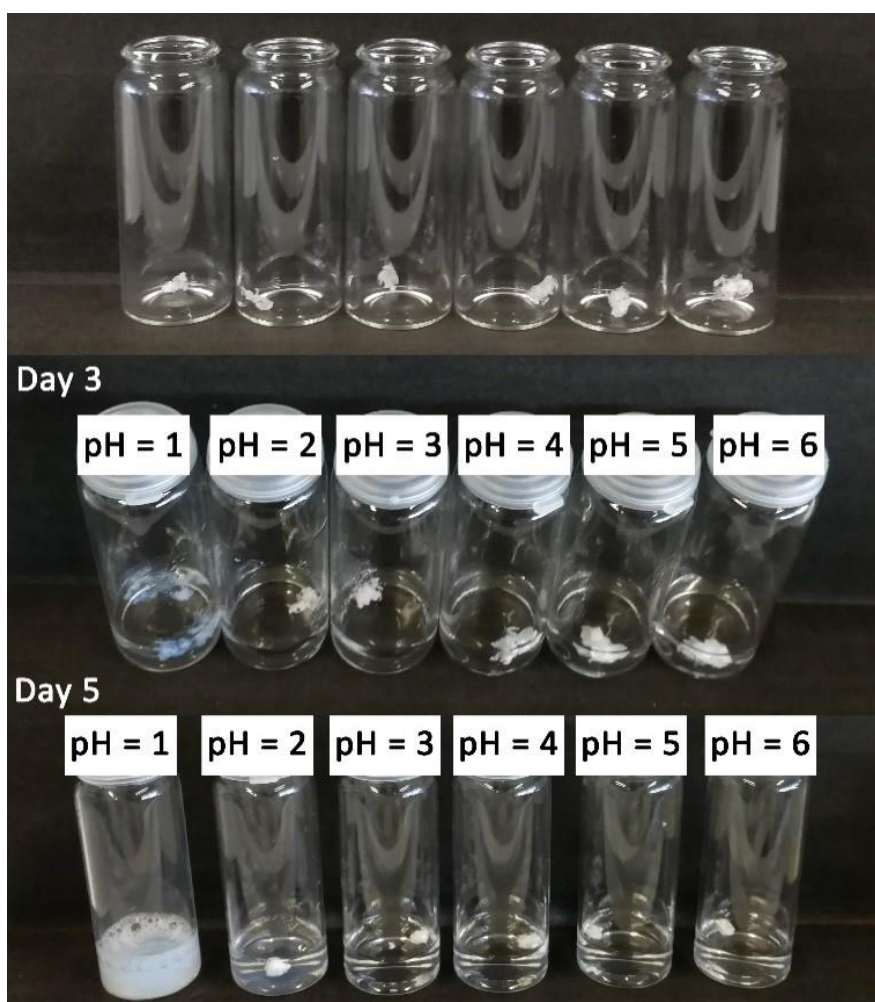


Figure 6: Light scattering measurements of P(2-VP-b-I-b-2-VP). The increasing particle size in dependence of the theoretically planned molecular weight and monomer ratio is observed. Solvent: DMF, concentration: 1 mg/mL.

In accordance with the results calculated from the SEC traces, the particle size increases with the molecular weight. Light scattering reveals a linear trend for both sets of polymers with a steeper slope of the 15-70-15 series. This underlines the tendency to form larger aggregates when the molar fraction of 2-VP is lower. In addition, the smaller particle size of the 20-60-20 series clearly shows that a higher molar fraction of 2-VP increases the steric demand of the shell as well as the interaction of the 2-VP blocks, thus resulting in the formation of a smaller particle core and an overall reduced particle size. Conversely, it can be clearly seen that the particle size of the 15-70-15 series increases significantly faster with increasing isoprene block length than the 20-60-20 series. This confirms that the influence of the interaction between the 2-VP blocks is less significant than the tendency of the isoprene blocks to form a hydrophobic core, which results in an increasing number of isoprene blocks in the core and thus in the particle growth. Since the shape of the aggregates could not be determined at this stage, this should be the focus of further work on this topic.

Besides the aggregation behaviour in DMF, the aqueous solubility of the polymers was also investigated. While it has been reported that P(2-VP) is insoluble in water at neutral pH and at a pH > 5, lower pH values lead to protonation at the aromatic nitrogen and thus solubility of the copolymer.<sup>11,52</sup> For the solubility tests, sample 20-60-20 – 4k was used. The higher molar fraction of the polar vinylpyridine and therefore the highest number of accessible protonation sites was expected to yield the best results. Six samples with different pH values from pH 1 to pH 6 were each mixed with 5 mg polymer and left to stand for a period of five days. Figure 7 displays the results.



*Figure 7: pH dependent solubility of P(2-VP-b-I-b-2-VP) 20-60-20 4k, observed for 5 days.*

As expected, the polymers are completely insoluble at pH 5 and 6, but this is also true for the samples stored at pH 3 and 4. Protonation at these pH values is not sufficient to compensate for the hydrophobicity of the isoprene block. However, after three days, swelling of the polymer sample at pH 1 can be observed. After five days, the pH 2 sample also shows first signs of solubility. There is still clearly undissolved polymer, however the solution shows a slight turbidity, as well as foaming when shaken, suggesting the presence of at least some dissolved amphiphilic polymer. At pH 1 no solid polymer residue was observed, a turbid solution at the limit of solubility of the polymer sample has formed. Strong foaming indicates the presence of the dissolved, amphiphilic polymer. Although these are relatively harsh conditions for solubility, they nevertheless show that it is possible to solubilise the structures in aqueous solution. A further change of the monomer ratio towards 2-VP should also allow solubility at higher pH values.

#### Material properties

The triblock copolymer structure with the highly flexible isoprene middle block and the high glass transition 2-VP outer blocks resembles the classical structure of a P(S-*b*-I-*b*-S) TPE. To investigate the capability of the polymers to behave in a TPE manner, polymer films were prepared by solvent-casting. A 10 w% solution of the 15-70-15 4k sample in THF was evaporated over several days and residual solvent was removed at reduced pressure.

The low  $T_g$  of isoprene and the high number of 1,4-units provide the basic requirements for an elastic material, yet these properties are quite weak. This can be attributed to the low molecular weight, Nevertheless, reversible elongation with fracture between ~20-25 % can be observed, as qualitatively shown in Figure 8.

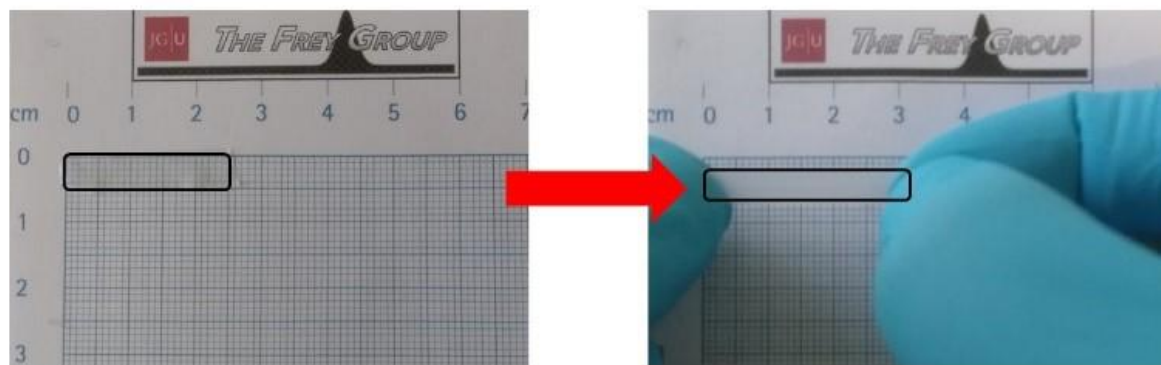


*Figure 8: TPE-like properties of P(2-VP-*b*-I-*b*-2-VP) 15-70-15 4k allow ~20% elongation of the solvent-cast polymer film.*

While high molecular weight TPEs with up to 1000% elongation benefit from loops and entanglements, these effects are not yet present in the samples since the molecular weight does not exceed  $27 \text{ kg}\cdot\text{mol}^{-1}$ . Overall, however, it can already be concluded that polymers of this type are certainly suitable as TPEs.



## 8.5 Experimental

### Materials and Methods

1,3-Dibenzoylbenzene was purchased from ABCR and used as received. Methylmagnesium iodide was purchased from Acros Organics and used as received. 2-Vinylpyridine as Isoprene were purchased from Acros Organics, filtered over basic aluminium oxide to remove the stabiliser and protic impurities, dried over  $\text{CaH}_2$  and freshly distilled prior to use. All solvents (Fisher Chemical, Carl Roth GmbH + Co. KG) were carefully dried with  $\text{CaH}_2$  (Sigma Aldrich) or butyllithium (Sigma Aldrich) and freshly distilled prior to use.

### Nuclear magnetic resonance (NMR) spectroscopy

$^1\text{H}$  measurements were performed on a Bruker Avance II 400 at a magnetic field strength of 400 MHz. DOSY measurements were performed using a Bruker Avance III HD 400 at a magnetic field strength of 400 MHz.

### Size exclusion chromatography (SEC)

All SEC measurements were performed with an Agilent 1100 Series chromatograph, equipped with HEMA columns (300/100/40, 95 cm length, 0.8 cm width, 50 °C) and an Agilent G1314A UV detector. Solvent: DMF, internal standard: toluene, calibration: polystyrene.

### Differential scanning calorimetry (DSC)

The DSC experiments were performed with a Perkin Elmer 8500 differential scanning calorimeter in a temperature range from -80 to 150 °C and a heating rate of 5 – 15 °C/min for the determination of the  $T_g$ .

### Zetasizer particle size measurements

The particle size was determined with a Malvern Nano ZS Zetasizer (Nano series). Measurements were performed in HPLC grade DMF at room temperature.

## Synthesis procedures

### Initiator synthesis

29.10 mL of methylmagnesium iodide (3M solution in Et<sub>2</sub>O, 87.31 mmol, 5 eq.) and dry THF (40 mL) were added to an argon-flushed three-neck round-bottomed flask equipped with a magnetic stir bar, a dropping funnel with pressure compensation, a Dimroth condenser and a rubber seal. 5 g of 1,3-dibenzoylbenzene (17.46 mmol, 1 eq.) were dissolved in 30 mL dry THF and the solution was added slowly *via* the dropping funnel, maintaining a slight reflux of the reaction mixture. After the complete addition, the mixture was allowed to reflux for an additional hour and quenched by the addition of a saturated NH<sub>4</sub>Cl solution. The ethereal phase was separated, washed with water, brine and water, dried over MgSO<sub>4</sub> and the solvent was removed under reduced pressure.

<sup>1</sup>H NMR: (DMSO-d<sub>6</sub>, 400 MHz)  $\delta$  [ppm] = 7.72 (t,  $J$  = 1.9 Hz, 1H), 7.44 (dt,  $J$  = 8.3, 1.4 Hz, 4H), 7.35-7.07 (m, 9H), 5.69 (d,  $J$  = 3.0 Hz, 2H), 1.85 (d,  $J$  = 2.3 Hz, 6H).

50 mL of 20% H<sub>2</sub>SO<sub>4</sub> solution in water were added to the intermediate and heated for 2 h under reflux, while the conversion was observed *via* TLC. After cooling, the product was extracted with Et<sub>2</sub>O. The resulting organic phase was separated, washed with water, brine and water, dried over MgSO<sub>4</sub> and the solvent was removed under reduced pressure. Column chromatographic purification of the crude product (solvent: petroleum ether) yields DDPE as colourless oil (91%, 4.49 g, 15.89 mmol).

$R_f$  : 0.4 (petroleum ether).

<sup>1</sup>H NMR (DMSO-d<sub>6</sub>, 400 MHz)  $\delta$  [ppm] = 7.46-7.27 (m, 13H), 7.15 (td,  $J$  = 1.8, 0.5 Hz, 1H), 5.49 (dd,  $J$  = 5.9, 1.1 Hz, 4H).

<sup>13</sup>C NMR (DMSO-d<sub>6</sub>, 101 MHz)  $\delta$  [ppm] = 148.89 (s, 2C), 140.60 (d,  $J$  = 30.2 Hz, 3C), 128.69 –127.28 (m, 31C), 114.99(s, 3C).

### Polymer synthesis

All polymerisations were carried out on a 5 g scale using a carefully flame dried all-glass apparatus with rubber seals and Teflon caps as well as standard high vacuum techniques. Both monomers were purified by filtration over basic aluminium oxide to remove the stabiliser and protic impurities, degassed with three *freeze-pump-thaw* cycles, stirred over  $\text{CaH}_2$  for one night and freshly distilled prior to the polymerisation. DDPE was placed in the reaction flask, lyophilised with pre-dried benzene to remove last traces of water and subsequently stirred under dynamic vacuum for one night. With the use of a graduated ampoule, a defined amount of benzene was added to DDPE, followed by the addition of 2.05 eq. *s*-BuLi to activate the initiator. The immediate formation of the red-coloured anionic species can be observed. After one hour, additional benzene was condensed into the reaction flask and isoprene was added *via* syringe, resulting in the colour change to light yellow. After 2 h, 1.5 eq. THF with respect to benzene were condensed to the reaction mixture and a chloroform-dry ice bath was applied to cool the reaction mixture to  $-64\text{ }^\circ\text{C}$ . 2-VP was added *via* syringe, leading to the immediate formation of the deep red coloured pyridinyl anions. After 1 h, the reaction was quenched with degassed methanol. The solvent was removed under reduced pressure to quantitatively yield the respective triblock copolymer as a colourless solid. See ESI for specific quantities of each individual sample.

## 8.6 Conclusion

According to a literature procedure for the synthesis of DPE, double 1,1-diphenylethylene (DDPE) has been obtained by a facile Grignard reaction from 1,3-dibenzoylbenzene and methyl magnesium iodide and subsequent dehydration. After purification, an optimised procedure for its universal use as efficient bifunctional initiator for carbanionic block copolymerisation reactions has been established, as demonstrated by the quantitative end-capping with ethylene oxide. Starting from the activated initiator species, the previous limitations in linear block copolymer synthesis of some monomers have been successfully circumvented. A sophisticated two-step synthesis route was established, in which isoprene was first polymerised in benzene and subsequently, upon addition of THF, 2-vinylpyridine was copolymerised in a controlled reaction at low temperatures. Novel, functional ABA triblock copolymers of 2-VP and isoprene with narrow molecular weight distributions have been obtained, which allowed the first characterisation of such structures. Although the determination of the exact molecular weight cannot be carried out accurately *via* NMR and SEC, a controlled polymerisation is assumed due to the distinct colour change to the respective living chain end, the uniform shift of the elugrams towards higher molecular weights with a stable dispersity as well as quantitative yields for all samples.

By means of  $^1\text{H}$  NMR spectroscopy, it was possible to precisely verify the molar monomer composition and to determine the incorporation ratio of 1,4-units in the isoprene block. Both values are in accordance with expectation. In particular, the microstructure of isoprene and the corresponding low glass transition temperature of around  $-62\text{ }^\circ\text{C}$  as well as the observed mechanical properties lay the foundation for a new type of TPE materials.

SEC and light scattering experiments display strong aggregation behaviour of the polymers in DMF, which is in accordance with earlier reported 2-VP copolymers and a clear trend of the aggregate/particle size in dependence of the molecular weight and molar monomer ratio. These results offer a good starting point for more in-depth

investigations into the shape of the aggregates, and thus the possibility of finding further examples of toroidal structures.

In addition to the protonation in the acidic medium, further post-polymerisation modifications - first and foremost the quaternisation with  $\alpha$ - $\omega$ -dialkyl halides or diphenols which leads to reversibly cross-linked systems - are possible in order to exploit the full potential of the pyridine groups in these novel materials.

## 8.7 References

- (1) Feng, H.; Lu, X.; Wang, W.; Kang, N.-G.; Mays, J. W. Block Copolymers: Synthesis, Self-Assembly, and Applications. *Polymers* **2017**, *9* (10). DOI: 10.3390/polym9100494. Published Online: Oct. 9, 2017.
- (2) Lazzari, M.; Torneiro, M. A Global View on Block Copolymers. *Polymers* **2020**, *12* (4). DOI: 10.3390/polym12040869. Published Online: Apr. 10, 2020.
- (3) Wang, W.; Lu, W.; Goodwin, A.; Wang, H.; Yin, P.; Kang, N.-G.; Hong, K.; Mays, J. W. Recent advances in thermoplastic elastomers from living polymerizations: Macromolecular architectures and supramolecular chemistry. *Progress in Polymer Science* **2019**, *95*, 1–31. DOI: 10.1016/j.progpolymsci.2019.04.002.
- (4) Chapman, B. K.; Kilian, D. High performance styrenic block copolymers in medical and damping applications. *TPE magazine international* **2012**, *4* (4), 28–31.
- (5) Lopes, P. A.; Fernandes, D. F.; Silva, A. F.; Marques, D. G.; Almeida, A. T. de; Majidi, C.; Tavakoli, M. Bi-Phasic Ag-In-Ga-Embedded Elastomer Inks for Digitally Printed, Ultra-Stretchable, Multi-layer Electronics. *ACS applied materials & interfaces* **2021**, *13* (12), 14552–14561. DOI: 10.1021/acsami.0c22206. Published Online: Mar. 10, 2021.
- (6) Rankin, L. A.; Lee, B.; Mineart, K. P. Effect of network connectivity on the mechanical and transport properties of block copolymer gels. *Journal of Polymer Science* **2021**, *59* (1), 34–42. DOI: 10.1002/pol.20200695.
- (7) Braun, V. D.; Daimon, H.; Becker, G. Über polystyrolerivate mit elementen der fünften hauptgruppe. *Makromol. Chem.* **1963**, *62* (1), 183–195. DOI: 10.1002/macp.1963.020620119.
- (8) Geerts, J.; van Beylen, M.; Smets, G. Anionic polymerization of o- and p-methoxystyrene. *J. Polym. Sci. A-1 Polym. Chem.* **1969**, *7* (10), 2859–2873. DOI: 10.1002/pol.1969.150071010.
- (9) Hirao, A.; Loykulant, S.; Ishizone, T. Recent advance in living anionic polymerization of functionalized styrene derivatives. *Progress in Polymer Science* **2002**, *27* (8), 1399–1471. DOI: 10.1016/S0079-6700(02)00016-3.
- (10) Fréchet, J. M. J.; Meftahi, M. V. de. Poly(vinyl pyridine)s: Simple reactive polymers with multiple applications. *Brit. Poly.J.* **1984**, *16* (4), 193–198. DOI: 10.1002/pi.4980160407.
- (11) Kennemur, J. G. Poly(vinylpyridine) Segments in Block Copolymers: Synthesis, Self-Assembly, and Versatility. *Macromolecules* **2019**, *52* (4), 1354–1370. DOI: 10.1021/acs.macromol.8b01661.
- (12) Luxton, A. R.; Quig, A.; Delvaux, M.-J.; Fetters, L. J. Star-branched polymers: 2. Linking reaction involving 2- and 4-vinyl pyridine and dienyl and styryllithium chain ends. *Polymer* **1978**, *19* (11), 1320–1324. DOI: 10.1016/0032-3861(78)90315-4.
- (13) Schmitz, F. P.; Hilgers, H.; Gemmel, B. Side reactions during preparation and handling of oligomers and polymers from 2-vinylpyridine. *Makromol. Chem.* **1990**, *191* (5), 1033–1049. DOI: 10.1002/macp.1990.021910506.
- (14) Szwarc, M. 'Living' Polymers. *Nature* **1956**, *178* (4543), 1168–1169. DOI: 10.1038/1781168a0.

- (15) Grubbs, R. B.; Grubbs, R. H. 50th Anniversary Perspective : Living Polymerization—Emphasizing the Molecule in Macromolecules. *Macromolecules* **2017**, *50* (18), 6979–6997. DOI: 10.1021/acs.macromol.7b01440.
- (16) Worsfold, D. J.; Bywater, S. Anionic Polymerization Of Isoprene. *Can. J. Chem.* **1964**, *42* (12), 2884–2892. DOI: 10.1139/v64-426.
- (17) Schoenberg, E.; Marsh, H. A.; Walters, S. J.; Saltman, W. M. Polyisoprene. *Rubber Chemistry and Technology* **1979**, *52* (3), 526–604. DOI: 10.5254/1.3535230.
- (18) Quirk, R. P. Anionic Polymerization of Nonpolar Monomers. In *Polymer Science: A Comprehensive Reference*; Elsevier, 2012; pp 559–590. DOI: 10.1016/B978-0-444-53349-4.00076-5.
- (19) Stavely, F. W.; Coworkers. Coral Rubber—A Cis -1,4-Polyisoprene. *Rubber Chemistry and Technology* **1956**, *29* (3), 673–686. DOI: 10.5254/1.3542582.
- (20) Watanabe, H.; Tirrell, M. Measurement of forces in symmetric and asymmetric interactions between diblock copolymer layers adsorbed on mica. *Macromolecules* **1993**, *26* (24), 6455–6466. DOI: 10.1021/ma00076a023.
- (21) Quirk, R. P.; Corona-Galvan, S. Controlled Anionic Synthesis of Polyisoprene–Poly(2-vinylpyridine) Diblock Copolymers in Hydrocarbon Solution. *Macromolecules* **2001**, *34* (5), 1192–1197. DOI: 10.1021/ma001044v.
- (22) Odani, H.; Uchikura, M.; Ogino, Y.; Kuarat, M. Permeation of Gases in Poly (2-vinylpyridine)-Block-Polyisoprene. *Bulletin of the Institute for Chemical Research, Kyoto* **1986**, *63* (4), 332–339.
- (23) Funaki, Y.; Kumano, K.; Nakao, T.; Jinnai, H.; Yoshida, H.; Kimishima, K.; Tsutsumi, K.; Hirokawa, Y.; Hashimoto, T. Influence of casting solvents on microphase-separated structures of poly(2-vinylpyridine)- block -polyisoprene. *Polymer* **1999**, *40* (25), 7147–7156. DOI: 10.1016/s0032-3861(99)00112-3.
- (24) Tsutsumi, K.; Funaki, Y.; Hirokawa, Y.; Hashimoto, T. Selective Incorporation of Palladium Nanoparticles into Microphase-Separated Domains of Poly(2-vinylpyridine)- block -polyisoprene. *Langmuir* **1999**, *15* (16), 5200–5203. DOI: 10.1021/la990246l.
- (25) Asai, Y.; Takano, A.; Matsushita, Y. Asymmetric Double Tetragonal Domain Packing from ABC Triblock Terpolymer Blends with Chain Length Difference. *Macromolecules* **2016**, *49* (18), 6940–6946. DOI: 10.1021/acs.macromol.6b01670.
- (26) Chernyy, S.; Mahalik, J. P.; Kumar, R.; Kirkensgaard, J. J. K.; Arras, M. M. L.; Kim, H.; Schulte, L.; Ndoni, S.; Smith, G. S.; Mortensen, K.; Sumpter, B. G.; Russell, T. P.; Almdal, K. On the morphological behavior of ABC miktoarm stars containing poly(cis 1,4-isoprene), poly(styrene), and poly(2-vinylpyridine). *J. Polym. Sci. Part B: Polym. Phys.* **2018**, *56* (22), 1491–1504. DOI: 10.1002/polb.24733.
- (27) Dai, K. Determining the temperature-dependent Flory interaction parameter for strongly immiscible polymers from block copolymer segregation measurements. *Polymer* **1994**, *35* (1), 157–161. DOI: 10.1016/0032-3861(94)90065-5.
- (28) Hirschberg, V.; Faust, L.; Rodrigue, D.; Wilhelm, M. Effect of Topology and Molecular Properties on the Rheology and Fatigue Behavior of Solid Polystyrene/Polyisoprene Di- and

Triblock Copolymers. *Macromolecules* **2020**, *53* (13), 5572–5587. DOI: 10.1021/acs.macromol.0c00632.

(29) Jiang, K.; Zhang, J.; Liang, Q. Self-Assembly of Asymmetrically Interacting ABC Star Triblock Copolymer Melts. *The journal of physical chemistry. B* **2015**, *119* (45), 14551–14562. DOI: 10.1021/acs.jpccb.5b08187. Published Online: Nov. 2, 2015.

(30) Zhang, G.; Qiu, F.; Zhang, H.; Yang, Y.; Shi, A.-C. SCFT Study of Tiling Patterns in ABC Star Terpolymers. *Macromolecules* **2010**, *43* (6), 2981–2989. DOI: 10.1021/ma902735t.

(31) Zioga, A.; Sioula, S.; Hadjichristidis, N. Synthesis and morphology of model 3-miktoarm star terpolymers of styrene, isoprene and 2-vinyl pyridine. *Macromol. Symp.* **2000**, *157* (1), 239–250. DOI: 10.1002/1521-3900(200007)157:1<239:AID-MASY239>3.0.CO;2-I.

(32) Chen, Z.; Cui, H.; Hales, K.; Li, Z.; Qi, K.; Pochan, D. J.; Wooley, K. L. Unique toroidal morphology from composition and sequence control of triblock copolymers. *Journal of the American Chemical Society* **2005**, *127* (24), 8592–8593. DOI: 10.1021/ja050290p.

(33) Pochan, D. J.; Chen, Z.; Cui, H.; Hales, K.; Qi, K.; Wooley, K. L. Toroidal triblock copolymer assemblies. *Science (New York, N.Y.)* **2004**, *306* (5693), 94–97. DOI: 10.1126/science.1102866.

(34) Huang, H.; Chung, B.; Jung, J.; Park, H.-W.; Chang, T. Toroidal micelles of uniform size from diblock copolymers. *Angewandte Chemie (International ed. in English)* **2009**, *48* (25), 4594–4597. DOI: 10.1002/anie.200900533.

(35) Nakahama, S.; Ishizone, T.; Hirao, A. Anionic living polymerization of styrenes containing electron-withdrawing groups. *Makromolekulare Chemie. Macromolecular Symposia* **1993**, *67* (1), 223–236. DOI: 10.1002/masy.19930670118.

(36) Matmour, R.; More, A. S.; Wadgaonkar, P. P.; Gnanou, Y. High performance poly(styrene-*b*-diene-*b*-styrene) triblock copolymers from a hydrocarbon-soluble and additive-free dicarbanionic initiator. *Journal of the American Chemical Society* **2006**, *128* (25), 8158–8159. DOI: 10.1021/ja062695v.

(37) Schultz, A. R.; Bobade, S.; Scott, P. J.; Long, T. E. Hydrocarbon-Soluble Piperazine-Containing Dilithium Anionic Initiator for High Cis -1,4 Isoprene Polymerization. *Macromol. Chem. Phys.* **2018**, *219* (1), 1700201. DOI: 10.1002/macp.201700201.

(38) Tung, L. H.; Lo, G. Y.-S.; Beyer, D. E. Dilithium Anionic Initiators Based on Double 1,1-Diphenylethylene Compounds. *Macromolecules* **1978**, *11* (3), 616–617. DOI: 10.1021/ma60063a036.

(39) Vasilakopoulos, T. C.; Hadjichristidis, N. Influence of (1,3-phenylene)bis(3-methyl-1-phenyl pentylidene)dilithium initiator concentration on the modality of polybutadiene. *J. Polym. Sci. A Polym. Chem.* **2013**, *51* (4), 824–835. DOI: 10.1002/pola.26435.

(40) Lu, Z.; Xu, H.; Li, Y.; Hu, Y. Synthesis of a difunctional organolithium compound as initiator for the polymerization of styrene-butadiene/isoprene-styrene triblock copolymer. *J. Appl. Polym. Sci.* **2006**, *100* (2), 1395–1402. DOI: 10.1002/app.23666.

(41) Iatrou, H.; Mays, J. W.; Hadjichristidis, N. Regular Comb Polystyrenes and Graft Polyisoprene/Polystyrene Copolymers with Double Branches (“Centipedes”). Quality of (1,3-



Phenylene)bis(3-methyl-1-phenylpentylidene)dilithium Initiator in the Presence of Polar Additives. *Macromolecules* **1998**, *31* (19), 6697–6701. DOI: 10.1021/ma980738p.

(42) Batesky, D. C.; Goldfogel, M. J.; Weix, D. J. Removal of Triphenylphosphine Oxide by Precipitation with Zinc Chloride in Polar Solvents. *The Journal of organic chemistry* **2017**, *82* (19), 9931–9936. DOI: 10.1021/acs.joc.7b00459. Published Online: Sep. 28, 2017.

(43) 1,1-Diphenylethylene. *Org. Synth.* **1926**, *6*, 32. DOI: 10.15227/orgsyn.006.0032.

(44) Hillmyer, M. A.; Bates, F. S. Synthesis and Characterization of Model Polyalkane–Poly(ethylene oxide) Block Copolymers. *Macromolecules* **1996**, *29* (22), 6994–7002. DOI: 10.1021/ma960774t.

(45) Hadjichristidis, N.; Hiraio, A., Eds. *Anionic polymerization: Principles, practice, strength, consequences and applications*; Springer Tokyo, 2015.

(46) Widmaier, J. M.; Meyer, G. C. Glass transition temperature of anionic polyisoprene. *Macromolecules* **1981**, *14* (2), 450–452. DOI: 10.1021/ma50003a041.

(47) Georgopoulos, P.; Rangou, S.; Gil Haenelt, T.; Abetz, C.; Meyer, A.; Filiz, V.; Handge, U. A.; Abetz, V. Analysis of glass transition and relaxation processes of low molecular weight polystyrene-b-polyisoprene diblock copolymers. *Colloid Polym Sci* **2014**, *292* (8), 1877–1891. DOI: 10.1007/s00396-014-3284-y.

(48) Wahlen, C.; Blankenburg, J.; Tiedemann, P. von; Ewald, J.; Sajkiewicz, P.; Müller, A. H. E.; Floudas, G.; Frey, H. Tapered Multiblock Copolymers Based on Farnesene and Styrene: Impact of Biobased Polydiene Architectures on Material Properties. *Macromolecules* **2020**, *53* (23), 10397–10408. DOI: 10.1021/acs.macromol.0c02118.

(49) Fickenscher, M.; Reimers, T.; Frey, H. Introducing a 1,1-diphenylethylene analogue for vinylpyridine: anionic copolymerisation of 3-(1-phenylvinyl)pyridine (m-PyPE). *Polym. Chem.* **2021**, *12* (24), 3576–3581. DOI: 10.1039/d1py00302j.

(50) Gan, Y.; Dong, D.; Hogen-Esch, T. E. Effects of Lithium Bromide on the Glass Transition Temperatures of Linear and Macrocyclic Poly(2-vinylpyridine) and Polystyrene. *Macromolecules* **1995**, *28* (1), 383–385. DOI: 10.1021/ma00105a055.

(51) Ogata, Y.; Iso, K.; Kura, S.; Hayakawa, T.; Makita, Y. Aggregation behavior of poly( $\gamma$ -benzyl-L-glutamate)-b-polyisoprene-b-poly( $\gamma$ -benzyl-L-glutamate) rod-coil-rod triblock copolymer in N,N-dimethylformamide. *J. Polym. Sci. Part B: Polym. Phys.* **2010**, *48* (15), 1740–1748. DOI: 10.1002/polb.22039.

(52) Yoshida, M.; Sakamoto, N.; Ikemi, K.; Arichi, S. Solution Properties of Polyvinylpyridine in Acidic Solvent. I. Solution Properties of Poly(2-vinylpyridine) in Aqueous Solution of Sulfuric Acid. *BCSJ* **1993**, *66* (6), 1598–1602. DOI: 10.1246/bcsj.66.1598.

## 8.8 Supporting Information

### $^{13}\text{C}$ NMR spectroscopy $\beta$ -/reactive-carbon shifts

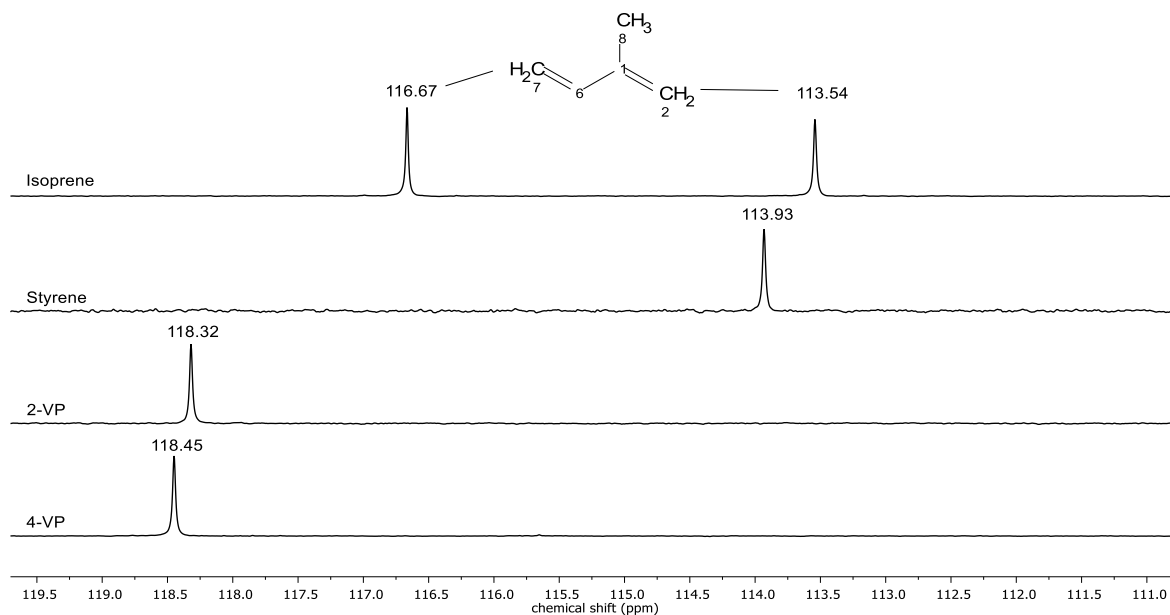


Figure S1:  $^{13}\text{C}$  NMR spectrum (400 MHz,  $\text{CDCl}_3$ ) of different monomers, showing the respective  $\beta$ -carbon shifts.

## DDPE characterisation



Figure S2:  $^1\text{H}$  NMR spectrum (400 MHz,  $\text{DMSO-d}_6$ ) of the intermediate diol (top) and DDPE (bottom).

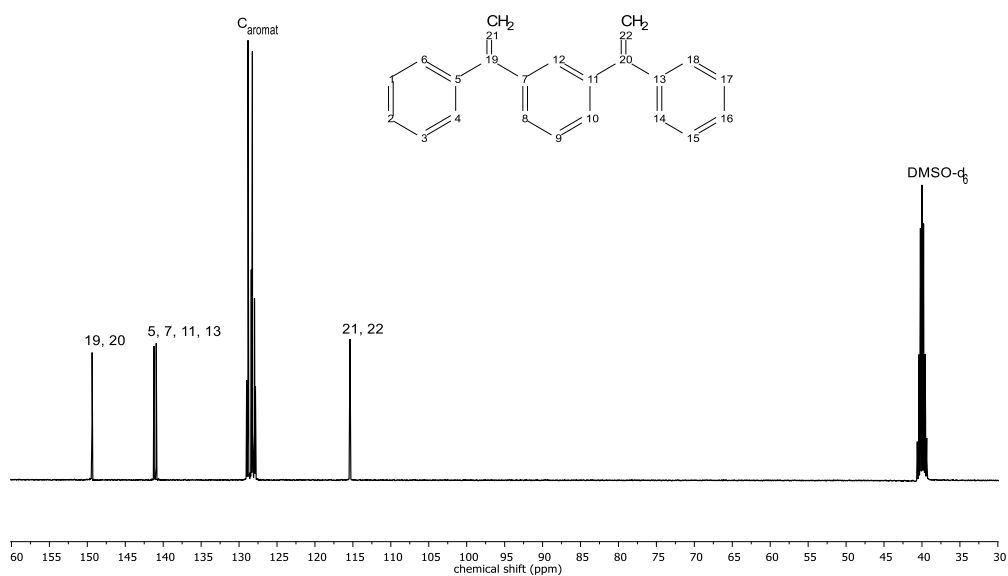


Figure S3:  $^{13}\text{C}$  NMR spectrum (400 MHz,  $\text{DMSO-d}_6$ ) of DDPE.

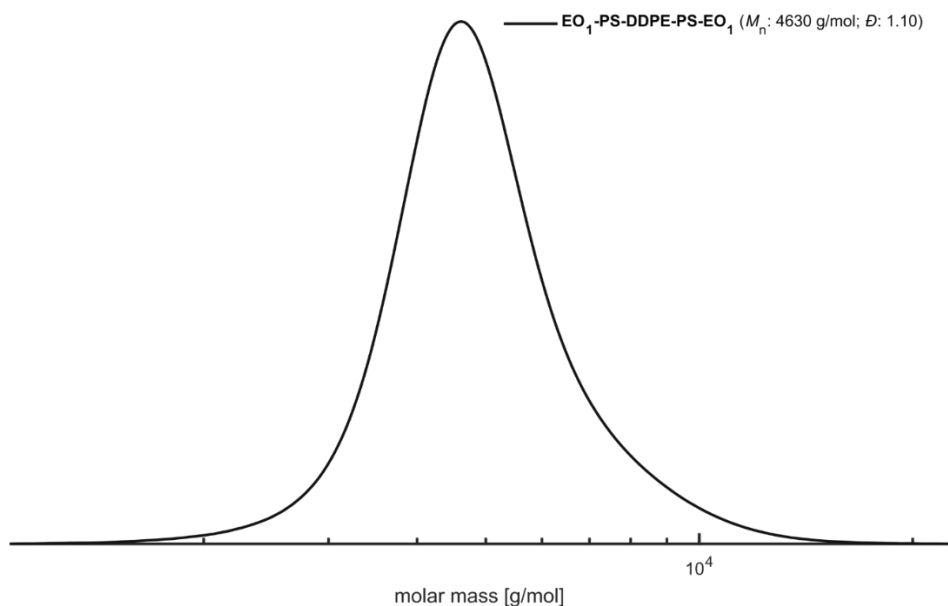


Figure S4: SEC elugram of  $EO\text{-PS-DDPE-PS-EO}$ ,  $M_w(\text{target}) = 5 \text{ kg mol}^{-1}$ , measured in THF with toluene as internal standard, polystyrene calibration and an UV detector.

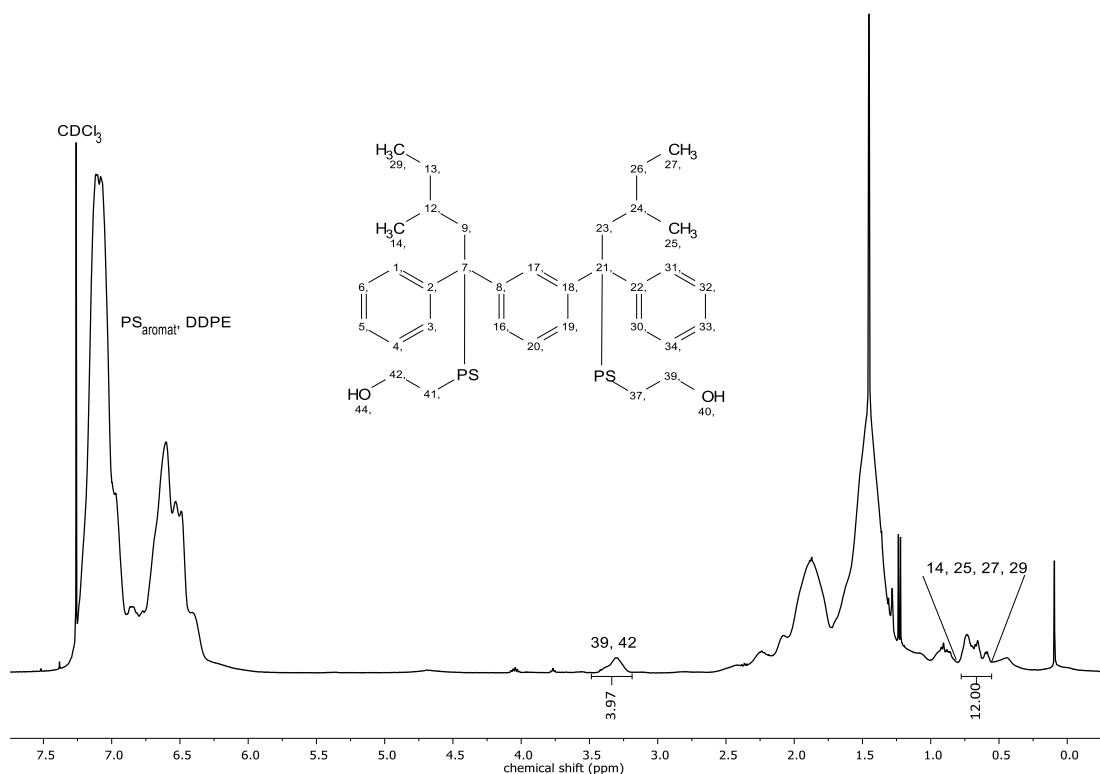


Figure S5:  $^1\text{H NMR}$  spectrum (400 MHz,  $\text{CDCl}_3$ ) of  $EO\text{-PS-DDPE-PS-EO}$ , showing only the successful bifunctional initiation via end-capping with EO.

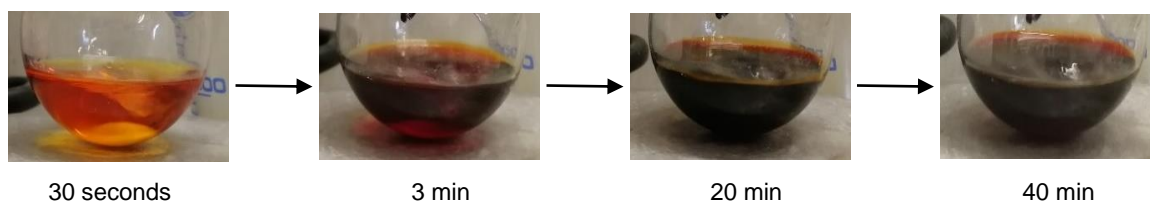
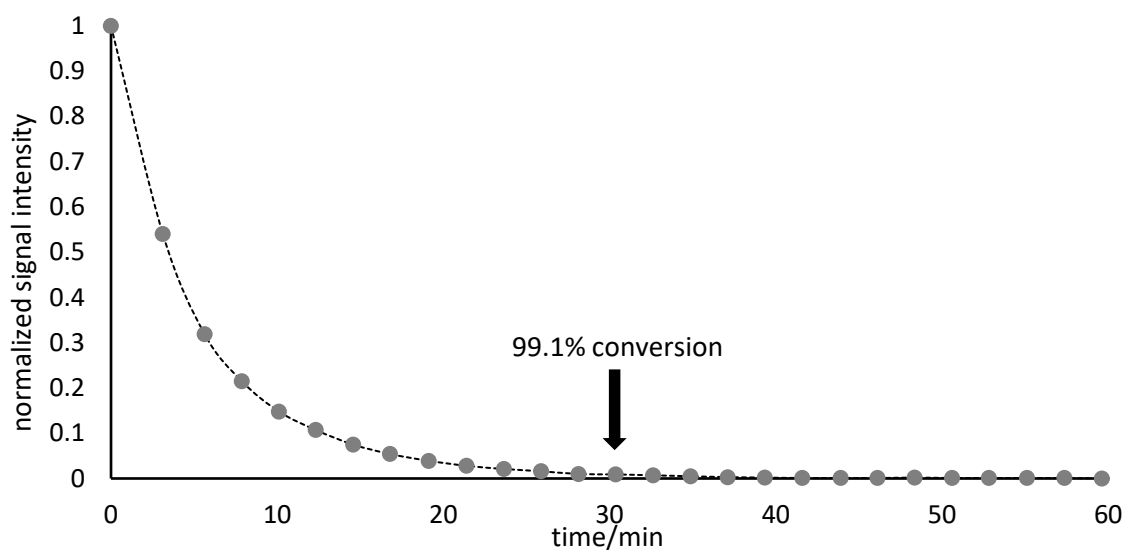
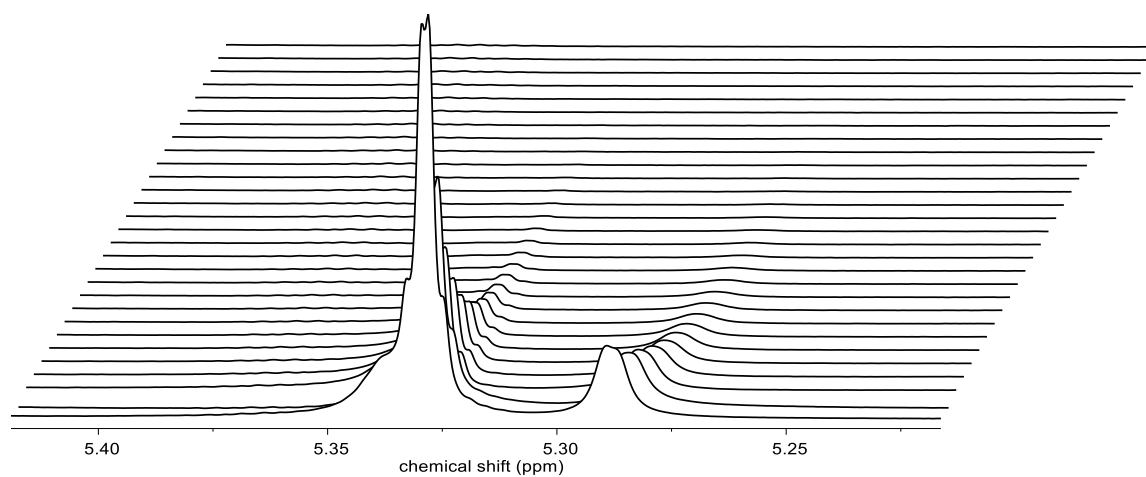


Figure S6: Top:  $^1\text{H}$  NMR spectrum (400 MHz, benzene- $d_6$ ) of the activation reaction of a 0.1 M DDPE solution in benzene with *s*-BuLi, depicting the depletion of the double bond signal. Mid: Corresponding time-intensity plot, indication 99% conversion after 30 minutes. Bottom: Visible change to the typical dark red coloured anionic solution after the addition of *s*-BuLi.

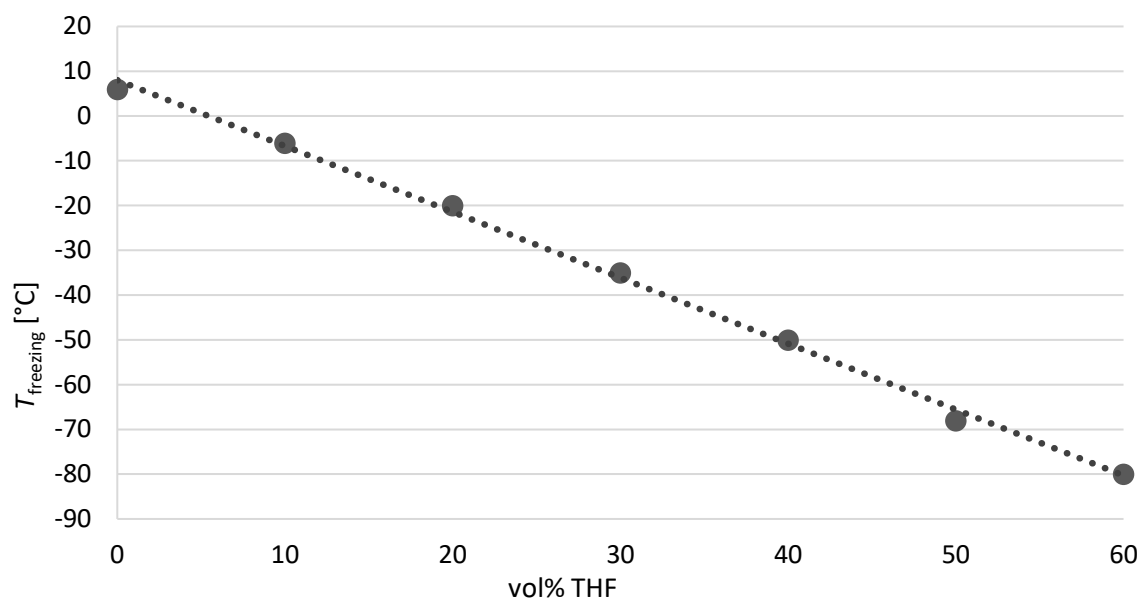


Figure S7: Melting temperature of benzene-THF mixtures. A minimum of 50% THF is required to prevent the mixture from freezing during the polymerisation.

Copolymer NMR spectroscopy characterisation

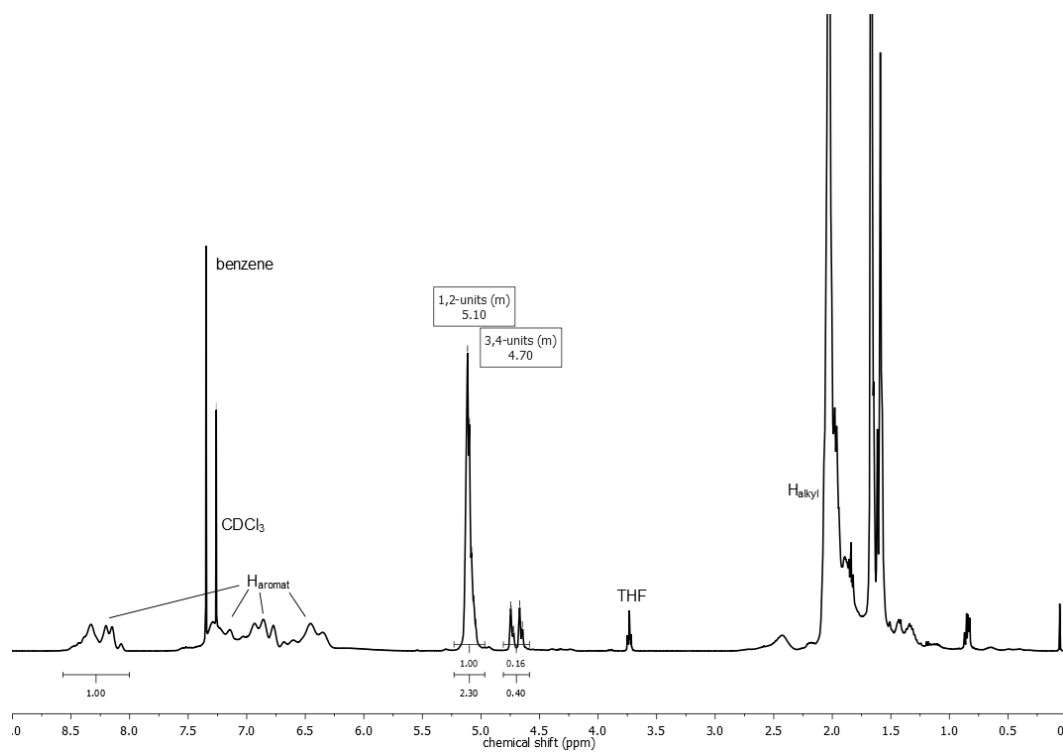


Figure S8: <sup>1</sup>H NMR spectrum (CDCl<sub>3</sub>, 400 MHz) of P(2-VP-b-I-b-2-VP) – 15-70-15 2k.

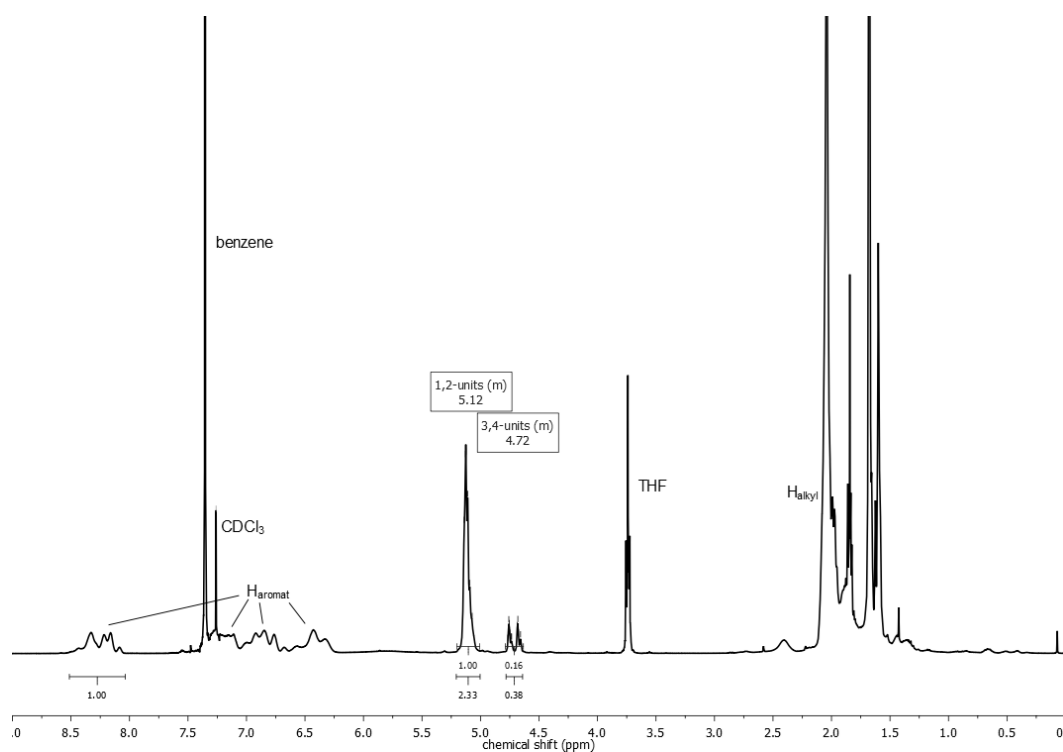


Figure S9: <sup>1</sup>H NMR spectrum (CDCl<sub>3</sub>, 400 MHz) of P(2-VP-b-I-b-2-VP) – 15-70-15 3k.

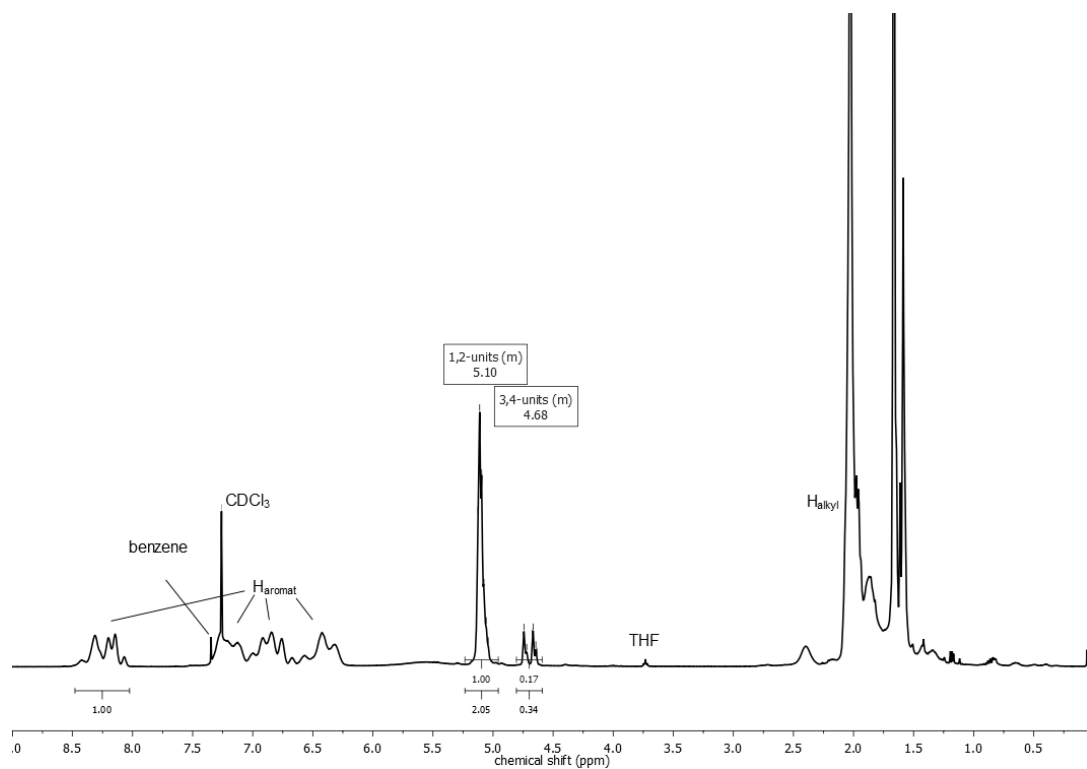


Figure S10:  $^1\text{H}$  NMR spectrum ( $\text{CDCl}_3$ , 400 MHz) of  $P(2\text{-VP-}b\text{-I-}b\text{-2-VP})$  – 15-70-15 4k.

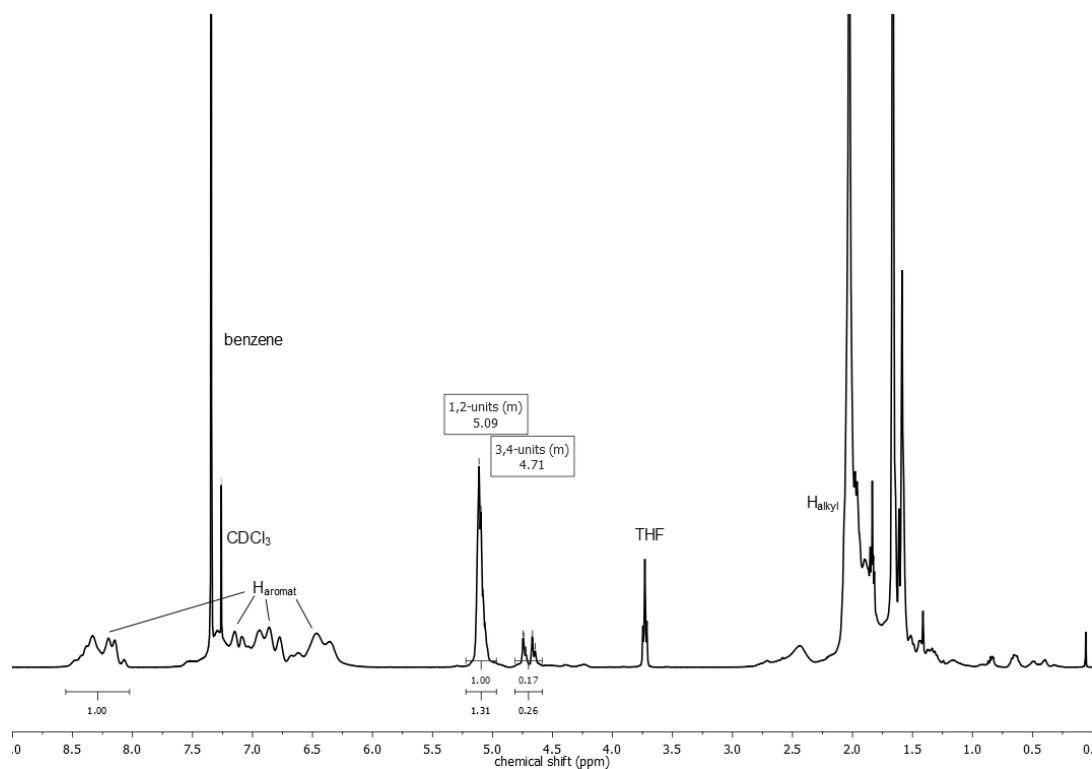


Figure S11:  $^1\text{H}$  NMR spectrum ( $\text{CDCl}_3$ , 400 MHz) of  $P(2\text{-VP-}b\text{-I-}b\text{-2-VP})$  – 20-60-20 2k.



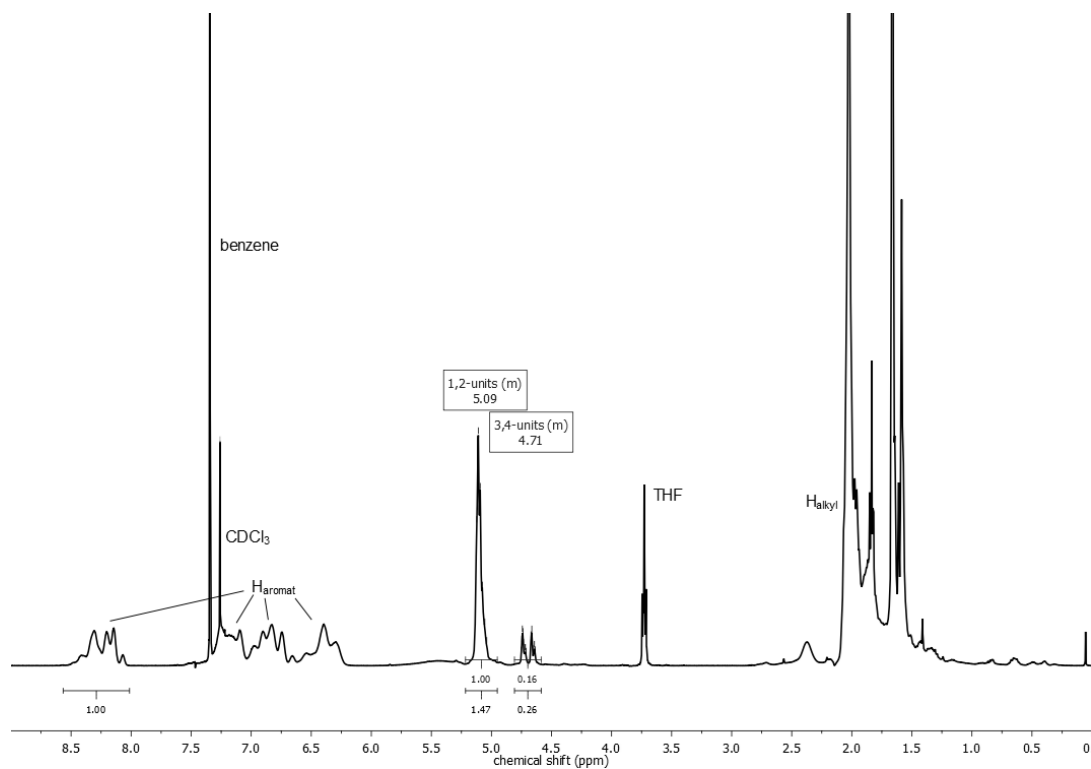


Figure S12:  $^1\text{H}$  NMR spectrum ( $\text{CDCl}_3$ , 400 MHz) of  $P(2\text{-VP-}b\text{-I-}b\text{-2-VP})$  - 20-60-20 3k.

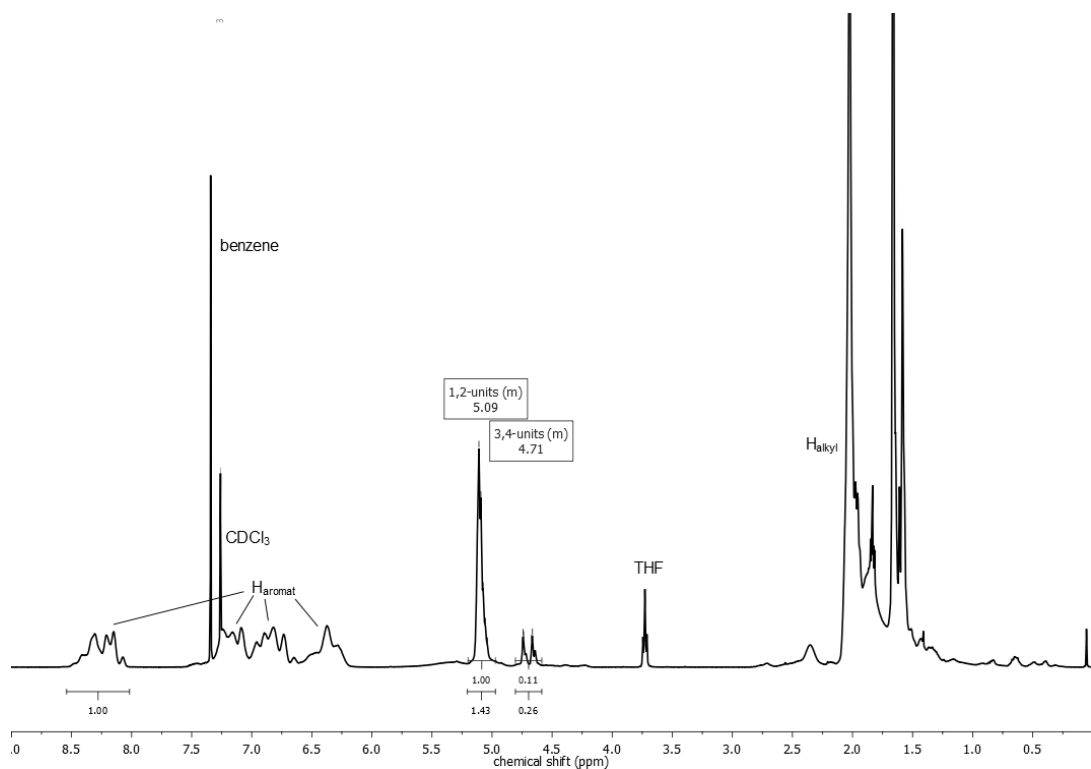


Figure S13:  $^1\text{H}$  NMR spectrum ( $\text{CDCl}_3$ , 400 MHz) of  $P(2\text{-VP-}b\text{-I-}b\text{-2-VP})$  - 20-60-20 4k.

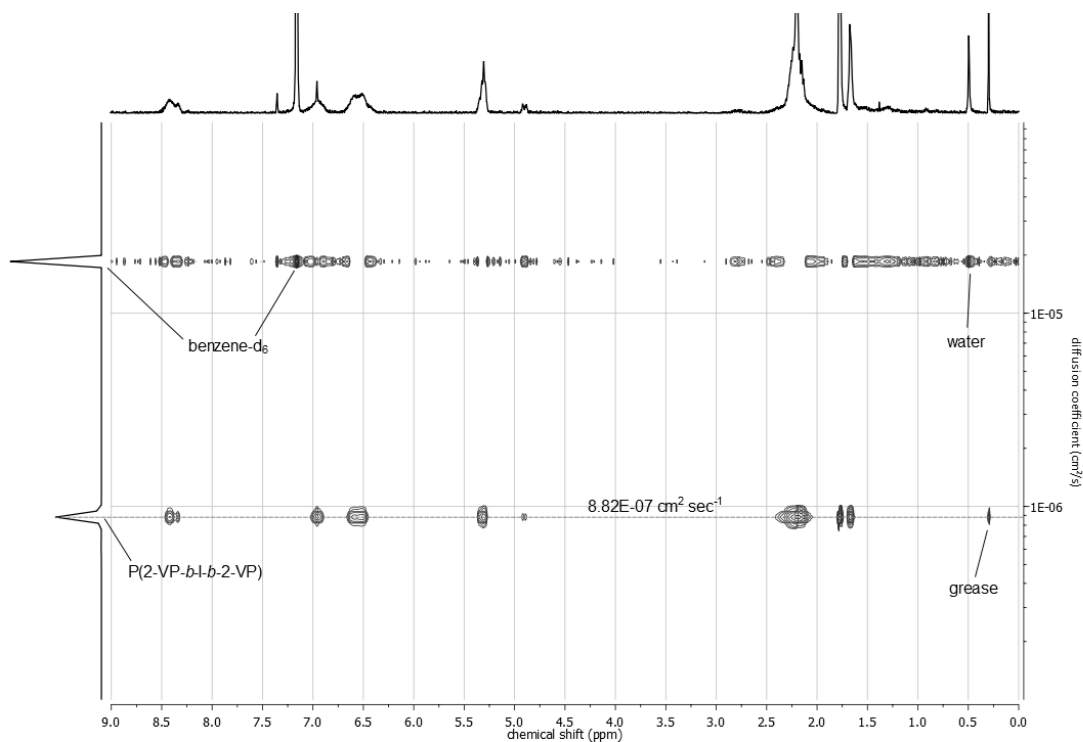


Figure S14: DOSY NMR spectrum (benzene-d<sub>6</sub>, 400 MHz) of P(2-VP-b-I-b-2-VP) – 20-60-20 4k.

Table S2: Monomer and microstructure ratios calculated from <sup>1</sup>H NMR spectroscopy.

Sample	mol% <sub>calc</sub> (2-VP)	mol% <sub>calc</sub> (I)	deviation(I) [%]	3,4-units [%]	1,4-units [%]
15-70-15 - 2k	28.6	71.4	2.0	8.7	91.3
15-70-15 - 3k	28.4	71.6	2.3	8.2	91.8
15-70-15 - 4k	31.1	68.9	1.5	8.3	91.7
20-60-20 - 2k	41.8	58.2	2.9	6.5	93.5
20-60-20 - 3k	39.1	60.9	1.6	9.1	90.9
20-60-20 - 4k	38.5	61.5	2.6	8.8	91.2

## Differential scanning calorimetry

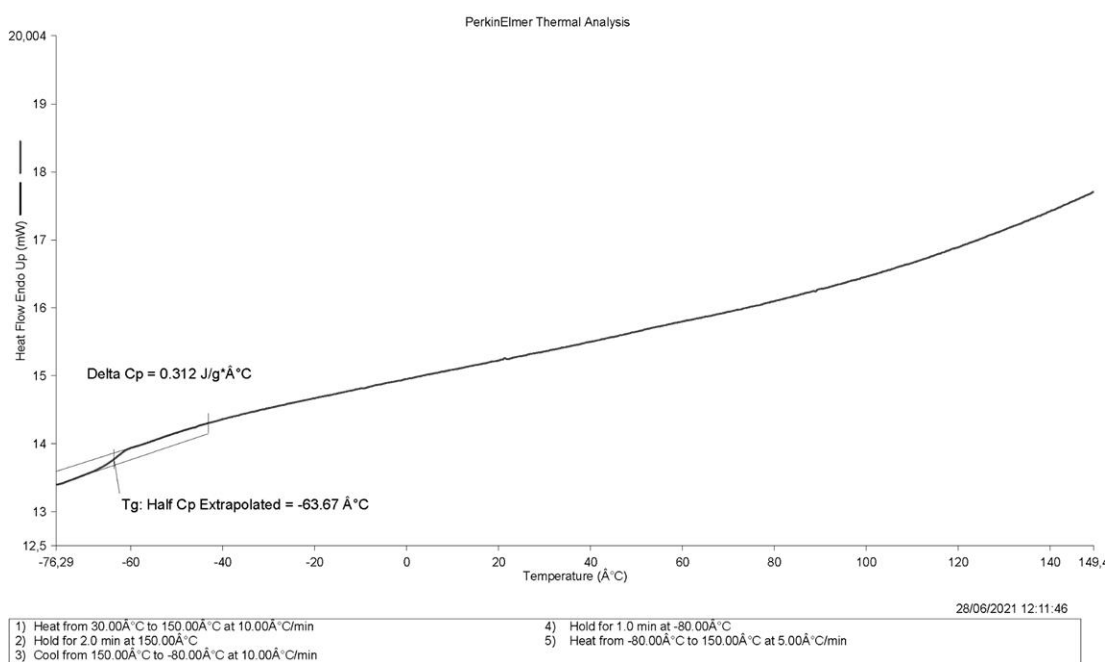


Figure S15: DSC curve of P(2-VP-b-I-b-2-VP) – 15-70-15 2k.

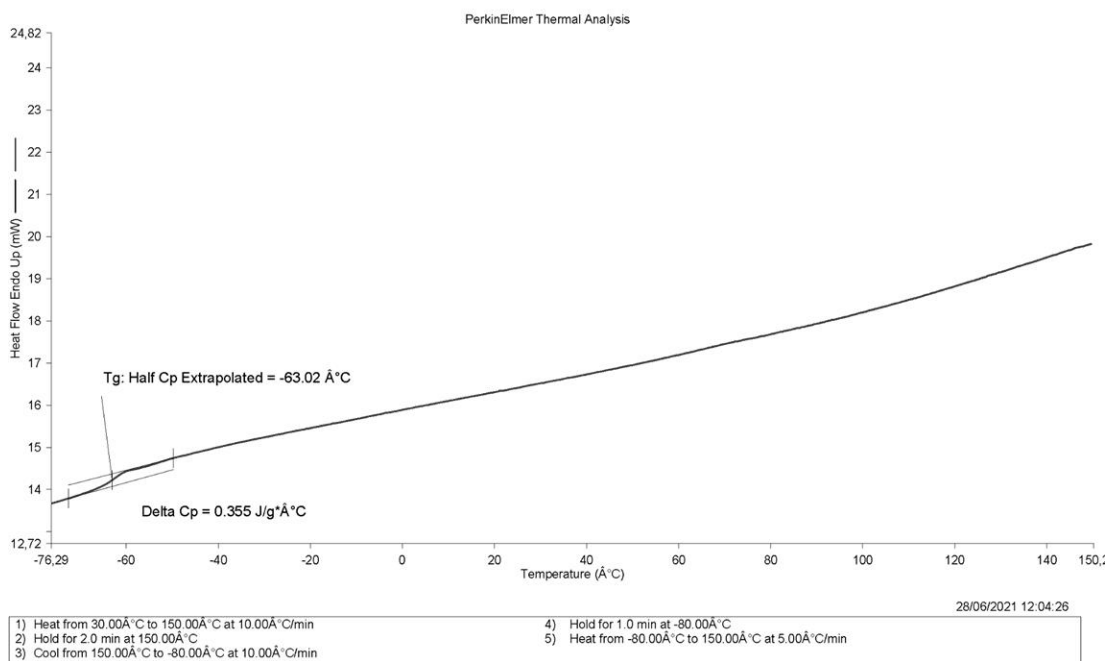


Figure S16: DSC curve of P(2-VP-b-I-b-2-VP) – 15-70-15 3k.

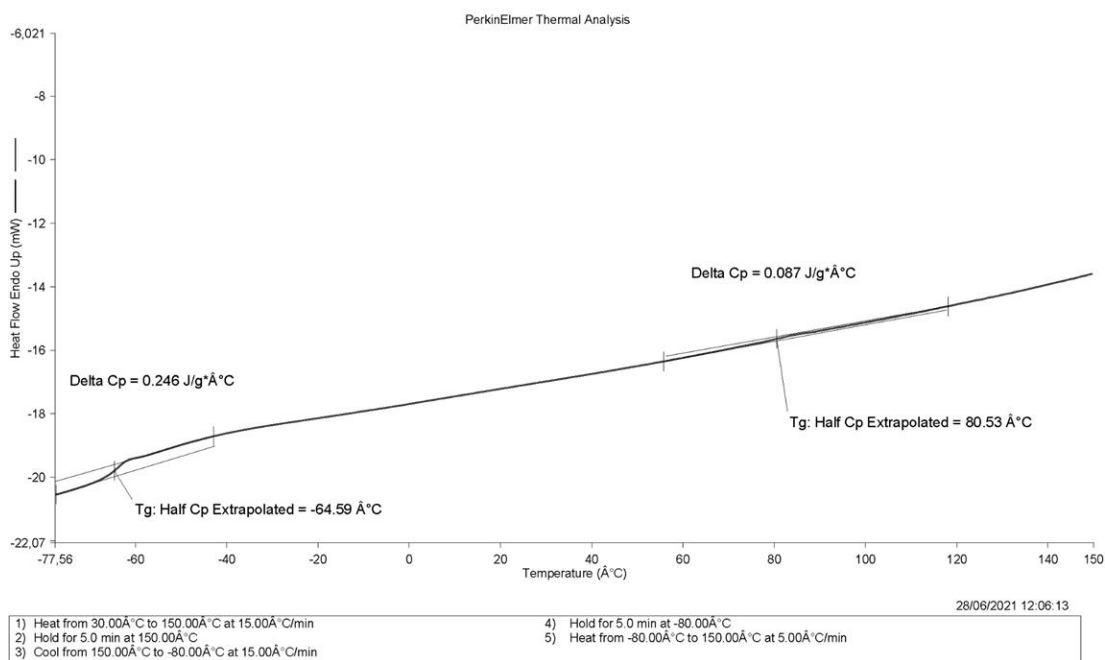


Figure S17: DSC curve of P(2-VP-b-I-b-2-VP) – 15-70-15 4k.

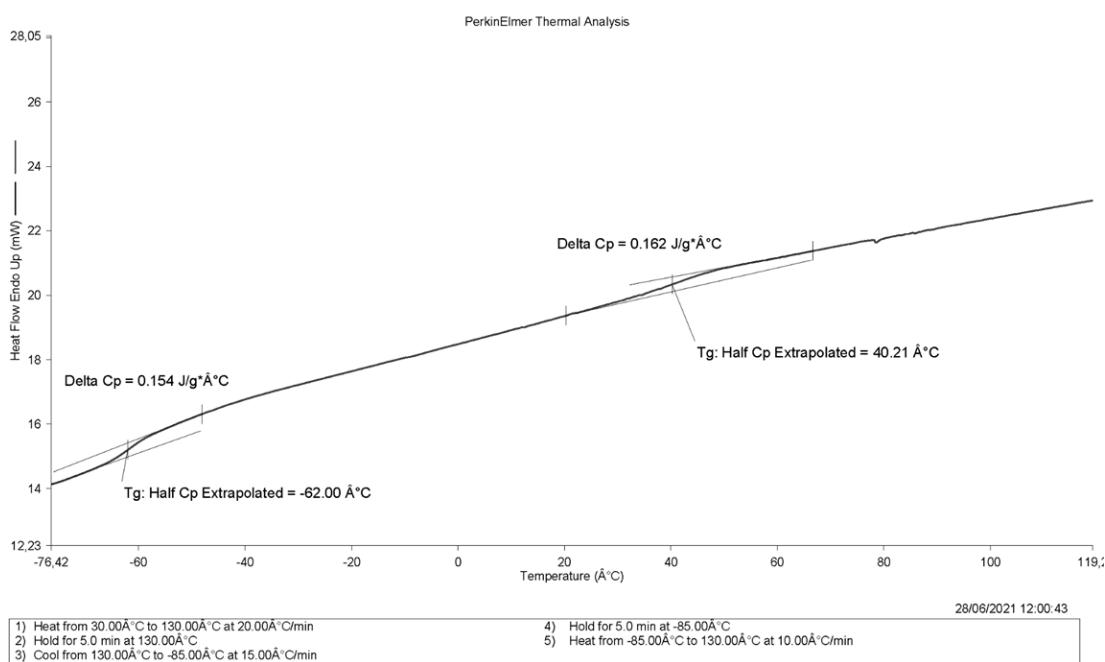


Figure S18: DSC curve of P(2-VP-b-I-b-2-VP) – 20-60-20 2k.

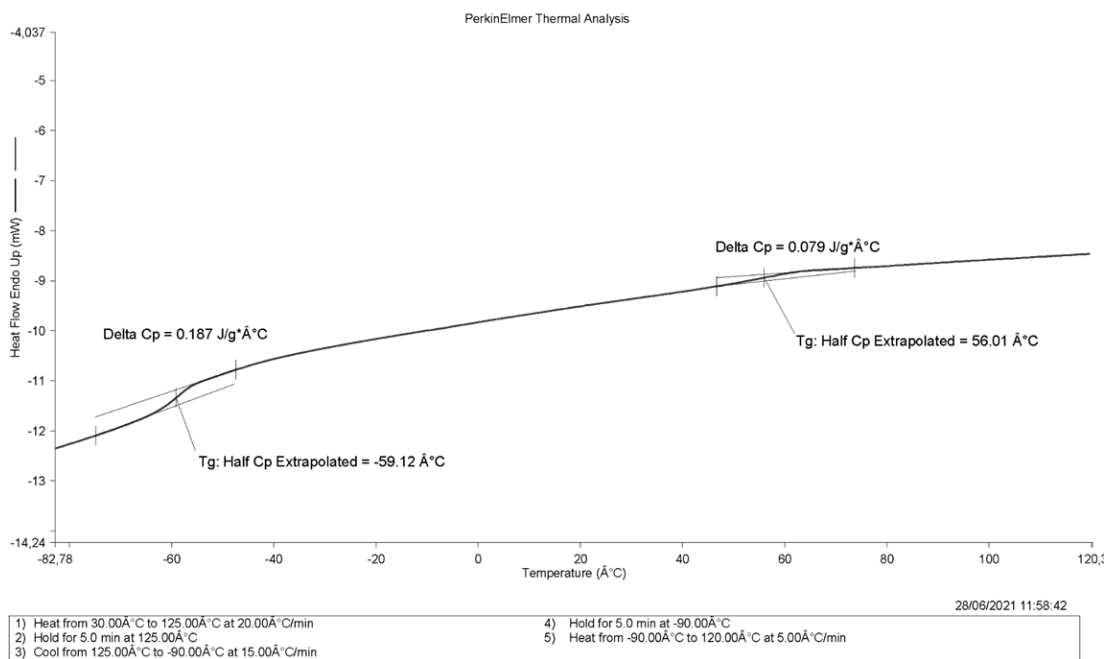


Figure S19: DSC curve of P(2-VP-b-I-b-2-VP) – 20-60-20 3k.

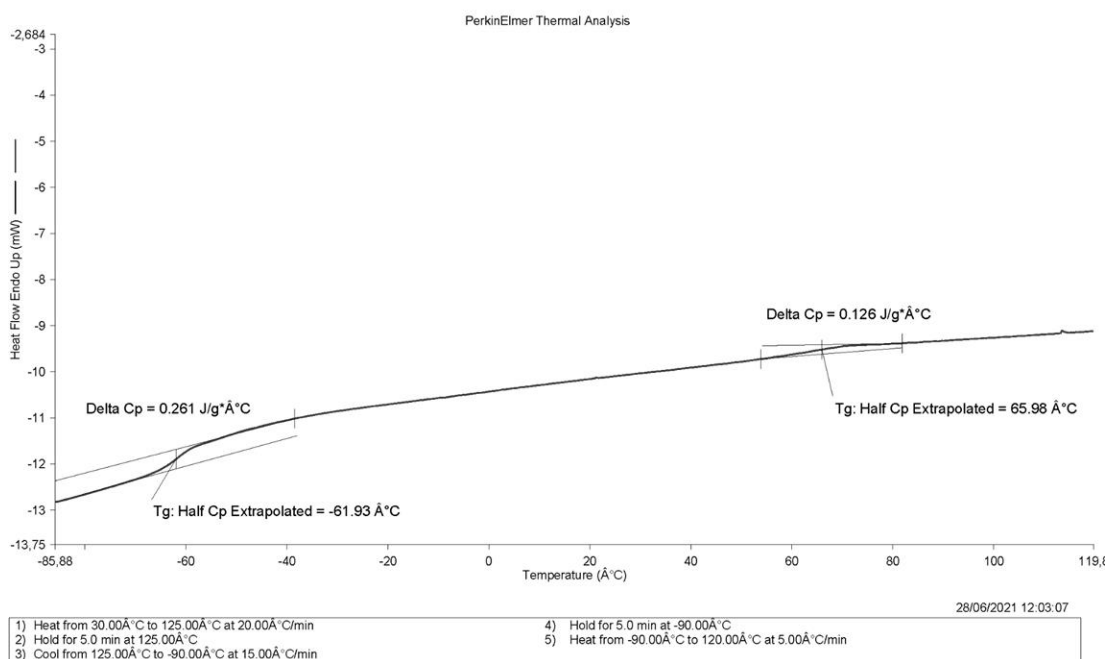


Figure S20: DSC curve of P(2-VP-b-I-b-2-VP) – 20-60-20 4k.

*Table S3: Overview of all measured glass transition temperatures.*

Sample	$T_g(I)$ [°C]	$T_g(2-VP)$ [°C]
15-70-15 - 2k	-64	-
15-70-15 - 3k	-63	-
15-70-15 - 4k	-65	81
20-60-20 - 2k	-62	40
20-60-20 - 3k	-60	56
20-60-20 - 4k	-62	66

## Experiments

Table S4: 15-70-15 2k.

$M_w(\text{tar})$	<b>13320 g/mol</b>	2-VP 15%	isoprene 70%	2-VP 15%	
$n(\text{anions}) =$	0.375 mmol	2000 g/mol	9320 g/mol	2000 g/mol	
$m(\text{DDPE}) =$	106.00 mg	2.05 eq. $V(s\text{-BuLi}) =$	0.59 mL	$V(\text{benzene}) =$ 3.75 mL	$c(\text{DDPE}) =$ 0.10 mol/L
70:30	$n(\text{total}) =$	0.063 mol			
$n(2\text{-VP})$ 30:70 $n(\text{l})$					
$m(\text{total}) =$	5.00 g				
$n(2\text{-VP}) =$	0.0189 mol	$n(\text{l}) =$	0.0442 mol		
$m(2\text{-VP}) =$	1.99 g	$m(\text{l}) =$	3.01 g		
$V(2\text{-VP}) =$	2.04 mL	$V(\text{l}) =$	4.42 mL		
$c(\text{anions}) =$ 16.99 mM					
$c(\text{l}) =$ 2.00 mol/L					
$V(\text{benzene}) =$ 22.09 mL					
$V(\text{THF}) =$ 44.18 mL					
$V(\text{ges}) =$ 66.27 mL					
$c(\text{ges}) =$ 0.95 mol/L					

Table S5: 15-70-15 3k.

$M_w(\text{tar})$	<b>19980 g/mol</b>	2-VP 15%	isoprene 70%	2-VP 15%	
$n(\text{anions}) =$	0.250 mmol	3000 g/mol	13980 g/mol	3000 g/mol	
$m(\text{DDPE}) =$	70.67 mg	2.05 eq. $V(s\text{-BuLi}) =$	0.39 mL	$V(\text{benzene}) =$ 2.50 mL	$c(\text{DDPE}) =$ 0.10 mol/L
70:30	$n(\text{total}) =$	0.063 mol			
$n(2\text{-VP})$ 30:70 $n(\text{l})$					
$m(\text{total}) =$	5.00 g				
$n(2\text{-VP}) =$	0.0189 mol	$n(\text{l}) =$	0.0442 mol		
$m(2\text{-VP}) =$	1.99 g	$m(\text{l}) =$	3.01 g		
$V(2\text{-VP}) =$	2.04 mL	$V(\text{l}) =$	4.42 mL		
$c(\text{anions}) =$ 11.33 mM					
$c(\text{l}) =$ 2.00 mol/L					
$V(\text{benzene}) =$ 22.09 mL					
$V(\text{THF}) =$ 44.18 mL					
$V(\text{ges}) =$ 66.27 mL					
$c(\text{ges}) =$ 0.95 mol/L					

Chapter 4 – Synthesis and characterisation of novel 2-vinylpyridine-isoprene ABA triblock copolymers - Supporting Information

Table S6: 15-70-15 4k.

$M_w(\text{tar})$	<b>26640 g/mol</b>	2-VP 15%	isoprene 70%	2-VP 15%
$n(\text{anions}) =$	0.188 mmol	4000 g/mol	18640 g/mol	4000 g/mol
$m(\text{DDPE}) =$	53.00 mg	2.05 eq. $V(\text{s-BuLi}) =$	0.30 mL	$V(\text{benzene}) =$ 1.88 mL
				$c(\text{DDPE}) =$ 0.10 mol/L
70:30	$n(\text{total}) =$	0.063 mol		
$n(\text{2-VP})$ 30:70 $n(\text{l})$				
$m(\text{total}) =$	5.00 g			
$n(\text{2-VP}) =$	0.0189 mol	$n(\text{l}) =$	0.0442 mol	
$m(\text{2-VP}) =$	1.99 g	$m(\text{l}) =$	3.01 g	
$V(\text{2-VP}) =$	2.04 mL	$V(\text{l}) =$	4.42 mL	
$c(\text{anions}) =$ 8.50 mM				
$c(\text{l}) =$ 2.00 mol/L				
$V(\text{benzene}) =$ 22.09 mL				
$V(\text{THF}) =$ 44.18 mL				
$V(\text{ges}) =$ 66.27 mL				
$c(\text{ges}) =$ 0.95 mol/L				

Table S7: 20-60-20 2k.

$M_w(\text{tar})$	<b>10000 g/mol</b>	2-VP 20%	isoprene 60%	2-VP 20%
$n(\text{anions}) =$	0.500 mmol	2000 g/mol	6000 g/mol	2000 g/mol
$m(\text{DDPE}) =$	141.19 mg	2.05 eq. $V(\text{s-BuLi}) =$	0.79 mL	$V(\text{benzene}) =$ 5.00 mL
				$c(\text{DDPE}) =$ 0.10 mol/L
60:40	$n(\text{total}) =$	0.060 mol		
$n(\text{2-VP})$ 40:60 $n(\text{l})$				
$m(\text{total}) =$	5.00 g			
$n(\text{2-VP}) =$	0.0241 mol	$n(\text{l}) =$	0.0362 mol	
$m(\text{2-VP}) =$	2.54 g	$m(\text{l}) =$	2.46 g	
$V(\text{2-VP}) =$	2.60 mL	$V(\text{l}) =$	3.62 mL	
$c(\text{anions}) =$ 27.64 mM				
$c(\text{l}) =$ 2.00 mol/L				
$V(\text{benzene}) =$ 18.09 mL				
$V(\text{THF}) =$ 36.18 mL				
$V(\text{ges}) =$ 54.26 mL				
$c(\text{ges}) =$ 1.11 mol/L				



Chapter 4 – Synthesis and characterisation of novel 2-vinylpyridine-isoprene ABA triblock copolymers - Supporting Information

Table S8: 20-60-20 3k.

$M_w(\text{tar})$	<b>15000 g/mol</b>	2-VP 20%	isoprene 60%	2-VP 20%												
$n(\text{anions}) =$	0.333 mmol	3000 g/mol	9000 g/mol	3000 g/mol												
$m(\text{DDPE}) =$	94.13 mg	2.05 eq. $V(\text{s-BuLi}) =$	0.53 mL	$V(\text{benzene}) =$ 3.33 mL	$c(\text{DDPE}) =$ 0.10 mol/L											
60:40	$n(\text{total}) =$	0.060 mol														
$n(\text{2-VP})$ 40:60 $n(\text{l})$																
$m(\text{total}) =$	5.00 g															
$n(\text{2-VP}) =$	0.0241 mol	$n(\text{l}) =$	0.0362 mol													
$m(\text{2-VP}) =$	2.54 g	$m(\text{l}) =$	2.46 g													
$V(\text{2-VP}) =$	2.60 mL	$V(\text{l}) =$	3.62 mL													
<table border="1"> <tr> <td><math>c(\text{anions}) =</math></td> <td>18.43 mM</td> </tr> <tr> <td><math>c(\text{l}) =</math></td> <td>2.00 mol/L</td> </tr> <tr> <td><math>V(\text{benzene}) =</math></td> <td>18.09 mL</td> </tr> <tr> <td><math>V(\text{THF}) =</math></td> <td>36.18 mL</td> </tr> <tr> <td><math>V(\text{ges}) =</math></td> <td>54.26 mL</td> </tr> <tr> <td><math>c(\text{ges}) =</math></td> <td>1.11 mol/L</td> </tr> </table>					$c(\text{anions}) =$	18.43 mM	$c(\text{l}) =$	2.00 mol/L	$V(\text{benzene}) =$	18.09 mL	$V(\text{THF}) =$	36.18 mL	$V(\text{ges}) =$	54.26 mL	$c(\text{ges}) =$	1.11 mol/L
$c(\text{anions}) =$	18.43 mM															
$c(\text{l}) =$	2.00 mol/L															
$V(\text{benzene}) =$	18.09 mL															
$V(\text{THF}) =$	36.18 mL															
$V(\text{ges}) =$	54.26 mL															
$c(\text{ges}) =$	1.11 mol/L															

Table S9: 20-60-20 4k.

$M_w(\text{tar})$	<b>20000 g/mol</b>	2-VP 20%	isoprene 60%	2-VP 20%												
$n(\text{anions}) =$	0.250 mmol	4000 g/mol	12000 g/mol	4000 g/mol												
$m(\text{DDPE}) =$	70.60 mg	2.05 eq. $V(\text{s-BuLi}) =$	0.39 mL	$V(\text{benzene}) =$ 2.50 mL	$c(\text{DDPE}) =$ 0.10 mol/L											
60:40	$n(\text{total}) =$	0.060 mol														
$n(\text{2-VP})$ 40:60 $n(\text{l})$																
$m(\text{total}) =$	5.00 g															
$n(\text{2-VP}) =$	0.0241 mol	$n(\text{l}) =$	0.0362 mol													
$m(\text{2-VP}) =$	2.54 g	$m(\text{l}) =$	2.46 g													
$V(\text{2-VP}) =$	2.60 mL	$V(\text{l}) =$	3.62 mL													
<table border="1"> <tr> <td><math>c(\text{anions}) =</math></td> <td>13.82 mM</td> </tr> <tr> <td><math>c(\text{l}) =</math></td> <td>2.00 mol/L</td> </tr> <tr> <td><math>V(\text{benzene}) =</math></td> <td>18.09 mL</td> </tr> <tr> <td><math>V(\text{THF}) =</math></td> <td>36.18 mL</td> </tr> <tr> <td><math>V(\text{ges}) =</math></td> <td>54.26 mL</td> </tr> <tr> <td><math>c(\text{ges}) =</math></td> <td>1.11 mol/L</td> </tr> </table>					$c(\text{anions}) =$	13.82 mM	$c(\text{l}) =$	2.00 mol/L	$V(\text{benzene}) =$	18.09 mL	$V(\text{THF}) =$	36.18 mL	$V(\text{ges}) =$	54.26 mL	$c(\text{ges}) =$	1.11 mol/L
$c(\text{anions}) =$	13.82 mM															
$c(\text{l}) =$	2.00 mol/L															
$V(\text{benzene}) =$	18.09 mL															
$V(\text{THF}) =$	36.18 mL															
$V(\text{ges}) =$	54.26 mL															
$c(\text{ges}) =$	1.11 mol/L															



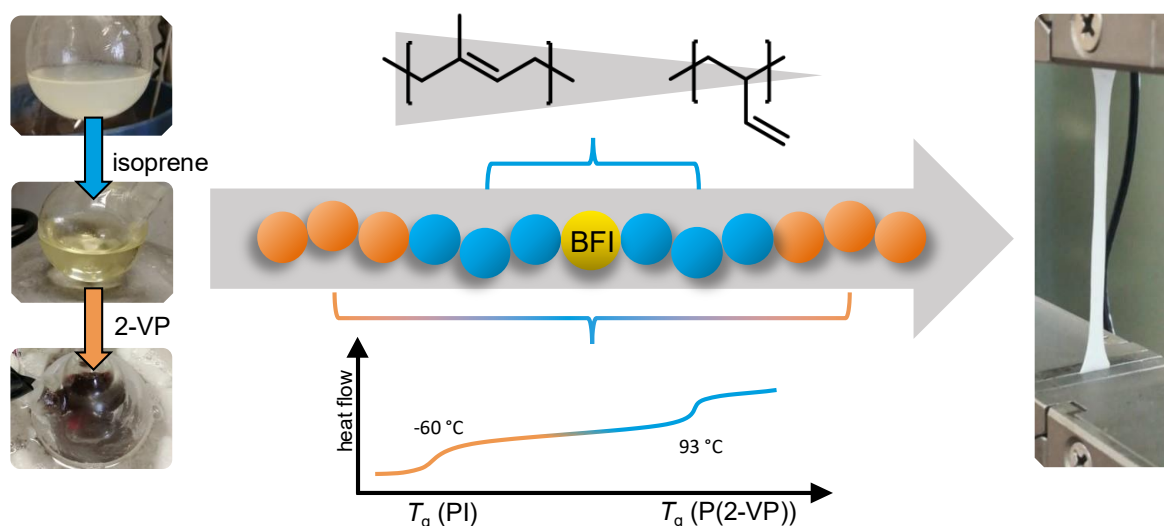
## 9. Chapter 5 – Synthesis and characterisation of ABA triblock copolymers based on isoprene and 2-vinylpyridine for TPE applications

Marcel Fickenscher and [REDACTED] \*

M. Sc. Marcel Fickenscher, Prof. [REDACTED]  
Department of Chemistry, Johannes Gutenberg University Mainz, Duesbergweg 10-14,  
55128 Mainz, Germany  
E-Mail: [REDACTED]

Keywords: 2-vinylpyridine, isoprene, bifunctional initiators, carbanionic polymerisation, triblock copolymers, thermoplastic elastomers

### 9.1 TOC & Short Abstract



Synthesis and characterisation of 2-vinylpyridine-isoprene triblock copolymers for TPE applications. The chemical structure, physical properties and stress-strain measurements were studied.

## 9.2 Abstract

1-bromo-4-(4-bromophenoxy)-2-pentadecylbenzene (DBPPB) is an efficient bifunctional carbanionic initiator, which enables the two-step synthesis of ABA triblock copolymers. The synthesis route overcomes limitations in terms of monomer reactivities and thus enables the synthesis of novel, functional TPEs, inspired by the commercial styrene-diene block copolymers, styrene being replaced by 2-vinylpyridine (2-VP). While the thermal properties are comparable to polystyrene, the increased polarity significantly alters the copolymer features and provides new areas of application, with post-polymerisation modification also being conceivable. Copolymers with Poly(2-VP) outer blocks and a high 1,4-polyisoprene mid-block with varying monomer ratios and molecular weights ( $M_n = 75$  to  $167 \text{ kg}\cdot\text{mol}^{-1}$ ) were synthesised. The synthesis route was optimised in terms of solvent and temperature, starting with the isoprene polymerisation in toluene at room temperature, then lowering the temperature and adding THF before the addition of 2-VP to allow for controlled polymerisation of the latter. SEC,  $^1\text{H}$  NMR spectroscopy and DSC measurements were used for characterisation of the polymers, as well as tensile test measurements of selected samples. High 1,4-content as well as separate  $T_g$ s for the PI and P(2-VP) blocks were observed, which forms the basis for the use as TPE materials. The following tensile tests showed that mechanical properties are present. Individual samples were elongated up to 342% before mechanical failure.

### 9.3 Introduction

Thermoplastic elastomers based on styrene and dienes such as butadiene or isoprene are a well-known class of polymers with a wide range of established uses, from everyday applications such as shoe soles to highly specialised plastics for medical applications.<sup>1</sup> Multifaceted publications in this area cover a wide range from academic to commercially oriented fields of interest.<sup>2</sup> Reviewing the current scientific work, the influence of polymer architectures and block numbers of (tapered) (multi) block copolymers with regard to the mechanical properties are investigated, as well as the influence of a variety of alternative dienes besides butadiene and isoprene.<sup>3-5</sup> Figure 1 gives an overview of different TPE structures and a selection of typical monomers, such as the established butadiene, isoprene, or bio-based alternatives such as myrcene<sup>6,7</sup>.

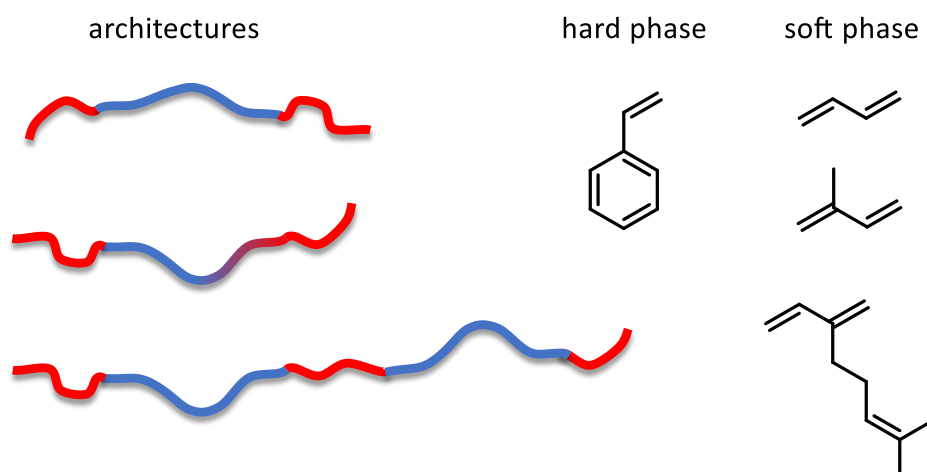


Figure 1: ABA triblock TPE, ABA tapered triblock TPE, multiblock TPE structure. Hard phase (red). Soft phase (blue), monomers butadiene, isoprene, myrcene.

Similar to alternative diene monomers, the variation of the hard phase monomer of the TPE also offers intriguing possibilities for new structures. Although a large number of different styrene derivatives is already known, 2-vinylpyridine as a functional, nitrogen-bearing styrene analogue represents an additional, promising starting point for new materials.<sup>8-10</sup> However, in comparison to styrene and its derivatives, vinylpyridine takes a special position since the reaction conditions have to be significantly adapted for the formation of block or tapered polymer architectures with dienes. On the one hand, the polymerisation of vinylpyridine requires the use of a polar

solvent and low temperatures to avoid precipitation during the polymerisation as well as side reactions. On the other hand, a linear, sequential copolymerisation of vinylpyridine and dienes such as isoprene is limited.<sup>11–13</sup> By means of the  $\beta$ -carbon shift of monomers in  $^{13}\text{C}$  NMR spectroscopy, which is given in Table 1, the reactivity of the resulting chain end can be estimated (Figure S1).

Table 1: ( $\beta$ -)carbon shifts of selected monomers measured via  $^{13}\text{C}$  NMR (400 MHz,  $\text{CDCl}_3$ , Figure S1) reflect the respective reactivity.

monomer	( $\beta$ -)carbon shift / [ppm]
isoprene	113.54 C-1 / 116.67 C-4
styrene	113.93
2-VP	118.32
4-VP	118.45

As a consequence of the electron-withdrawing character of the nitrogen atom, the 2-vinylpyridine chain end shows reduced nucleophilicity, which is reflected by the significant difference of  $\sim 5$  ppm between 2-VP and styrene, the latter being much closer to the value of isoprene. This indicates that in a 2-VP/isoprene copolymerisation a cross-over from 2-VP to isoprene is not possible, and linear diblock copolymers are limited to isoprene/2-VP diblock structures, with the polyisoprene block prepared first.<sup>14</sup>

Table 2 shows a brief comparison of the properties of styrene and 2-vinylpyridine with respect to anionic polymerisation. Different post-polymerisation reactions for P(2-VP) are schematically presented in Figure 2, demonstrating the manifold options for postpolymerisation reactions.

Table 2: Comparison of different properties between 2-VP and styrene.<sup>14–20</sup>

	2-VP	styrene
reaction solvents	rather polar	polar or non-polar
common reaction temperatures	-78 °C to -50 °C	r.t. and above
$T_g$	60 – 104 °C	100 - 107 °C
polymer polarity	polar	non-polar
post-polymerisation reactions	various	hydrogenation
entanglement molecular weight $M_e$	17.0 kg·mol <sup>-1</sup>	18.0 kg·mol <sup>-1</sup>

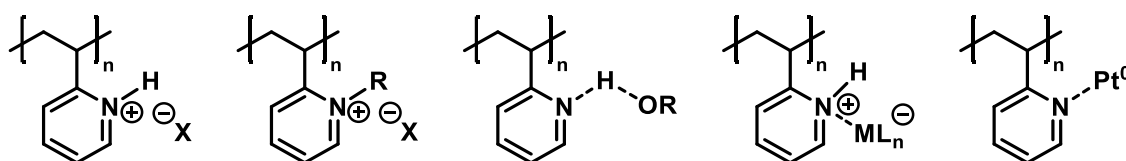


Figure 2: Post-polymerisation reactions of 2-VP, left to right: protonation, quaternisation, hydrogen bonding, metal ligand coordination

The polarity difference between 2-VP and styrene is evident and has an impact on both the choice of the reaction medium for the VP polymerisation and the properties of PVP. The possibility of protonation or quaternisation allows for subsequent introduction of charges and thus further increase of the polarity. The influence of this is particularly noticeable in the Flory-Huggins interaction parameter  $\chi$  of the corresponding copolymers with isoprene. While no conclusive reports for exact values can be found in literature yet, the trend  $\chi_{(PS-PI)} \leq \chi_{(P(2-VP)-PS)} < \chi_{(PI-P(2-VP))}$  is uniformly confirmed and it is believed that  $\chi_{(PI-P(2-VP))}$  is 1.5 to 3.5 times, in some reports even 8 times, higher than  $\chi_{(PS-PI)}$ .<sup>18,22–27</sup>

In contrast to the different polarity, the  $T_g$  and the entanglement molecular weight ( $M_e$ ) of P(2-VP) are similar to those of PS. The  $T_g$  of 60 °C for P(2-VP), which is quite low at

low molecular weights, increases to a value of about 100 °C for higher molecular weights. These values are comparable to corresponding TPEs with a minimum chain length of 15 kg·mol<sup>-1</sup>, which ultimately is similar to polystyrene. While the  $M_e$  is slightly below the literature value for PS, this nevertheless suggests comparable behaviour regarding the mechanical properties. Overall, the comparison between styrene and 2-VP shows the suitability of 2-VP for the use in TPEs and thus represents a promising alternative for existing high-performance applications, such as adhesion promoters for tire cords, which currently rely on styrene-isoprene-vinylpyridine triblock copolymers.<sup>28</sup>

In order to realise tri- or multiblock architectures based on VP and isoprene, two main challenges have to be addressed.

(I) The need for polar solvents during the polymerisation of 2-VP also significantly affects the polymerisation of isoprene. While in non-polar media, and using lithium-based initiators, mainly the 1,4-isomer is incorporated in the polyisoprene chain, the proportion of the 3,4-isomer increases drastically when using a polar solvent. This has to be avoided to exclude a deterioration of the mechanical properties due to the shortened chain length as well as the facilitated cross-linking due to dangling vinyl groups at the polymer backbone.

(II) The second challenge is the significant reactivity difference between 2-VP and isoprene, which does not allow the synthesis of 2-VP-isoprene-2-VP ABA triblock copolymers. Both of these challenges can be overcome with the help of a bifunctional initiator by first synthesising a polyisoprenyl-dilithium prepolymer in non-polar solvents and the subsequent addition of a polar solvent and 2-VP at reduced temperature, as shown schematically in Figure 3.



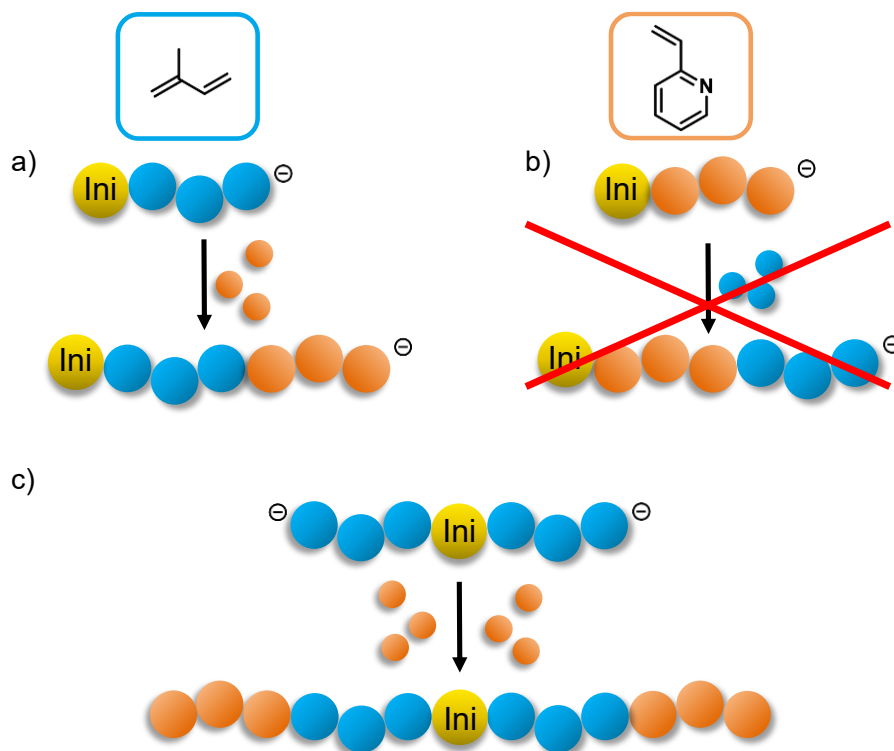


Figure 3: Synthesis scheme for P(2-VP-b-I-b-2-VP) ABA triblock copolymers. a), b): linear approach, leading to mono- or diblock copolymers only. c): bifunctional approach, leading to the desired triblock copolymer structures (orange: 2-VP, blue: isoprene).

According to this route, three sets of polymers with varies monomer ratios and chain lengths were synthesised and characterised with regard to their structures and mechanical properties with respect to suitability for TPEs.

## 9.4 Results and Discussion

### Synthesis of initiator and copolymers

In the following, the synthesis of the bifunctional initiator 1-bromo-4-(4-bromophenoxy)-2-pentadecylbenzene (DBPPB) as well as the sequential carbanionic polymerisation of P(2-VP-*b*-I-*b*-2-VP) are described.

Following the synthesis route described by Gnanou et al., DBPPB was synthesised, starting from the readily available 3-pentadecylphenol and bromobenzene. Figure 4 shows the chemical structure of the bifunctional initiator.<sup>29</sup> The first step of the reaction relies on the formation of the potassium salt of 3-pentadecylphenol, followed by the coupling reaction with bromobenzene, ultimately forming the intermediate 1-pentadecyl-3-phenoxybenzene. Bromination of the ladder leads to the formation of DBPPB, which is obtained as a colourless powder after careful purification by means of column chromatography in an overall yield of 58% (Figure S1).

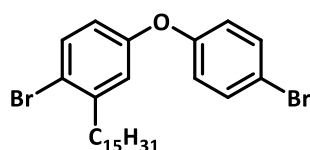


Figure 4: Chemical structure of the synthesised 1-bromo-4-(4-bromophenoxy)2-pentadecylbenzene (DBPPB).

The activation of the initiator is described in detail in Chapter 3. In accordance with this universal approach, the initiator was lyophilised, a 0.03 M stock solution was prepared and stored under an inert argon atmosphere, prior to its use.

### Polymer synthesis

All polymerisation reactions were carried out using standard high-vacuum techniques in carefully dried all-glass reaction vessels, sealed with rubber and Teflon caps. Both monomers were degassed in several freeze-pump-thaw cycles, dried over CaH<sub>2</sub> for one night. Isoprene was freshly distilled prior to the reaction. 2-Vinylpyridine was distilled in a second flask, equipped with trioctylaluminium as a second drying step, stirred for an additional night, and freshly distilled prior to the reaction. A 0.03 M solution of

DBPPB in benzene was initially placed in the reaction flask, activated with *s*-BuLi and stirred for one hour to ensure the quantitative conversion into the active species and subsequently further diluted with the respective solvent prior to the addition isoprene.

Figure 5 gives an overview of the polymerisation steps.

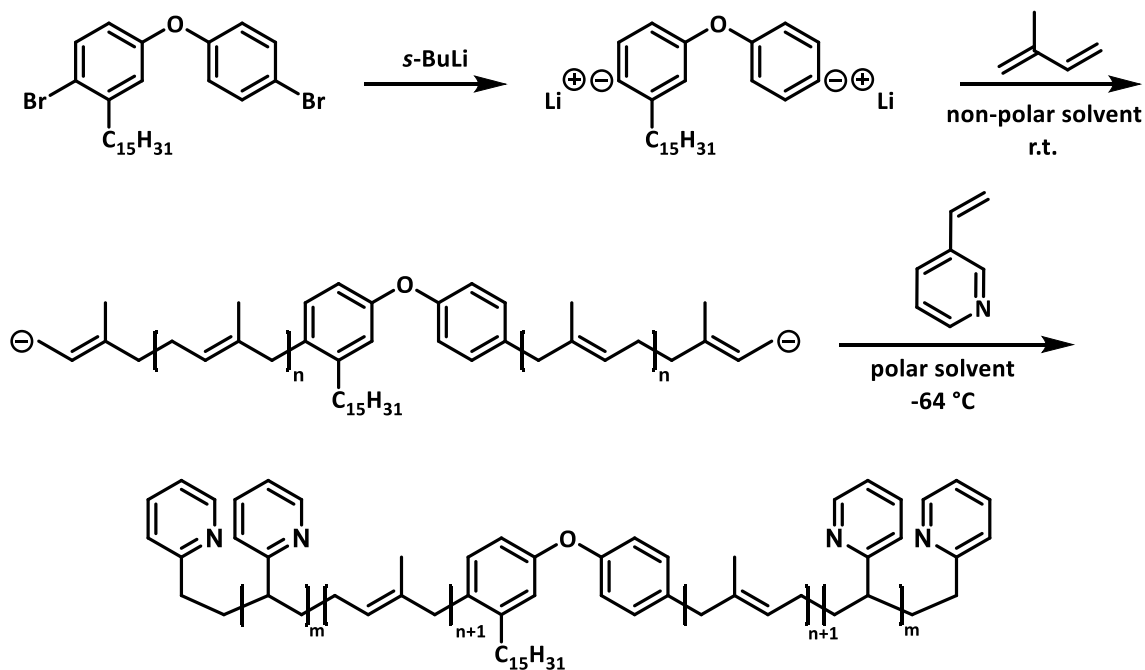


Figure 5: Synthesis of P(2-VP-*b*-I-*b*-2-VP) starting from the bifunctional initiator in non-polar solvents at room temperature and the subsequent addition of a polar solvent and 2-VP at  $-64\text{ }^\circ\text{C}$  leads to the desired triblock copolymer structures

The development of suitable reaction conditions started by identifying a suitable solvent for monomers and polymers and the most efficient solution concentration. All solvents used were dried using standard methods, degassed and freshly distilled into the reaction solution. In each case, three polymerisations were carried out on a 5 g scale, with a monomer ratio of 15:70:15 and targeted total molecular weights of 100, 133 and  $167\text{ kg}\cdot\text{mol}^{-1}$ . Isoprene polymerisation was carried out at  $35\text{ }^\circ\text{C}$  for 24 hours, 2-VP was polymerised at  $-64\text{ }^\circ\text{C}$  using a dry ice chloroform cold bath for 3 to 5 hours. The monomers were added *via* syringe. To prevent freezing of cyclohexane and benzene, a freezing point determination of cyclohexane/benzene:THF mixtures was performed (Figure S3). At least 1 eq. THF with respect to cyclohexane or benzene had to be added to prevent the freezing of the solution. Table 3 gives an overview of the different conditions used.

Table 3: Overview of screening of the different reaction conditions for the efficient synthesis of *P(2-VP-*b*-I-*b*-2-VP)*.

	non-polar solvent	eq. THF	concentration [M]	comment
1	cyclohexane	1.00	0.4	precipitation
2	cyclohexane	1.00	0.3	precipitation
3	cyclohexane	1.00	0.2	precipitation
4	cyclohexane	1.25	0.3	precipitation
5	cyclohexane	1.50	0.3	precipitation
6	cyclohexane	2.00	0.3	precipitation
7	cyclohexane	2.00	0.2	precipitation
8	benzene	2	0.4	no precipitation
9	benzene	1.5	0.7	high viscosity
10	benzene	1.5	0.4	difficult PI thawing
11	toluene	1.5	0.4	-
12	toluene	1.5	0.7	high viscosity
13	toluene	1.5	0.6	high viscosity
14	toluene	1.5	0.5	-

When using cyclohexane and THF, major problems were encountered when cooling the solution, as the polyisoprenyl-dilithium species which had already been formed had to be frozen together with cyclohexane in order to carry out the cold distillation of THF. To obtain a homogeneous solution for subsequent steps, it is essential to heat the mixture well above the freezing point of cyclohexane. However, due to the high viscosity of the already formed polymer, homogeneous mixing could only be achieved with great effort. Before adding 2-VP, the solution was cooled down to -64 °C again. In the first reaction series, turbidity of the polymerisation solution was observed in each

case, indicating precipitation of the resulting copolymer. This was confirmed by the fact that no quantitative yield could be obtained. To counteract this, the amount of THF added was increased up to 2 eq. in relation to cyclohexane to enhance polymer solubility, yet without achieving any improvement.

In order to achieve better solubility during 2-VP polymerisation and to suppress the precipitation, cyclohexane was replaced with benzene. Also in this case, homogeneous mixing prior to 2-VP addition was challenging, yet the precipitation could be suppressed while the required amount of THF was reduced to 1.5 eq. with respect to benzene. While the addition of 1 eq. is also sufficient for polymers with a lower molecular weight, a significantly increased viscosity was observed, as expected with increasing molecular weight, which can be reduced by using 1.5 eq. THF. Although the use of benzene aided to suppress these issues during the 2-VP polymerisation, thawing of the frozen benzene-polyisoprenyl-dilithium solution was still a critical step.

Switching from benzene to toluene resulted in a major improvement, since the freezing point of toluene is  $-95\text{ }^{\circ}\text{C}$ , which is significantly lower than the reaction temperature, and at the same time the cold distillation of THF is also possible at  $-64\text{ }^{\circ}\text{C}$ , which eliminates the need to thaw the reaction mixture after the addition of THF.

Employing toluene as the solvent of choice for the polymerisation of isoprene, the necessary total solvent quantity was determined experimentally. Entry 14 shows a universal set of reaction parameters for the synthesis of P(2-VP-*b*-I-*b*-2-VP), the corresponding, optimised procedure is summarised in the following:

A 0.03 M solution of DBPPB in benzene was activated with *s*-BuLi for 60 minutes, followed by the addition of toluene for sufficient dilution during the isoprene polymerisation. Isoprene was added *via* syringe and stirred for 24 h. After full conversion of isoprene, the reaction flask was cooled to  $-64\text{ }^{\circ}\text{C}$  with a chloroform-dry ice bath and 1.5 eq. THF with respect to toluene were condensed into the reaction mixture under reduced pressure. 2-VP was injected *via* syringe and allowed to polymerise for 4 h prior to the quenching of the reaction mixture with degassed

methanol. In the course of the reaction, two important colour changes were observed: Starting from the turbid and very pale yellow active solution of DBPPB, the addition of isoprene and the formation of the isoprenyllithium chain end turned the solution to a pale yellow colour, that changed to an intensive red once 2-VP is added (Figure 6).

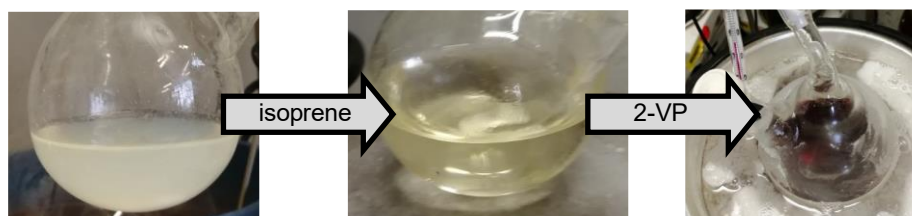


*Figure 6: Colour change during the different reaction steps indicates the successful cross-over between DBPPB, isoprene and 2-VP.*

The purification of the resulting polymers is challenging as a result of their amphiphilic character, precipitation is hardly possible, therefore the solvent was removed under reduced pressure to afford P(2-VP-*b*-I-*b*-2-VP) as a colourless solid with quantitative yields.

Two sets of polymers with varying molar monomer ratios and different total molecular weights in dependence of the 2-VP block molecular weights were synthesised. The different ratios allow the comparison of composition effects, while the 2-VP block size varies around the entanglement molecular weight of P(2-VP) and allows further comparison of material properties of the polymers belonging to the same ratio group.

### Sample characterisation

The sample IDs are composed of the monomer composition and the molecular weight of the P(2-VP) blocks, e.g. the monomer ratio of sample 15-70-15 15k is 70 mol% isoprene and 30 mol% 2-VP, the latter split on both outer blocks, each with a molecular weight of 15 kg·mol<sup>-1</sup>. Both, NMR spectroscopy and SEC experiments show results which, when interpreting the data, indicate a similarly complex behaviour as the polymers described in Chapter 4.

With regard to the interpretation of the NMR spectra, a meaningful determination of the molecular weight is not possible, since the initiator signal is hardly detectable and therefore does not allow a valid integration. An exemplary spectrum is shown in Figure 7 (sample 15-70-15 15k).

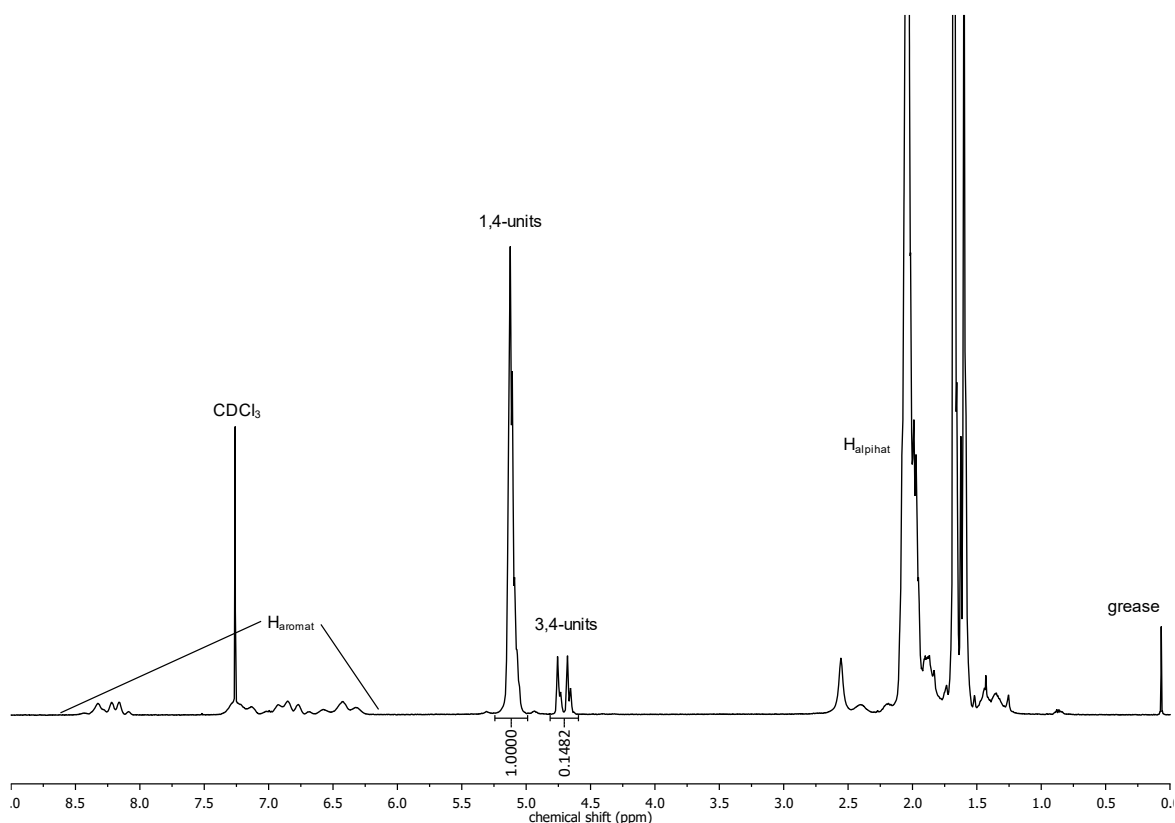


Figure 7: <sup>1</sup>H NMR spectrum (CDCl<sub>3</sub>, 400 MHz) of P(2-VP-*b*-I-*b*-2-VP) – 15-70-15 15k.

The absence of the double bond signal of 2-VP combined with the quantitative yield of the synthesis allows the conclusion that the complete incorporation was achieved. According to Equation 1 the percentage of 1,4-units is given by the integral ratio

of both vinyl signals (1,4-units: 5.1 ppm, 1H; 3,4-units: 4.7 ppm, 2H; see ESI). It is at all times 93% and therefore represents an excellent result with regard to the desired material properties, an overview is given in Table 4.

$$\%(1,4) = 100 - \frac{(0.5 \cdot I(3,4))}{I(1,4) + 0.5 \cdot I(3,4)} \cdot 100 \quad \text{Equation 1}$$

Table 4: NMR spectroscopy results of the copolymer samples (CHCl<sub>3</sub>, 400 MHz).

Sample ID	1,4-units [%]
15-70-15 - 15k	93.1
15-70-15 - 20k	93.0
15-70-15 - 25k	93.0
20-60-20 - 15k	93.4
20-60-20 - 20k	92.8
20-60-20 - 25k	93.0

Table 5 gives an overview of the SEC data, measured in CHCl<sub>3</sub>. The measurements were performed at a rather low concentration of 1 mg·mL<sup>-1</sup>, it was not possible to vary the concentrations nor the solvents due to the strong aggregation, samples prepared in DMF and THF showed no signal, it can be assumed that the aggregates were too large and separated by the precolumn.



Table 5: SEC measurements of the synthesised polymers (solvent:  $\text{CHCl}_3$  with toluene as an internal standard, PS calibration and UV detector).

Sample ID	$M_{n, \text{tar}}$ [ $\text{kg}\cdot\text{mol}^{-1}$ ]	$M_{n, \text{SEC, exp}}$ [ $\text{kg}\cdot\text{mol}^{-1}$ ]	$\bar{D}$
15-70-15 - 15k	100	140	1.41
15-70-15 - 20k	133	158	1.50
15-70-15 - 25k	167	349	1.84
20-60-20 - 15k	75	238	2.83
20-60-20 - 20k	100	340	2.04
20-60-20 - 25k	125	299	2.46

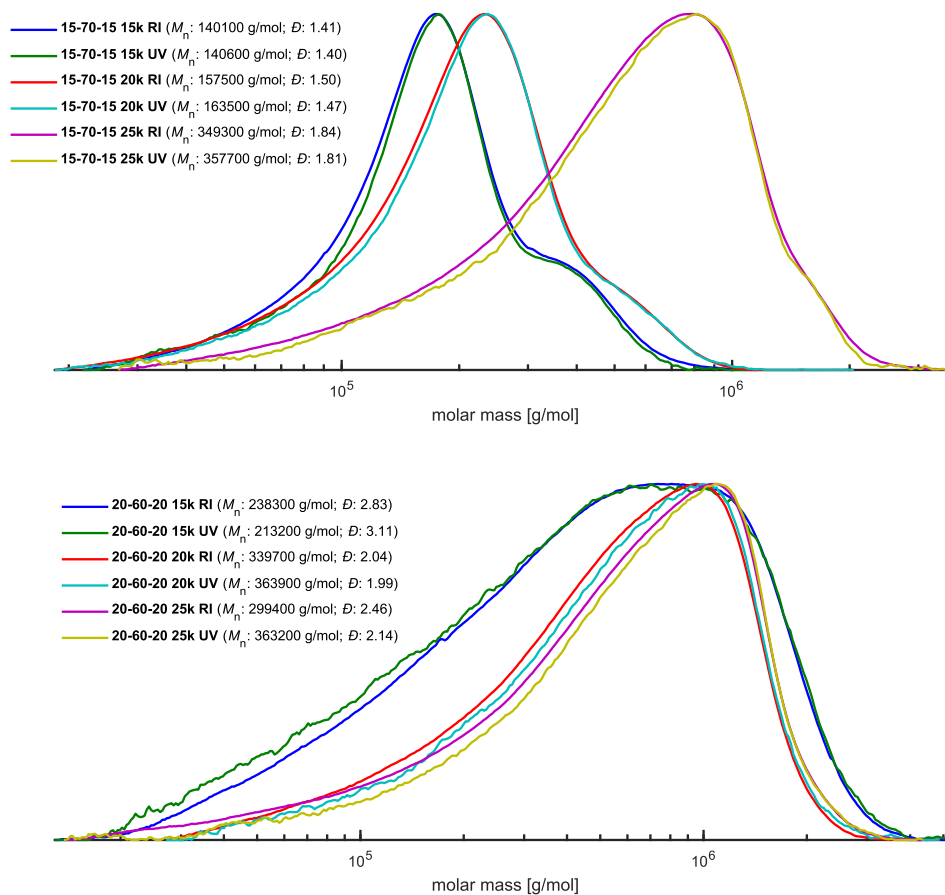


Figure 8: SEC traces of both polymer sets. Top: 15-70-15, bottom: 20-60-20. Measurements were performed in  $\text{CHCl}_3$  with toluene as an internal standard, PS calibration, UV and RI detector.

Considering the results of the SEC elugrams (Figure 8), the significant deviation of the measured values from the theoretically planned ones as a result of the aggregation behaviour, as discussed in Chapter 4, was recognized. However, a clear trend is observable for the 15-70-15 series. This is in line with the expectations since the molecular weight of each sample increases. The samples of the 20-60-20 series elute almost at the same time, which again can be attributed to the polymers tendency to aggregate and is the reason why the samples exhibit an unreasonably high molecular weight close to the exclusion volume of the column. Comparing both series, it can be seen that the polymers of the 20-60-20 series, which should actually have a lower molecular weight than the 15-70-15 series, the overestimation is even more pronounced. In analogy to Chapter 4, this effect is also attributed to the aggregation; if the vinylpyridine chain length exceeds a critical value, aggregation increases significantly. This effect is also reflected in sample 15-70-15 25k.

While the samples of the 15-70-15 series already show a rather broad distribution of 1.4 to 1.8, dispersities between 2 and 3 are obtained for the 20-60-20 series. This effect is also ascribed to the aggregation behaviour, due to the assumed large aggregate size, the efficient separation is hardly possible anymore, leading to the broadening of the signal. However, the absence of other signals than the expected and the excellent overlap of RI and UV signals shows that no isoprene homopolymer was formed and therefore confirms the control over the reaction.

In summary, it is clear that the analysis by means of NMR spectroscopy and SEC is associated with certain difficulties. Mainly the amphiphilic character of the polymers, which contributes to the formation of aggregates complicates the proper evaluation of the measurement data. Nevertheless, the results, especially the high content of 1,4-isoprene units and the monomodal distribution of the SEC, allow the conclusion of a successful and controlled polymerisation.

Thermal analysis of the samples by means of DSC confirms the results of the isomer distribution *via* NMR spectroscopy, as presented in Table 6.

Table 6: Overview of the DSC measurements of the synthesised polymers, displaying both glass transition temperatures.

Sample ID	$T_g(\text{isoprene})$ [°C]	$T_g(\text{2-VP})$ [°C]
15-70-15 - 15k	-61	97
15-70-15 - 20k	-59	90
15-70-15 - 25k	-58	93
20-60-20 - 15k	-59	96
20-60-20 - 20k	-66	73
20-60-20 - 25k	-58	91

The  $T_g$  of the isoprene midblock varies in the range of -66 to -58 °C and thus in the expected range for polymers with a high 1,4-content.<sup>30-33</sup> The  $T_g$  of the P(2-VP) outer blocks is in a high range with values between 90 and 97 °C, which is also in line with expectations and comparable to polystyrene. An exception here is the value for sample 20-60-20, where both values are slightly lower. A possible explanation are solvent residues, which falsify the results. Overall, this is not a problem for the further analysis of the material properties. Compared to the triblock copolymers from Chapter 4, the  $T_g$  is both more visible and about 30 to 50 °C higher due to the significantly higher molecular weight of the 2-VP blocks. The detectability of both  $T_g$ s clearly shows the presence of both polymer blocks and thus indicate the efficient microphase separation which forms the basis for the applicability of the materials as TPEs.

## Material properties

To test the material properties, the synthesised polymers were processed into thin films by means of solvent evaporation. Benzene and chloroform were used as solvents and 1.5 g of each polymer were dissolved in the respective solvent. After a slow evaporation over 3-5 days, the samples were freed from solvent residues under reduced pressure. To remove the films from the moulds, they were cooled with liquid nitrogen to a temperature range around the  $T_g$  of polyisoprene to ensure sufficient strength for removal, further thermal annealing was not performed. The films produced had a thickness of 0.2 to 0.4 mm. Already at this point, a difference between the different solvents could be observed. The films cast from benzene were characterised by higher transparency and showed better elasticity. Dogbones were stamped out of the films, which were then measured in stress-strain experiments at room temperature. Figure 9 displays the successfully cast thin films and dogbone samples, as well as an exemplary measurement. An overview of the stress-strain measurement results is given in Table 5.

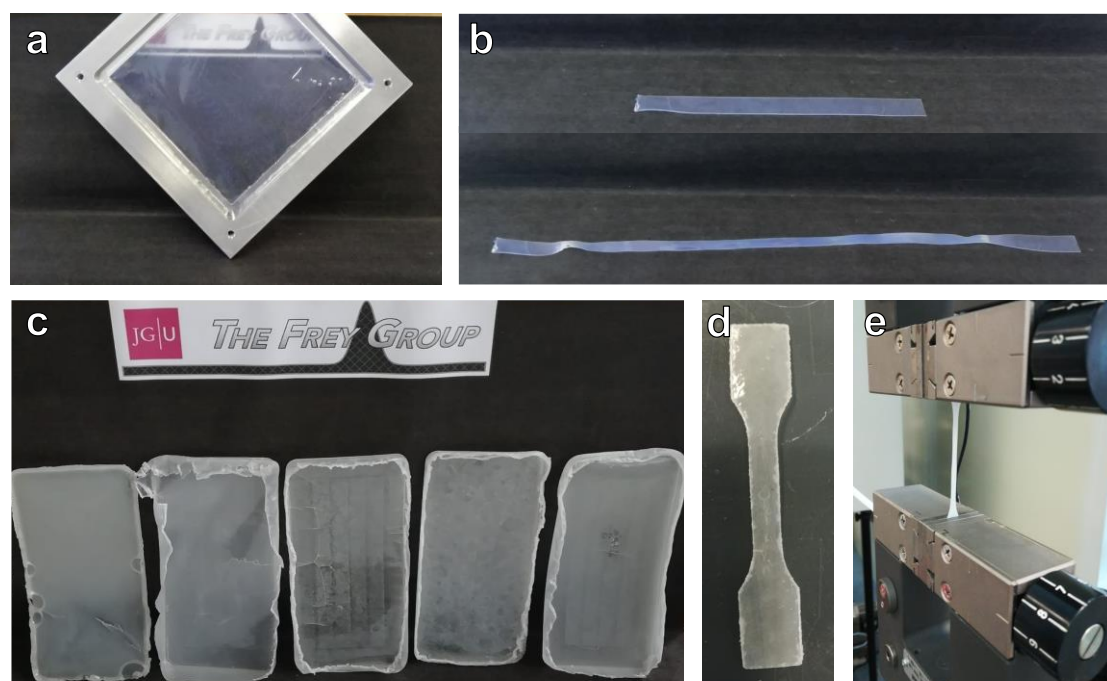


Figure 9: a, b: Large thin film, cast from benzene for qualitative pretests. c: Thin films cast from  $\text{CHCl}_3$ , left to right: 15-70-15 20k, 15-70-15 25k, 20-60-20 15k, 20-60-20 20k, 20-60-20 25k. d, e: Dogbone and tensile test measurement.

Table 7: Overview of tensile test measurement of P(2-VP-*b*-I-*b*-2-VP) thin films (see ESI).

Sample	$\epsilon$ (benzene) [%]	$\sigma$ (benzene) [Nm/mm <sup>2</sup> ]	$\epsilon$ (CHCl <sub>3</sub> ) [%]	$\sigma$ (CHCl <sub>3</sub> ) [Nm/mm <sup>2</sup> ]
15-70-15 - 15k	-	-	-	-
15-70-15 - 20k	195	2.5	3	9.0
15-70-15 - 25k	-	-	128	0.1
20-60-20 - 15k	173	0.9	1	9
20-60-20 - 20k	342	0.9	9	13.8
20-60-20 - 25k	33	1.0	30	0.2

Sample 15-70-15 15k could not be measured, since the film did not show sufficient strength as well as a highly viscous behaviour at room temperature after removal from the mould. The reason for this is that the molecular weight of the P(2-VP) blocks is too low, no entanglements are possible, and in combination with the rather high isoprene content no sufficient microphase separation was achieved. Sample 15-70-15 25k, cast from benzene, showed a too high brittleness in the frozen state and broke immediately on removal. The reason for this can be attributed the higher number of entanglements, which improves the stability of the sample, but at the same time causes increased brittleness, which cannot be compensated for by the flexibility of the isoprene block in the cooled state.

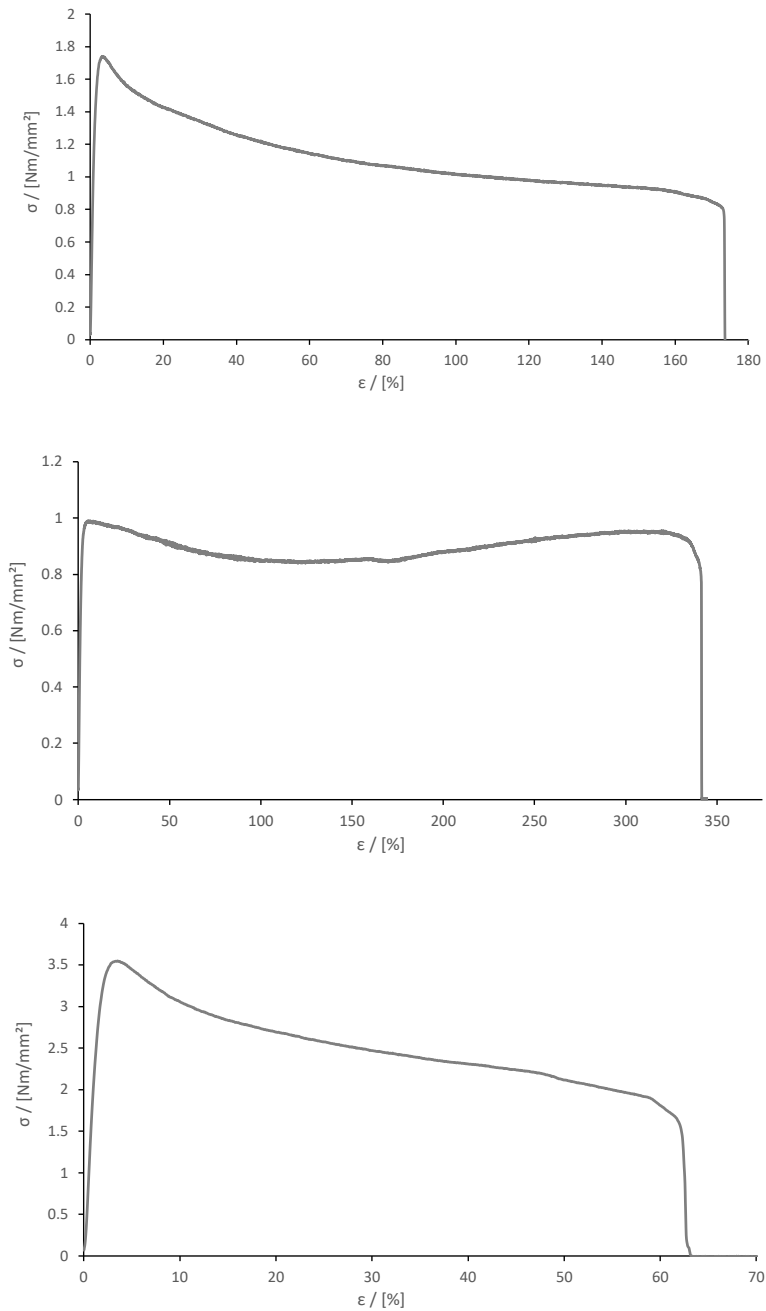


Figure 10: Selected stress-strain curves of the 20-60-20 series, cast from benzene. Top to bottom: 15k, 20k, 25k.

The films of the 20-60-20 series cast from benzene (Figure 10) were slightly easier to handle due to the higher hard phase content. Sample 20-60-20 25k shows a comparatively low elongation at break  $\epsilon$  with a mean value of 33%, while high values of 173% and 342% could be determined for the remaining samples of the series. This is attributed to the influence of the entanglement molecular weight of P(2-VP), with 15  $\text{kg}\cdot\text{mol}^{-1}$  blocks, the  $M_e$  is not yet reached, while 20  $\text{kg}\cdot\text{mol}^{-1}$  are sufficient and cause

a stronger cohesion of the hard phase. This is confirmed within the series by the reduced ductility of the  $25 \text{ kg}\cdot\text{mol}^{-1}$  samples; as expected, the increasing entanglement causes the material to behave more brittle.

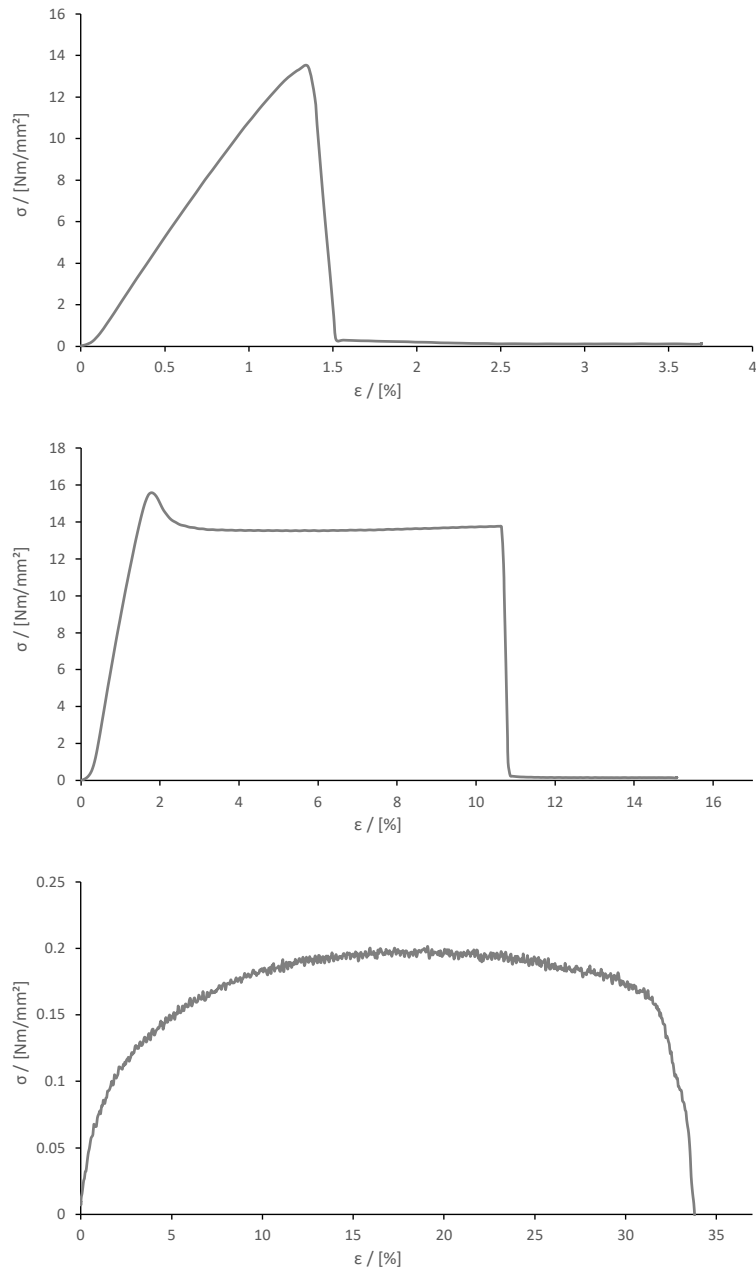


Figure 11: Selected stress-strain curves of the 20-60-20 series, cast from  $\text{CHCl}_3$ . Top to bottom: 15k, 20k, 25k.

In contrast, the samples of the 20-60-20 series cast from chloroform (Figure 11) show an overall significantly lower elongation at break  $\epsilon$ . Although a trend towards increasing  $\epsilon$  within the series can also be seen here, this does not drop again for the

25 kg·mol<sup>-1</sup> samples. It can be assumed that chloroform is no suitable solvent for the thin film preparation and prevents proper microphase separation, resulting in a rather brittle, plastic behaviour. While the results obtained from the benzene cast films are promising towards the materials applications as TPEs, it can be assumed that benzene is not yet the most suitable solvent. Both blocks are not dissolved equally well, which limits the formation of microphase separated film and thus significantly worsens the material properties.

Comparing the results obtained with values of triblocks based on styrene and isoprene, it becomes clear that there is further room for optimisation. While P(S-*b*-I-*b*-S) with a comparable monomer composition reaches  $\epsilon$  values of more than 1200%, the values of P(2-VP-*b*-I-*b*-2-VP) with maximum of 342% are significantly lower.<sup>34</sup> Overall, however, the potential of the material can be recognised and forms good basis for further work on this topic; in particular, the choice of a suitable solvent for thin-film production as well as the analysis of samples with different monomer ratios should be prioritised.



## 9.5 Experimental

### Materials and methods

3-Pentadecylphenol was purchased from TCI and used as received. Bromobenzene and bromine was purchased from Fisher Chemical and used as received. Copper was purchased from Sigma-Aldrich and used as received. 2-Vinylpyridine as Isoprene were purchased from Acros Organics, filtered over basic aluminium oxide to remove the stabiliser and protic impurities, dried over  $\text{CaH}_2$  and freshly distilled prior to use. All solvents (Fisher Chemical, Carl Roth GmbH + Co. KG) were carefully drier with  $\text{CaH}_2$  (Sigma Aldrich) or butyllithium (Sigma Aldrich) and freshly distilled prior to use.

### Nuclear magnetic resonance (NMR) spectroscopy

$^1\text{H}$  NMR measurements were performed on a Bruker Avance II 400 at a magnetic field strength of 400 MHz.

$^{13}\text{C}$  NMR measurements were performed on a Bruker Avance II 400 at a magnetic field strength of 400 MHz.

### Size exclusion chromatography (SEC)

All SEC measurements were performed with an Agilent 1100 Series chromatograph, equipped with HEMA columns (300/100/40, 95 cm length, 0.8 cm width, 50 °C) and an Agilent G1314A UV detector. Solvent:  $\text{CHCl}_3$ , internal standard: toluene, calibration: polystyrene.

### Differential scanning calorimetry (DSC)

The DSC experiments were performed with a Perkin Elmer 8500 differential scanning calorimeter in a temperature range from -80 to 150 °C and a heating rate of 5 – 15 °C/min for the determination of the  $T_g$ .

## Tensile tests

Tensile tests were performed using a materials testing machine Z005 (Zwick/Roell, Germany). Tensile tests were carried out by exposing the stamped polymer dogbones to a uniaxial tension. Bone shape samples with thicknesses around 0.2 – 0.4 mm were drawn with rate of 10 mm/min at room temperature. All thin films were obtained by slow evaporation from a benzene or chloroform solution followed a full removal of the solvent under reduced pressure.

## Synthesis procedures

### Initiator synthesis

DBPPB was synthesised based on the prescription of Gnanou et al.<sup>29</sup>

25 g (82.10 mmol, 1 eq.) of 3-pentadecylphenol were placed in a two-neck round bottom flask with a reflux condenser and a Dean-Stark apparatus, dissolved in 75 mL of N,N-dimethylacetamide and 38 mL of toluene and mixed with 5.12 g (98.39 mmol, 1.2 eq.) potassium hydroxide and heated under reflux for 5 h until the water formed was completely separated. The solvent was then removed using a rotary evaporator, 40 mL of N,N-dimethylacetamide was added to the resulting potassium salt and 12.89 g (82.10 mmol, 1 eq.) of bromobenzene and 0.56 g Cu (8.81 mmol, 0.11 eq.) were added and heated to 150 °C for 8 h. The resulting reaction solution was then filtered off at reduced pressure and the product extracted with ethyl acetate (4x 200 mL). The organic phase was washed with water, brine and water, dried, concentrated and purified *via* column chromatography (petroleum ether). Yield: 18.13 g, 47.62 mmol, 58%.

In the second reaction step, 18.13 g (47.62 mmol, 1 eq.) of the intermediate were placed in a three-neck flask with reflux condenser, dropping funnel and thermometer and dissolved in 75 mL dichloromethane. The reaction solution was protected from light and 5.09 mL of bromine (15.87 g, 99.31 mmol, 2.1 eq.) were added under stirring. The temperature was kept at 0 °C during the addition. After the addition of bromine,

the solution was further stirred at the same temperature for one hour and then heated under reflux for 18 hours. Excess bromine was neutralised with an aqueous ammonia solution, the organic phase separated, washed with water, brine and water, concentrated, dried and purified by means of twofold column chromatography ( $R_f$ : 0.4, solvent: petroleum ether) to yield 25.46 g (47.29 mmol, 100%) DBPPB as colourless solid.

$^1\text{H}$  NMR: ( $\text{CDCl}_3$ , 400 MHz)  $\delta$  [ppm] = 7.48-7.42 (m, 3H), 6.89-6.85 (m, 3H), 6.69 (dd,  $J = 8.3$  Hz, 1H), 2.70-2.65 (m, 2H), 1.63-1.53 (m, 2H), 1.26 (s, 24H), 0.88 (t,  $J = 7.0$  Hz, 3H).

#### Polymer synthesis

All polymerisations were carried out in a 5 g scale using a carefully flame dried all-glass apparatus with rubber seals and Teflon caps as well as standard high vacuum techniques. Both monomers were purified by filtration over basic aluminium oxide to remove the stabiliser and protic impurities, degassed with three *freeze-pump-thaw* cycles and stirred over  $\text{CaH}_2$  for one night. Isoprene was freshly distilled prior to the polymerisation. 2-VP was additionally distilled on trioctylaluminium, stirred for one night and freshly distilled prior to the polymerisation. A 0.03 M solution of DBPPB in dried, degassed benzene was placed in the reaction flask, followed by the addition of 4 eq. *s*-BuLi to activate the initiator. The gelation of the solution as well as a turbidity can be observed in the course of the activation time of one hour. After the quantitative activation of the initiator, the required amount of freshly distilled toluene was transferred into the reaction flask and isoprene was added *via* syringe, resulting in the colour change to light yellow. After 24 h, a chloroform-dry ice bath was applied to cool the reaction mixture to  $-64$  °C and 1.5 eq. THF with respect to toluene were condensed to the reaction mixture. 2-VP was added *via* syringe, leading to the immediate formation of the deep red coloured pyridinyl anions. After 3 to 5 h, the reaction mixture was quenched with degassed methanol. The solvent was removed under reduced pressure to quantitatively yield the respective triblock copolymer as a colourless solid. See ESI for specific quantities of each individual sample.

## 9.6 Conclusion

The use of the bifunctional initiator DBPPB allows the synthesis of triblock copolymers that are not accessible *via* the conventional linear reaction pathway due to the reduced reactivity of the pyridinyl chain end. By optimising the solvent mixture and changing from cyclohexane over benzene to toluene, existing difficulties in the synthesis pathway have successfully been overcome to yield the desired materials.

The polymers produced in this manner were characterised by means of SEC and  $^1\text{H}$  NMR spectroscopy. In both cases, the evaluation proved to be difficult, however, the SEC and NMR spectroscopy results indicate the desired control over the reaction, as well as a high proportion of 1,4-units of 93% in the isoprene mid-block. This, together with the resulting low isoprene  $T_g$  ( $-60\text{ }^\circ\text{C}$ ) which, as well as the high  $T_g$  of the 2-VP block ( $90\text{ }^\circ\text{C}$ ), could be determined by means of DSC measurements, indicates the suitability of the material for TPE applications.

Subsequently, thin films were obtained using the solvent evaporation technique and tensile test measurements were performed. The results thus obtained clearly show that there is still potential for optimisation. In particular, the samples of the 20-60-20 series cast from  $\text{CHCl}_3$  showed a rather plastic behaviour, while the films cast from benzene proved to be more elastic and hint at a possible use of the materials for TPE applications. In particular, the choice of solvent or the use of a solvent mixture should be the focus here in order to obtain uniform and reliable results of the tensile test measurements and, following on from this, to examine the morphology of the films with the aid of TEM or SAXS measurements.

Another promising topic is the influence of the post-polymerisation modification of the 2-VP block in these types of functional TPEs. Besides the common protonation reaction of the 2-VP block, the reversible cross-linking of the structures is conceivable with the help of quaternisation reactions, which provides additional stability and broadens the range of processing possibilities.

## 9.7 References

- (1) Holden, G.; Kricheldorf, H. R.; Quirk, R. P., Eds. *Thermoplastic elastomers*, 3. ed.; Hanser; Hanser Gardner Publications, 2004.
- (2) Feng, H.; Lu, X.; Wang, W.; Kang, N.-G.; Mays, J. W. Block Copolymers: Synthesis, Self-Assembly, and Applications. *Polymers* **2017**, *9* (10). DOI: 10.3390/polym9100494.
- (3) Steube, M.; Plank, M.; Gallei, M.; Frey, H.; Floudas, G. Building Bridges by Blending: Morphology and Mechanical Properties of Binary Tapered Diblock/Multiblock Copolymer Blends. *Macromol. Chem. Phys.* **2021**, *222* (4), 2000373. DOI: 10.1002/macp.202000373.
- (4) Knoll, K.; Nießner, N. Styrolux + and styroflex + - from transparent high impact polystyrene to new thermoplastic elastomers: Syntheses, applications and blends with other styrene based polymers. *Macromol. Symp.* **1998**, *132* (1), 231–243. DOI: 10.1002/masy.19981320122.
- (5) Fuchs, D. A. H.; Hübner, H.; Kraus, T.; Niebuur, B.-J.; Gallei, M.; Frey, H.; Müller, A. H. E. The effect of THF and the chelating modifier DTHFP on the copolymerisation of  $\beta$ -myrcene and styrene: kinetics, microstructures, morphologies, and mechanical properties. *Polym. Chem.* **2021**, *12* (32), 4632–4642. DOI: 10.1039/D1PY00791B.
- (6) Wahlen, C.; Frey, H. Anionic Polymerization of Terpene Monomers: New Options for Bio-Based Thermoplastic Elastomers. *Macromolecules* **2021**, *54* (16), 7323–7336. DOI: 10.1021/acs.macromol.1c00770.
- (7) Wahlen, C.; Blankenburg, J.; Tiedemann, P. von; Ewald, J.; Sajkiewicz, P.; Müller, A. H. E.; Floudas, G.; Frey, H. Tapered Multiblock Copolymers Based on Farnesene and Styrene: Impact of Biobased Polydiene Architectures on Material Properties. *Macromolecules* **2020**, *53* (23), 10397–10408. DOI: 10.1021/acs.macromol.0c02118.
- (8) Braun, V. D.; Daimon, H.; Becker, G. Über polystyrolerivate mit elementen der fünften hauptgruppe. *Makromol. Chem.* **1963**, *62* (1), 183–195. DOI: 10.1002/macp.1963.020620119.
- (9) Geerts, J.; van Beylen, M.; Smets, G. Anionic polymerization of o- and p-methoxystyrene. *J. Polym. Sci. A-1 Polym. Chem.* **1969**, *7* (10), 2859–2873. DOI: 10.1002/pol.1969.150071010.
- (10) Hirao, A.; Loykulnant, S.; Ishizone, T. Recent advance in living anionic polymerization of functionalized styrene derivatives. *Progress in Polymer Science* **2002**, *27* (8), 1399–1471. DOI: 10.1016/S0079-6700(02)00016-3.
- (11) Watanabe, H.; Shimura, T.; Kotaka, T.; Tirrell, M. Synthesis, characterization, and surface structures of styrene-2-vinylpyridine-butadiene three-block polymers. *Macromolecules* **1993**, *26* (24), 6338–6345. DOI: 10.1021/ma00076a006.
- (12) Luxton, A. R.; Quig, A.; Delvaux, M.-J.; Fetters, L. J. Star-branched polymers: 2. Linking reaction involving 2- and 4-vinyl pyridine and dienyl and styryllithium chain ends. *Polymer* **1978**, *19* (11), 1320–1324. DOI: 10.1016/0032-3861(78)90315-4.
- (13) Hirao, A.; Goseki, R.; Ishizone, T. Advances in Living Anionic Polymerization: From Functional Monomers, Polymerization Systems, to Macromolecular Architectures. *Macromolecules* **2014**, *47* (6), 1883–1905. DOI: 10.1021/ma401175m.

- (14) Nakahama, S.; Ishizone, T.; Hirao, A. Anionic living polymerization of styrenes containing electron-withdrawing groups. *Makromolekulare Chemie. Macromolecular Symposia* **1993**, *67* (1), 223–236. DOI: 10.1002/masy.19930670118.
- (15) Fréchet, J. M. J.; Meftahi, M. V. de. Poly(vinyl pyridine)s: Simple reactive polymers with multiple applications. *Brit. Poly.J.* **1984**, *16* (4), 193–198. DOI: 10.1002/pi.4980160407.
- (16) Fickenscher, M.; Reimers, T.; Frey, H. Introducing a 1,1-diphenylethylene analogue for vinylpyridine: anionic copolymerisation of 3-(1-phenylvinyl)pyridine (m -PyPE). *Polym. Chem.* **2021**, *12* (24), 3576–3581. DOI: 10.1039/d1py00302j.
- (17) Gan, Y.; Dong, D.; Hogen-Esch, T. E. Effects of Lithium Bromide on the Glass Transition Temperatures of Linear and Macrocyclic Poly(2-vinylpyridine) and Polystyrene. *Macromolecules* **1995**, *28* (1), 383–385. DOI: 10.1021/ma00105a055.
- (18) Kennemur, J. G. Poly(vinylpyridine) Segments in Block Copolymers: Synthesis, Self-Assembly, and Versatility. *Macromolecules* **2019**, *52* (4), 1354–1370. DOI: 10.1021/acs.macromol.8b01661.
- (19) Rieger, J. The glass transition temperature of polystyrene. *Journal of Thermal Analysis* **1996**, *46* (3-4), 965–972. DOI: 10.1007/BF01983614.
- (20) Lo, C.-T.; Tsui, K.-H. The dispersion of magnetic nanorods in poly(2-vinylpyridine). *Polym. Int.* **2013**, n/a-n/a. DOI: 10.1002/pi.4462.
- (21) Inoue, T.; Onogi, T.; Yao, M.-L.; Osaki, K. Viscoelasticity of low molecular weight polystyrene. Separation of rubbery and glassy components. *J. Polym. Sci. Part B: Polym. Phys.* **1999**, *37* (4), 389–397. DOI: 10.1002/(SICI)1099-0488(19990215)37:4<389:AID-POLB12>3.0.CO;2-G.
- (22) Asai, Y.; Takano, A.; Matsushita, Y. Asymmetric Double Tetragonal Domain Packing from ABC Triblock Terpolymer Blends with Chain Length Difference. *Macromolecules* **2016**, *49* (18), 6940–6946. DOI: 10.1021/acs.macromol.6b01670.
- (23) Chernyy, S.; Mahalik, J. P.; Kumar, R.; Kirkensgaard, J. J. K.; Arras, M. M. L.; Kim, H.; Schulte, L.; Ndoni, S.; Smith, G. S.; Mortensen, K.; Sumpter, B. G.; Russell, T. P.; Almdal, K. On the morphological behavior of ABC miktoarm stars containing poly(cis 1,4-isoprene), poly(styrene), and poly(2-vinylpyridine). *J. Polym. Sci. Part B: Polym. Phys.* **2018**, *56* (22), 1491–1504. DOI: 10.1002/polb.24733.
- (24) DAI, K. Determining the temperature-dependent Flory interaction parameter for strongly immiscible polymers from block copolymer segregation measurements. *Polymer* **1994**, *35* (1), 157–161. DOI: 10.1016/0032-3861(94)90065-5.
- (25) Hirschberg, V.; Faust, L.; Rodrigue, D.; Wilhelm, M. Effect of Topology and Molecular Properties on the Rheology and Fatigue Behavior of Solid Polystyrene/Polyisoprene Di- and Triblock Copolymers. *Macromolecules* **2020**, *53* (13), 5572–5587. DOI: 10.1021/acs.macromol.0c00632.
- (26) Jiang, K.; Zhang, J.; Liang, Q. Self-Assembly of Asymmetrically Interacting ABC Star Triblock Copolymer Melts. *The journal of physical chemistry. B* **2015**, *119* (45), 14551–14562. DOI: 10.1021/acs.jpcc.5b08187. Published Online: Nov. 2, 2015.

- (27) Odani, H.; Uchikura, M.; Ogino, Y.; Kurata, M. Diffusion and solution of methanol vapor in poly(2-vinylpyridine)- block- polyisoprene and poly(2-vinylpyridine)-block-polystyrene. *Journal of Membrane Science* **1983**, *15* (2), 193–208. DOI: 10.1016/S0376-7388(00)80398-1.
- (28) Kurz, G.; Manuel, S. Adhesive Formulation, Method for Production and Use Thereof. DE102005052025A.
- (29) Matmour, R.; More, A. S.; Wadgaonkar, P. P.; Gnanou, Y. High performance poly(styrene-b-diene-b-styrene) triblock copolymers from a hydrocarbon-soluble and additive-free dicarbanionic initiator. *Journal of the American Chemical Society* **2006**, *128* (25), 8158–8159. DOI: 10.1021/ja062695v.
- (30) Burfield, D. R. Polymer glass transition temperatures. *J. Chem. Educ.* **1987**, *64* (10), 875. DOI: 10.1021/ed064p875.
- (31) Müller, A. H. E.; Matyjaszewski, K. *Controlled and Living Polymerizations*; Wiley, 2009. DOI: 10.1002/9783527629091.
- (32) Stavely, F. W.; Coworkers. Coral Rubber—A Cis -1,4-Polyisoprene. *Rubber Chemistry and Technology* **1956**, *29* (3), 673–686. DOI: 10.5254/1.3542582.
- (33) Widmaier, J. M.; Meyer, G. C. Glass Transition Temperature of Anionic Polyisoprene. *Rubber Chemistry and Technology* **1981**, *54* (5), 940–943. DOI: 10.5254/1.3535854.
- (34) Cunningham, R. E.; Treiber, M. R. Preparation and stress–strain properties of ABA-type block polymers of styrene and isoprene or butadiene. *J. Appl. Polym. Sci.* **1968**, *12* (1), 23–34. DOI: 10.1002/app.1968.070120104.

## 9.8 Supporting Information

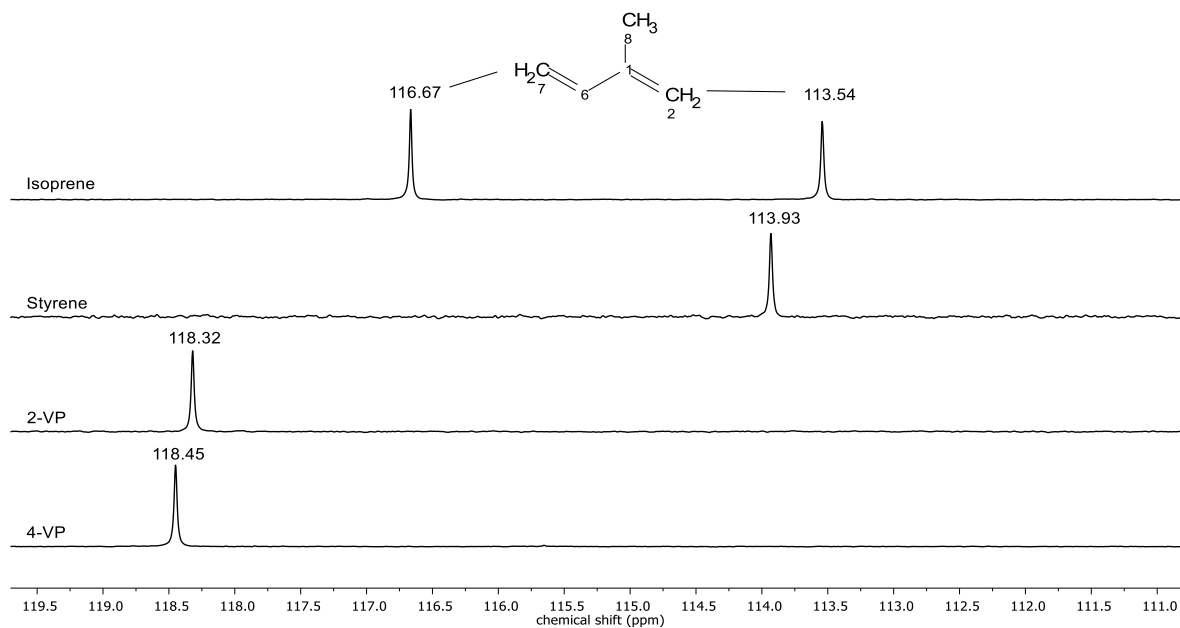


Figure S1:  $^{13}\text{C}$  NMR spectrum (400 MHz,  $\text{CDCl}_3$ ) of different monomers, showing the respective  $\beta$ -carbon shifts.

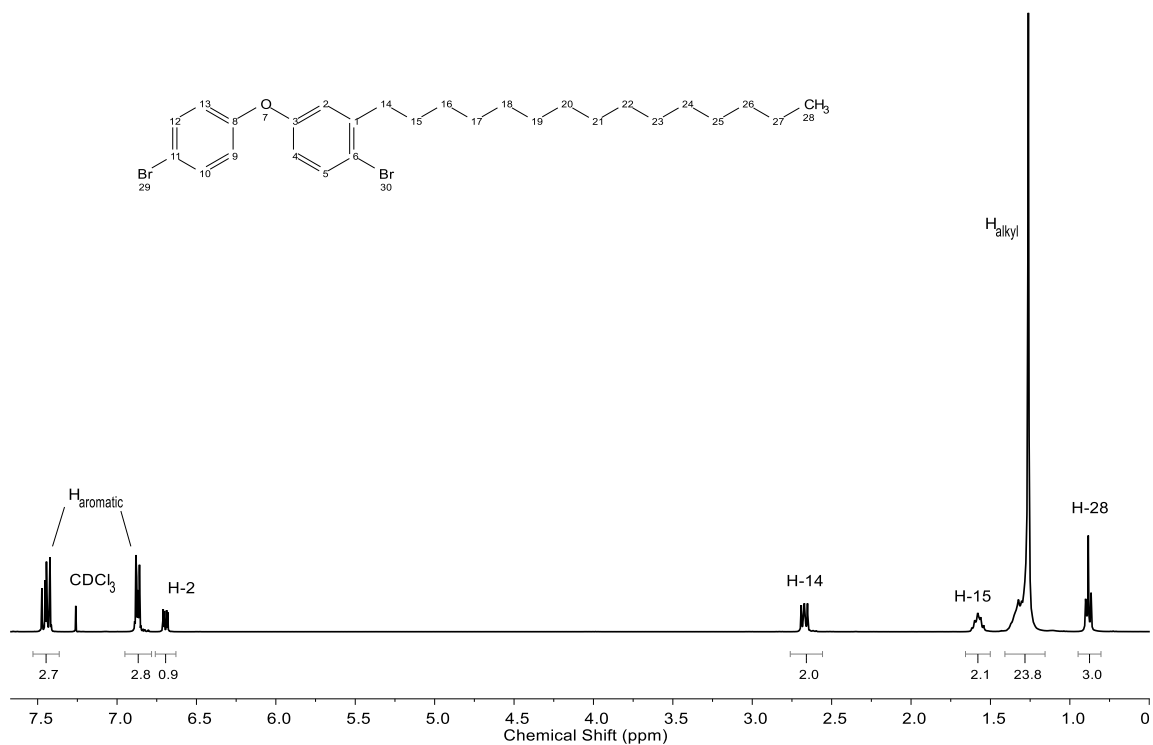


Figure S2:  $^1\text{H}$  NMR spectrum (400 MHz,  $\text{CDCl}_3$ ) of DBPPB.



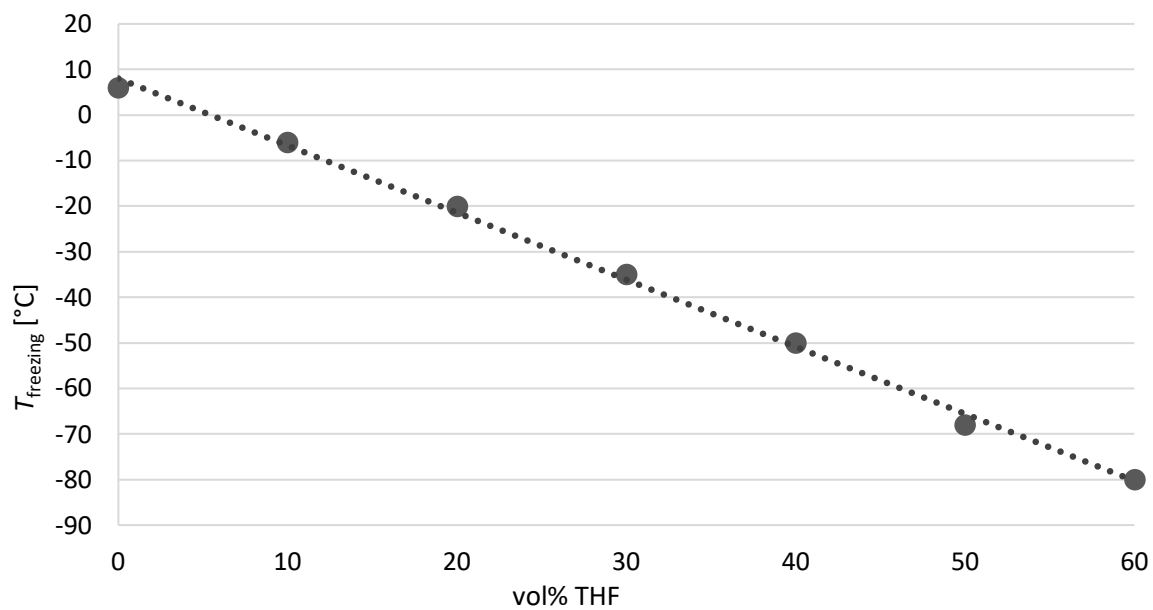


Figure S3: Melting temperature of benzene-THF mixtures. A minimum of 50% THF is required to prevent the mixture from freezing during the polymerisation.

Copolymer NMR spectroscopy characterisation

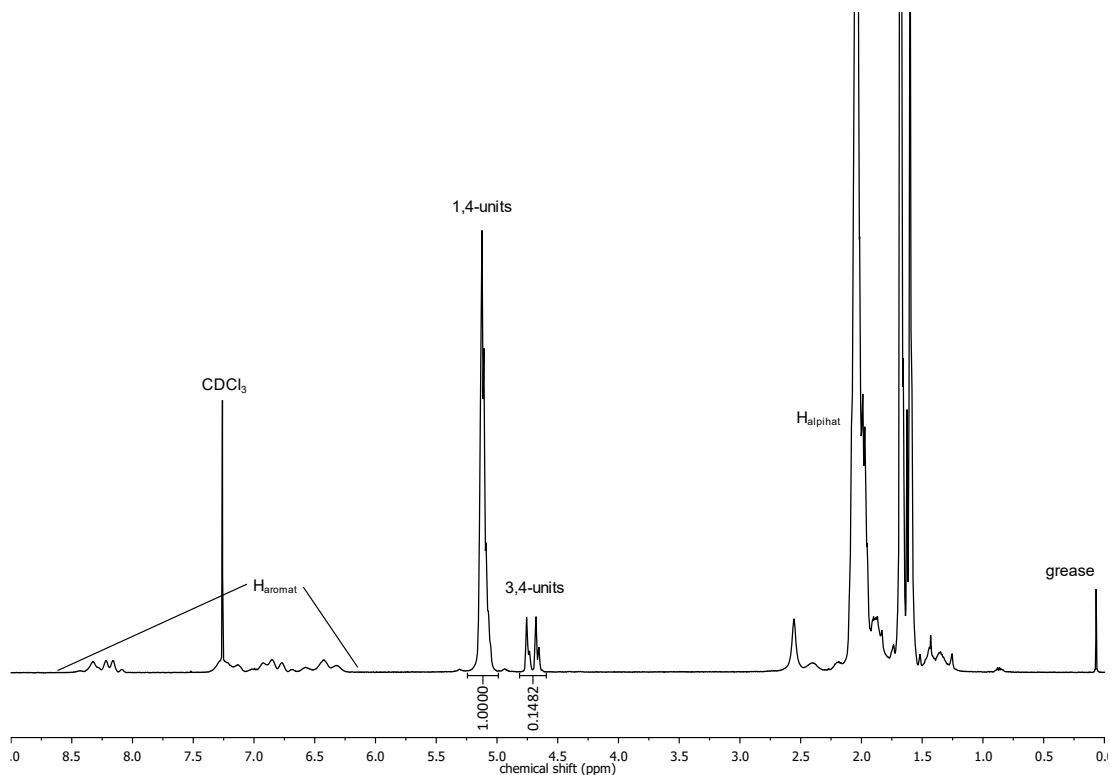


Figure S4: <sup>1</sup>H NMR spectrum (CDCl<sub>3</sub>, 400 MHz) of P(2-VP-b-l-b-2-VP) – 15-70-15 15k.

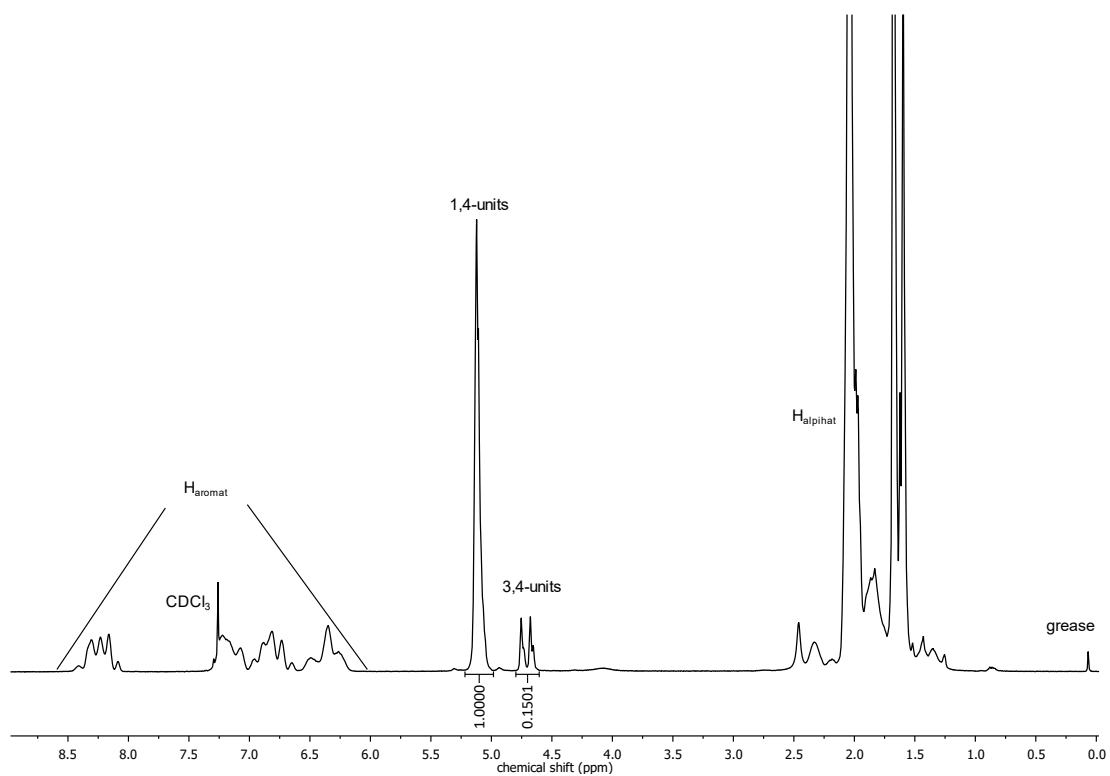


Figure S5: <sup>1</sup>H NMR spectrum (CDCl<sub>3</sub>, 400 MHz) of P(2-VP-b-l-b-2-VP) – 15-70-15 20k.

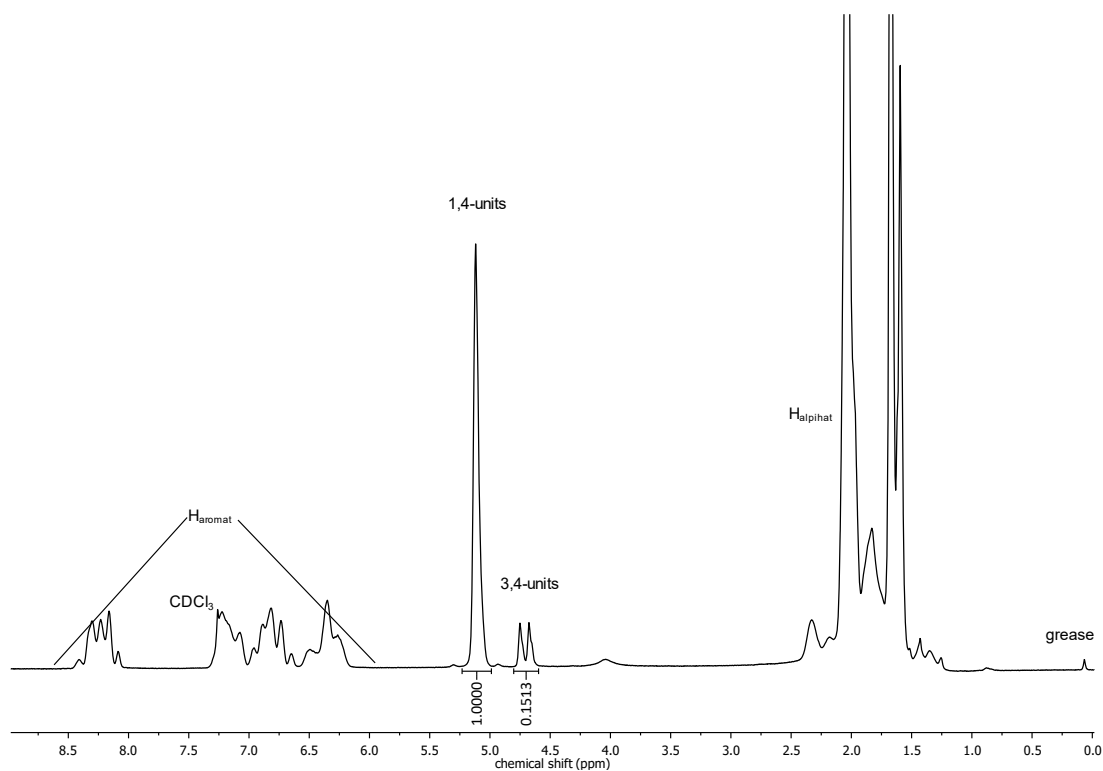


Figure S6:  $^1\text{H}$  NMR spectrum ( $\text{CDCl}_3$ , 400 MHz) of  $P(2\text{-VP-}b\text{-I-}b\text{-2-VP})$  – 15-70-15 25k.

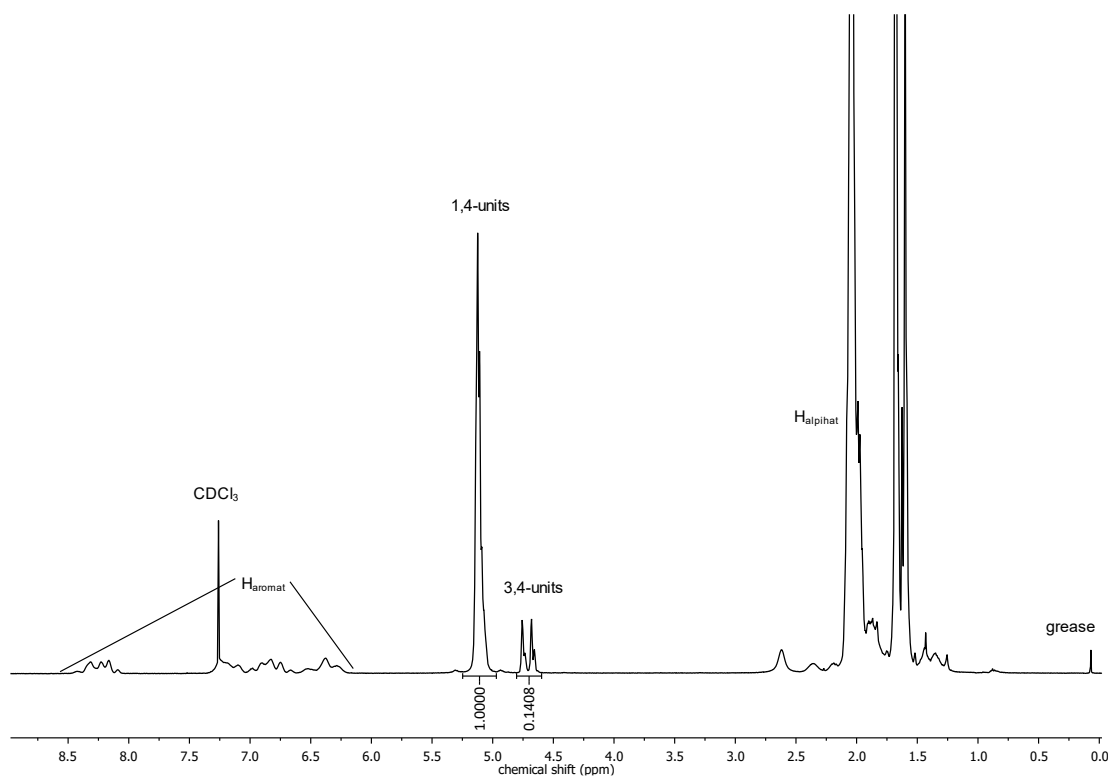


Figure S7:  $^1\text{H}$  NMR spectrum ( $\text{CDCl}_3$ , 400 MHz) of  $P(2\text{-VP-}b\text{-I-}b\text{-2-VP})$  – 20-60-20 15k.

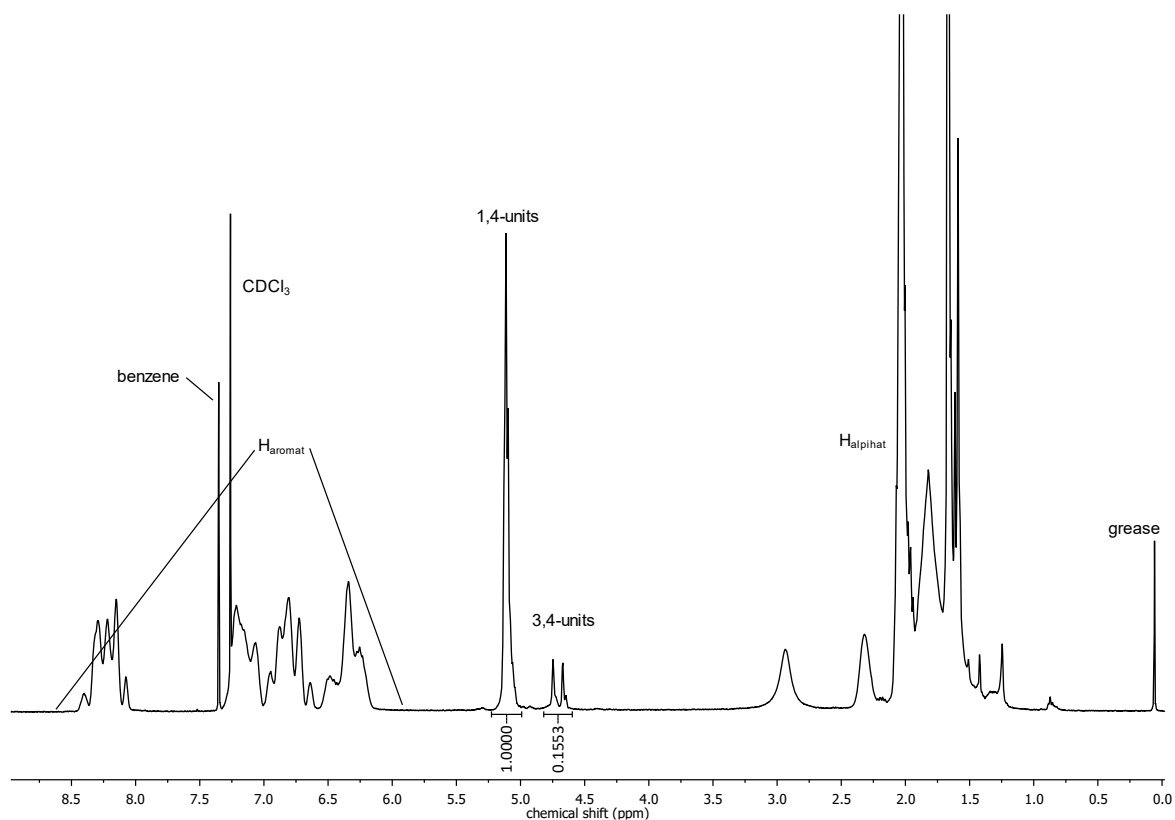


Figure S8: <sup>1</sup>H NMR spectrum (CDCl<sub>3</sub>, 400 MHz) of P(2-VP-b-I-b-2-VP) – 20-60-20 20k.

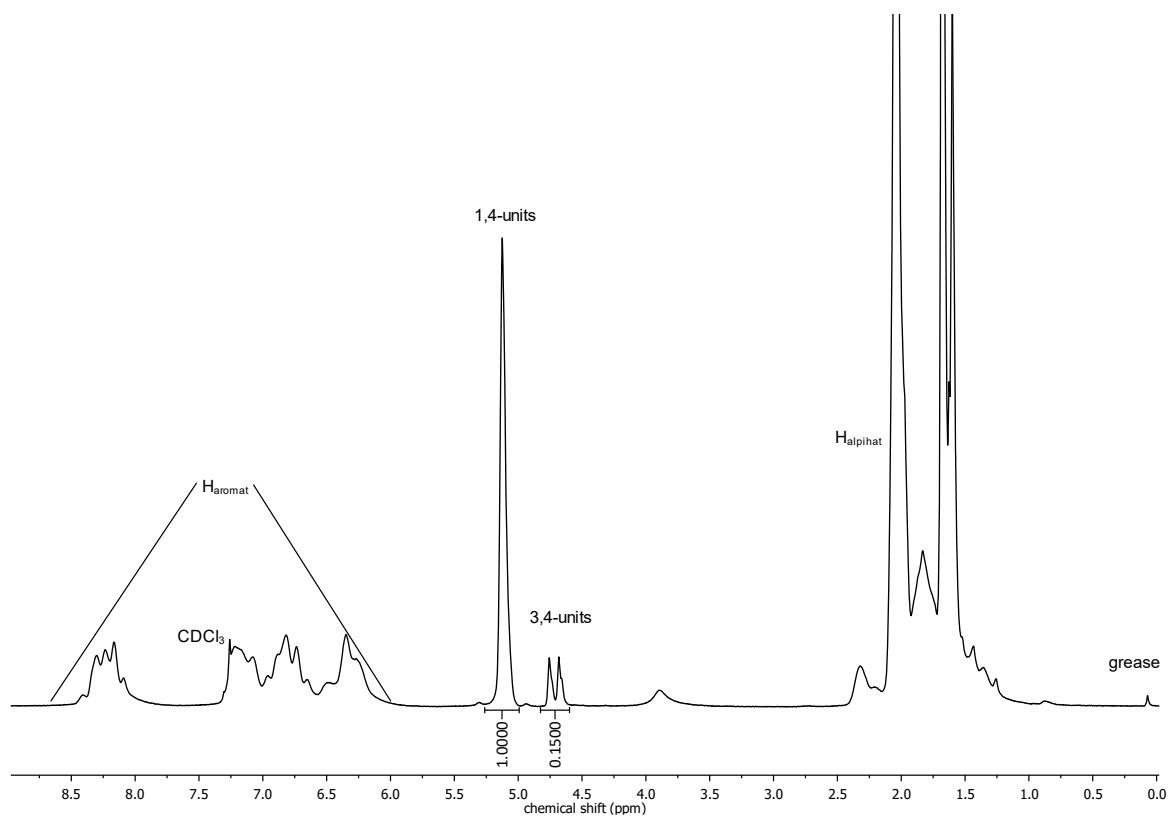


Figure S9: <sup>1</sup>H NMR spectrum (CDCl<sub>3</sub>, 400 MHz) of P(2-VP-b-I-b-2-VP) – 20-60-20 25k.

Table S1: Microstructure ratios calculated from  $^1\text{H}$  NMR spectroscopy.

Sample	I(1,4-units)	$0.5 \cdot I(3,4\text{-units})$	3,4-units [%]	1,4-units [%]
15-70-15 - 15k	1	0.0741	6.9	93.1
15-70-15 - 20k	1	0.0751	7.0	93.0
15-70-15 - 25k	1	0.0757	7.0	93.0
20-60-20 - 15k	1	0.0704	6.6	93.4
20-60-20 - 20k	1	0.0777	7.2	92.8
20-60-20 - 25k	1	0.0750	7.0	93.0

Differential scanning calorimetry

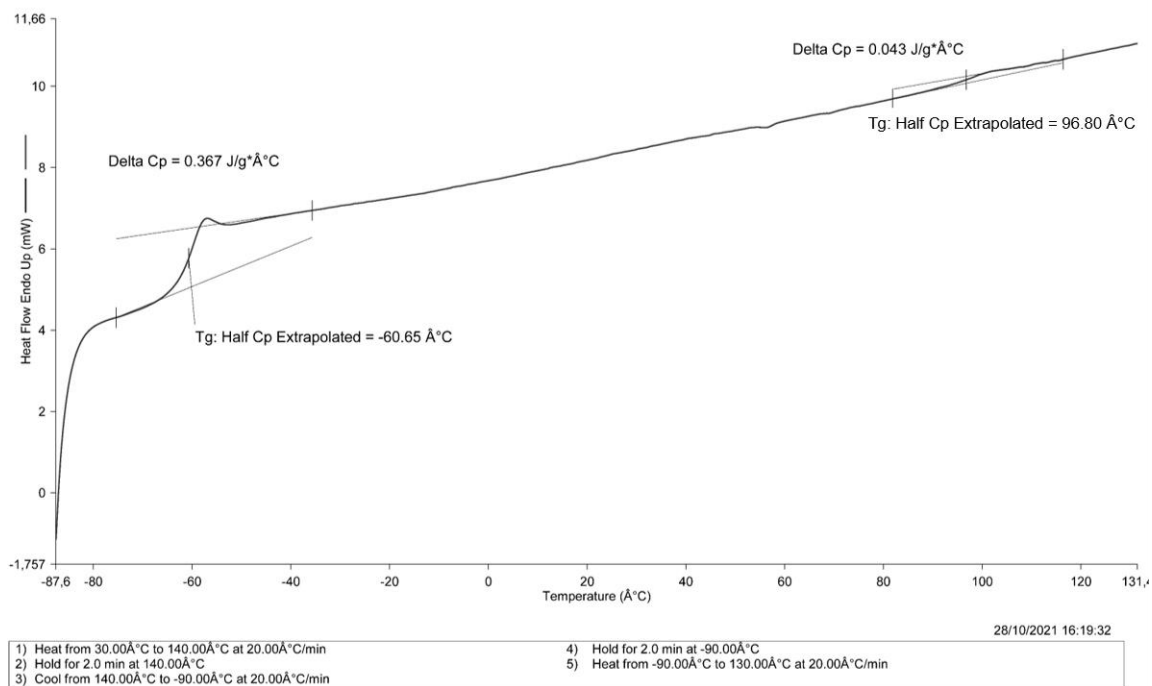


Figure S10: DSC curve of P(2-VP-b-I-b-2-VP) – 15-70-15 15k.

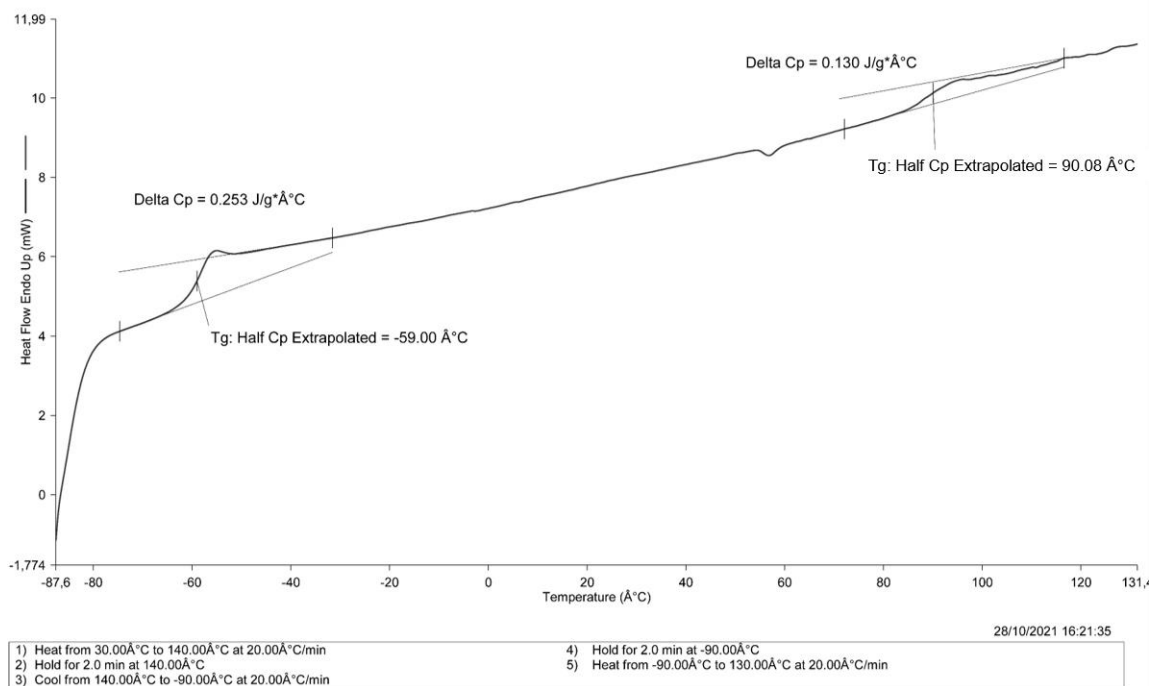


Figure S11: DSC curve of P(2-VP-b-I-b-2-VP) – 15-70-15 20k.

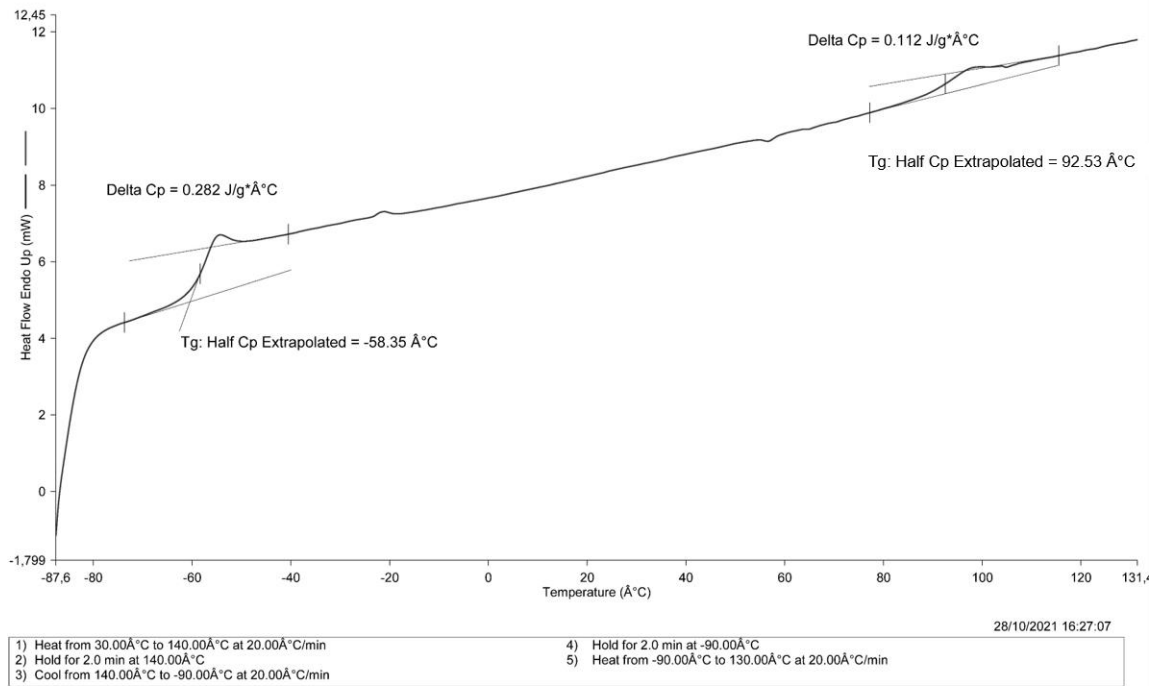


Figure S12: DSC curve of P(2-VP-b-I-b-2-VP) – 15-70-15 25k.

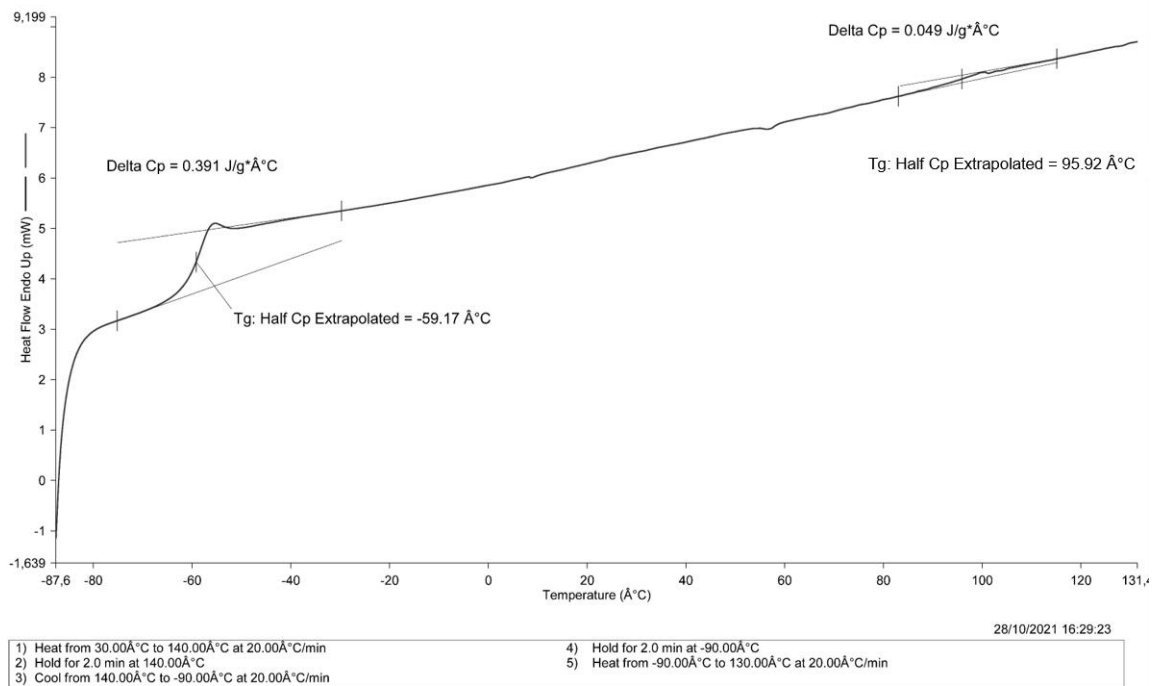


Figure S13: DSC curve of P(2-VP-b-I-b-2-VP) – 20-60-20 15k.

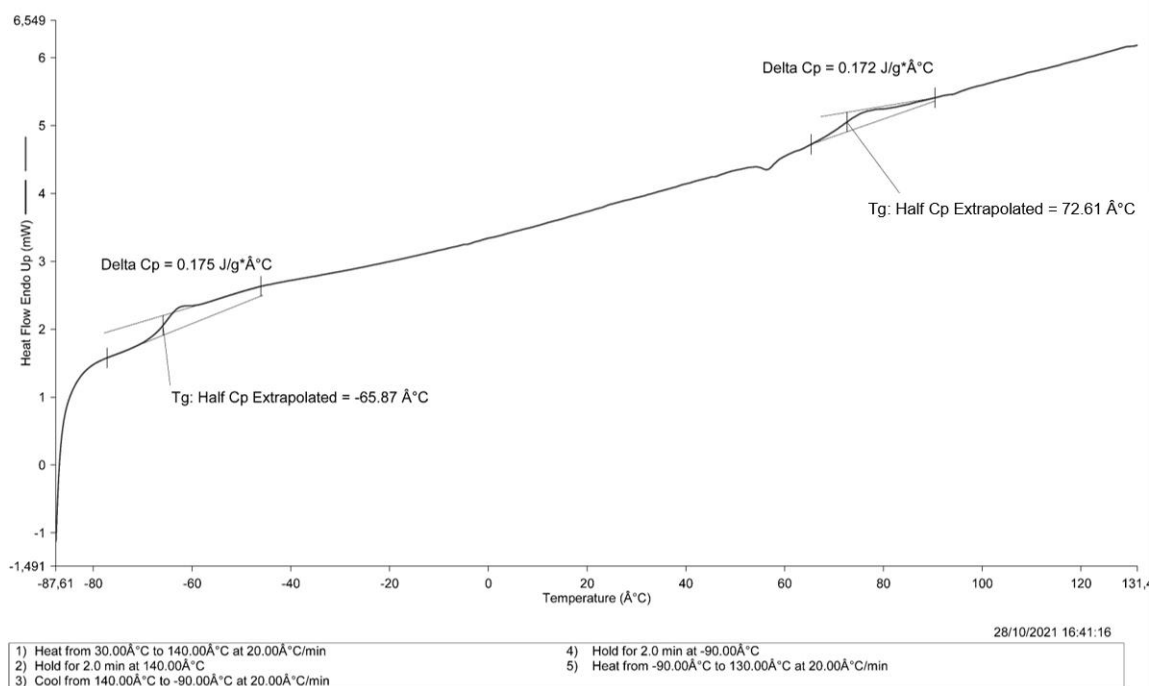


Figure S14: DSC curve of P(2-VP-b-I-b-2-VP) – 20-60-20 20k.

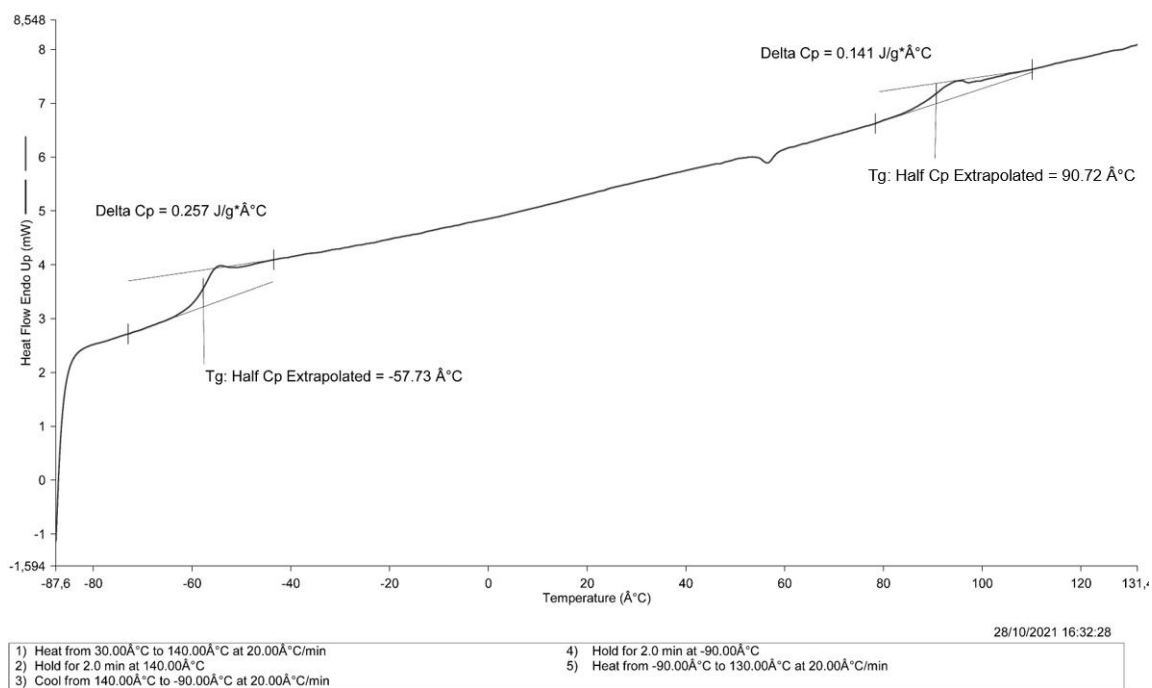


Figure S15: DSC curve of P(2-VP-b-I-b-2-VP) – 20-60-20 25k.



Table S2: Overview of all measured glass transition temperatures.

Sample	$T_g(I)$ [°C]	$T_g(2-VP)$ [°C]
15-70-15 - 15k	-61	97
15-70-15 - 20k	-59	90
15-70-15 - 25k	-58	93
20-60-20 - 15k	-59	96
20-60-20 - 20k	-66	73
20-60-20 - 25k	-58	91

### Tensile tests

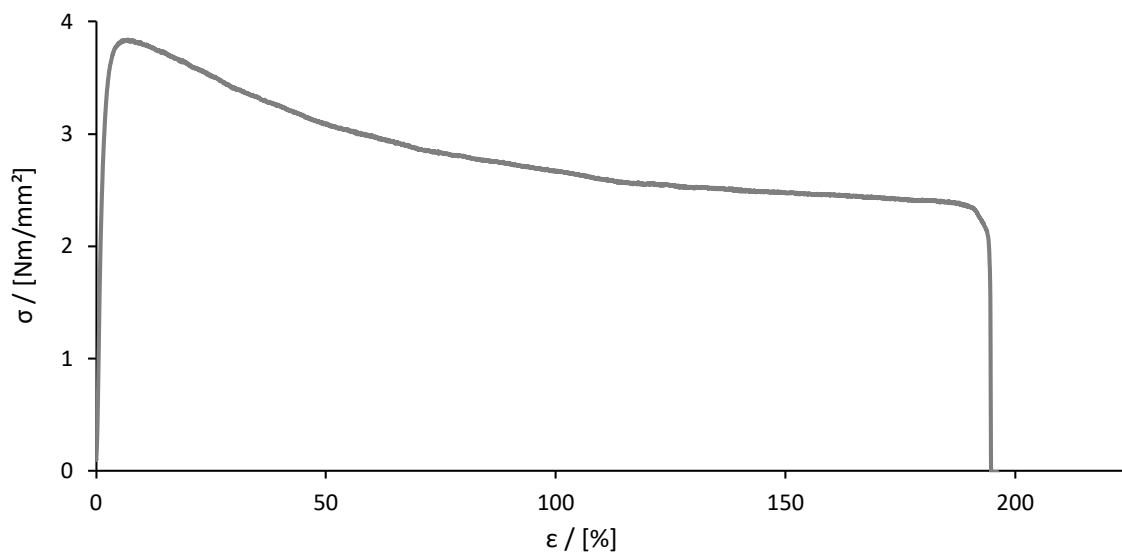


Figure S16: Stress-strain curve of sample 15-70-15 20k, cast from benzene.

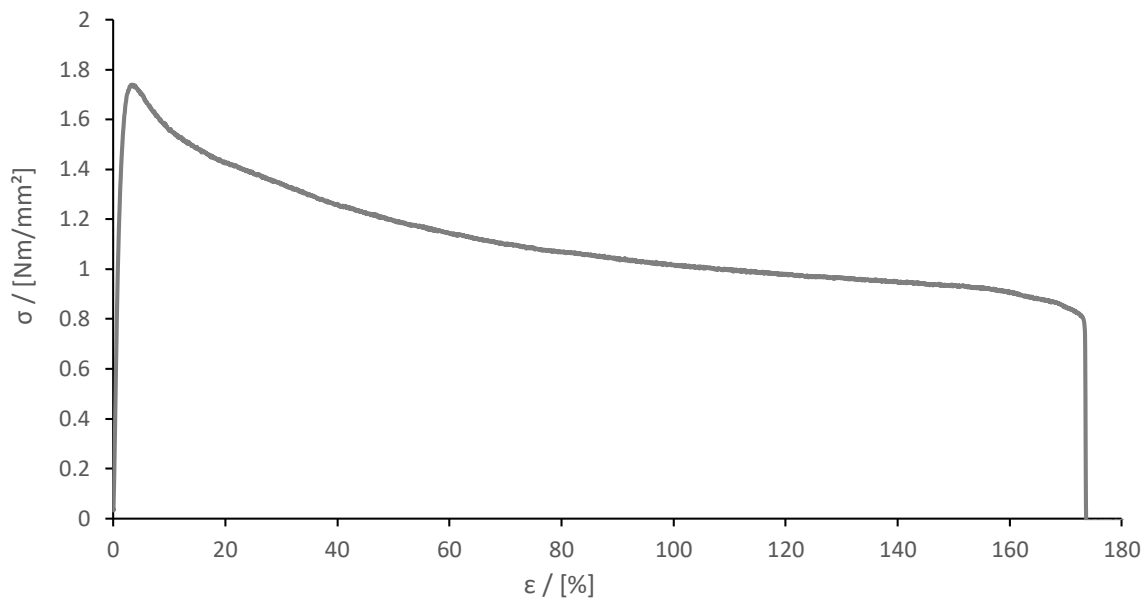


Figure S17: Stress-strain curve of sample 20-60-20 15k, cast from benzene.

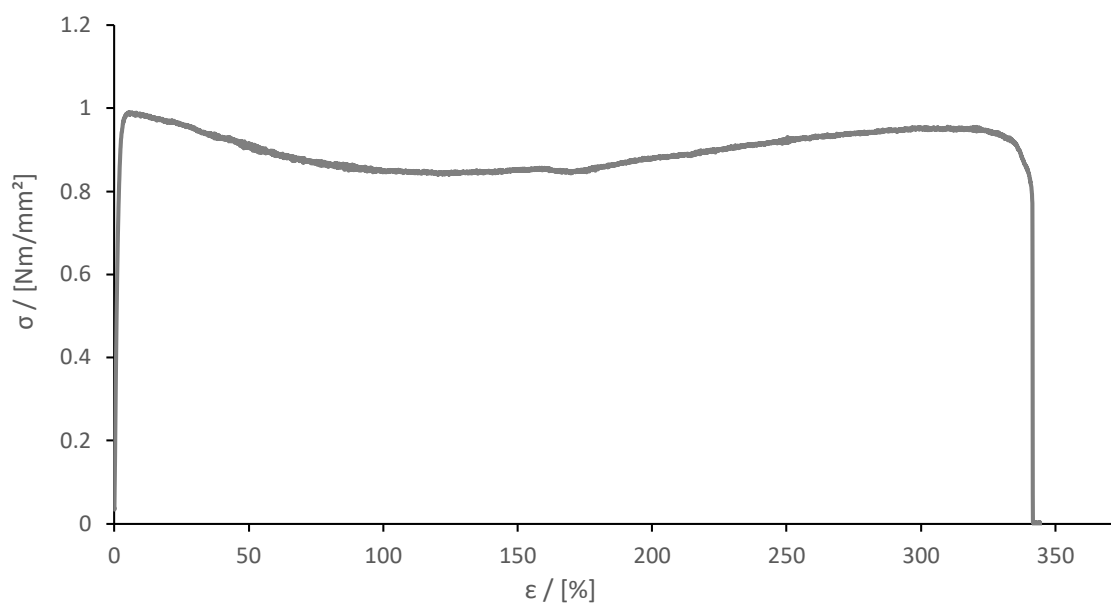


Figure S18: Stress-strain curve of sample 20-60-20 20k, cast from benzene.

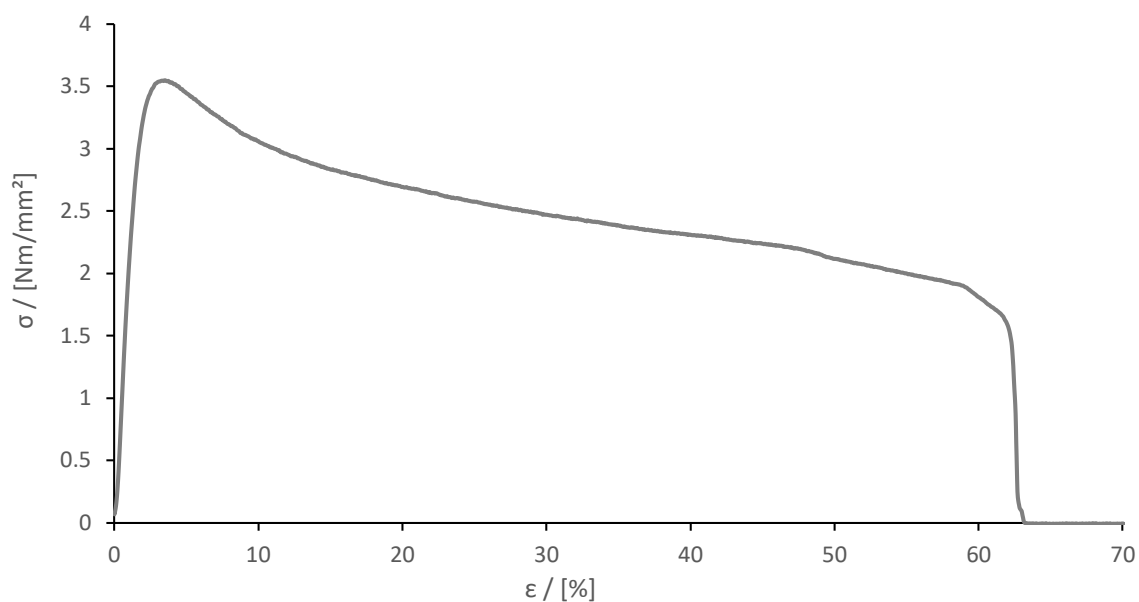


Figure S19: Stress-strain curve of sample 20-60-20 25k (#1), cast from benzene.

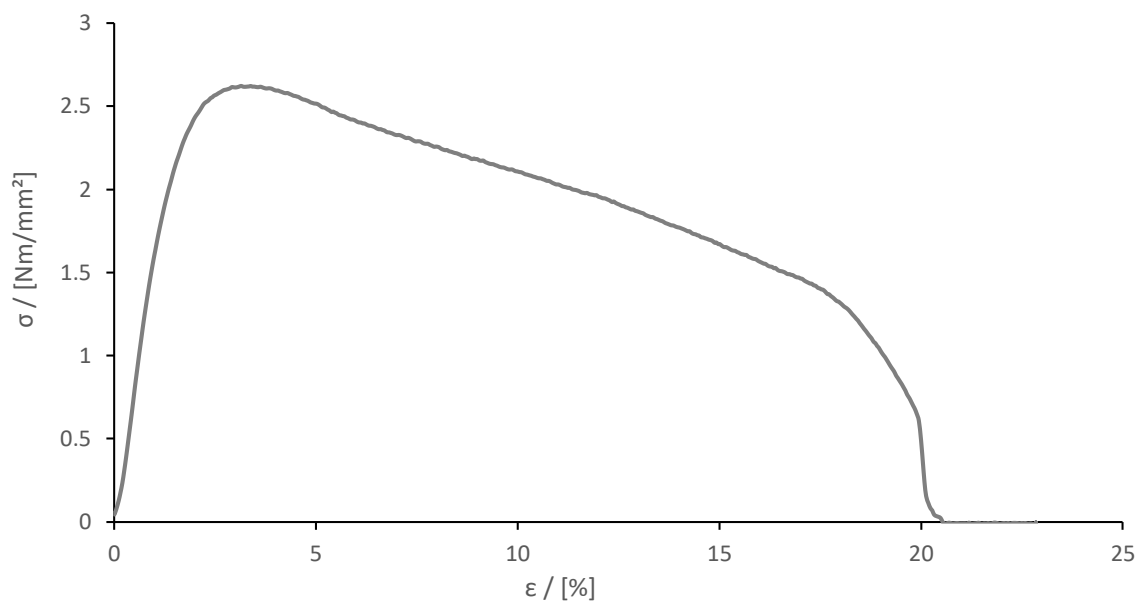


Figure S20: Stress-strain curve of sample 20-60-20 25k (#2), cast from benzene.

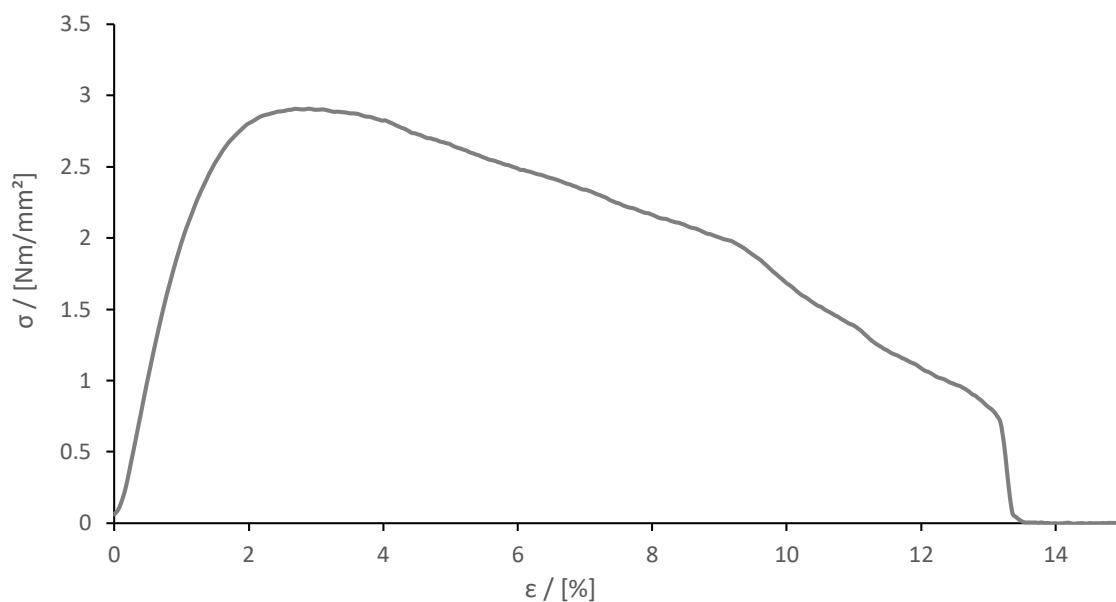


Figure S21: Stress-strain curve of sample 20-60-20 25k (#3), cast from benzene.

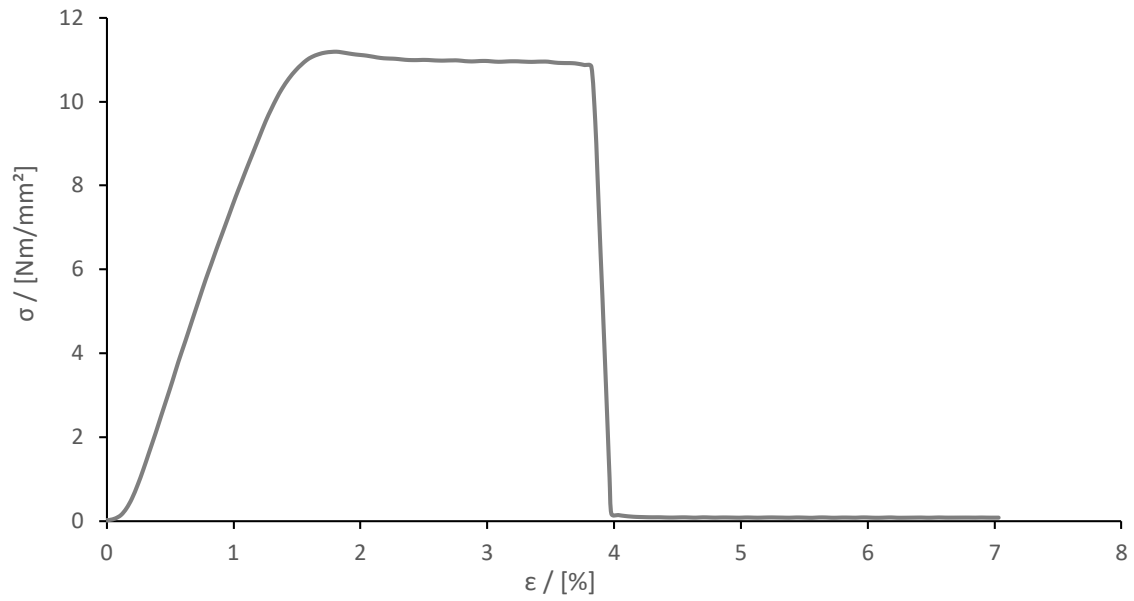


Figure S22: Stress-strain curve of sample 15-70-15 20k (#1), cast from  $\text{CHCl}_3$ .

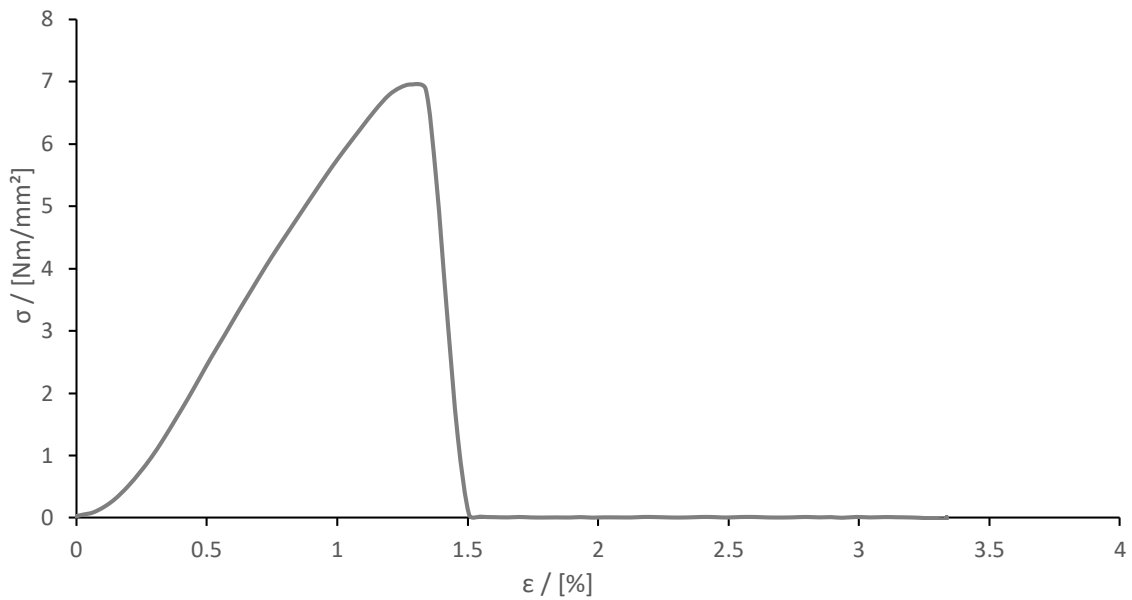


Figure S23: Stress-strain curve of sample 15-70-15 20k (#2), cast from  $\text{CHCl}_3$ .

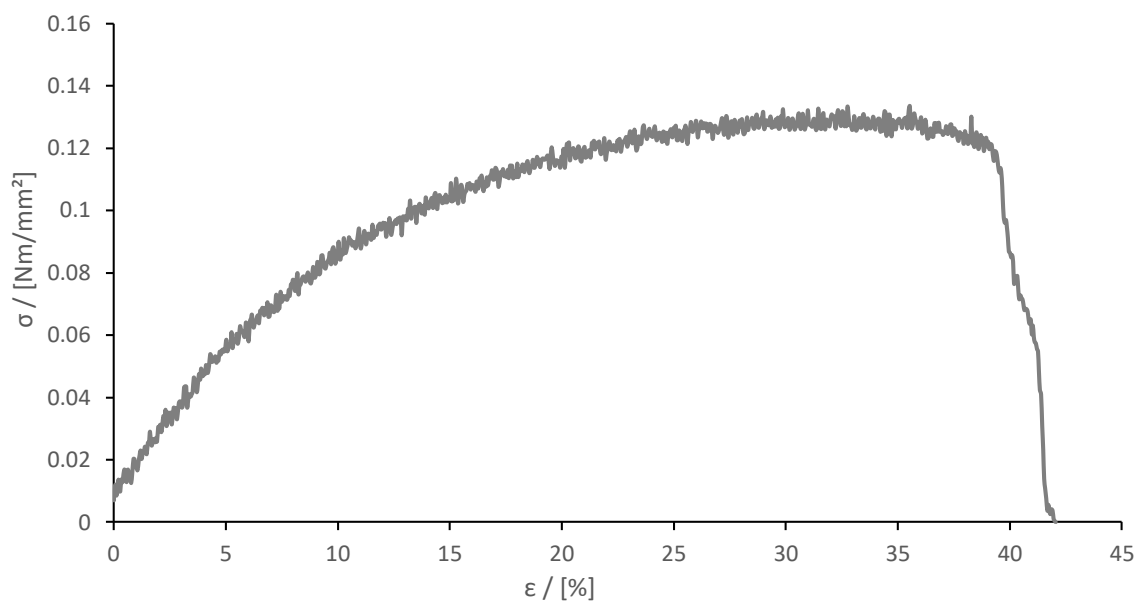


Figure S24: Stress-strain curve of sample 15-70-15 25k (#1), cast from  $\text{CHCl}_3$ .

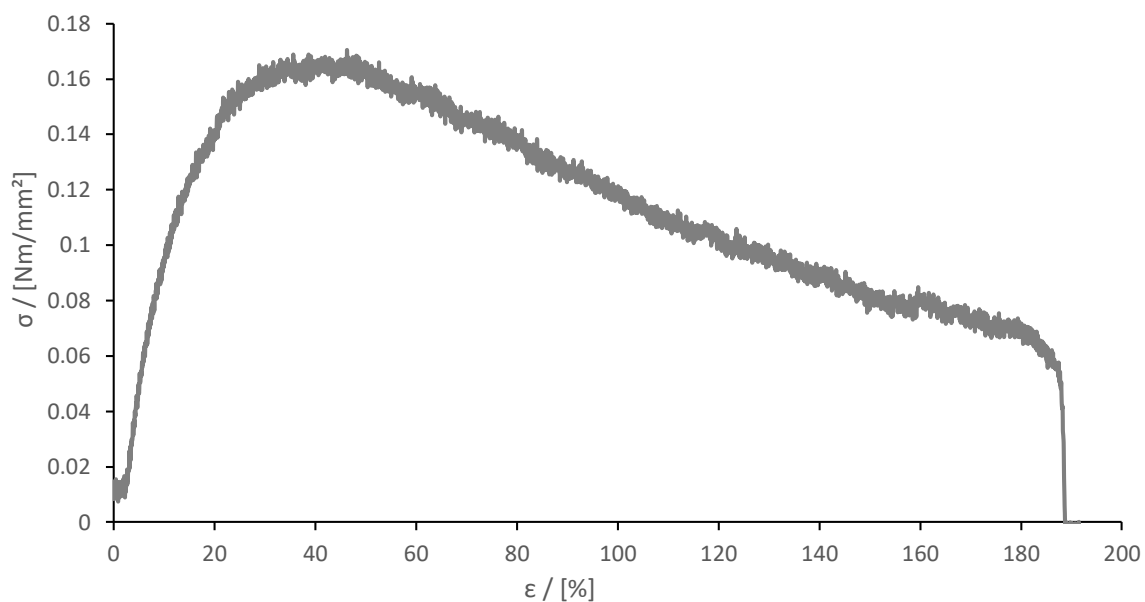


Figure S25: Stress-strain curve of sample 15-70-15 25k (#2), cast from  $\text{CHCl}_3$ .

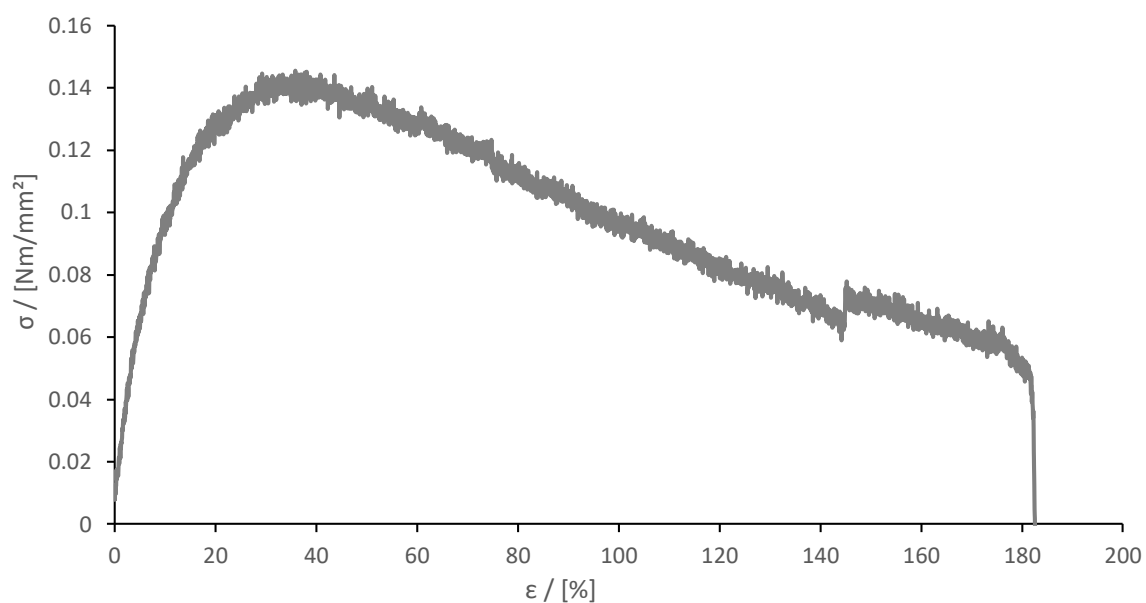


Figure S26: Stress-strain curve of sample 15-70-15 25k (#3), cast from  $\text{CHCl}_3$ .

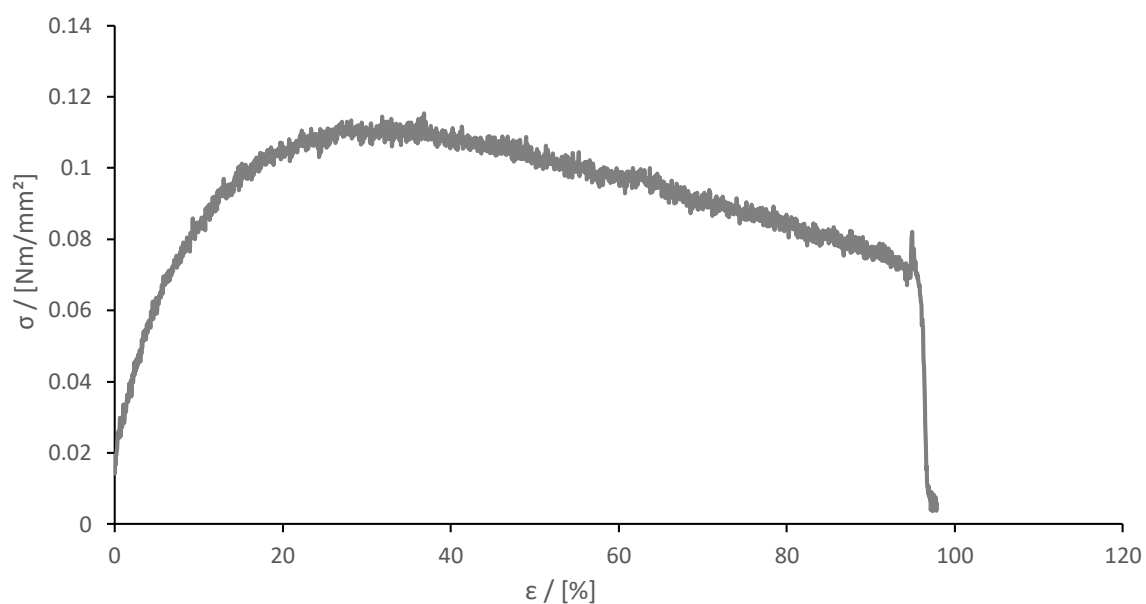


Figure S27: Stress-strain curve of sample 15-70-15 25k (#4), cast from  $\text{CHCl}_3$ .

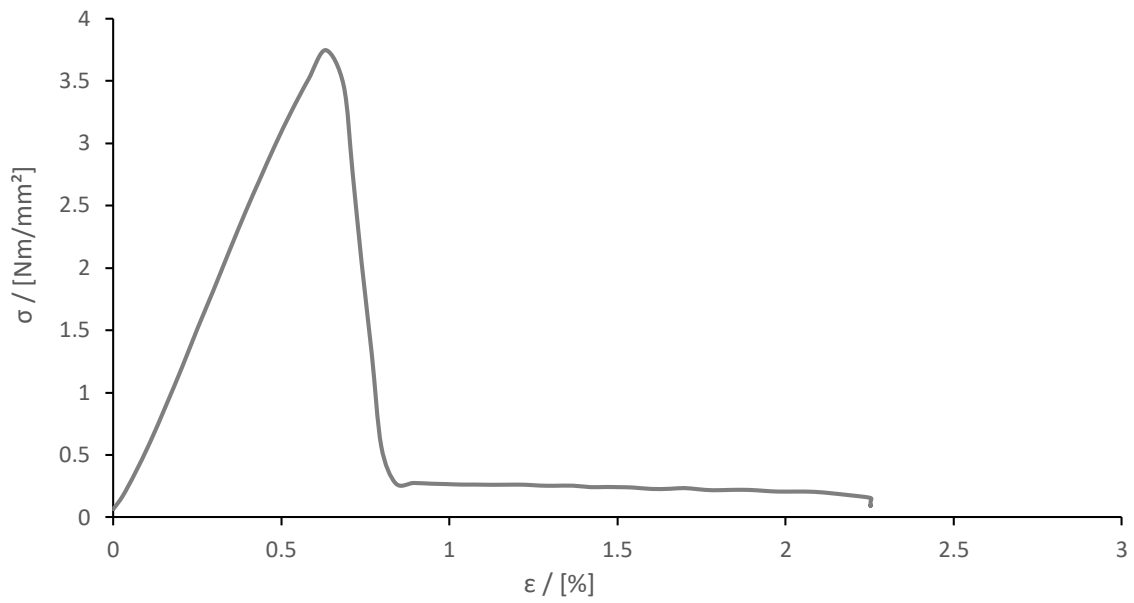


Figure S28: Stress-strain curve of sample 20-60-20 15k (#1), cast from  $\text{CHCl}_3$ .

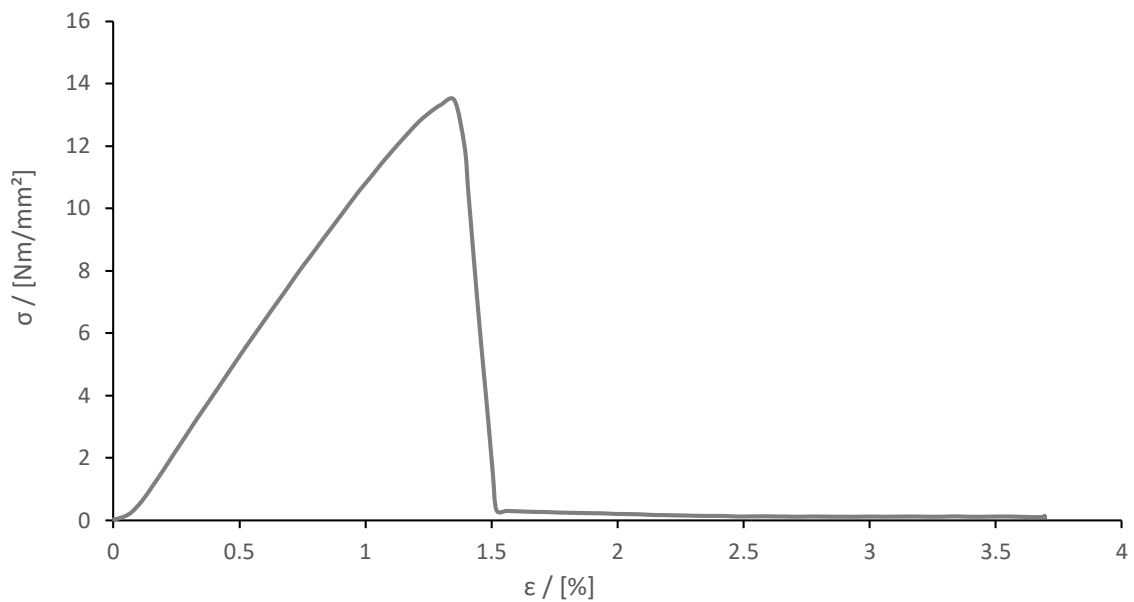


Figure S29: Stress-strain curve of sample 20-60-20 15k (#2), cast from  $\text{CHCl}_3$ .



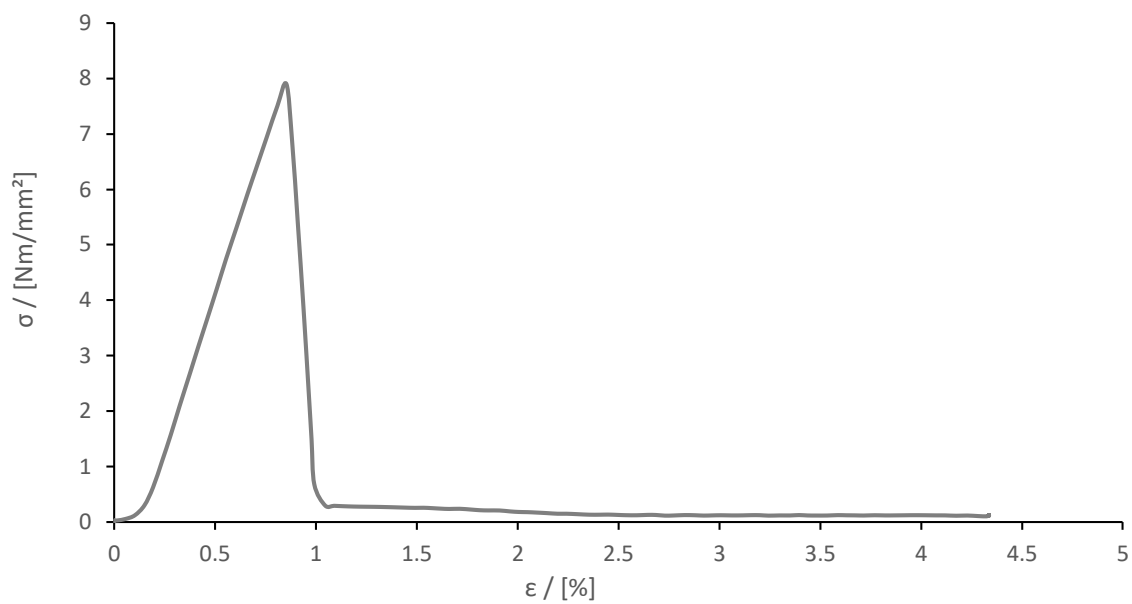


Figure S30: Stress-strain curve of sample 20-60-20 15k (#3), cast from  $\text{CHCl}_3$ .

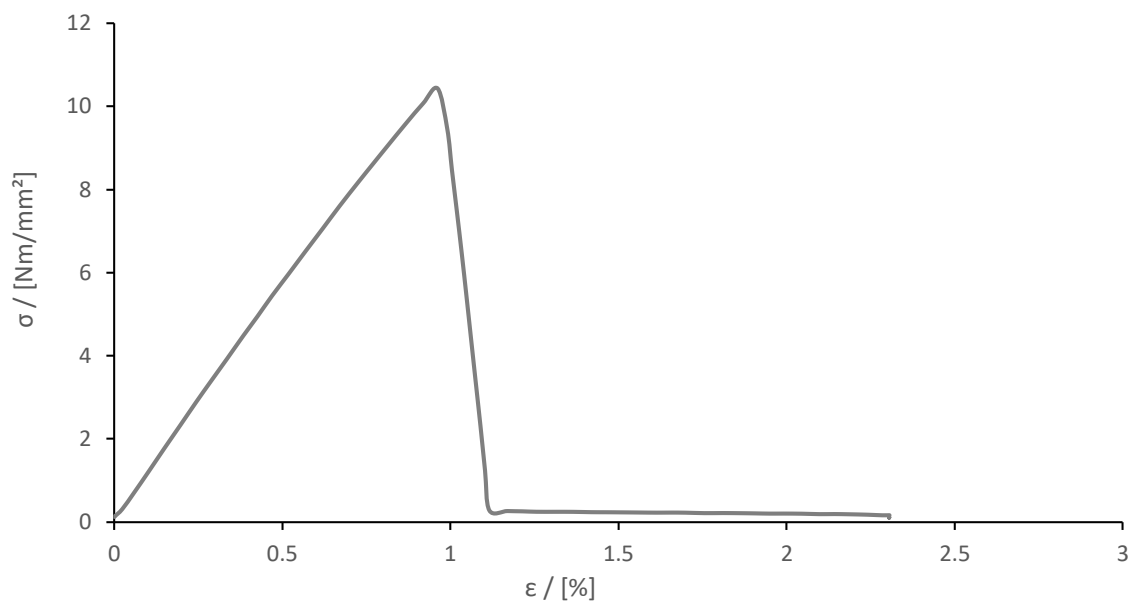


Figure S31: Stress-strain curve of sample 20-60-20 15k (#4), cast from  $\text{CHCl}_3$ .

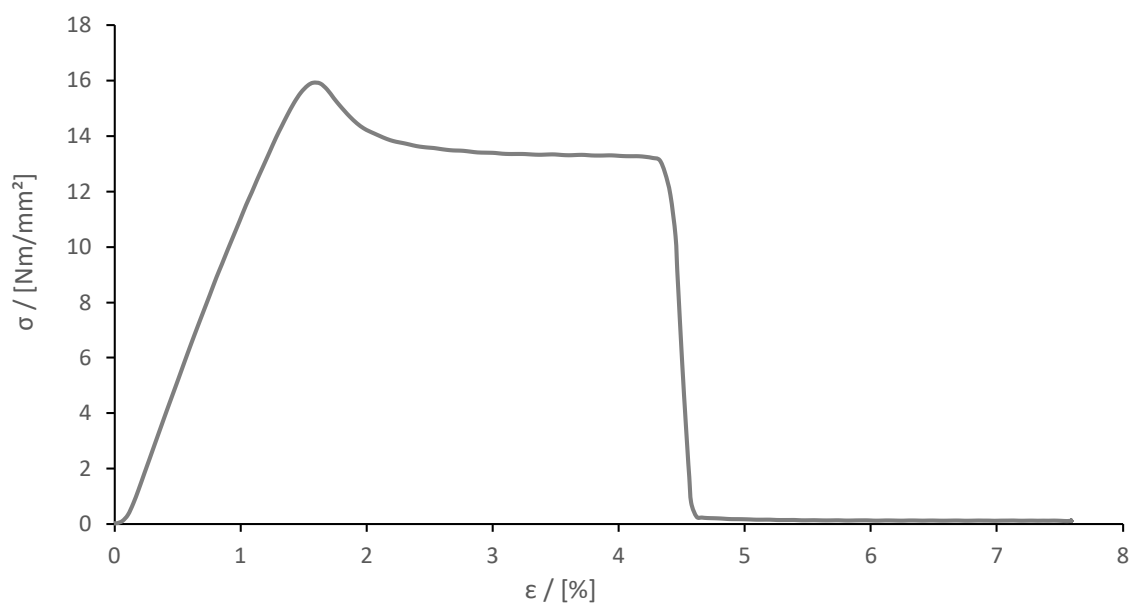


Figure S32: Stress-strain curve of sample 20-60-20 20k (#1), cast from CHCl<sub>3</sub>.

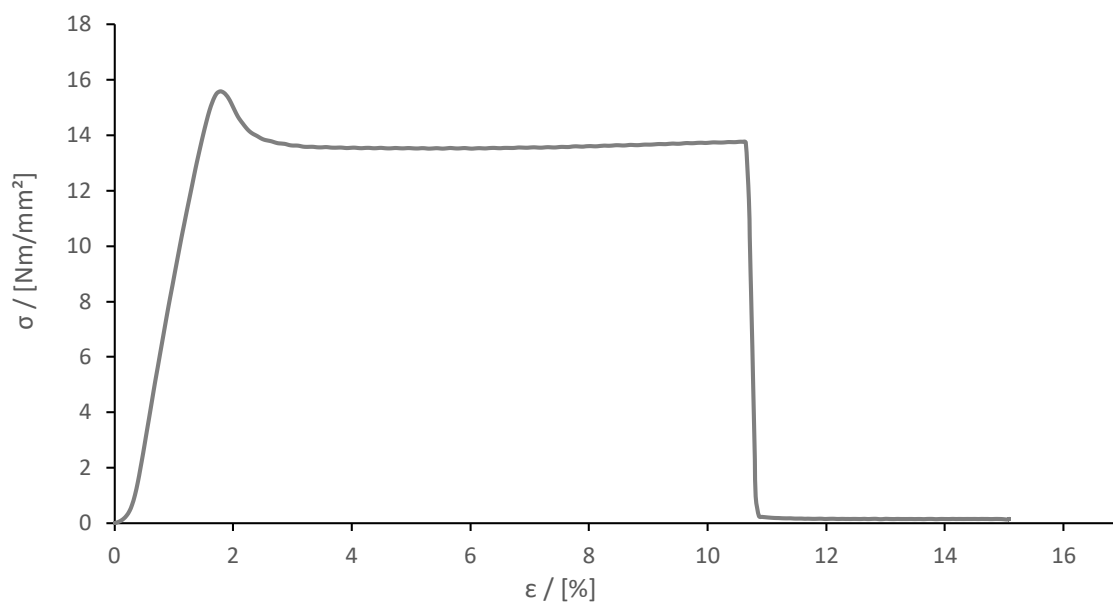


Figure S33: Stress-strain curve of sample 20-60-20 20k (#2), cast from CHCl<sub>3</sub>.

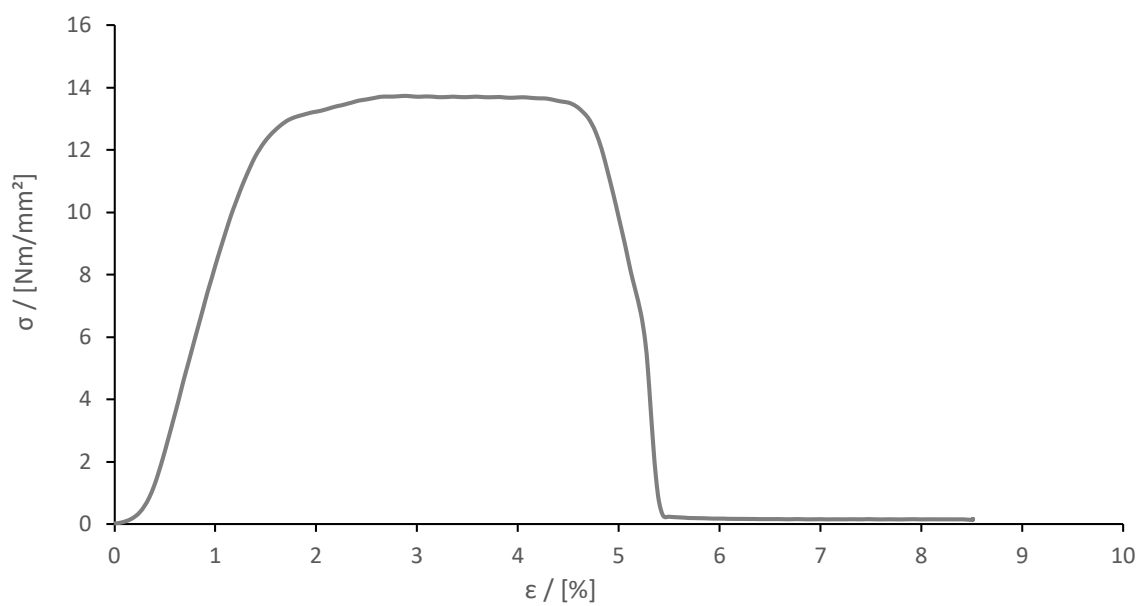


Figure S34: Stress-strain curve of sample 20-60-20 20k (#3), cast from CHCl<sub>3</sub>.

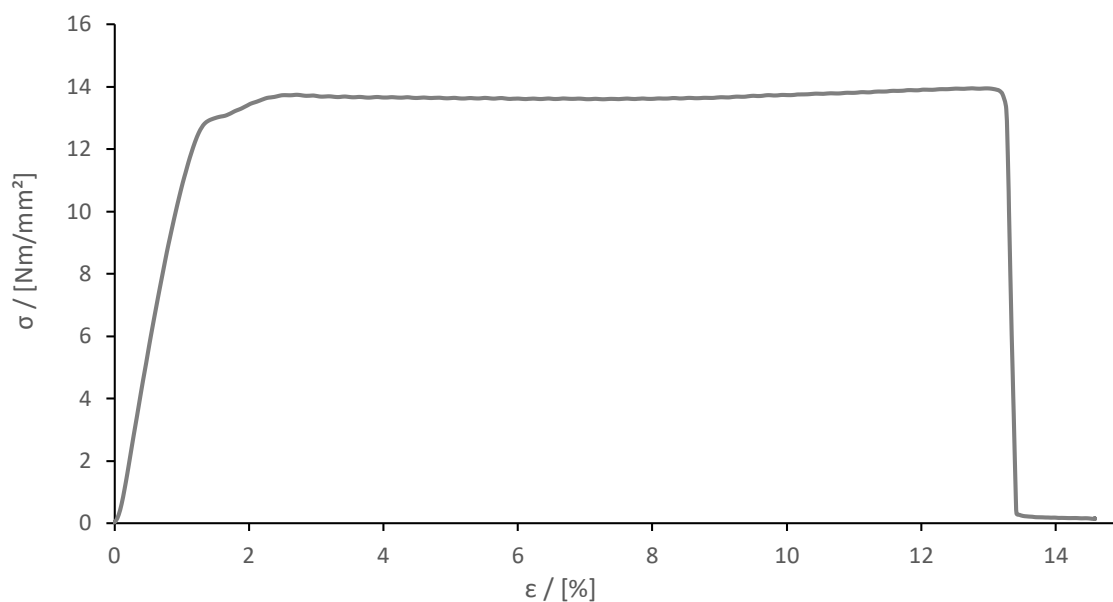


Figure S35: Stress-strain curve of sample 20-60-20 20k (#4), cast from CHCl<sub>3</sub>.

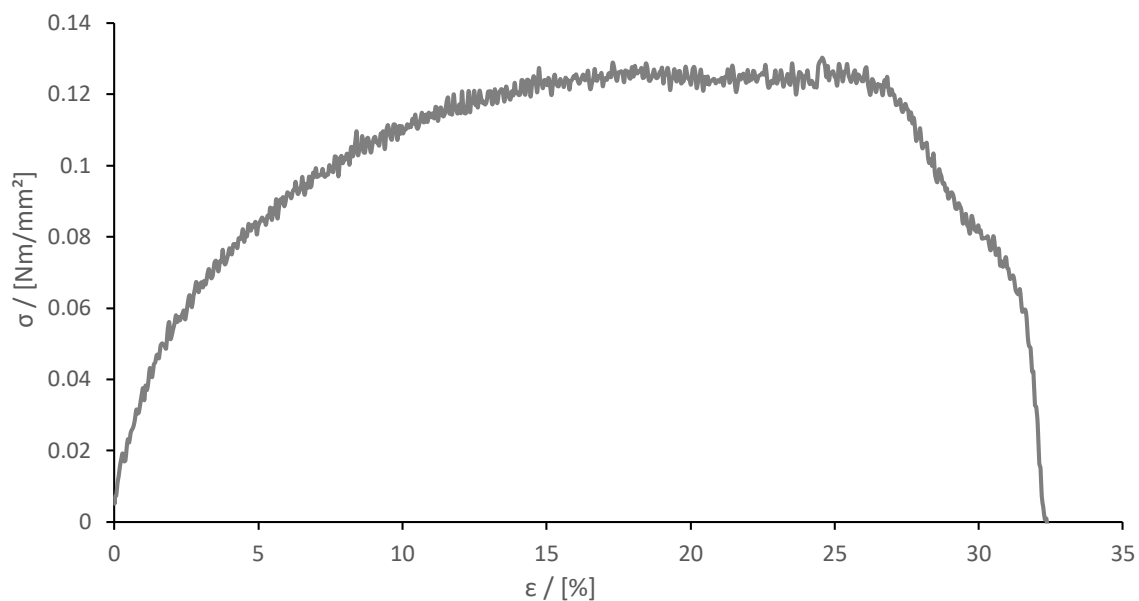


Figure S36: Stress-strain curve of sample 20-60-20 25k (#1), cast from CHCl<sub>3</sub>.

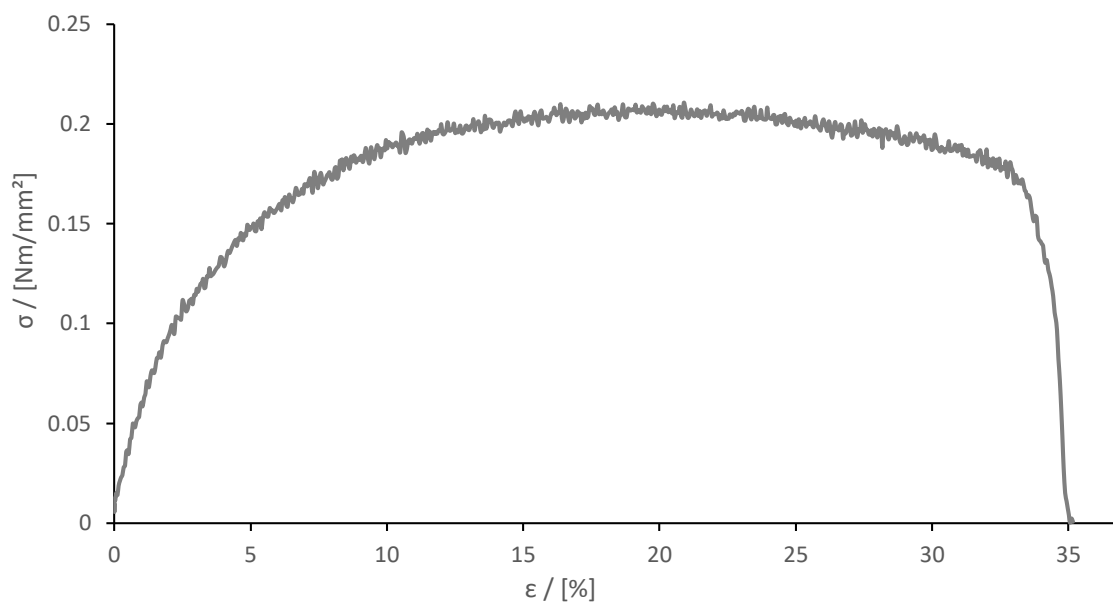


Figure S37: Stress-strain curve of sample 20-60-20 25k (#2), cast from CHCl<sub>3</sub>.

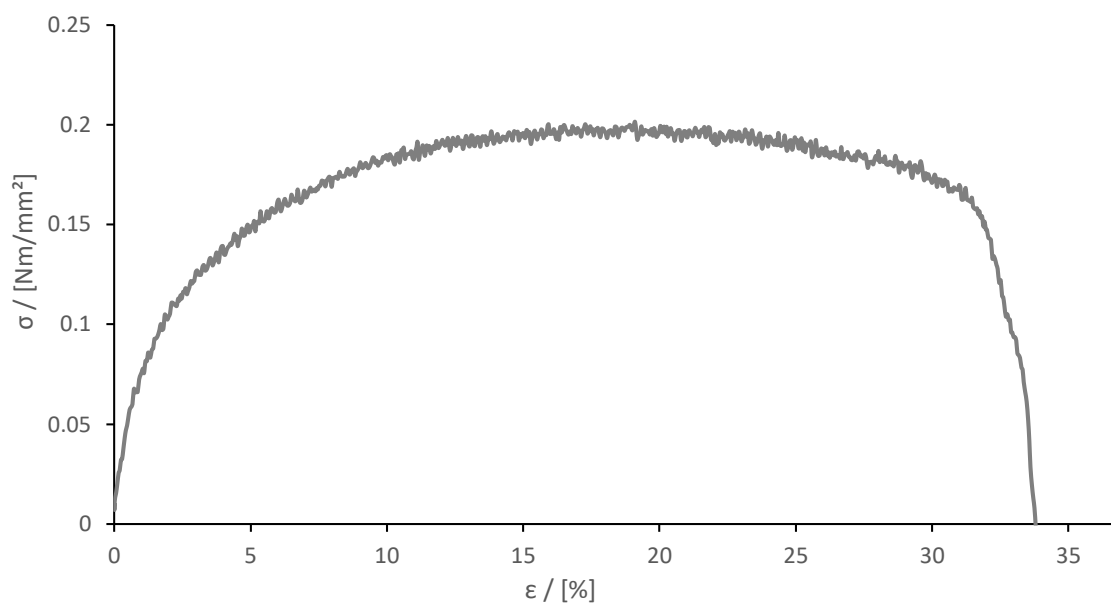


Figure S38: Stress-strain curve of sample 20-60-20 25k (#3), cast from  $\text{CHCl}_3$ .

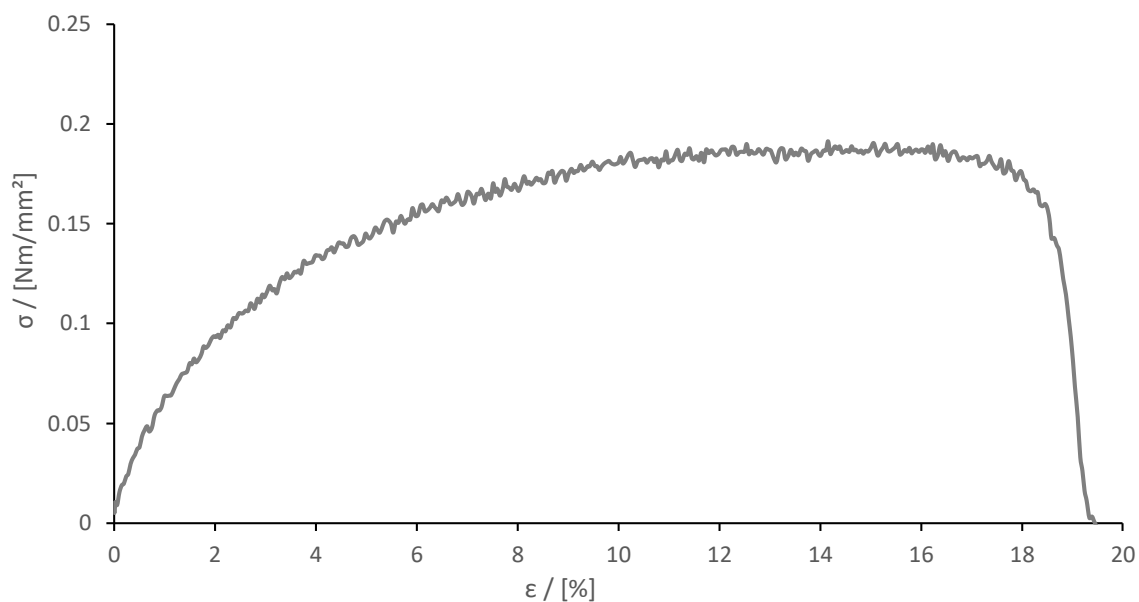


Figure S39: Stress-strain curve of sample 20-60-20 25k (#4), cast from  $\text{CHCl}_3$ .

Chapter 5 – Synthesis and characterisation of ABA triblock copolymers based on isoprene and 2-vinylpyridine for TPE applications - Supporting Information

Experiments

Table S3: 15-70-15 15k.

$M_w(\text{tar})$	<b>99900 g/mol</b>	2-VP 15%	isoprene 70%	2-VP 15%			
$n(\text{DBPPB}) =$	0.050 mmol	15000 g/mol	69900 g/mol	15000 g/mol			
$m(\text{DBPPB}) =$	26.95 mg	4 eq. V(s-BuLi) =	0.154 mL	V(initiator) =	1.67 mL	c(DDPE) =	0.03 mol/L
70:30	$n(\text{total}) =$	0.063 mol					
$n(2\text{-VP})$ 30:70 $n(\text{l})$							
$m(\text{total}) =$	5.00 g						
$n(2\text{-VP}) =$	0.0189 mol	$n(\text{l}) =$	0.0442 mol				
$m(2\text{-VP}) =$	1.99 g	$m(\text{l}) =$	3.01 g				
$V(2\text{-VP}) =$	2.04 mL	$V(\text{l}) =$	4.42 mL				
$c(\text{anions}) =$ 1.7 mM $c(\text{l}) =$ 1.50 mol/L $V(\text{toluene}) =$ 29.45 mL $V(\text{THF}) =$ 58.90 mL <hr/> $V(\text{ges}) =$ 88.35 mL $c(\text{ges}) =$ 0.71 mol/L							

Table S4: 15-70-15 20k.

$M_w(\text{tar})$	<b>99900 g/mol</b>	2-VP 15%	isoprene 70%	2-VP 15%			
$n(\text{DBPPB}) =$	0.038 mmol	20000 g/mol	93200 g/mol	20000 g/mol			
$m(\text{DBPPB}) =$	20.21 mg	4 eq. V(s-BuLi) =	0.116 mL	V(initiator) =	1.25 mL	c(DDPE) =	0.03 mol/L
70:30	$n(\text{total}) =$	0.063 mol					
$n(2\text{-VP})$ 30:70 $n(\text{l})$							
$m(\text{total}) =$	5.00 g						
$n(2\text{-VP}) =$	0.0189 mol	$n(\text{l}) =$	0.0442 mol				
$m(2\text{-VP}) =$	1.99 g	$m(\text{l}) =$	3.01 g				
$V(2\text{-VP}) =$	2.04 mL	$V(\text{l}) =$	4.42 mL				
$c(\text{anions}) =$ 1.27 mM $c(\text{l}) =$ 1.50 mol/L $V(\text{toluene}) =$ 29.45 mL $V(\text{THF}) =$ 58.90 mL <hr/> $V(\text{ges}) =$ 88.35 mL $c(\text{ges}) =$ 0.71 mol/L							

Chapter 5 – Synthesis and characterisation of ABA triblock copolymers based on isoprene and 2-vinylpyridine for TPE applications - Supporting Information

Table S5: 15-70-15 25k.

		2-VP 15%	isoprene 70%	2-VP 15%						
$M_w(\text{tar})$	<b>166500 g/mol</b>	25000 g/mol	116500 g/mol	25000 g/mol						
$n(\text{DBPPB}) =$	0.030 mmol									
$m(\text{DBPPB}) =$	16.17 mg	4 eq. $V(\text{s-BuLi}) =$	0.092 mL	$V(\text{initiator}) =$ 1.00 mL						
		$c(\text{DDPE}) =$ 0.03 mol/L								
70:30	$n(\text{total}) =$	0.063 mol								
$n(\text{2-VP})$ 30:70 $n(\text{l})$										
$m(\text{total}) =$ 5.00 g										
$n(\text{2-VP}) =$ 0.0189 mol		$n(\text{l}) =$ 0.0442 mol								
$m(\text{2-VP}) =$ 1.99 g		$m(\text{l}) =$ 3.01 g								
$V(\text{2-VP}) =$ 2.04 mL		$V(\text{l}) =$ 4.42 mL								
<table border="1"> <tr> <td><math>c(\text{anions}) =</math> 1.02 mM</td> </tr> <tr> <td><math>c(\text{l}) =</math> 1.50 mol/L</td> </tr> <tr> <td><math>V(\text{toluene}) =</math> 29.45 mL</td> </tr> <tr> <td><math>V(\text{THF}) =</math> 58.90 mL</td> </tr> <tr> <td><math>V(\text{ges}) =</math> 88.35 mL</td> </tr> <tr> <td><math>c(\text{ges}) =</math> 0.71 mol/L</td> </tr> </table>					$c(\text{anions}) =$ 1.02 mM	$c(\text{l}) =$ 1.50 mol/L	$V(\text{toluene}) =$ 29.45 mL	$V(\text{THF}) =$ 58.90 mL	$V(\text{ges}) =$ 88.35 mL	$c(\text{ges}) =$ 0.71 mol/L
$c(\text{anions}) =$ 1.02 mM										
$c(\text{l}) =$ 1.50 mol/L										
$V(\text{toluene}) =$ 29.45 mL										
$V(\text{THF}) =$ 58.90 mL										
$V(\text{ges}) =$ 88.35 mL										
$c(\text{ges}) =$ 0.71 mol/L										

Table S6: 20-60-20 15k.

		2-VP 20%	isoprene 60%	2-VP 20%						
$M_w(\text{tar})$	<b>75000 g/mol</b>	15000 g/mol	69900 g/mol	15000 g/mol						
$n(\text{DBPPB}) =$	0.067 mmol									
$m(\text{DBPPB}) =$	35.89 mg	4 eq. $V(\text{s-BuLi}) =$	0.205 mL	$V(\text{initiator}) =$ 2.22 mL						
		$c(\text{DDPE}) =$ 0.03 mol/L								
60:40	$n(\text{total}) =$	0.060 mol								
$n(\text{2-VP})$ 40:60 $n(\text{l})$										
$m(\text{total}) =$ 5.00 g										
$n(\text{2-VP}) =$ 0.0241 mol		$n(\text{l}) =$ 0.0362 mol								
$m(\text{2-VP}) =$ 2.54 g		$m(\text{l}) =$ 2.46 g								
$V(\text{2-VP}) =$ 2.60 mL		$V(\text{l}) =$ 3.62 mL								
<table border="1"> <tr> <td><math>c(\text{anions}) =</math> 2.76 mM</td> </tr> <tr> <td><math>c(\text{l}) =</math> 1.50 mol/L</td> </tr> <tr> <td><math>V(\text{toluene}) =</math> 24.12 mL</td> </tr> <tr> <td><math>V(\text{THF}) =</math> 48.23 mL</td> </tr> <tr> <td><math>V(\text{ges}) =</math> 72.35 mL</td> </tr> <tr> <td><math>c(\text{ges}) =</math> 0.83 mol/L</td> </tr> </table>					$c(\text{anions}) =$ 2.76 mM	$c(\text{l}) =$ 1.50 mol/L	$V(\text{toluene}) =$ 24.12 mL	$V(\text{THF}) =$ 48.23 mL	$V(\text{ges}) =$ 72.35 mL	$c(\text{ges}) =$ 0.83 mol/L
$c(\text{anions}) =$ 2.76 mM										
$c(\text{l}) =$ 1.50 mol/L										
$V(\text{toluene}) =$ 24.12 mL										
$V(\text{THF}) =$ 48.23 mL										
$V(\text{ges}) =$ 72.35 mL										
$c(\text{ges}) =$ 0.83 mol/L										

Chapter 5 – Synthesis and characterisation of ABA triblock copolymers based on isoprene and 2-vinylpyridine for TPE applications - Supporting Information

Table S7: 20-60-20 20k.

$M_w(\text{tar})$	<b>100000 g/mol</b>	2-VP 20%	isoprene 60%	2-VP 20%
n(DBPPB) =	0.050 mmol	20000 g/mol	60000 g/mol	20000 g/mol
m(DBPPB) =	26.92 mg	4 eq. V(s-BuLi) = 0.154 mL		V(initiator) = 1.67 mL
		c(DDPE) = 0.03 mol/L		
60:40	n(total) =	0.060 mol		
n(2-VP) 40:60 n(l)				
m(total) = 5.00 g				
n(2-VP) = 0.0241 mol		n(l) = 0.0362 mol		
m(2-VP) = 2.54 g		m(l) = 2.46 g		
V(2-VP) = 2.60 mL		V(l) = 3.62 mL		
c(anions) = 2.07 mM				
c(l) = 1.50 mol/L				
V(toluene) = 24.12 mL				
V(THF) = 48.23 mL				
V(ges) = 72.35 mL				
c(ges) = 0.83 mol/L				

Table S8: 20-60-20 25k.

$M_w(\text{tar})$	<b>125000 g/mol</b>	2-VP 20%	isoprene 60%	2-VP 20%
n(DBPPB) =	0.040 mmol	25000 g/mol	75000 g/mol	25000 g/mol
m(DBPPB) =	21.54 mg	4 eq. V(s-BuLi) = 0.123 mL		V(initiator) = 1.33 mL
		c(DDPE) = 0.03 mol/L		
60:40	n(total) =	0.060 mol		
n(2-VP) 40:60 n(l)				
m(total) = 5.00 g				
n(2-VP) = 0.0241 mol		n(l) = 0.0362 mol		
m(2-VP) = 2.54 g		m(l) = 2.46 g		
V(2-VP) = 2.60 mL		V(l) = 3.62 mL		
c(anions) = 1.66 mM				
c(l) = 1.50 mol/L				
V(toluene) = 24.12 mL				
V(THF) = 48.23 mL				
V(ges) = 72.35 mL				
c(ges) = 0.83 mol/L				



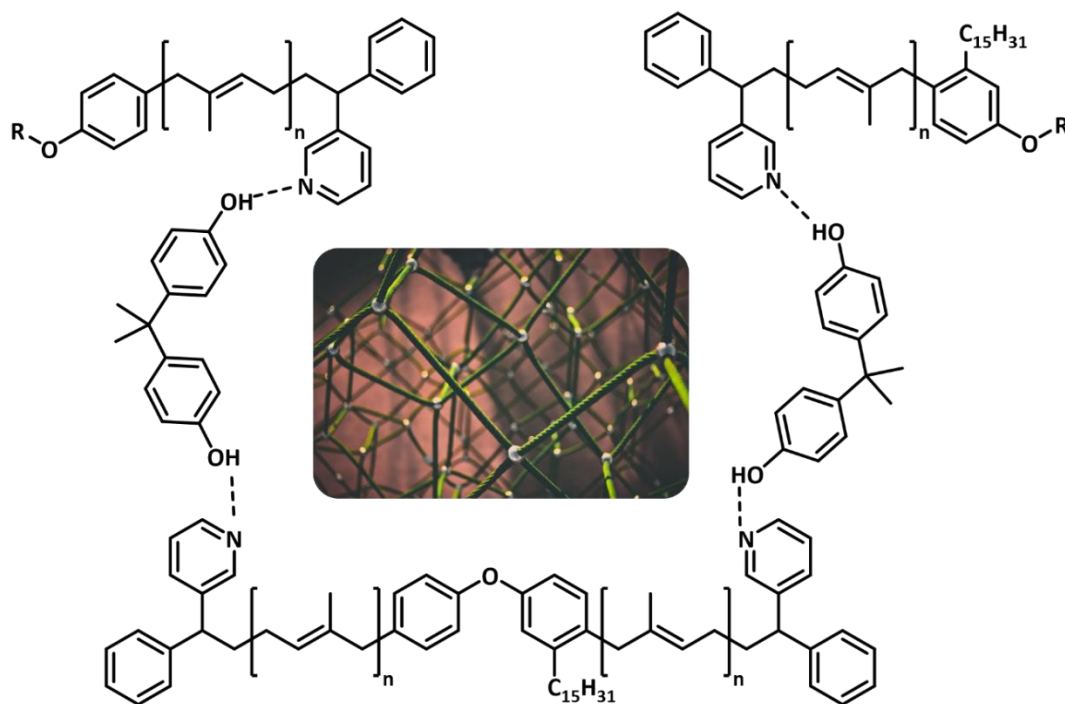
## 10. Chapter 6 – End-capping of bifunctional initiated polyisoprene with *m*-PyPE

Marcel Fickenscher and [REDACTED] \*

M. Sc. Marcel Fickenscher, Prof. [REDACTED]  
Department of Chemistry, Johannes Gutenberg University Mainz, Duesbergweg 10-14,  
55128 Mainz, Germany  
E-Mail: [REDACTED]

Keywords: telechelic isoprene, bifunctional initiators, carbanionic polymerisation, DPE derivatives

### 10.1 TOC & Short Abstract



Endcapping of bifunctional initiated polyisoprene with *m*-PyPE yields telechelic PI, bearing an aminofunctional DPE derivate at each chain end. Different reaction parameters were screened, and the products characterised by means of SEC chromatography and <sup>1</sup>H NMR spectroscopy.

## 10.2 Abstract

Diphenylethylene (DPE) is a well-known monomer and widely used in carbanionic polymerisations. As a result of its sterical bulk, the homopolymerisation is not possible. This was exploited in several publications to synthesise various copolymer structures with different comonomer ratios up to alternating structures with 50 mol% DPE content. Ultimately, the stiffness of the polymer backbone increases, leading to an increased glass transition temperature  $T_g$ . Additionally, DPE derivatives offer an excellent way to introduce functional groups, since they are easily accessible and most benzylic side groups do not alter the reactivity of the monomer double bond. A special field of application for DPE derivatives is the endcapping of living polymers: Due to the limited homopolymerisability, precisely one DPE unit is incorporated at the end of each chain, allowing the introduction of a single functional group per carbanion. In this work, an attempt was made to synthesise a telechelic polyisoprene, bearing two *m*-PyPE units, an amine functional DPE derivative with one phenyl group being replaced by pyridine, with the aim of forming dynamically crosslinked structures by means of post-polymerisation modification. Different reaction parameters were screened to enable a controlled bifunctional polymerisation of isoprene and the subsequent crossover to *m*-PyPE. Depending on the chosen reaction conditions, the synthesis shows different difficulties, which were analysed by means of  $^1\text{H}$  NMR spectroscopy and SEC chromatography.

## 10.3 Introduction

The carbanionic polymerisation of functional monomers enables the synthesis of well-defined materials with unique properties. One of the most popular monomers used for the tailored functionalisation is DPE and its respective derivatives. DPE itself offers an excellent way to alter the material properties with regard to the glass transition temperature  $T_g$  and the mechanical toughness, frequently used for the synthesis of styrene and isoprene based thermoplastic elastomers.<sup>1</sup> Since it cannot homopolymerise due to its steric bulk, the incorporation limit of DPE is 50 mol%, resulting in a perfectly alternating copolymer.<sup>2,3</sup> For styrene-DPE copolymers, the  $T_g$  rises from ~100 °C to ~180 °C as a consequence of the increased stiffness of the polymer backbone.<sup>4</sup> In addition to the changing material properties, DPE derivatives are of particular interest from a chemical point of view. Various derivatives with functional groups are known in literature, a selection is shown in Figure 1:

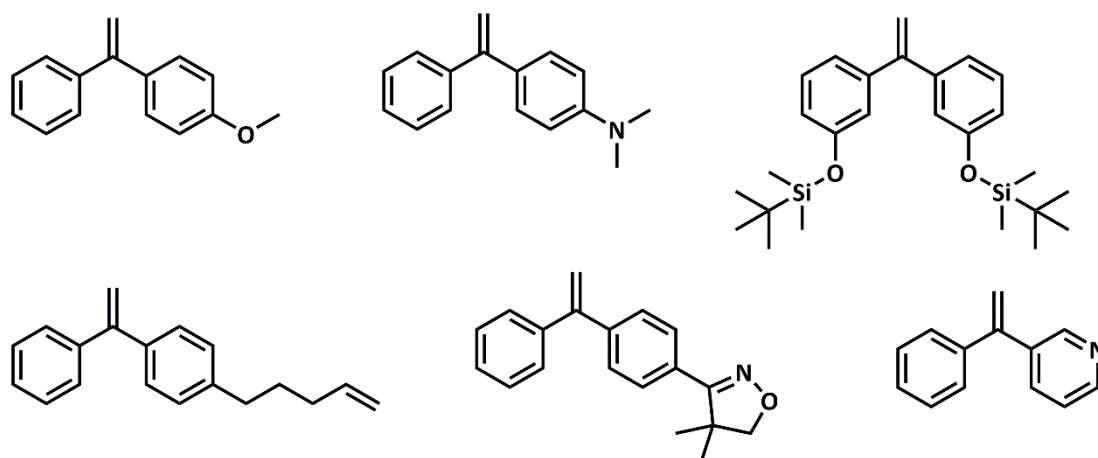


Figure 1: Various DPE derivatives, demonstrating the versatility for functionalisation by means of copolymerisation.<sup>5-10</sup>

The wide range of functional groups shows the universal applicability of DPE derivatives: ether groups, amines, silicon groups, cyanides, or more complex substituents such as oxazolines are possible. While most of these structures carry their functional group in the phenyl position, few examples modify one of the phenyl groups itself. Ma *et al.* employ 1-cyclopropylvinylbenzene (CPVB) as a monomer for the thermally controlled living anionic polymerisation which includes an anion migrated

ring-opening mechanism. Starting at 20 °C, the addition of *s*-BuLi results in the opening of the cyclopropyl group, yet no further polymerisation is observed. Raising the temperature to 60 °C enables the addition of monomers by means of an anion migrated ring opening mechanism.<sup>11</sup>

Similar to CPVB, 3-(1-phenylvinyl)pyridine (*m*-PyPE) is a special representative of DPE derivatives due to the pyridinyl group that substitutes one phenyl group. As already discussed in Chapter 2, this modification changes the reactivity of the double bond, but also offers a variety of possibilities for post-polymerisation modification.<sup>12</sup> Similar to vinylpyridine, protonation, quaternisation or metal salt inclusion is conceivable. With the help of bifunctional initiators, telechelic structures can be synthesised which, in combination with the exact incorporation of a single pyridine unit per chain end, offer the possibility of reversible crosslinking of polymers via the introduction of organic guest molecules such as phenols. Figure 2 gives an overview over the different modifications.<sup>13</sup>

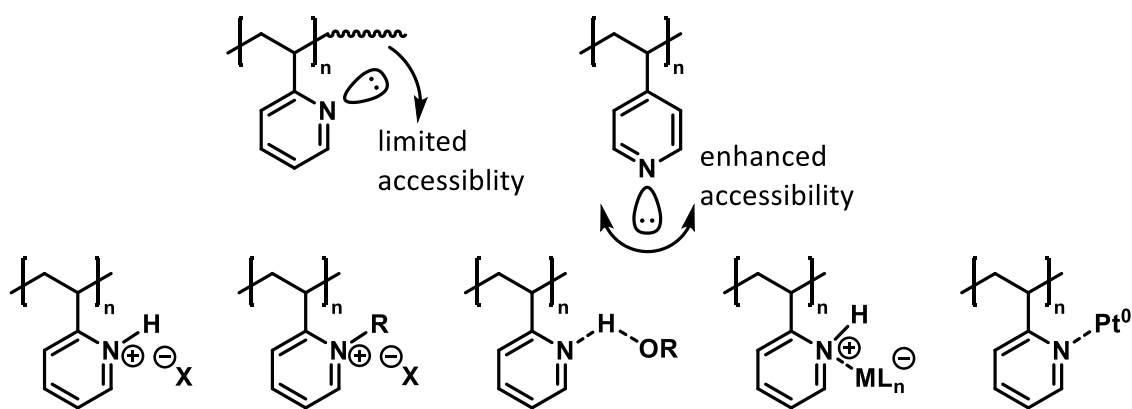


Figure 2: Post-polymerisation modifications of 2-VP and dynamic crosslinking of *m*-PyPE-endcapped polyisoprene with bisphenol A.

Especially the modification with alkyl halides and phenols are of special interest since the use of bihalides and -phenols enables the formation of ionic or hydrogen bond based networks. This self-assembly based reversible crosslinking is a powerful tool in modern chemistry, its potential is demonstrated in several articles and points towards improved self-healing materials.

Brinke et al. present an overview, describing the general concept of self-assembling functional materials. Comb-shaped polymers form hierarchical structures by simple hydrogen bonds, favouring plasticisation and ultimately leading to solid films and enhanced processing options.<sup>14</sup> Loos et al. show the change in morphology using the example of P4VP-*b*-PS-*b*-PAPI and the introduction of 3-nonadecylphenol (NDP). The formation of hydrogen bonds between NDP and 4-VP as well as PAPI efficiently alters the observed morphology in dependence on the NDP concentration from triple lamellar towards different structures such as spheres or tetragonally packed cylinders *in-lamellae*.<sup>15</sup> A more application-related example of the use of dynamically crosslinked elastomers with a strong focus on the self-healing potential is shown by Kutsumizu *et al.*. The introduction of carboxy groups into polyisoprene yields a pH-responsive polymer that forms ionic aggregates in the hydrophobic PI matrix, when treated with sodium hydroxide solution. After the solvent removal, a cast film was obtained, that shows efficient self-healing behaviour at 28 °C when cut.<sup>16</sup>

Similar behaviour is expected for telechelic *m*-PyPE endcapped PI samples when treated with dihalides or -phenols. Figure 3 displays an exemplary network formation with bisphenol A. In contrast to the previously discussed structures, the use of *m*-PyPE as linking point has several advantages. Since *m*-PyPE cannot homopolymerise under carbanionic conditions due to steric hindrance, exactly one pyridine unit is added to each living chain end. This allows precise control over the molecular structure of the polymer as well as excellent control over post-polymerisation modification. This control over the functionalisation allows the full potential of the supramolecular reversible network to be realised. Whereas with crosslinking sites along the chain the mesh size is difficult to determine, in this case the full elasticity of the PI strands can be exploited. This also allows the mechanics of the network to be precisely tuned, as the length of the PI parts and thus the mesh size can be adjusted during synthesis. In this case, exceeding the entanglement molecular weight results in a further increase in the mechanical properties.

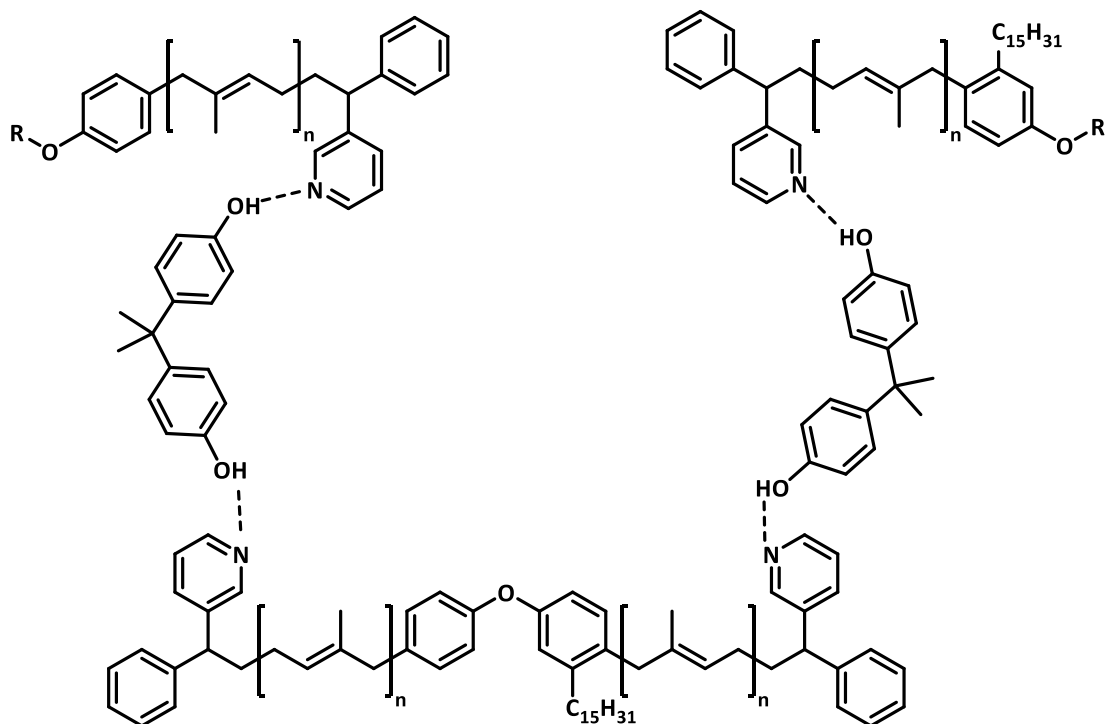


Figure 3: Hydrogen bonding between the pyridine groups and bisphenol A forms a reversible crosslinked network of telechelic PI.

In this study, we synthesised living PI via the bifunctional initiator 1-bromo-4-(4-bromophenoxy)-2-pentadecylbenzene (DBPPB), readily available from a coupling reaction of 3-pentadecylphenol and bromobenzene, and the subsequent bromination. After the activation of the initiator with *s*-BuLi, isoprene is added, followed by the addition of *m*-PyPE after full monomer conversion. Different reaction conditions were screened to yield the telechelic PI.

## 10.4 Results and Discussion

### Synthesis and sample overview

In the following we describe the synthesis of the initiator, the endcapping reagent *m*-PyPE, the polymerisation of isoprene and various approaches for the endcapping reaction.

According to the synthesis described by Gnanou et al., DBPPB was synthesised, starting from 3-pentadecylphenol and bromobenzene.<sup>17</sup> Figure 4 shows the reactions scheme.

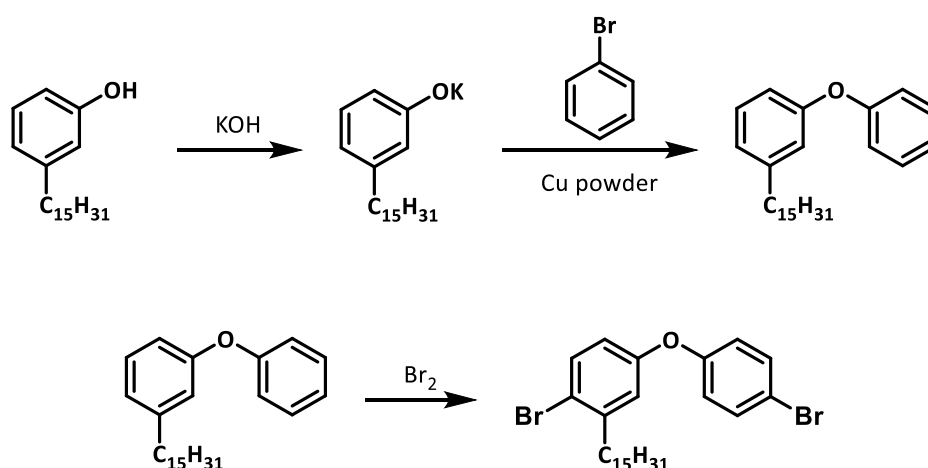


Figure 4: Reaction scheme for the two-step synthesis of DBPPB. Formation of the 3-pentadecylphenol potassium salt and subsequent coupling with bromobenzene yields 1-pentadecyl-3-phenoxybenzene which is brominated to yield the bifunctional initiator.<sup>17</sup>

The bromination of the intermediate 1-pentadecyl-3-phenoxybenzene leads to the formation of the initiator DBPPB, which is obtained as a colourless powder after careful purification by means of column chromatography (yield: 58%, Figure S1). Prior to use, the initiator was lyophilised and a 0.01 M stock solution in benzene was prepared.

*m*-PyPE was synthesised as described in Chapter 2 lyophilised and degassed prior to use (Figure S2).

Starting from the activation of the initiator solution with *s*-BuLi, the mixture is stirred for 60 minutes to ensure the full activation. Subsequently, the reaction solution was further diluted with benzene or toluene respectively prior to the addition of the dried and degassed isoprene to the activated initiator solution. The polymerisation was

stirred for 3 h at room temperature prior to the addition of *m*-PyPE. Ultimately, the reaction was quenched with degassed MeOH after different time spans, depending on the chosen reaction conditions. Figure 5 shows the reaction scheme, a summary of the different conditions is given in table 1. Polymers with 2, 5 and 10 kg·mol<sup>-1</sup> were synthesised for each given sample.

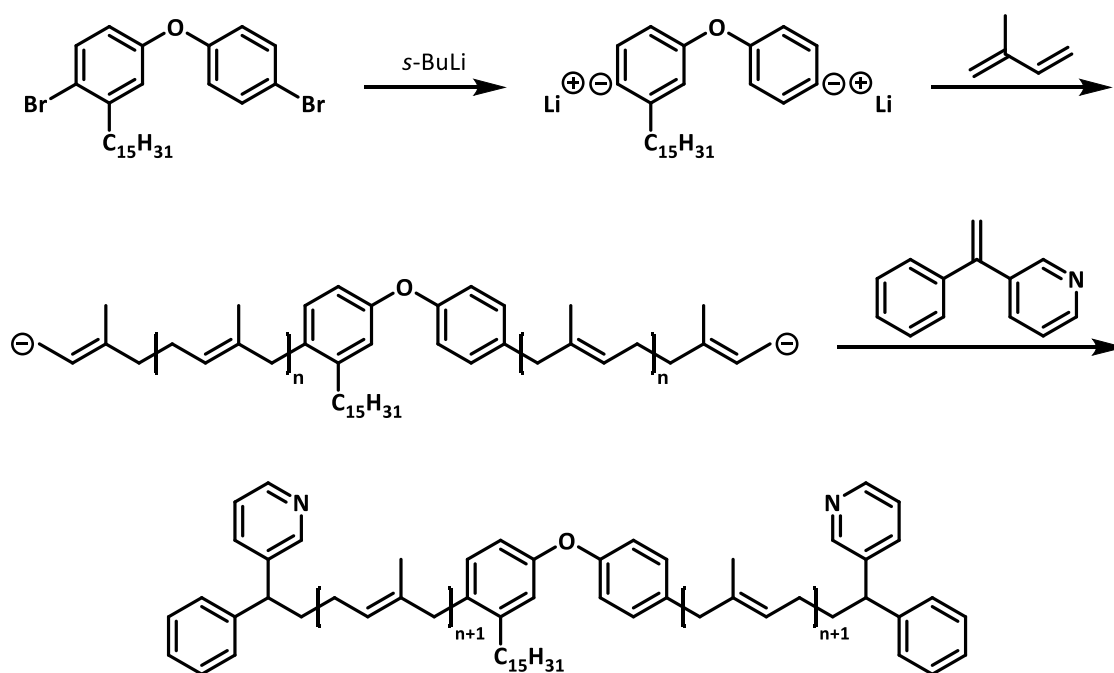


Figure 5: Reaction scheme for the bifunctional stepwise synthesis of *m*-PyPE endcapped polyisoprene.



Table 1: Overview of the different reaction conditions.

Sample	isoprene	<i>m</i> -PyPE	comment
A1	3 h, r.t., benzene	30 min, r.t., undiluted	crosslinked
A2	3 h, r.t., benzene	20 min, r.t., undiluted	crosslinked
A3	3 h, r.t., benzene	10 min, r.t., undiluted	crosslinked
A4	3 h, r.t., benzene	1 min, r.t., undiluted	crosslinked
B1	3 h, r.t., toluene	30 min, 0 °C, undiluted	crosslinked
B2	3 h, r.t., toluene	20 min, 0 °C, undiluted	crosslinked
B3	3 h, r.t., toluene	10 min, 0 °C, undiluted	crosslinked
B4	3 h, r.t., toluene	1 min, 0 °C, undiluted	crosslinked
C1	3 h, r.t., toluene	20 min, -78 °C, undiluted	no crossover
C2	3 h, r.t., toluene	60 min, -78 °C, undiluted	no crossover
C3	3 h, r.t., toluene	2 h, -78 °C, undiluted	no crossover
C4	3 h, r.t., toluene	4 h, -78 °C, undiluted	no crossover
D1	3 h, r.t., benzene	15 min, r.t., 0.5 M, benzene	crosslinked
D2	3 h, r.t., toluene	15 min, -78 °C, 0.5 M, toluene	no crossover
D3	3 h, r.t., toluene	15 min, -78 °C, 0.5 M, THF	multimodal
D4	3 h, r.t., toluene	15 min, -78 °C, 0.1 M, THF	monomodal, molecular weight too high

In a first attempt to synthesise the desired endcapped polymer structure, an excess of 6 eq. pure *m*-PyPE was to add to the living polyisoprene solution at room temperature (A1). Upon addition, the colourless reaction mixture immediately turned yellow, indicating the formation of living *m*-PyPE chain ends. The reaction mixture was stirred for 30 minutes, after purification an insoluble product was obtained, indicating

crosslinking by side reactions, and not allowing for deeper analysis. Figure 6 show the side reaction leading to the crosslinking of *m*-PyPE-endcapped polyisoprene, similar to the known side reaction of vinylpyridine.

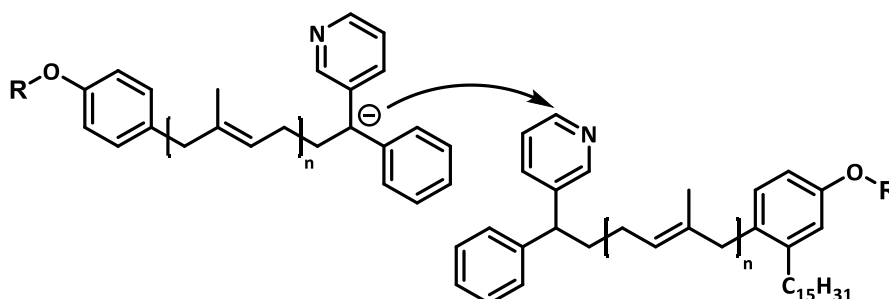


Figure 6: Crosslinking reaction between two *m*-PyPE moieties, leading to the formation of an insoluble product.

Similar to DPE, *m*-PyPE is not able to homopolymerise under carbanionic reaction conditions, therefore 6 eq. of *m*-PyPE were chosen to ensure complete functionalisation of the chain ends. Since the immediate colour change is a sign of a very fast reaction, the amount of *m*-PyPE used was reduced to 2.05 eq. in the following syntheses to avoid enhanced side reactions due to excess *m*-PyPE on the one hand and to facilitate the purification on the other hand, as the removal of excess *m*-PyPE is challenging. At the same time, the reaction time was gradually reduced to decrease the probability of crosslinking. While even reducing the reaction time to 1 minute still results in an insoluble product and further optimisation is needed, it is evident from this that the reaction of polyisoprene with *m*-PyPE is possible and proceeds very fast.

In order to suppress the occurring side reactions, the conditions were changed in a further reaction series B in favour of an increased reaction control and thus the temperature was reduced to 0 °C during the addition of *m*-PyPE. To avoid the freezing of the reaction mixture, toluene was used instead of benzene as solvent for the polymerisation. Different reaction times were employed with no improvement with regard to the side reactions.

Lower temperatures such as -78 °C, that are commonly used for the polymerisation of vinylpyridine in polar media, were screened in the reaction series C. The reaction time

was varied between 20 minutes and 4 h, yet no crossover can be observed. As known in literature, the reactivity of dienes at low temperatures such as  $-78\text{ }^{\circ}\text{C}$  is limited which in this case results in the lack of a crossover reaction.<sup>18</sup> Additionally, it can be assumed that, similar to vinylpyridine, *m*-PyPE requires a more polar environment for its successful and controlled copolymerisation at low temperatures.

A more promising approach is presented in the reaction series D, where a stock solution of *m*-PyPE with different solvents was used. In accordance with series A, room temperature leads to the side reactions and ultimately the crosslinking of the polymer. If a non-polar solvent such as toluene is used to dilute *m*-PyPE and the temperature is lowered to  $-78\text{ }^{\circ}\text{C}$ , no crossover is observed in this case either.

SEC and  $^1\text{H}$  NMR spectroscopy

In comparison, the addition of a *m*-PyPE/THF solution (D3) leads to a more controlled addition of *m*-PyPE due to the increased polarity even at low temperatures. This can be observed on the one hand by the colour change, which indicates the crossover, and on the other hand by the fact that the product is no longer insoluble.

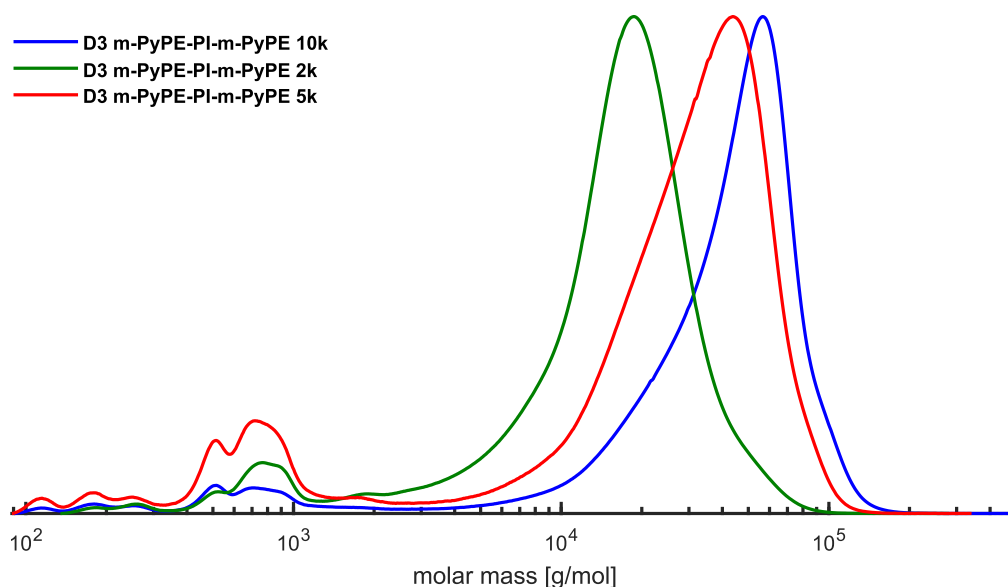


Figure 7: SEC traces of three D3 samples with varying molecular weight. Multimodality as well as an increased molecular weight as a result of polymer linkage is observed. Measured in THF with a polystyrene standard and a RI detector.

The corresponding SEC traces of the three underlying reactions for the polymers with 2, 5 and 10 kg·mol<sup>-1</sup> are shown in Figure 7 and clearly reflect the trend of the molecular weight increase within the series. However, the molecular weight itself deviates strongly from the targeted one and is significantly too high, which is attributed to the presence of linked polymer chains, yet no insoluble network was formed. Although an overall multimodal distribution is observed, the signals of the main products show a monomodal distribution with dispersities between 1.3 and 1.4, suggesting a controlled polymerisation with successful end functionalisation. Figure 8 shows an example of the superposition of the UV and RI signals of the 2k sample, confirming the presence of the UV-active *m*-PyPE.

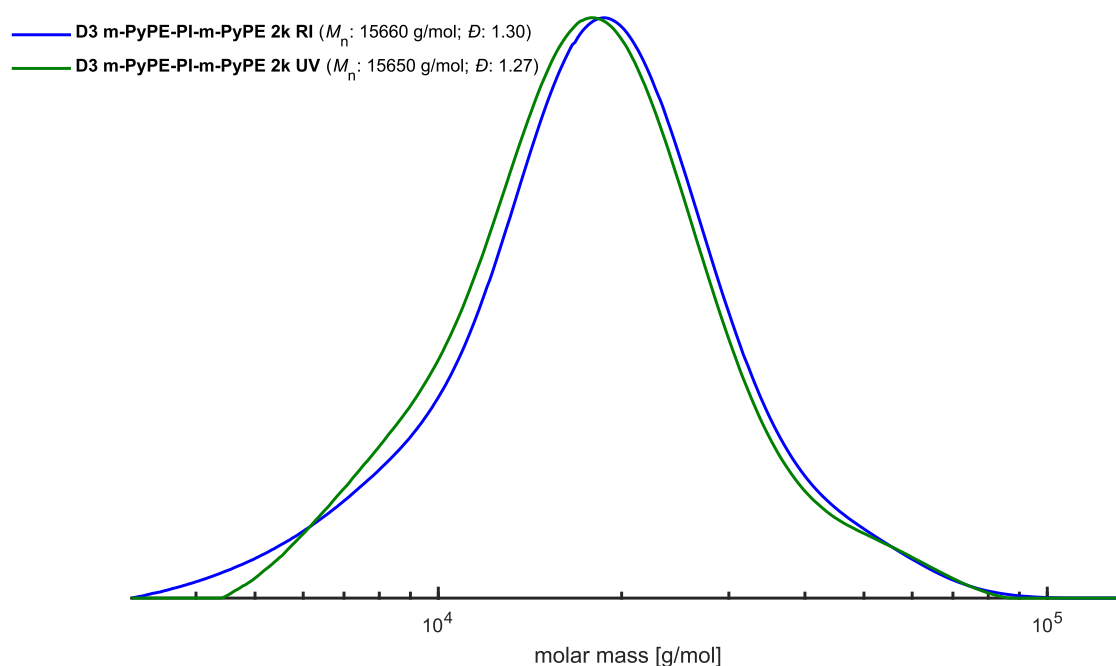


Figure 8: Superpositioned SEC traces of the D3 2 kg·mol<sup>-1</sup> sample, indicating the quantitative endcapping of PI. Measured in THF with a polystyrene standard and a RI detector.

Further dilution of the added *m*-PyPE (D4) causes the side reactions to recede further, and monomodal elugrams are obtained, as shown in Figure 9. Similar to D3, a clearly too high molecular weight is observed, however, overall it can be assumed that the control over the reaction was significantly increased. Analysing the SEC traces in detail, it is particularly noteworthy that in all cases the UV and RI signals agree very well. Based on this, it can be assumed that the quantitative endcapping has been achieved.

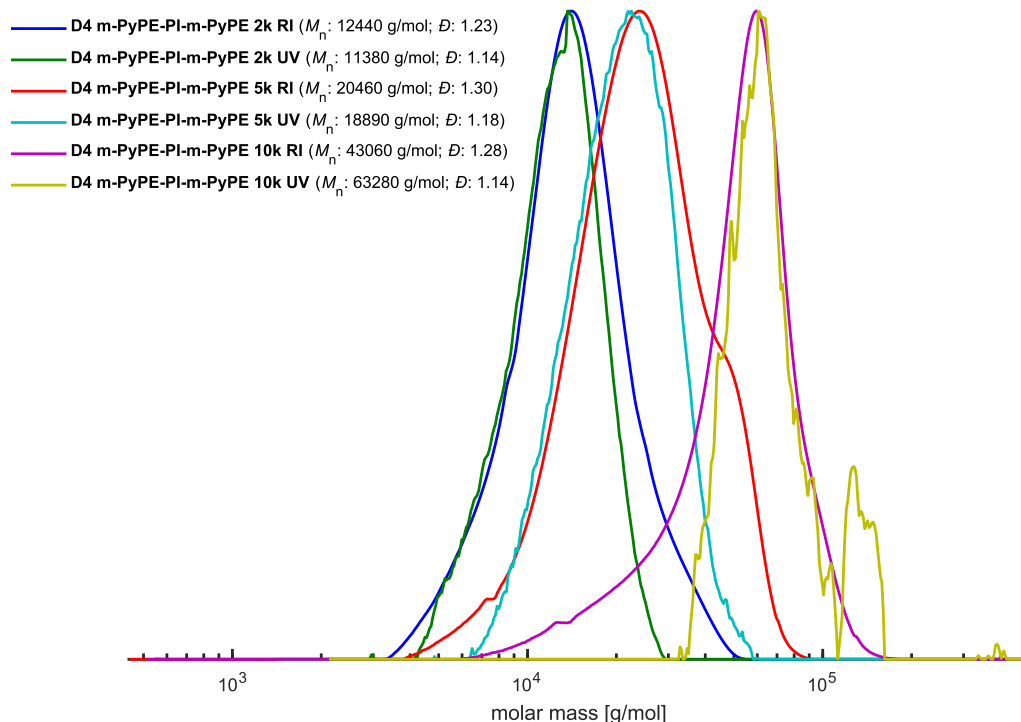


Figure 9: Superpositioned RI and UV detected SEC traces of three D4 samples with varying molecular weight. Monomodality as well as an increased molecular weight as a result of polymer linkage is observed. Measured in THF with a polystyrene standard.

A comparison of the molecular weights and dispersities (RI detector) between the D3 and D4 series is given in Table 2:

Table 2: Comparison of SEC results of the polymerisation series D3 and D4. Measured in THF with a polystyrene standard and a RI detector.

D3	$\bar{D}$	$M_n / [\text{kg}\cdot\text{mol}^{-1}]$	$M_n / [\text{kg}\cdot\text{mol}^{-1}]$	$\bar{D}$	D4
2k	1.30	15.7	12.4	1.23	2k
5k	1.34	28.1	20.5	1.30	5k
10k	1.36	35.8	43.1	1.28	10k

Although the D4 5k sample exhibits a slight shoulder, these samples as a whole are distinguished by the fact that no low-molecular signals were detected and thus imply more control over the reaction. Overall, the trend of the increasing molecular weight corresponding to the target molecular weights is clearly evident in both series. While

the detected molecular weights differ significantly from the targeted ones, the samples D4 2k and 5k show a lower molecular weight and dispersity than the corresponding polymers of the D3 series, therefore a reduction of the side reactions resulting from the increased dilution is assumed here as well.

In addition to the SEC analysis,  $^1\text{H}$  NMR spectra of the polymers were measured. Figure 10 shows an example of the spectrum of the D4 2k sample.

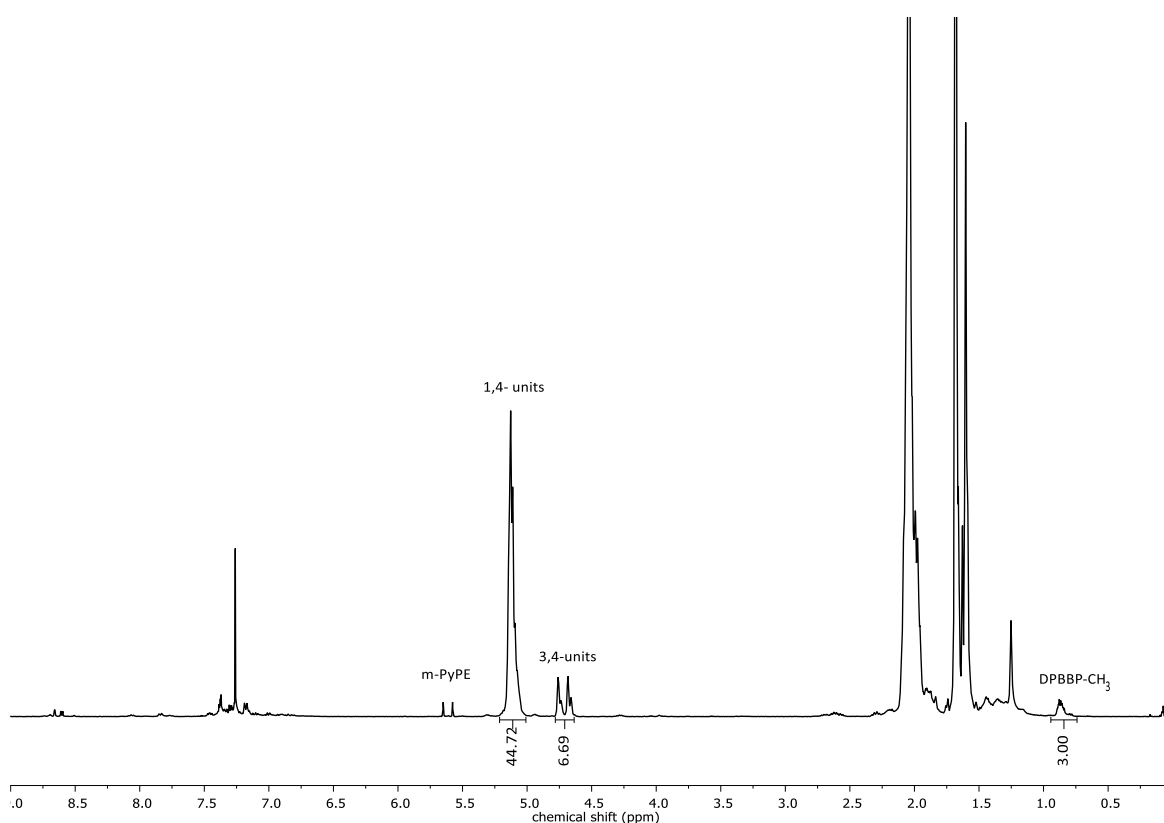


Figure 10:  $^1\text{H}$  NMR spectrum of D4 2k ( $\text{CDCl}_3$ , 400 MHz). The microstructure composition as well as leftover m-PyPE is observed.

The integration on the methyl signal of the alkyl anchor of the initiator allows the determination of the microstructure composition of isoprene (ratio of 1,4- to 3,4-units). While the incorporation ratio of 7.5 to 8.5% 3,4-units is within the expected range for carbanionic polymerisations in non-polar solvents, the calculated molecular weights are on the one hand not consistent within the series but on the other hand not reliable at all, since the assumed chain coupling affects the signal used as reference as well. The respective values for the D4 series are displayed in Table 3:

Table 3: Isoprene microstructure composition and molecular weight, calculated from  $^1\text{H}$  NMR spectra (400 MHz,  $\text{CDCl}_3$ ).

D4	3,4-units / [%]	$M_n$ / [ $\text{kg}\cdot\text{mol}^{-1}$ ]
2k	7.5	3.3
5k	8.5	2.6
10k	7.8	4.3

To improve this, it is necessary to control the amount of *m*-PyPE used more precisely. Since only small amounts are employed, this is quite challenging, but an increase in the size of the reaction batch would remedy this. A major problem in this context is the presence of unreacted *m*-PyPE, which can be seen from the doublet signal at 5.6 ppm (*m*-PyPE double bond), which hints towards another reason for the leftover *m*-PyPE, the undesired side reaction of living isoprenyllithium chain ends with already end-capped *m*-PyPE chain ends. In addition, a coupling of chains cannot be seen in NMR spectra, since the calculated molecular weight is only the ratio of initiator group to monomer units; if chains are coupled, the ratio does not change, since there is then also more than one initiator group in the molecule. Further optimisation of the reaction parameters is mandatory in order to carry out a reliable analysis.

Although the polymers produced have not yet been fully optimised, the interaction with diols in a qualitative test series should be investigated. For this purpose, a small amount of the viscous polymer was dissolved in benzene, mixed with a 0.5 M bisphenol A solution and the solvent was evaporated. As expected, the viscosity should increase, yet this could not be observed. A possible reason for this could be the linking of the polymers that has already taken place and the associated high molecular weight, which is why further crosslinking of the end groups no longer has any influence. Another explanation could be a steric hindrance between bisphenol A and *m*-PyPE, both groups are comparably voluminous. To rule this out, the possibility of

quaternisation with 1,2-dibromoethane was investigated, but no other results were observed in this case either.



## 10.5 Experimental

### Materials and methods

Isoprene was purchased from Acros Organics, filtered over basic aluminium oxide to remove the stabiliser and protic impurities, dried over CaH<sub>2</sub> and freshly distilled prior to use. All solvents (Fisher Chemical, Carl Roth GmbH + Co. KG) were carefully dried with CaH<sub>2</sub> (Sigma Aldrich) or butyllithium (Sigma Aldrich) and freshly distilled prior to use.

### Nuclear magnetic resonance (NMR) spectroscopy

<sup>1</sup>H NMR measurements were performed on a Bruker Avance II 400 at a magnetic field strength of 400 MHz.

### Size exclusion chromatography (SEC)

All SEC measurements were performed with an Agilent 1100 Series chromatograph, equipped with HEMA columns (300/100/40, 95 cm length, 0.8 cm width, 50 °C) and an Agilent G1314A UV detector. Solvent: THF, internal standard: toluene, calibration: polystyrene.

### Synthesis procedures

*m*-PyPE was synthesised following the route described in Chapter 2. DBPPB was synthesised following the route described in Chapter 5.

All polymerisations were carried out in a 2 g scale using a carefully flame dried all-glass apparatus with rubber seals and Teflon caps as well as standard high vacuum techniques. Isoprene was purified by filtration over basic aluminium oxide to remove the stabiliser and protic impurities, degassed with three *freeze-pump-thaw* cycles and stirred over CaH<sub>2</sub> for one night. Isoprene was freshly distilled prior to the polymerisation. *m*-PyPE was lyophilised and stored under an inert argon atmosphere. A 0.03 M solution of DBPPB in dried, degassed benzene was placed in the reaction flask, followed by the addition of 4 eq. *s*-BuLi to activate the initiator. The gelation of the solution as well as a turbidity can be observed in the course of the activation time of

one hour. After the quantitative activation of the initiator, the required amount of freshly distilled toluene was transferred into the reaction flask and isoprene was added *via* syringe, resulting in the colour change to light yellow. After 3 h, *m*-PyPE was added *via* syringe, leading to the immediate formation of yellow coloured pyridinyl anions. After 1 min to 4 h, the reaction mixture was quenched with degassed methanol. The solvent was removed under reduced pressure to quantitatively yield the respective polymers.

## 10.6 Conclusion

The successful synthesis of *m*-PyPE and the development of a synthesis route for the endcapping of living bifunctional polyisoprene was studied in this work. While high temperatures (room temperature) result in uncontrolled crosslinking of the attached, living *m*-PyPE groups, the absence of endcapping was observed at low temperatures (-78 °C) in non-polar solvents. The addition of a polar solvent as well as the dilution of *m*-PyPE prior to the addition increases the reaction control significantly. By means of SEC and <sup>1</sup>H NMR spectroscopy, it could be shown that monomodal distributions with a high fraction of 1,4-units within the isoprene block are available by a suitable choice of reaction conditions. The deviation in molecular weight as a result of side reactions during endcapping is the most important issue to be addressed in follow-up work. The polymers obtained still show clear potential for optimisation, yet overall it could be shown that endcapping is feasible. Based on this, an interesting method for modifying isoprene was opened up, which can be further optimised in the future and has the potential to expand the already wide range of possible applications for polyisoprene. The prospect of developing bisphenol-based networks provides a promising starting point for further work on this topic. The screening of alternative bisphenols is the most important point of material characterisation, and a rheological investigation of viscosity to quantitatively verify successful crosslinking should be the focus after the successful synthesis.

## 10.7 References

- (1) Quirk, R. P.; Yoo, T.; Lee, Y.; Kim, J.; Lee, B. Applications of 1,1-Diphenylethylene Chemistry in Anionic Synthesis of Polymers with Controlled Structures. In *Biopolymers · PVA Hydrogels, Anionic Polymerisation Nanocomposites*; Advances in Polymer Science; Springer Berlin Heidelberg, 2000; pp 67–162. DOI: 10.1007/3-540-46414-X\_3.
- (2) Liu, K.; an Li; Yang, Z.; Jiang, A.; Xie, F.; Li, S.; Xia, J.; She, Z.; Tang, K.; Zhou, C. Synthesis of strictly alternating copolymers by living carbanionic copolymerization of diphenylethylene with 1,3-pentadiene isomers. *Polym. Chem.* **2019**, *10* (14), 1787–1794. DOI: 10.1039/C9PY00008A.
- (3) Hirao, A.; Hayashi, M.; Haraguchi, N. Synthesis of well-defined functionalized polymers and star branched polymers by means of living anionic polymerization using specially designed 1,1-diphenylethylene derivatives. *Macromol. Rapid Commun.* **2000**, *21* (17), 1171–1184. DOI: 10.1002/1521-3927(20001101)21:17<1171:AID-MARC1171>3.0.CO;2-C.
- (4) Hutchings, L. R.; Brooks, P. P.; Shaw, P.; Ross-Gardner, P. Fire and Forget! One-Shot Synthesis and Characterization of Block-Like Statistical Terpolymers via Living Anionic Polymerization. *J. Polym. Sci. A Polym. Chem.* **2019**, *57* (3), 382–394. DOI: 10.1002/pola.29208.
- (5) Natalello, A.; Hall, J. N.; Eccles, E. A. L.; Kimani, S. M.; Hutchings, L. R. Kinetic control of monomer sequence distribution in living anionic copolymerisation. *Macromolecular rapid communications* **2011**, *32* (2), 233–237. DOI: 10.1002/marc.201000482. Published Online: Nov. 15, 2010.
- (6) Hirao, A.; Hayashi, M. Synthesis of Well-Defined Functionalized Polystyrenes with a Definite Number of Chloromethylphenyl Groups at Chain Ends or in Chains by Means of Anionic Living Polymerization in Conjunction with Functional Group Transformation. *Macromolecules* **1999**, *32* (20), 6450–6460. DOI: 10.1021/ma990618x.
- (7) Hirao, A.; Loykulant, S.; Ishizone, T. Recent advance in living anionic polymerization of functionalized styrene derivatives. *Progress in Polymer Science* **2002**, *27* (8), 1399–1471. DOI: 10.1016/S0079-6700(02)00016-3.
- (8) Quirk, R. P. Scope and limitations of 1,1-diphenylethylene chemistry in anionic polymer synthesis. *Makromolekulare Chemie. Macromolecular Symposia* **1992**, *63* (1), 259–269. DOI: 10.1002/masy.19920630119.
- (9) Yang, L.; Shen, H.; Han, L.; Ma, H.; Li, C.; Lei, L.; Zhang, S.; Liu, P.; Li, Y. Sequence regulation in living anionic terpolymerization of styrene and two categories of 1,1-diphenylethylene (DPE) derivatives. *Polym. Chem.* **2020**, *11* (32), 5163–5172. DOI: 10.1039/D0PY00731E.
- (10) Brooks, P. P.; Natalello, A.; Hall, J. N.; Eccles, E. A. L.; Kimani, S. M.; Bley, K.; Hutchings, L. R. Monomer Sequencing in Living Anionic Polymerization Using Kinetic Control. *Macromol. Symp.* **2013**, *323* (1), 42–50. DOI: 10.1002/masy.201100111.
- (11) Bai, H.; Leng, X.; Han, L.; Yang, L.; Li, C.; Shen, H.; Lei, L.; Zhang, S.; Wang, X.; Ma, H. Thermally Controlled On/Off Switch in a Living Anionic Polymerization of 1-Cyclopropylvinylbenzene with an Anion Migrated Ring-Opening Mechanism. *Macromolecules* **2020**, *53* (21), 9200–9207. DOI: 10.1021/acs.macromol.0c01589.

- (12) Fickenscher, M.; Reimers, T.; Frey, H. Introducing a 1,1-diphenylethylene analogue for vinylpyridine: anionic copolymerisation of 3-(1-phenylvinyl)pyridine (m -PyPE). *Polym. Chem.* **2021**, *12* (24), 3576–3581. DOI: 10.1039/D1PY00302J.
- (13) Kennemur, J. G. Poly(vinylpyridine) Segments in Block Copolymers: Synthesis, Self-Assembly, and Versatility. *Macromolecules* **2019**, *52* (4), 1354–1370. DOI: 10.1021/acs.macromol.8b01661.
- (14) Ikkala, O.; Brinke, G. ten. Functional materials based on self-assembly of polymeric supramolecules. *Science (New York, N.Y.)* **2002**, *295* (5564), 2407–2409. DOI: 10.1126/science.1067794.
- (15) Hofman, A. H.; Terzic, I.; Stuart, M. C. A.; Brinke, G. ten; Loos, K. Hierarchical Self-Assembly of Supramolecular Double-Comb Triblock Terpolymers. *ACS macro letters* **2018**, *7* (10), 1168–1173. DOI: 10.1021/acsmacrolett.8b00570. Published Online: Sep. 13, 2018.
- (16) Miwa, Y.; Kurachi, J.; Sugino, Y.; Udagawa, T.; Kutsumizu, S. Toward strong self-healing polyisoprene elastomers with dynamic ionic crosslinks. *Soft matter* **2020**, *16* (14), 3384–3394. DOI: 10.1039/D0SM00058B.
- (17) Matmour, R.; More, A. S.; Wadgaonkar, P. P.; Gnanou, Y. High performance poly(styrene-b-diene-b-styrene) triblock copolymers from a hydrocarbon-soluble and additive-free dicarbanionic initiator. *J. Am. Chem. Soc.* **2006**, *128* (25), 8158–8159. DOI: 10.1021/ja062695v.
- (18) Bareuther, J.; Plank, M.; Kuttich, B.; Kraus, T.; Frey, H.; Gallei, M. Temperature Variation Enables the Design of Biobased Block Copolymers via One-Step Anionic Copolymerization. *Macromol. Rapid Commun.* **2021**, *42* (8), e2000513. DOI: 10.1002/marc.202000513. Published Online: Oct. 12, 2020.

## 10.8 Supporting Information

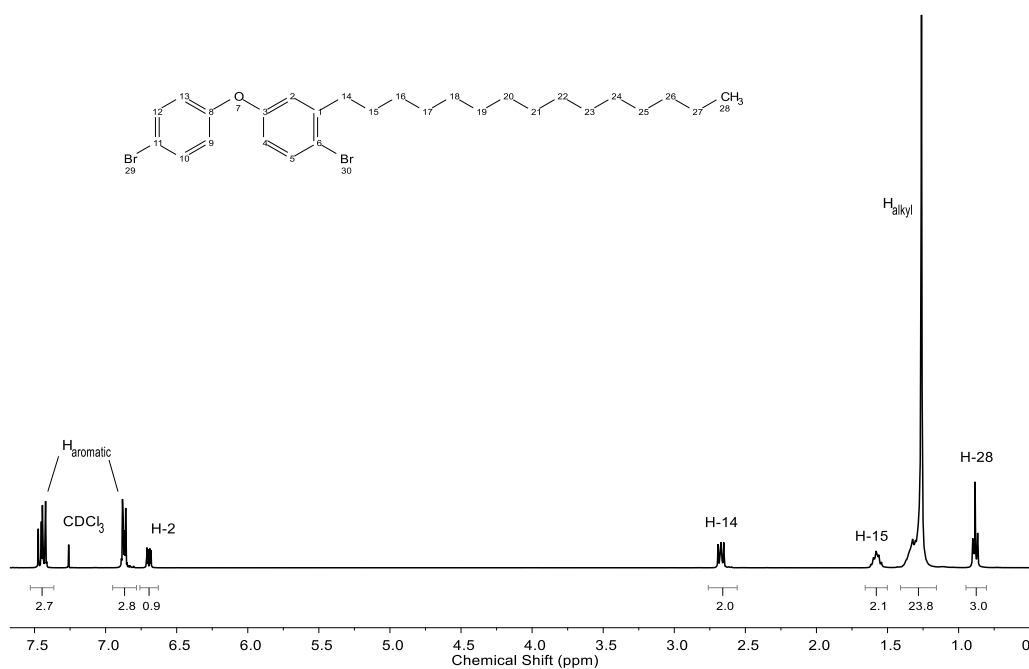


Figure S1:  $^1\text{H}$  NMR spectrum of DBPPB ( $\text{CDCl}_3$ , 400 MHz).

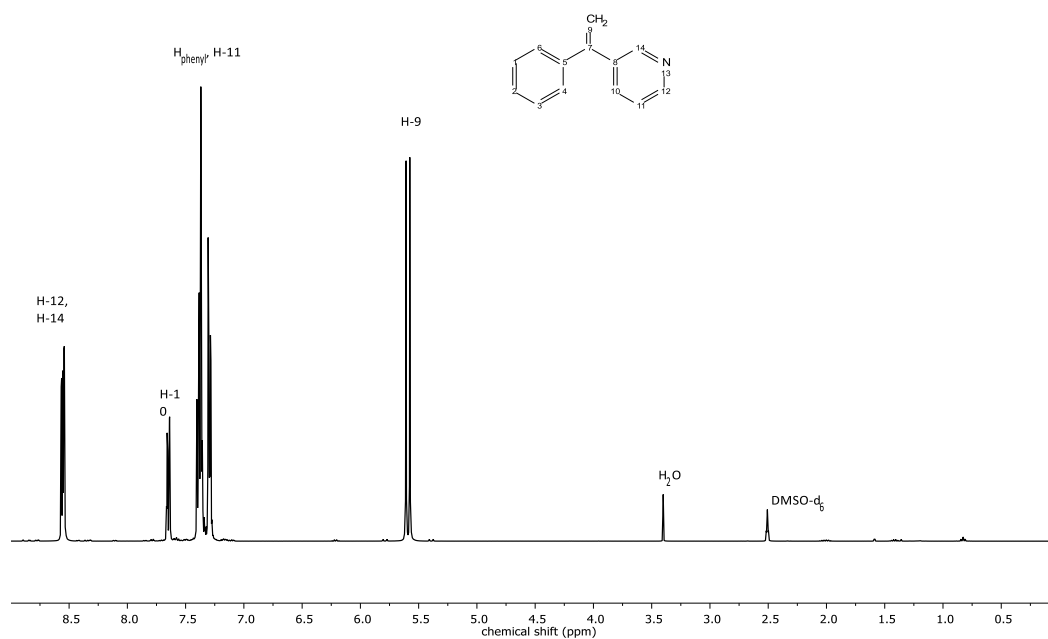


Figure S2:  $^1\text{H}$  NMR spectrum of m-PyPE ( $\text{DMSO-d}_6$ , 400 MHz).

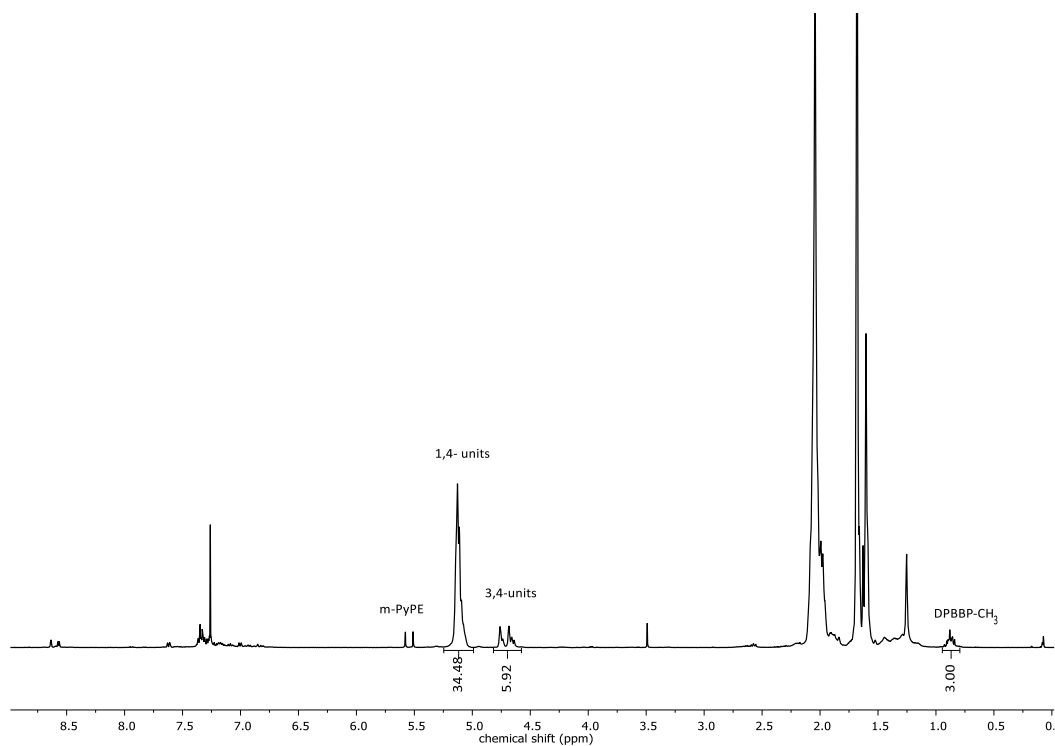


Figure S3: <sup>1</sup>H NMR spectrum of D4 5k (CDCl<sub>3</sub>, 400 MHz).

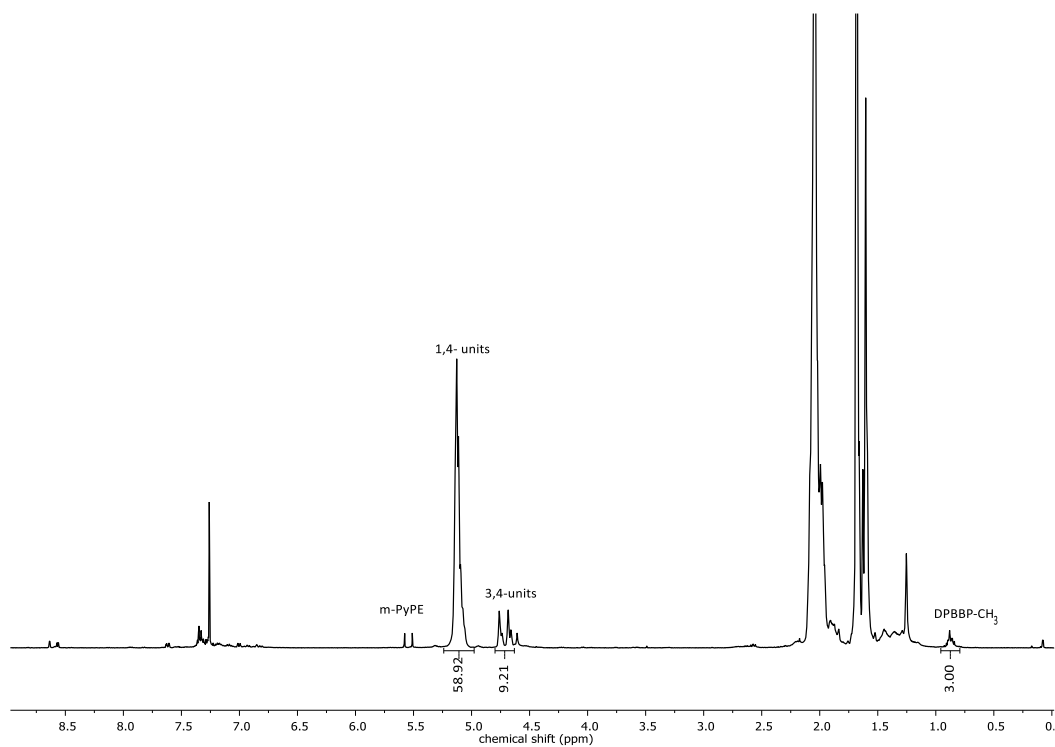


Figure S4: <sup>1</sup>H NMR spectrum of D4 10k (CDCl<sub>3</sub>, 400 MHz).







**09/2001 – 06/2010** Abitur at the [REDACTED]

Work Experience

**06/2015 – 12/2015** Internship at the Johannes Gutenberg University Mainz  
Working group of Prof. Dr. [REDACTED]

Further Education

Courses of the general doctoral programme of the Johannes Gutenberg University Mainz

- Project Management
- Presenting in English
- Intercultural Communication
- Academic Writing in English
- Research Data Management
- What to do with a PhD? Professional Orientation for PhD Students

Languages

German (native)

English (fluent)

French (basic)

Skills

Organic synthesis

- Inert reaction environments and high-purity substance isolation
- Reaction tracking via *online* and *offline*  $^1\text{H}$  NMR spectroscopy

Polymer synthesis

- Synthesis preparation using the *glovebox*
- Carbanionic syntheses by means of high-vacuum techniques
- Design of custom glass reactors for high-boiling monomers and sequential solvent additions of multi-step syntheses
- Development and optimisation of complex synthesis routes

Analytical methods

- NMR spectroscopy
- Differential scanning calorimetry
- Lightscattering (Zetasizer)
- Size exclusion chromatography
- UV-Vis spectroscopy
- IR spectroscopy

Materials characterisation

- Contact angle determination
- Extrusion
- Film production via *solvent evaporation casting*
- Tensile strain measurements

- IT Skills
- Microsoft Office
  - Adobe Photoshop
  - WordPress (administration and design of the working group homepage)
  - Citavi
  - MestreNova
  - PSS WinGPC UniChrom
  - FindMolecule (chemical inventory, management and ordering)
  - SciFinder and Reaxys

Interests

[REDACTED]  
[REDACTED]  
[REDACTED]

Conferences

- 2021 Macromolecular Colloquium, Freiburg, Germany (Online)  
Poster: Introducing a 1,1-diphenylethylene analogue for vinylpyridine: anionic copolymerisation of 3-(1-phenylvinyl)pyridine (*m*-PyPE)
- 2019 International Symposium in Ionic Polymerisation, Beijing, China  
Poster: Copolymerisation of 2-vinylpyridine with an amine functional DPE derivative: 3-(1-phenylvinyl)pyridine

Publications

Graphical Design of an *ACS Macromolecules Supplementary Cover Image*, 54, 16, **2021**.

[REDACTED], M. Fickenscher, [REDACTED]

Introducing a 1,1-diphenylethylene analogue for vinylpyridine: anionic copolymerisation of 3-(1-phenylvinyl)pyridine (*m*-PyPE)

M. Fickenscher, [REDACTED], [REDACTED], *Polymer Chemistry* **2021**. DOI: 10.1039/D1PY00302J